Mode of action and target identification of anti-inflammatory natural products

Dissertation

To Fulfil the
Requirements for the Degree of
“doctor rerum naturalium” (Dr. rer. nat.)

Submitted to the Council of the Faculty
of Biological Sciences
of the Friedrich Schiller University Jena

by Dipl.-Pharm. Stefanie König
born on January 24st, 1990 in Karl-Marx-Stadt

1st Reviewer Prof. Dr. Oliver Werz
Friedrich-Schiller-University Jena
Faculty of Biological Sciences
Institute of Pharmacy
Department of Pharmaceutical and Medicinal Chemistry
Philosophenweg 14
07743 Jena, Germany

2nd Reviewer Prof. Dr. Dirk Hoffmeister
Friedrich-Schiller-University Jena
Faculty of Biological Sciences
Institute of Pharmacy
Department of Pharmaceutical Microbiology at the Hans Knöll Institute
Winzerlaer Straße 2
07745 Jena, Germany

3rd Reviewer Prof. Dr. Alexandra Kiemer
Saarland University
Faculty of Natural Sciences and Technology
Institute of Pharmaceutical Sciences
Department of Pharmaceutical Biology
Campus C2 3
66123 Saarbrücken, Germany

Date of oral defense: November 21, 2019

TABLE OF CONTENTS

TABLE OF CONTENTS I
ABBREVIATIONS III
SUMMARY V
ZUSAMMENFASSUNG VIII
1. **INTRODUCTION** 1
1.1 Inflammatory response and cancer 1
1.1.1 Arachidonic acid pathway 2
1.1.1.1 5-Lipoxygenase and its helper protein FLAP 3
1.1.1.2 Leukotriene A_4 hydrolase and leukotrienes 5
1.2 Cell death 7
1.2.1 Apoptosis 8
1.2.2 Autophagy and autophagic cell death 9
1.2.3 Necrosis 10
1.3 Natural products 10
1.3.1 Gliotoxin from *Aspergillus fumigatus* 11
1.3.2 Melleolides from *Armillaria mellea* 12
1.3.3 Myxochelin A from *Pyxidicoccus fallax* 12
2. **AIM OF THE THESIS** 13
3. **MANUSCRIPTS** 14
3.1 Manuscript I (M-I) 15
3.2 Manuscript II (M-II) 17
3.3 Manuscript III (M-III) 19
3.4 Manuscript IV (M-IV) 20
3.5 Manuscript V (M-V) 21
4. **DISCUSSION** 22
4.1 Natural compounds and their effect on inflammatory key processes 23
4.2 Natural compounds and their influence on cell viability in human cells 29
4.3 Conclusion 34
5. **LITERATURE** 36
APPENDIX 1: ADDITIONAL DATA I
A.1 Effects of natural products on cancer cell proliferation I
A.1.1 Myxochelin A reduces primarily cell viability of leukemic cancer cells I
APPENDIX 2: MANUSCRIPTS III

M-I: Melleolides from honey mushroom inhibit 5-lipoxygenase via C159 III

M-II: Gliotoxin from *Aspergillus fumigatus* abrogates leukotriene B_4 formation through inhibition of leukotriene A_4 hydrolase XXV

M-III: Myxochelins target human 5-lipoxygenase XLIV

M-IV: Melleolides induce rapid cell death in human primary monocytes and cancer cells XLVIII

M-V: Rapid cell death induction by the honey mushroom mycotoxin dehydroarmillylorsellinate through covalent reaction with membrane phosphatidylethanolamines LIV

APPENDIX 3: AUTHORS´ CONTRIBUTIONS TO THE MANUSCRIPTS LXXXVIII

APPENDIX 3: ACKNOWLEGDMENTS XCIII

APPENDIX 4: PUBLICATIONS AND CONFERENCE CONTRIBUTIONS XCVI

A3.1 Publications XCVI

A3.2 Conference contributions XCVIII

A3.2.1 Oral presentations XCVIII

A3.2.2 Poster presentations XCVIII

APPENDIX 5: CURRICULUM VITAE XCIX

APPENDIX 6: EIGENSTÄNDIGKEITSERKLÄRUNG C

ABBREVIATIONS

AA	arachidonic acid
AMPK	5´adenosine monophosphate-activated protein kinase
AP-1	activator protein 1
Apaf-1	apoptotic protease-activating factor-1
Atg5	autophagy protein 5
ATP	adenosine triphosphate
Bak	Bcl-2 homologous antagonist/killer
Bax	Bcl-2-associated X protein
Bcl-2	B-cell lymphoma 2
Bid	BH3 interacting-domain death agonist
COPD	chronic obstructive pulmonary disease
COX	cyclooxygenase
$cPLA_2$	cytosolic phospholipase A_2
CYP	cytochrome P
cysLT	cysteinyl leukotrienes
DAMP	danger associated molecular patterns
DAO	dehydroarmillylorsellinate
DISC	death initiation signaling complex
DNA	deoxyribonucleic acid
EA	ethanolamine
EET	epoxyeicosatrienoic acid
e.g.	for example (lat. exempli gratia)
ER	endoplasmic reticulum
e(t)-LTB_4	LTB_4 isomers: 6-trans-LTB_4, 6-trans-12-epi-LTB_4
FLAP	5-lipoxygenase activating protein
fMLP	N-formyl-methionyl-leucyl-phenylalanine
Golgi	Golgi apparatus
GPCR	G-protein coupled receptor
GSH	glutathione
HEK	human embryonic kidney cell line
H(p)ETE	hydroxy(peroxy)eicosatetraenoic acid
IA	invasive aspergillosis
IC_{50}	half maximal inhibitory concentration

IL	interleukin
JNK	c-Jun N-terminal kinase
LDH	lactate dehydrogenase
LM	lipid mediators
LOX	lipoxygenase
LPS	lipopolysaccharide
LT	leukotriene(s)
LTA_4H	leukotriene A_4 hydrolase
LTC_4S	leukotriene C_4 synthase
MAPEG	membrane-associated proteins in eicosanoid and GSH metabolism
MAPK	mitogen-activated protein kinase
MCP-1	monocyte chemoattractant protein 1
mPGES-1	microsomal prostaglandin E synthase 1
mRNA	messenger RNA
mTOR	mammalian target of rapamycin
MTT	3-(4,5-dimethylthiazol-2-yl)-2,5-diphenyltetrazolium bromide
NFκB	nuclear factor “kappa-light-chain-enhancer” of activated B-cells
NO	nitric oxide
PAF	platelet activating factor
PAMP	pathogen-associated molecular patterns
PARP	poly(ADP-ribose)-polymerase 1
PC	phosphatidylcholine
PE	phosphatidylethanolamine
PGP	proline-glycine-proline (tripeptide)
PK	protein kinase
PMA	phorbol-12 myristate 13-acetate
PMNL	polymorph nuclear leukocytes
PS	phosphatidylserine
RNA	ribonucleic acid
ROS	reactive oxygen species
sEH	soluble epoxide hydrolase
TLR	Toll-like receptor
TNF(R)	tumor necrosis factor (receptor)
UPLC-MS/MS	ultra performance liquid chromatography tandem mass spectrometry

SUMMARY

In the present thesis, the mode of action of three different natural secondary metabolites was clarified in human cancer cells and primary immune cells. The investigated compounds of this work were (I) the mycotoxin gliotoxin from *Aspergillus fumigatus* targeting leukotriene A_4 hydrolase (LTA_4H), identifying thereby the cause of neutropenia during invasive aspergillosis (IA), (II) the melleolide dehydroarmillylorsellinate (DAO) and several structural analogs exhibiting, on the one hand, anti-inflammatory features by abrogating 5-lipoxygenase (5-LOX) product formation, and on the other hand, manipulate monocyte functions by covalent binding of the cellular membrane constituent phosphatidylethanolamine (PE), and finally (III), the myxobacterial compound myxochelin A hampering 5-LOX activity by iron chelation. Over the last decades, the link between inflammation and cancer gains relevance. Hence, it is important to investigate new anti-inflammatory drugs to prevent chronic diseases, and to elucidate the mechanism of action of cytotoxic compounds to develop new strategies of action for anti-cancer drugs. Both approaches are the basis of this work.

Gliotoxin is known as important virulence factor of *A. fumigatus* [1] causing IA by affecting neutrophils [2, 3], but the underlying molecular mechanism is still elusive. Our data revealed that gliotoxin inhibits the biosynthesis of the important neutrophil chemoattractant leukotriene B_4 (LTB_4) [4, 5] *in vivo* using the zymosan-induced peritonitis model in mice and the carrageenan-induced pleurisy model in rats. Furthermore, gliotoxin caused a reduced neutrophil infiltration into the peritoneal or thoracic cavity. Interestingly, gliotoxin suppressed solely LTB_4 formation without compromising other eicosanoids. The well-known 5-LOX inhibitor zileuton [6] was deployed as reference drug reducing all 5-LOX products. Similar results were reached *in vitro* in human primary monocytes and neutrophils in comparison to zileuton and the selective LTA_4H inhibitor SC-57461A [7, 8]. In addition, we confirmed gliotoxin as virulence factor of *A. fumigatus* by using an *A. fumigatus* strain containing a deletion of the gliP gene, which is responsible for gliotoxin biosynthesis (Δ*gliP*) [9]. Supernatants of this strain failed to inhibit LTB_4 production in neutrophils, and in line with this finding, histopathological investigations confirmed our hypothesis. Leukotrienes (LT) are formed by 5-LOX, which convert arachidonic acid (AA) in a two-step reaction to LTA_4 followed by a hydrolysis to LTB_4 performed by LTA_4H [10]. Interestingly, gliotoxin failed to impede LTA_4H activity in non-cellular systems but pre-incubation with GSH enables inhibition of LTA_4H activity by gliotoxin indicating that reducing conditions were crucial to cleave the intramolecular disulfide bond. The formed free thiol groups chelated the zinc ion in the active epoxide hydrolase center of the bifunctional enzyme [11] causing covalent and irreversible inhibition of LTA_4H. Beside epoxide hydrolase activity, LTA_4H exhibits also an aminopeptidase function involved in the resolution of inflammation by hydrolysis and inactivation of the tripeptide matrikine proline-glycine-proline (PGP) [12, 13]. We measured the enzymatic degradation of PGP in gliotoxin-treated

neutrophils by UPLC-MS/MS resulting in an exclusively abrogation of the epoxide hydrolase activity by gliotoxin. Additional, we excluded an inhibition of other bifunctional enzymes containing an epoxide hydrolase activity by investigating sEH activity [14] after treatment with gliotoxin.

In contrast to gliotoxin, we identified myxochelin A biosynthesized by *Pyxidicoccus fallax* as direct 5-LOX inhibitor in cell-free assays (IC_{50}=1.9 µM ± 0.2 µM), correlating with its anti-proliferative effects in leukemic cells. As expected, the catechol basic structure was crucial for hampering LT biosynthesis, whereas methylation of aromatic hydroxyl residues caused detrimental effects on 5-LOX inhibition. Structure-activity relationships formed a basis for further investigations and structural modifications.

Besides myxochelins, also DAO act as direct and irreversible 5-LOX inhibitor in cellular (IC_{50}=0.3 µM ± 0.1 µM) and non-cellular (IC_{50}=2.8 µM ± 0.9 µM) experimental settings. Furthermore, DAO hampered the interaction between 5-LOX and its helper protein 5-LOX activating protein (FLAP) determined by a proximity ligation assay, and DAO inhibited solely the 5-LOX pathway without targeting other enzymes of the AA cascade. Screening of various melleolides for 5-LOX inhibition provided detailed information on the underlying structure-activity relationships. Especially the α,β-unsaturated aldehyde turned out to be crucial for potent 5-LOX inhibition. This structural element is also known as Michael acceptor. Compounds containing a Michael acceptor structure showed interactions with cysteines located at the entrance to the catalytic center of 5-LOX [15, 16]. Using stable transfected HEK cells with 5-LOX cysteine mutants, we showed that cysteines are catalytically relevant causing reduced 5-LOX activity and mediated diminished product formation. 5-LOX translocation was not affected by DAO, but the interaction with FLAP at the nuclear membrane was hampered, especially by the 5-LOX_C^{159} mutant. Interestingly, DAO interacted with C^{159} triggering abrogated 5-LOX/FLAP interaction and impaired 5-LOX activity resulting in reduced LT formation.

Besides its anti-inflammatory effects, DAO displayed remarkable cytotoxic properties towards human primary monocytes and cancer cells. DAO induced cell death in an unusual rapid onset, characterized by apoptotic and necrotic features. The apoptosis marker PARP was cleaved within 15 min with preceding a slight activation of caspases, whereas the potent cytotoxic compound staurosporine [17, 18] triggered PARP cleavage only after 5 hrs. Furthermore, DAO affected also the membrane integrity after 15 min measured by an LDH assay indicating an untypical mode of action for its cytotoxicity. We clarified the cytotoxic mode of action of DAO, which is seemingly due to a covalent binding of its α,β-unsaturated aldehyde group to the ethanolamine residue of membrane PE by UPLC-MS/MS. Furthermore, we excluded an effect on serine or choline residues of other phospholipids. With the help of subcellular fractionation, we identified that DAO interacted primarily with plasma and lysosomal

membrane parts of cells causing an abrogation of PE in the membrane fraction. Hence, destabilization of lysosomes and the related decreased intracellular pH might be induced by a DAO-PE interaction on lysosomal membranes mediating necrotic features of cell death.

In conclusion, the results of this thesis clarified the mode of action and targets of two fungal toxins and of the myxobacterial compound myxochelin A in human cells. Inhibition of LTA_4H activity in case of gliotoxin seems to be the reason for neutropenia during IA, providing the basis for new therapeutic approaches of this disorder. Myxochelin A and its derivatives represent an interesting substance class for new 5-LOX inhibitors, but further investigations are essential, e.g., the *in vivo* confirmation of the anti-inflammatory efficiency. Finally, the melleolide DAO influences 5-LOX activity, but it exhibits also potent cytotoxic activity in human cells due to its unusual rapid onset of cell death induction by covalent binding to membrane PE.

ZUSAMMENFASSUNG

In der vorliegenden Arbeit wurde der Wirkmechanismus von drei verschiedenen natürlich vorkommenden Sekundärmetaboliten in Krebszellen und primären Immunzellen aufgeklärt. Die untersuchten Substanzen sind (I) Gliotoxin aus *Aspergillus fumigatus*, welches mit LTA_4H interagiert und damit ein potentieller Auslöser für die Neutropenie während einer IA festgestellt werden konnte, (II) das Melleolid DAO und verwandte Strukturanaloga, welche aufgrund einer 5-LOX-Hemmung anti-inflammatorische Eigenschaften besitzen, aber auch kovalent an das Membranlipid PE binden und damit wichtige monozytäre Funktionen manipulieren, und zu guter Letzt (III) Myxochelin A aus Myxobakterien, welches die 5-LOX Aktivität durch eine Chelatisierung des zentralen Eisen-Atoms beeinflusst. Innerhalb der letzten Jahrzehnte verfestigte sich der bestehende Zusammenhang zwischen Entzündung und Krebsgeschehen. Deshalb ist es von großer Bedeutung neue Wirkstoffe zu identifizieren und weiterzuentwickeln, die eine chronische Entzündung verhindern und Wirkmechanismen zytotoxischer Substanzen zu untersuchen, um neue Ansatzpunkte für die Krebsmedikation finden zu können. Beide Aspekte werden mit dieser Arbeit angesprochen und behandelt.

Gliotoxin ist bekannt als bedeutender Virulenzfaktor von *A. fumigatus* [1], der durch gezielte Beeinflussung von Neutrophilen eine IA auslöst [2, 3]. Unsere Untersuchungen ergaben, dass Gliotoxin die Biosynthese von LTB_4, welches ein wichtiger Signalstoff für die Chemotaxis von Neutrophilen ist [4, 5], *in vivo* und *in vitro* hemmt. LTB_4 entsteht durch die von LTA_4H ausgelöste Hydrolyse aus LTA_4, welches durch 5-LOX aus Arachidonsäure (AA) gebildet wird [10]. Für die Untersuchungen *in vivo* nutzten wir zwei Entzündungsmodelle: (1) eine durch Zymosan ausgelöste Bauchfellentzündung (Peritonitis) in Mäusen und (2) eine durch Carrageen ausgelöste Brustfellentzündung (Pleuritis) in Ratten. In den Tiermodellen reduzierte Gliotoxin die Einwanderung von Neutrophilen in die spezifischen Gewebe und hemmte selektiv die LTA_4H. Als Kontrollsubstanz diente der klinisch relevante 5-LOX Inhibitor Zileuton [6]. Diese Ergebnisse konnten ebenso *in vitro* in primären Monozyten und Neutrophilen im Vergleich zu Zileuton und dem LTA_4H Inhibitor SC-57461A [7, 8] nachgewiesen werden. Zusätzlich wurde die Bedeutung von Gliotoxin als Virulenzfaktor mit Hilfe eines *A. fumigatus* Stammes, bei dem das verantwortliche Enzym gliP für die Gliotoxin Biosynthese eliminiert worden ist (Δ*gliP*) [9], bestätigt. Kulturüberstände dieses Stammes zeigten keine Reduktion von LTB_4 in behandelten Neutrophilen. Interessanterweise konnte eine Aktivität von Gliotoxin nur intrazellulär nachgewiesen werden, da ein reduzierendes Milieu notwendig ist, um die intramolekulare Disulfidbrücke zu spalten. Die entstehenden freien Thiolgruppen bilden einen Chelatkomplex mit dem zentralen Zink-Ion in der Epoxidhydrolase Bindungstasche [11], was eine kovalente und irreversible Hemmung der LTA_4H bewirkt. LTA_4H ist ein bifunktionales Enzym, welches neben der Epoxidhydrolaseaktivität noch eine Aminopeptidaseaktivität aufweist [12, 13]. Diese ist an der Resolution einer Entzündung durch die Hydrolyse und

Inaktivierung des Matrikins PGP beteiligt. Mittels UPLC-MS/MS konnten wir nachweisen, dass Gliotoxin die Degradation von PGP und damit die Aminopeptidaseaktivität nicht beeinflusst. Des Weiteren wurde eine Beeinflussung anderer bifunktionaler Enzyme wie die sEH, welche ebenso eine Epoxidhydrolase Aktivität besitzt [14], ausgeschlossen.

Im Gegensatz zu Gliotoxin, identifizierten wir Myxochelin A, welches von dem Myxobakterium *Pyxidicoccus fallax* gebildet wird, als direkten 5-LOX Inhibitor (IC_{50}=1,9 ± 0,2 µM) aufgrund einer Komplexierung des zentralen Eisenions [19] im zellfreien Milieu, was mit seinen anti-proliferativen Eigenschaften in Leukämie-Zellen korreliert. Wie zu erwarten war, ist die Catechol-Grundstruktur verantwortlich für die verringerte LT-Bildung, da O-Methylierungen zu einem gravierenden Wirkungsverlust führen. Struktur-Wirkungsbeziehungen bilden die Grundlage für Strukturmodifikationen und weitere Untersuchungen.

Des Weiteren hemmt das Melleolid DAO selektiv die 5-LOX Aktivität und verhindert damit auch die Biosynthese pro-inflammatorischer LT. DAO ist ein direkter und irreversibler 5-LOX Inhibitor unter zellulären (IC_{50}=0,3 µM ± 0,1 µM) oder zellfreien (IC_{50}=2,8 µM ± 0,9 µM) Bedingungen. DAO verhindert die Interaktion zwischen 5-LOX und dem Helferprotein FLAP an der nukleären Membran, was wir mittels eines Proximity Ligation Assays analysiert haben. Neben DAO untersuchten wir auch andere Melleolide auf eine potentielle 5-LOX-Hemmung, um Informationen über Struktur-Wirkungsbeziehungen zu erhalten. Dabei ergab sich, dass das α,β-ungesättigte Aldehyd essentiell für die Interaktion mit 5-LOX ist. Dieses Strukturelement kann auch als Michael-Akzeptor bezeichnet werden und interagiert unter anderem mit Cysteinen, welche am Eingang zum katalytischen Zentrum der 5-LOX angeordnet sind [15, 16]. Wir nutzten stabil transfizierte HEK Zellen mit verschiedenen 5-LOX Cysteinmutanten und bestätigten aufgrund einer verminderten 5-LOX-Produktbildung, dass diese Cysteine katalytisch relevant für die LT-Biosynthese sind. Interessanterweise beeinflussten die Cysteinmutanten nicht die 5-LOX-Translokation, sondern die Interaktion mit FLAP, welche vorrangig über C^{159} gesteuert wird. DAO interagierte mit C^{159} und verursachte damit die gestörte 5-LOX/FLAP Interaktion, was eine verringerte 5-LOX Aktivität zur Folge hatte.

Neben seinen anti-inflammatorischen Eigenschaften weist DAO auch zytotoxische Charakteristika in humanen Monozyten und Krebszellen auf. DAO induzierte untypisch schnell den Zelltod, welcher sowohl apoptotische als auch nekrotische Merkmale aufweist. So aktiviert DAO den Apoptosemarker PARP innerhalb von 15 min, wofür Staurosporin, ein bekannter Apoptose auslösender Pan-Kinase Inhibitor [17, 18], mindestens 5 h benötigt. Des Weiteren schädigt DAO auch innerhalb von 15 min die Membranintegrität von Zellen, was wir mittels LDH Assay nachweisen konnten. Diese Aspekte lassen einen eher untypischen Wirkmechanismus für die Zytotoxizität vermuten. Wir zeigten, dass die α,β-ungesättigte Aldehydgruppe von DAO kovalent an die Ethanolamin-Kopfgruppe von membranständigen

Phospholipiden bindet, während Phosphatidylcholin und –serin nicht betroffen waren. Aufgrund einer durchgeführten subzellulären Fraktionierung stellten wir fest, dass DAO vorrangig mit PE aus der Plasmamembran/Lysosomen-Fraktion interagierte, welches die Reduktion des PE-Gehaltes in diesen Fraktionen erklärte. Gleichzeitig könnten damit die zu beobachtende Degradierung von Lysosomen und der sinkende intrazelluläre pH-Wert erklärt werden.

Zusammenfassend identifizierten wir den Wirkmechanismus und die Zielstrukturen der beiden Pilzgifte Gliotoxin und DAO und der myxobakteriellen Substanz Myxochelin A. Gliotoxin hemmt die LTA_4H Aktivität, was die Neutropenie während einer IA verursacht. Myxochelin A und Strukturanaloga stellen eine vielversprechende Substanzklasse für neue 5-LOX Inhibitoren dar, wofür allerdings weitere Untersuchungen wie zum Beispiel die Bestätigung der Wirksamkeit *in vivo* notwendig sind. DAO hemmt ebenfalls die 5-LOX-Aktivität und weist ein interessantes Wirkprofil nicht zuletzt wegen seiner untypisch schnellen zytotoxischen Wirkung durch die kovalente Bindung von PE an humanen Zellmembranen auf.

1. INTRODUCTION

1.1 Inflammatory response and cancer

Acute inflammation is a self-limiting innate immune response to internal or external harmful stimuli aiming to restore the homeostatic balance and to protect the organism against infection or any tissue damage. Inflammation is characterized by five major symptoms: (I) redness, (II) swelling, (III) pain, (IV) heating, and (V) loss of function. Classical initiators of acute inflammation are tissue injury or infection by pathogens [20]. During acute inflammation, various pro-inflammatory mediators, e.g., cytokines, chemokines, and eicosanoids are released by macrophages or mast cells initiating the recruitment of leukocytes and plasma proteins to the site of infection or injury. Due to the direct contact with pathogens or pro-inflammatory mediators, neutrophils are activated leading in a release of detoxifying agents, e.g., reactive oxygen species (ROS), to eliminate infectious agents. In a second step, monocytes and macrophages access the inflammatory site, where alternatively activated macrophages promote the resolution phase of inflammation [20, 21]. Thus, the recruitment of neutrophils is interrupted, and an alteration in lipid mediator (LM) biosynthesis occurs from pro-inflammatory prostaglandins and leukotrienes (LT) to anti-inflammatory lipoxins, protectins, maresins, and resolvins, mainly produced by macrophages [22, 23]. Macrophages initiate tissue repair and phagocytosis of apoptotic neutrophils and other dead cells. In the case that the acute inflammatory response fails to remedy the infection or injury, inflammation becomes chronic [20, 21]. Dysregulated inflammation leads to a homeostatic imbalance and can promote several diseases, e.g., rheumatoid arthritis, cardiovascular diseases, and ultimately also cancer. Several pro-inflammatory mediators and enzymes, e.g., cytokines, chemokines, matrix metalloproteinases, vascular endothelial growth factors, cyclooxygenase-2 (COX-2), and 5-lipoxygenase (5-LOX) are involved in inflammation but play also an important role in tumorigenesis as part of a pro-tumorigenic tissue microenvironment [24, 25]. This tumor microenvironment arises during persistent inflammatory states surrounding tumor cells and triggering tumor growth via the above-mentioned released mediators of infiltrating immune cells. Beside innate immune cells and cancer cells, the microenvironment consists of adaptive immune cells and surrounding stroma containing blood vessels, fibroblasts, and extracellular matrix [26-28]. Furthermore, two transcription factors are mainly involved in (inflammation-triggered) tumor development: (I) signal transducer and activator of transcription 3 (STAT3) inducible by interleukin (IL)-6, and (II) nuclear factor κ B (NFκB). NFκB is responsible for pro-inflammatory, proliferative, and pro-survival gene expression leading to suppression of apoptosis and support of cell cycle progression in cancer cells [29-31]. As mentioned before, neutrophils release ROS, inter alia, to eliminate injuring agents, but excessive formation of ROS can also initiate tumorigenesis by subsequent DNA damage. Considering, that 20% of cancers are associated with chronic inflammation [32], and that the tumorigenesis process is

biased by inflammation, it is concluded that inflammation is one key regulator of tumor development through various pathophysiological processes.

1.1.1 Arachidonic acid pathway

Arachidonic acid (AA) is a notable polyunsaturated fatty acid (20:4 ω-6) in mammalian cells. Due to its esterification within membrane phospholipids, AA is a marked component of human cellular membranes and affects membrane fluidity and flexibility [33, 34]. Furthermore, as essential precursor of pro- and anti-inflammatory bioactive LM, AA plays an important biochemical role in the initiation and resolution of inflammation [34, 35]. Three various types of oxygenases convert AA to bioactive LM in mammals: (I) cyclooxygenases (COX), (II) lipoxygenases (LOX), and cytochrome P450 (CYP450) enzymes. Initially, AA can be released from cellular membranes by the cytosolic phospholipase A_2 ($cPLA_2$) [4]. Free AA may then be metabolized by COX-1 or COX-2 to pro-inflammatory prostanoids, that encompass prostaglandins and thromboxanes, which are crucial mediators of inflammation [36]. But also LOX, including 5-LOX, 8-LOX, 12-LOX, and 15-LOX, generate pro-inflammatory LT and anti-inflammatory lipoxins from AA [4, 37, 38], and CYP450 isoenzymes form epoxyeicosatrienoic acid (EET) [39]. In the last decades, many chemically synthesized or natural compounds have been investigated, that interfere with the AA pathway and possess a promising potential as anti-inflammatory drugs, but only a few compounds reached the pharmaceutical market until now [40-42].

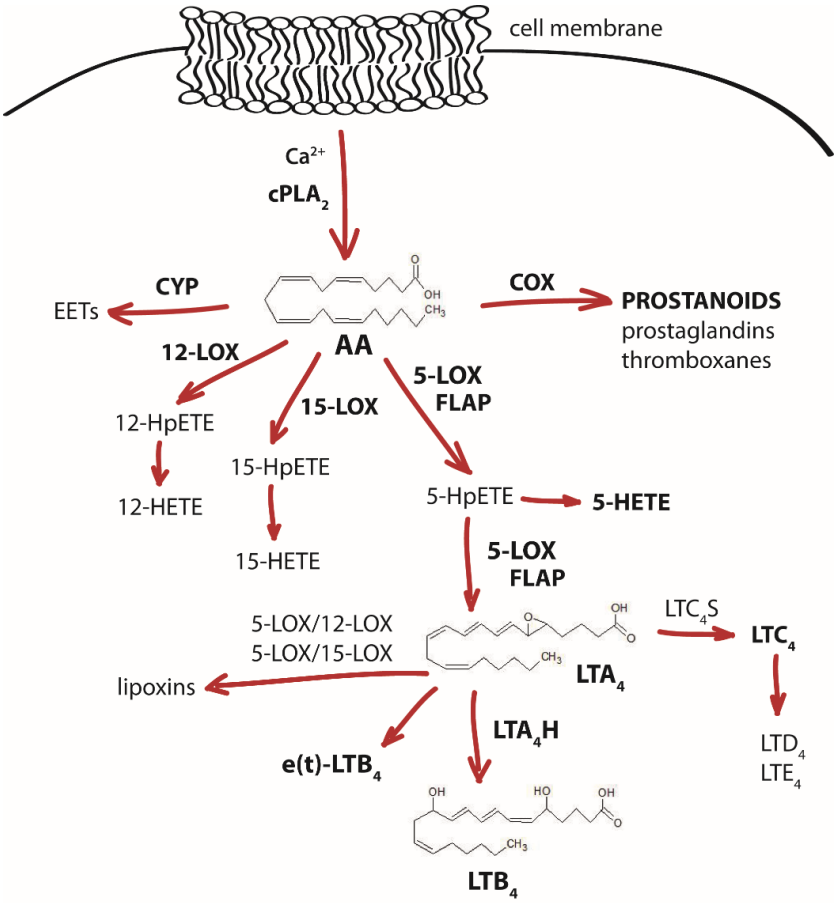

Fig. 1 The arachidonic acid pathway.

AA – arachidonic acid, $cPLA_2$ – cytosolic phospholipase A_2, COX – cyclooxygenase, EET – epoxyeicosatrienoic acid, FLAP – 5-lipoxygenase activating protein, LOX – lipoxygenase, LT – leukotriene, LTA_4H – leukotriene A_4 hydrolase, LTC_4S – leukotriene C_4 synthase

1.1.1.1 5-Lipoxygenase and its helper protein FLAP

5-LOX is one of the six known LOX in humans and was first discovered in the year 1976 [43-45]. 5-LOX is a soluble, 78 kDa protein expressed in the cytosol or inside the nucleoplasm of leukocytes (neutrophils, eosinophils, monocytes/macrophages, dendritic cells, mast cells, and B-lymphocytes) [46]. Mammalian 5-LOX exhibits a monomeric structure with 672 or 673 amino acids possessing two different functional domains: (I) an N-terminal C2-like domain (residues 1-112), and (II) an α-helical C-terminal domain (residues 126-673) [19, 47]. The regulatory C2-like domain consists of β-sheets and is responsible for Ca^{2+}, membrane, and coactosin-like protein (CLP) binding. In contrast, the C-terminal domain represents the catalytic center of 5-LOX with a non-hem iron [19]. This non-hem iron functions during the 5-LOX reaction mechanism as electron acceptor or donor forming a redox cycle between the inactive ferrous (Fe^{2+}) and the active ferric (Fe^{3+}) form promoted by lipid hydroxyperoxides [48]. Three conserved histidines (His^{367}, His^{372}, His^{550}) and the carboxylate of the C-terminal Ile^{673} coordinate the iron [10, 19]. The crystal structure reveals additionally a unique variation of small helix α2 in the catalytic domain controlling the entrance to the iron like a mobile lid [49], and the side chain of Phe^{177} and Tyr^{181} seals access to the catalytic domain, thereby called “FY cork” [19]. Usually, 5-LOX is described as monomeric protein, but also a homodimer formation of two monomers is reported [50, 51]. Dimer formation is caused by four cysteines (C^{159}, C^{300}, C^{416}, C^{418}) located at the region around the entrance to the catalytic center generating disulfide bonds by cross linking among each other [50, 51]. As monomer, 5-LOX exhibits an increased enzyme activity but after dimerization, the catalytic activity is reduced [51]. The C2- and the catalytic domain interact by a salt bridge between Arg^{101} of the β-sandwich and Asp^{166} located at the catalytic domain [49].

FLAP

The 5-LOX activating protein (FLAP) is an 18 kDa integral membrane protein embedded in the inner and outer leaflet of nuclear and endoplasmic membranes. FLAP belongs to the membrane-associated proteins in eicosanoid and glutathione metabolism (MAPEG) family and shows contrarily to other MAPEG family members no catalytic activity or GSH binding site [52, 53]. FLAP was firstly discovered in the late 1980s as target of MK-886 that was found to inhibit LT biosynthesis devoid of targeting other enzymes of the AA cascade [54, 55]. In 2007, the crystal structure of FLAP in complex with the inhibitor MK-591 was determined [56]. This study demonstrated by X-ray crystallography a formed homotrimer anchored in the nuclear membrane, whereby each monomer consists of four transmembrane helices linked by two cytosolic and one luminal loop [56]. During LT biosynthesis, FLAP interacts as 5-LOX helper protein to transfer AA to 5-LOX by a so far unknown mechanism [57] and thus stimulating conversion of exogenous AA to 5-HpETE and additionally triggering dehydration of AA to LTA_4

[58]. However, FLAP inhibitors are able to efficiently block LT biosynthesis gaining an interesting drug development field against inflammatory diseases [59].

Activation of 5-LOX and leukotriene formation

Activation of 5-LOX can be mediated by cell stress or various external stimuli. Cell stress as a Ca^{2+}-independent mechanism is caused by heat shock, osmotic stress, oxidative, or genotoxic agents [60]. These factors initiate activation of mitogen-activated protein kinases (MAPK) followed by phosphorylation of 5-LOX on several serine residues with divergent impacts [61]. External stimuli like N-formyl-methionyl-leucyl-phenylalanine in combination with lipopolysaccharide (fMLP/LPS), ionophores [62], platelet activating factor (PAF), thapsigargin [63], C5a, LTB_4, and cytokines increase the intracellular Ca^{2+} concentration, and thus, 5-LOX and $cPLA_2$ are activated [46]. $cPLA_2$ translocates together with 5-LOX to the nuclear membrane and liberates, among other things, AA from arachidonyl-phosphatidylcholine. Accordingly, FLAP transfers AA to the membrane-associated 5-LOX for LT biosynthesis [64]. 5-LOX generates pro-inflammatory LT in a two-step reaction: (I) oxygenation of AA to 5(S)-hydroxyperoxy-6-*trans*-8,11,14-*cis*-eicosatetranoic acid (5-HpETE), and (II) dehydration to the instable epoxide 5(*S*)-*trans*-5,6-oxido-7,9-*trans*-11,14-*cis*-eicosatetraenoic acid (LTA_4) [37, 65]. Alternatively, 5-HpETE can be reduced by glutathione peroxidases to 5(*S*)-hydroxy-6-*trans*-8,11,14-*cis*-eicosatetraenoic (5-HETE) [66]. The instable LTA_4 can be stereospecific hydrolyzed by LTA_4 hydrolase (LTA_4H) to the important chemoattractant 5(*S*),12(*R*)-dihydroxy-6,14-*cis*-8,10-*trans*-eicosatetraenoid acid (LTB_4). Additional, LTA_4 degrades non-enzymatically into two inactive isomers (6-*trans*-LTB_4, and 6-*trans*-12-epi-LTB_4) [67]. Alternatively, LTA_4 is transformed by LTC_4 synthase (LTC_4S) conjugating a glutathione (GSH) residue at the epoxide moiety to 5(*S*)-hydroxy-6(*R*)-S-glutathionyl-7,9-*trans*-11,14-*cis*-eicosatetraenoic acid (LTC_4) in monocytes, macrophages, dendritic cells, and mast cells [68, 69]. Several enzymes can metabolize LTC_4 to 5(*S*)-hydroxy-6(*R*)-S-cysteinylglycyl-7,9-*trans*-11,14-*cis*-eicosatetraenoic acid (LTD_4) and 5(*S*)-hydroxy-6(*R*)-cysteinyl-7,9-*trans*-11,14-*cis*-eicosatetraenoic acid (LTE_4), which can be summarized together with LTC_4 to cysteinyl-LT (cysLT).

5-LOX inhibitors

LT play an important role in acute and chronic inflammatory diseases and promote also the development and progression of cancer [37, 41, 65]. Different strategies are conceivable to interfere with LT: direct inhibition of enzymes involved in the AA pathway like $cPLA_2$, 5-LOX, FLAP, LTA_4H, LTC_4S or antagonists of LT receptors like the compound montelukast [70]. Besides $cPLA_2$, direct inhibition of 5-LOX is a common strategy to suppress a diversity of eicosanoids especially AA-derived LM. Direct 5-LOX inhibitors can be subdivided, based on their therapeutic mode of action, in four different inhibitor types: (I) redox active compounds

(e.g., natural compounds like coumarins, or flavonoids [71]) influencing mainly the 5-LOX redox cycle by reducing the active site iron (Fe^{3+}) to its inactive ferrous (Fe^{2+}) state, thereby, interrupting the catalytic reaction of 5-LOX [40, 41], (II) iron-chelating compounds characterized by hydroxamic acid (e.g., BWA4C [72]), or N-hydroxyurea residues (e.g., zileuton [6]) that cause reduced 5-LOX activity by chelating the active site iron, (III) non-redox active agents (e.g., embelin, and its derivatives [73, 74], ZD2138 [75], L-739,010 [76]), which are independent of redox characteristics competing with AA or lipid hydroxyperoxides for the binding to 5-LOX [40, 41], and (IV) novel inhibitors with unknown modes of action. These inhibitors of the latter group show interactions with different binding sites of the C2-like domain like hyperforin with the PC binding site [77, 78], or indirubin derivatives with the ATP binding site [79]. Furthermore, Michael acceptor-containing agents (e.g., thymoquinone, nitro fatty acids, U73122) are considered as additional new class of 5-LOX inhibitors by interacting with surface cysteines (C^{159}, C^{300}, C^{416}, C^{418}) at the dimerization interface of the catalytic center of 5-LOX [16].

1.1.1.2 Leukotriene A_4 hydrolase and leukotrienes

LTA_4H, a soluble 69 kDa protein, is widely expressed in mammalian cells preferable in neutrophils but negligibly in eosinophils. The enzyme is localized in the cytosol or in the extracellular space [47, 80], but nuclear distribution has also been observed [81]. Additionally, LTA_4H is a monomeric Zn^{2+} metalloenzyme that exhibits two distinct enzymatic activities: (I) an epoxide hydrolase activity that metabolizes LTA_4 to the pro-inflammatory chemoattractant LTB_4 predominantly in the cytosol, and (II) during the resolution state of inflammation an aminopeptidase activity that hydrolyzes and thus inactivates the pro-inflammatory tripeptide proline-glycine-proline (PGP) mainly in the extracellular space [12, 13, 82]. The aminopeptidase and epoxide hydrolase activities are exerted via distinct but overlapping active sites [82]. Interestingly, LTA_4H can be inhibited by its own substrate LTA_4 through a suicide inactivation mechanism interacting with Tyr^{378} within the active site [80, 83]. The crystal structure discloses three different domains: (I) an N-terminal domain (residues 1-207), (II) a Zn^{2+} containing catalytic domain (residues 461-450), and (III) an α-helical C-terminal domain (residues 461-610). The active site is situated between all three domains, and the catalytic Zn^{2+} ion is coordinated by two histidines (His^{295}, His^{299}), and Glu^{318} [84]. Close to the Zn^{2+}, the residue Glu^{271} is shared between the two catalytic pockets and is responsible for both enzyme activities [85]. The binding site for LTA_4 appears to be localized in the L-shaped hydrophobic pocket and contains the catalytic Zn^{2+} and Arg^{563} playing important roles for the epoxide hydrolase as well as the aminopeptidase activity [13, 86]. A mutation of Asp^{375} supported a crucial role of this residue for hydrolyzing LTA_4 into LTB_4 [87], and in contrast, mutations of the residues Glu^{296} and Tyr^{383} show a selective elimination of the aminopeptidase activity [88]. Besides LTA_4, the tripeptide PGP is a physiological substrate of LTA_4H [89] and exhibits similar

to LTB_4 chemoattractant properties for neutrophils [90, 91]. PGP belongs to the family of matrikines and is generated from extracellular matrix collagen by metalloproteinases and prolylenpeptidases [92]. Normally, PGP is degraded by the aminopeptidase activity of LTA_4H. If LTA_4H is blocked, the enzyme fails to decompose PGP, and thus, PGP accumulates and induces neutrophil infiltration especially in the lung [12, 93]. For this reason, PGP plays an important role in pathology and development of chronic lung diseases and is used as biomarker for chronic obstructive pulmonary disease (COPD) [94].

LTA_4H inhibitors

LTA_4H constitutes an attractive therapeutic target for the treatment of chronic inflammatory diseases, e.g., respiratory disease [89], inflammatory bowel diseases [95], or cancer [96], due to its high importance in the biosynthesis of inflammatory mediators. Until now, a variety of LTA_4H inhibitors were discovered and developed, but most potent selective inhibitors failed in clinical trials due to their minimal efficacy [97]. Furthermore, the problem of most identified inhibitors is to block also the aminopeptidase activity, which plays a crucial role in the resolution of inflammation by degradation of the tripeptide PGP, beside hampering the epoxide hydrolase activity [98], e.g., JNJ-40929837 [99], SC-57461A [7, 8, 100], or SC-22716 [101]. Interestingly, inhibitors of other Zn^{2+} metalloproteinases, for example, bestatin [102], captopril [103], or kelatorphan [11], affect additionally both LTA_4H activities by chelating the central Zn^{2+} ion. According to the importance of the PGP-degrading activity of LTA_4H [12, 89], the novel route in drug design is to create new LTA_4H inhibitors with a selective blockade of epoxide hydrolase activity without affecting the aminopeptidase activity [104, 105]. Recently, two selective epoxide hydrolase inhibitors were developed, 4-methoxydipehnylmethane (4-MDM) [106], and 4-(4-benzylphenyl)thiazol-2-amine (ARM-1) [107]. These two compound classes are used to design analogues with an improved potency for clinical trials and an unaffected selectivity for inhibition of LTB_4 biosynthesis [104, 105].

Leukotrienes

LT are bioactive LM involved in the innate and adaptive immune response and play physiological and pathological roles in inflammation and in several diseases like asthma bronchiale, psoriasis, rheumatoid arthritis, cardiovascular diseases, allergy, and cancer. They are produced by pro-inflammatory cells, mainly by leukocytes, through the AA/5-LOX pathway, released from the cells by ATP-dependent efflux pumps and deliver their biological activity via specific G-protein coupled receptors (GPCR). LT can be divided into two classes: (I) the chemoattractant LTB_4, and (II) the multi-functional cysLT.

LTB_4 is one of the most potent chemoattractants for neutrophils [4, 5] and plays an important role for the immune defense. LTB_4 triggers the recruitment of immune cells like granulocytes, monocytes, macrophages, and T-cells into inflammatory tissue, their adherence

to the endothelium, and their activation [108]. Additional, LTB_4 promotes the activation of phagocytosis of neutrophils and macrophages and triggers the generation of cytokines (IL1, IL2, IL6), and chemokines (MCP-1) in macrophages [108, 109]. These effects confirm the relevance of LTB_4 in host defense against infections and pathologies of acute and chronic diseases like atherosclerosis [110], rheumatoid arthritis [111, 112], and cancer [4, 113]. LTB_4 mediates its effects by two GPCRs: (I) BLT_1, and (II) BLT_2. The expression of BLT_1 is confined to leukocytes and represents a high affinity receptor. In contrast, the BLT_2 receptor is ubiquitously expressed with low affinity for LTB_4. A participation of BLT_2 for host defense was reported, but the physiological role is poorly understood [114, 115].

Biological effects of cysLT were first discovered in the year 1938 without any knowledge about chemical features and their mode of action [116]. As described before, cysLT are GSH-conjugated LT including LTC_4, LTD_4, and LTE_4 known as slow acting substances of anaphylaxis but also as powerful smooth muscle contracting agents [116, 117] primarily in eosinophils, basophiles, mast cells, monocytes, and macrophages [68]. CysLT exhibit pro-inflammatory, bronchoconstrictive, and vasoconstrictive properties and increase the recruitment of eosinophils by the release of chemokines (MCP-1), mucus secretion from bronchial epithelial cells, and the pulmonary vascular permeability [118, 119]. Besides their effects on asthma bronchiale, they play also a role in allergic rhinitis, atopic dermatitis, and chronic diseases, e.g., cardiovascular diseases [119-121]. CysLT can bind to three GPCR – $CysLT_1$, $CysLT_2$, and $CysLT_3$. All cysLT bind to $CysLT_1$ conveying most of their pro-inflammatory effects but with different levels of affinity (LTD_4>LTC_4>LTE_4) [122]. Potent selective LTD_4 antagonists like montelukast, zafirlukast (withdrew from the pharmaceutical market since 2019) , and pranlukast (with primary usage in Japan) are used for the treatment of asthma bronchiale [123]. In contrast, LTC_4 and LTD_4 bind with equal affinity to $CysLT_2$, and again LTE_4 shows a reduced binding affinity (LTC_4=LTD_4>LTE_4) [119, 124]. Recently discovered, the third cysLT receptor ($CysLT_3$) exhibited a selective binding of LTE_4 [125], but its role in inflammation has to be clarified.

1.2 Cell death

Cell death belongs to essential basic processes in mammalian cells mediating development and regulation of tissue homeostasis. On the basis of morphological and biochemical characteristics, cell death can be classified into three subgroups: (I) apoptosis (section **1.2.1**), (II) autophagic cell death (section **1.2.2**), and (III) necrosis (section **1.2.3**) [126-128], whereby in many cases no clear distinction exists between individual forms, and composited processes occur.

1.2.1 Apoptosis

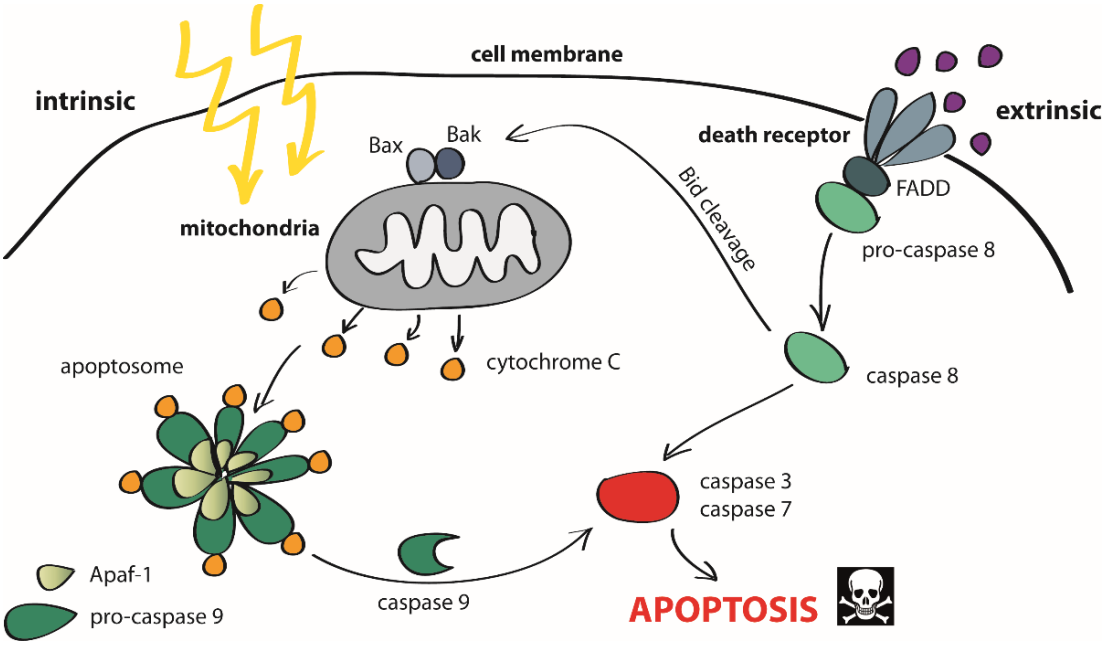

Fig. 2 Apoptosis pathway. *I) intrinsic pathway; II) extrinsic pathway.*

Apoptosis is the classical programmed cell death without induction of inflammation and is characterized by several morphological alterations to protect cells from an undesirable immune response [129, 130]. Typical morphological changes are chromatin condensation, and nuclear fragmentation, cell shrinkage, mitochondrial outer membrane permeabilization, and formation of apoptotic bodies [128-130]. These apoptotic bodies are small intact plasma membrane vesicles of disintegrated cells, containing cellular components and organelles, and can be eliminated by phagocytosis via neighboring cells [129]. Beside morphological features, apoptosis exhibits also biochemical characteristics. One major role plays the contribution of caspases, which are cysteine aspartyl proteases [131]. Under non-apoptotic conditions, caspases are inactive enzymes, called zymogens, and these pro-caspases can be activated by cleavage or dimerization [132, 133]. Caspase-mediated apoptosis can occur through two predominant pathways: (I) the extrinsic pathway, and (II) the intrinsic pathway. The extrinsic pathway is induced by extracellular signals, e.g., Fas ligands, TNFα, and TNF-related apoptosis-inducing ligands (TRAIL) binding to trans-membrane death receptors. Activated receptors form together with pro-caspase 8 a multi-protein death initiation signaling complex (DISC), which cleaves pro-caspase 8 in its active form. Subsequently, caspase 8 activates itself by autocleavage and triggers the cleavage of caspase 3 or induces the intrinsic mitochondrial pathway [134, 135]. Additionally, in response to stressing conditions, e.g., DNA damage, oxidative stress, growth factor withdrawal, cytotoxic compounds, or toxic insults, the mitochondrial outer membrane permeabilization increases by oligomerization of Bax/Bak [136], and the mitochondrial membrane potential dissipates resulting in an elimination of ATP

production [129, 137]. Consequently, mitochondria release several proteins like Cytochrome c, and these trigger together with ATP and the apoptotic protease-activating factor-1 (Apaf-1) the assembly of an apoptosome [138]. This complex initiates the recruitment and activation of caspase 9, which is able to cleave and therefore to activate caspase 3. Both pathways result in an activation of caspase 3 provoking the subsequent cleavage of poly-(ADP-ribose) polymerase-1 (PARP-1), which is essential for DNA repair and thus for cell survival. Furthermore, a caspase-independent PARP cleavage is also possible [139, 140].

1.2.2 Autophagy and autophagic cell death

Autophagy is a lysosomal degradation pathway, which is a pro-survival mechanism with spatial restriction. In short, cytoplasmic components are degraded and recycled in double-membraned vacuoles with the help of lysosomal hydrolases [141, 142]. Autophagic digestion is essential for survival, development, differentiation, and homeostasis, and it protects organisms from pathologies, e.g., cancer and infections [141]. In general, autophagy can be classified in (I) chaperone-mediated autophagy, (II) microautophagy, and (III) macroautophagy, whereby the latter is the major degradation process, which is primarily used by cells to generate energy in the form of ATP for their cell survival [143]. The basic macroautophagy process begins with isolated membrane residues, so-called phagophores. These membrane residues can originate from plasma membrane, endoplasmic reticulum (ER), Golgi, or mitochondria. Expansion of phagophores generates a double membrane-layered vesicle, the autophagosome. This autophagosome, containing cell organelles, protein aggregates, and endosomes, merges with lysosomes, holding lysosomal hydrolases, to the autolysosome. Within the autolysosome, captured material is degraded by hydrolases, and component parts are released to the cytosol for biosynthetic processes or for energy generation [142-144]. Autophagy can be regulated by many different factors which are specific for the respective organism, e.g., the up- and downstream pathway of the mechanistic target of rapamycin (mTOR), protein kinase A (PKA), proteins of the Bcl-2 family, and AMP-activated protein kinase (AMPK) as possible regulators for the mammalian macroautophagy [143-145]. The autophagic process is upregulated for generation of intracellular nutrients and energy or during oxidative stress, infection, and protein aggregate accumulation to remove intracellular pathogens [141, 145]. Furthermore, autophagy can also be activated by caspases [146]. Hyperactive autophagy provokes a breakdown of cellular organelles and proteins to generate energy comparable with a self-cannibalism that finally leads to cell death [141]. Cell death is mediated through autophagy, and on the other hand, cell death occurs with autophagy. In fact, the complete mechanism of autophagic cell death have not yet been fully clarified, but it is known that an increased autophagy activates the c-Jun N-terminal kinase (JNK) generating death signals [147]. Furthermore, autophagic cell death is mediated through the Bcl-2 family proteins Bax/Bak, located at the lysosomal

monomeric membrane, which cause an enhanced lysosomal membrane permeability resulting in an increased acidity [148].

1.2.3 Necrosis

In contrast to the previous types of cell death, necrosis is an uncontrolled process lacking the characteristics of apoptosis and autophagic cell death [128, 149] and can be elicited by direct chemical or radiologic insult [150]. Necrosis is originally characterized by a rapid rupture of plasma membrane caused by cytoplasmic swelling, dismantling of swollen organelles, and the involvement of the immune system leading to the release of pro-inflammatory intracellular factors [128, 149, 151]. Furthermore, necrosis exhibits several highly regulated mechanisms. These include early signs of mitochondrial dysfunction, e.g., ATP depletion, failed Ca^{2+} homeostasis, swelling, and enhanced ROS production, lysosomal rupture, and activation of proteases like calpains and cathepsins [149, 152, 153]. In fact, necrosis plays also a relevant role in many biological and immunological processes like microbial infections, adaptive immune responses, septic shock, cell homeostasis, and cancer [151, 153]. Three different types of necrosis are described: (I) pyroptosis, (II) necroptosis, and (III) lysosome-mediated necrosis (LMN) [151]. The best characterized form is pyroptosis, mediated through caspase 1 activation and inflammasome signaling [154]. Also known as back up cell death pathway, necroptosis combines apoptotic and necrotic features. In the presence of caspase inhibitors, necrosis is initiated by death receptor ligands (TNFα, TRAIL, or Fas) and is regulated by receptor-interacting kinase 1 and 3 (RIP1/RIP3), and mixed lineage kinase domain-like (MLKL) [155]. Both necrotic forms are linked to inflammation. In contrast, LMN is linked to the adaptive immunity [156] and is induced by alum, silicea crystals, cholesterol crystals, amyloid proteins, and the dipeptide methyl ester Leu-Leu-OMe (LLOMe). One major characteristic feature is an early lysosome rupture followed by irreversible plasma membrane damage and proteolysis of proteins with low-molecular weight [151, 157, 158]. These effects are regulated by cathepsins [157].

1.3 Natural products

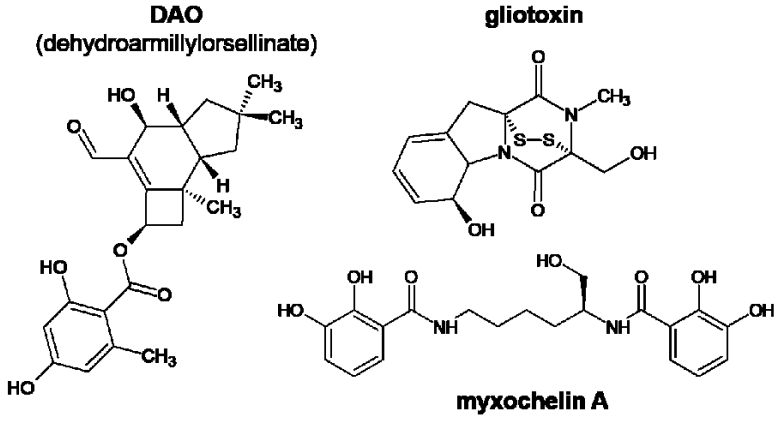

Fig. 3 Structures of investigated natural compounds.

1.3.1 Gliotoxin from *Aspergillus fumigatus*

The fungal secondary metabolite gliotoxin is an epidithiodioxopiperazine mycotoxin, and it is characterized by an intramolecular sulfur bridge and a dipiperazine core [159-161]. This intramolecular disulfide bond is responsible for the majority of biological activities [162] by triggering ROS production and interaction with cysteines within proteins [160], due to an intracellular redox cycle of gliotoxin. Gliotoxin is produced by various fungal species like *Eurotium chevalieri* and *Trichoderma vireus* but most commonly produced in *Aspergillus fumigatus* [160, 163]. The mycotoxin shows a variety of biological activities including antiviral effects by decreasing of multiplication of RNA through inhibition of RNA-dependent RNA polymerase [164, 165], inhibition of angiogenesis [166], and immunosuppressive impact [167, 168]. These immunosuppressive effects are conferred by effects on the cytoskeleton of immune cells, features as potent virulence factor, and also by its cytotoxicity [160]. Gliotoxin abrogates phagocytosis of polymorphonuclear leukocytes (PMNL) and affects the actin cytoskeleton organization resulting in alterations of cell morphology and cell adhesion [169-171]. In RAW264.7 macrophages, gliotoxin interferes with the inositol triphosphate metabolism impeding integrin activation, dysfunction in the actin cytoskeleton remodeling, and finally reduced phagocytosis [172]. Furthermore, gliotoxin shows inhibitory effects on farnesyltransferase and geranylgeranyltransferase [160], and it interferes with nicotinamide adenine dinucleotide phosphate oxidase complex formation leading to reduced ROS formation in phagocytes [173, 174]. Moreover, gliotoxin induces apoptosis in various cell types, except PMNL [175], through different pathways. Gliotoxin is able to stabilize IκBα preventing its degradation by proteasome [176], and thus, the transcription factor NFκB cannot be activated [177], causing a diminished pro-inflammatory cytokine release *in vivo* and *in vitro* [178]. Additional, gliotoxin increases the cellular concentration of cyclic adenosine monophosphate (AMP) by phosphorylation of histone H3 leading to an activation of PKA in thymocytes [179]. Another pathway of gliotoxin to trigger apoptosis is the interference with the Bcl-2 family member Bak resulting in a stimulation of the mitochondrial apoptosis pathway. As result, ROS production is increased and mediates the release of proapoptotic proteins like cytochrome C and leads eventually to apoptosis [180]. Finally, gliotoxin is a significant virulence factor in the pathology of *A. fumigatus* [1] eliciting IA [2]. IA affects primarily immunocompromised patients as well as immunocompetent patients with a high mortality rate varying between 30 to 90% [181]. During the infection process, *A. fumigatus* produces various mycotoxins with gliotoxin as most abundant and best characterized compound [163]. Indeed, gliotoxin is detectable in lung and sera of mice and human patients [182], and it is able to evoke aspergillosis in mice [2]. Due to its immunosuppressive characteristics, gliotoxin is used as diagnostic marker for IA [160].

1.3.2 Melleolides from *Armillaria mellea*

Melleolides are fungal secondary metabolites of the basidiomycete genus *Armillaria mellea*, a global widespread and edible genus with particular saprotrophic and parasitic characteristics [183, 184]. Constituents are sesquiterpene aryl esters with orsellinic acid from the polyketide pathway [185] as basic structure esterified with a protoilludene type secondary alcohol derived from the sesquiterpene pathway [184]. These combined structural elements are unique for the genus *Armillaria* [186]. The cultured mycelium of *A. mellea* is used as “Tienma” in traditional Chinese medicine to treat dizziness, headache, neurothenia, and insomnia [187, 188]. Melleolides show, besides antioxidative properties [189], also antimicrobial and antifungal activities [184, 188, 190, 191]. The modes of action for antimicrobial and antifungal effects are still unclear. Moreover, melleolides increase the maturation of dendritic cells [192] and enhance concanavalin A- or LPS-mediated lymphocyte proliferation [193]. Additional, melleolides exhibit cytotoxic properties towards various cancer cells [194] with several modes of action. Armillarikin induces apoptosis in human leukemia cells and hepatocellular carcinoma cells by caspase activation and increased ROS production followed by collapse of mitochondrial transmembrane potential [187]. In contrast, armillaridin causes autophagy-mediated cell death in human leukemia cells by reduction of the mitochondrial transmembrane potential and effects on autophagic flux and on autophagosome-lysosome fusion resulting in an induction of autophagosome formation [195, 196]. Also arnamial possesses cytotoxic features [197] with a still unclear mechanism. Additional, some melleolides causes decreased DNA biosynthesis in human cancer cells hypothesizing this effect as reason for their cytotoxicity [194]. During the last years, several structure-activity relationship studies were performed and some structural properties disclosure, whether melleolides exhibit antifungal or cytotoxic effects. Of interest, structural elements causing antifungal or cytotoxic activity are dissimilar. While the position of the double bond within the sesquiterpene moiety causes antifungal activity [186], the degree of hydroxylation within the sesquiterpene moiety and a low number of alcohol functionalities are responsible for cytotoxicity [194].

1.3.3 Myxochelin A from *Pyxidicoccus fallax*

Pyxidicoccus fallax belongs to the family of Gram negative bacteria - these so-called predatory myxobacteria contain diverse macrolide antibiotics, e.g., gulmirecins [198], disciformycins [199], and anti-cancer agents, e.g., myxochelin A [200-202]. Myxochelins are assumed to mediate their biological activity as siderophores and thus securing the iron supply of the producing bacterium as iron chelating agents [203]. Besides their antiproliferative effects in leukemic cancer cell lines [200], myxochelins exert also antimetastatic effects [204, 205]. The catechol residues seem to be responsible for the biological activity, whereas methylation of the catechol hydroxyl residues diminishs their effects [200, 206].

2. AIM OF THE THESIS

Acute inflammation is a physiological process to protect the host organism against infection and to restore homeostasis upon injury by an immune response. This response is mediated by various internal signals, e.g., eicosanoids, cytokines, and chemokines, or external signals, e.g., diverse microbes, leading to chronic inflammation and cancer in some cases. As member of the Excellence Graduate School “Jena School for microbial communication” (JSMC), which addresses microbial communication between microorganisms, their metabolic products and host organisms, this thesis aimed to investigate several natural secondary metabolites with potential anti-inflammatory and/or cytotoxic effects in primary immune cells and cancer cells for their immunomodulatory actions and to resolve the underlying molecular mechanisms. In view of the growing link between inflammation and cancer and the role of primary immune cells in tumorigenesis, the identification of crucial effectors is key for understanding their connection and may offer potential targets for therapeutic approaches.

First, the effect of these secondary metabolites on LT biosynthesis have been investigated with the aim to clarify and to characterize the mechanisms for the underlying inhibition of LT formation. LT are bioactive LM, which are formed by 5-LOX and LTA_4H, or LTC_4S from the polyunsaturated fatty acid AA, playing a pivotal role in the innate and adaptive immune response, inflammation, and several diseases due to the recruitment of leukocytes to the site of infection or injury. In the last decades, a variety of 5-LOX, LTA_4H, and LTC_4S inhibitors were designed, investigated, and tested in clinical trials, but only a few compounds reached the pharmaceutical market, e.g., the 5-LOX inhibitor zileuton [6]. Main focus of this thesis was placed on an abrogation of LT biosynthesis by inhibition of 5-LOX or LTA_4H. Therefore, inhibitory effects in cell-free assays were compared with the efficacy in various leukocytes including the influence of different stimuli or redox active agents. Furthermore, selectivity of inhibition was confirmed by the exclusion of effects on other enzymes involved in the AA metabolic pathway. In the case of 5-LOX inhibition, interaction with the 5-LOX helper protein was analyzed by immunofluorescence, and the detailed impact of concerned compounds was investigated. Moreover, physiological data for LTA_4H inhibition were collected by distinct animal models of inflammation and infection.

Second, the effects of natural compounds on human cell viability have been investigated to elucidate their mode of action as new approach for the development of anti-cancer drugs. Hence, the cytotoxic properties of melleolides were studied in human primary monocytes and cancer cells including the characterization of apoptotic and necrotic features by flow cytometry experiments. Additionally, modifications in cell morphology were analyzed by light microscopy followed by a new established UPLC-MS/MS method to detect phospholipid-compound interactions, and subcellular fractionation was performed to address a specific accumulation in various cell organelles including cell membranes.

3. MANUSCRIPTS

Manuscript I (M-I)

Melleolides from honey mushroom inhibit 5-lipoxygenase via C159

Stefanie König, Erik Romp, Verena Krauth, Michael Rühl, Maximilian Dörfer, Stefanie Liening, Bettina Hofmann, Ann-Kathrin Häfner, Dieter Steinhilber, Michael Karas, Ulrike Garscha, Dirk Hoffmeister, Oliver Werz, Cell Chemical Biology **2019** 26(1), 60-70

Manuscript II (M-II)

Gliotoxin from *Aspergillus fumigatus* abrogates leukotriene B_4 formation through inhibition of leukotriene A_4 hydrolase

Stefanie König, Simona Pace, Helmut Pein, Thorsten Heinekamp, Jan Kramer, Erik Romp, Maria Straßburger, Fabiana Troisi, Anna Proschak, Jan Dworschak, Kirstin Scherlach, Antonietta Rossi, Lidia Sautebin, Jesper Z. Haeggström, Christian Hertweck, Axel A. Brakhage, Jana Gerstmeier, Ewgenij Proschak, Oliver Werz, Cell Chemical Biology **2019** 26(4), 524-534

Manuscript III (M-III)

Myxochelins target human 5-lipoxygenase

Sebastian Schieferdecker, Stefanie König, Andreas Koeberle, Hans-Martin Dahse, Oliver Werz, Markus Nett, Journal of Natural Products **2015** 78(2), 335-338

Manuscript IV (M-IV)

Melleolides induce rapid cell death in human primary monocytes and cancer cells

Markus Bohnert, Olga Scherer, Katja Wiechmann, Stefanie König, Hans-Martin Dahse, Dirk Hoffmeister, Oliver Werz, Bioorganic & Medicinal Chemistry **2014** 22(15), 3856-61

Manuscript V (M-V)

Rapid cell death induction by the honey mushroom mycotoxin dehydroarmillylorsellinate through covalent reaction with membrane phosphatidylethanolamines

Stefanie König*, Konstantin Löser*, Helmut Pein*, Konstantin Neukirch, Anna Czapka, Stephanie Hoeppener, Maximilian Dörfer, Dirk Hoffmeister, Andreas Koeberle, Oliver Werz

* contributed equally; manuscript in preparation, planned submission 3rd quarter 2019 to Cell Chemical Biology

3.1 Manuscript I (M-I)

Melleolides from honey mushroom inhibit 5-lipoxygenase via C159

Stefanie König, Erik Romp, Verena Krauth, Michael Rühl, Maximilian Dörfer, Stefanie Liening, Bettina Hofmann, Ann-Kathrin Häfner, Dieter Steinhilber, Michael Karas, Ulrike Garscha, Dirk Hoffmeister, Oliver Werz

Cell Chemical Biology 2019 26(1), 60-70

In the present work, we characterized four melleolides isolated from *Armillaria mellea* and their effects on LT biosynthesis in human primary neutrophils. Melleolides abrogated the formation of LTB_4 due to a selective inhibition of 5-LOX. In more detail, melleolides prevented the interaction between 5-LOX and its helper protein FLAP at the nuclear membrane by covalent binding of their α,β-unsaturated aldehyde moiety to cysteines located around the entrance to the catalytic center. Moreover, experiments with 5-LOX mutants, where selected cysteines have been substituted by serine, revealed two possible modes of actions caused by melleolides. First, the direct interaction with more than two of the cysteines C^{159}, C^{300}, C^{416}, and C^{418} leading to a reduced 5-LOX activity, and second, the selective influence on C^{159}, which prevented the 5-LOX/FLAP complex assembly at the nuclear envelope. Taken together, melleolides harboring a Michael acceptor functionality mediated the 5-LOX inhibition by targeting C^{159}.

Own contribution: Experimental design and performance of 5-LOX assays, immunofluorescence analysis, proximity ligation assays; assistance to HEK cell transfection; measurement of 5-LOX expression, FLAP expression, and phosphorylation of $cPLA_2$, ERK-1/2, p38 MAPK by Western Blot; maintenance of cell culture and performance of blood cell isolation; data analysis; writing the manuscript. **Total contribution: 80%.**

Article

Cell Chemical Biology

Melleolides from Honey Mushroom Inhibit 5-Lipoxygenase via Cys159

Graphical Abstract

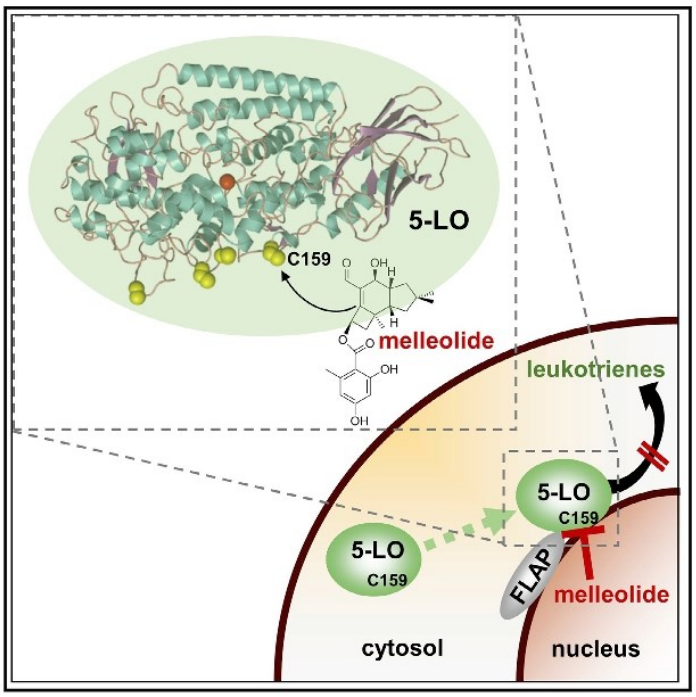

Highlights

- Human 5-lipoxygenase (5-LO) was identified as a molecular target of melleolides
- Melleolides inhibit 5-LO via two or more of the cysteines 159, 300, 416, and 418
- Melleolides prevent interaction of 5-LO with its helper protein via Cys159 in 5-LO
- Cys159 in 5-LO determines interaction with its helper protein and 5-LO activity

Authors

Stefanie König, Erik Romp, Verena Krauth, ..., Ulrike Garscha, Dirk Hoffmeister, Oliver Werz

Correspondence

oliver.werz@uni-jena.de

In Brief

König et al. revealed human 5-lipoxygenase as a functional target of melleolides from honey mushroom, where cysteines at the substrate entrance of 5-lipoxygenase mediate enzyme inhibition. Exploiting melleolides as a tool they identified Cys159 as a determinant for interaction of 5-lipoxygenase with its helper protein.

König et al., 2019, Cell Chemical Biology *26*, 1–11
January 17, 2019 © 2018 Elsevier Ltd.
https://doi.org/10.1016/j.chembiol.2018.10.010

CellPress

3.2 Manuscript II (M-II)

Gliotoxin from *Aspergillus fumigatus* abrogates leukotriene B_4 formation through inhibition of leukotriene A_4 hydrolase

Stefanie König, Simona Pace, Helmut Pein, Thorsten Heinekamp, Jan Kramer, Erik Romp, Maria Straßburger, Fabiana Troisi, Anna Proschak, Jan Dworschak, Kirstin Scherlach, Antonietta Rossi, Lidia Sautebin, Jesper Z. Haeggström, Christian Hertweck, Axel A. Brakhage, Jana Gerstmeier, Ewgenij Proschak, Oliver Werz

Cell Chemical Biology 2019 26(4), 524-534

This publication presents the effects of gliotoxin isolated from *Aspergillus fumigatus* on LTB_4 biosynthesis caused by inhibition of LTA_4H in human primary immune cells. The potent neutrophil chemoattractant LTB_4 is involved in several inflammatory diseases, e.g., IA caused by *A. fumigatus* leading to high mortality rates, especially for immunocompromised patients. The major virulence factor of *A. fumigatus*, gliotoxin, inhibited selectively the biosynthesis of LTB_4 *in vivo* in two distinct animal models: (I) murine peritonitis, and (II) pleurisy in rats. Furthermore, we confirmed selective LTB_4 inhibition *in vitro* in human primary immune cells. Intracellular GSH was crucial to cleave the disulfide bond of gliotoxin in order to chelate the zinc ion in the active center of the epoxide hydrolase pocket of LTA_4H without affecting the aminopeptidase function and thus preventing neutrophil recruitment to the site of inflammation. Conclusively, we identified the target and a potential mode of action of gliotoxin in *A. fumigatus* pathology.

Own contribution: Experimental design and performance of 5-LOX assays with several cell types, purified enzyme, agents, and stimuli, LM extraction for UPLC-MS/MS analysis; extraction of LM from animal samples and their analysis by UPLC-MS/MS and ELISA; experimental design, optimization, and performance of epoxide hydrolase and aminopeptidase activity assays of LTA_4H; maintenance of cell culture and performance of blood cell isolation; data analysis; writing the manuscript. **Total contribution: 75%.**

Article

Cell Chemical Biology

Gliotoxin from *Aspergillus fumigatus* Abrogates Leukotriene B_4 Formation through Inhibition of Leukotriene A_4 Hydrolase

Graphical Abstract

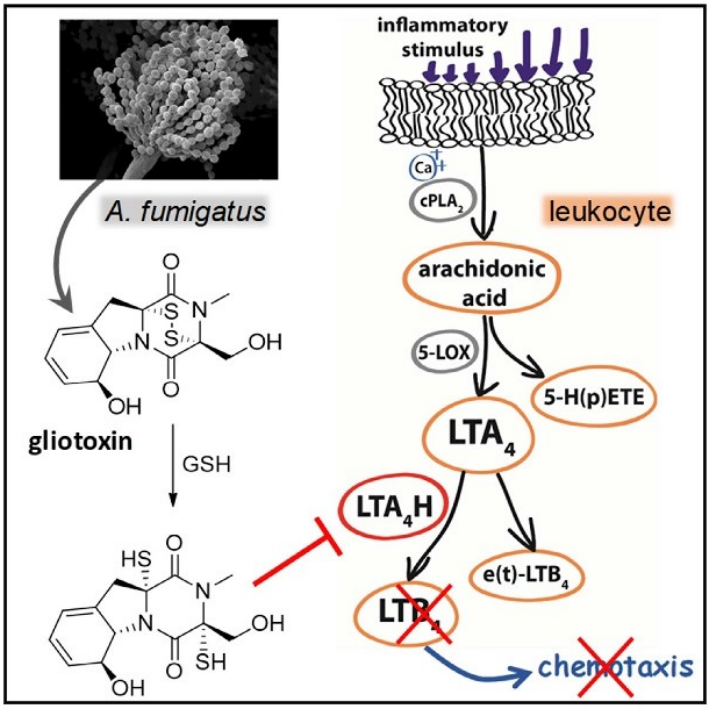

Highlights

- Gliotoxin suppresses neutrophil influx and LTB_4 formation in mice and rats
- Gliotoxin selectively inhibits LTB_4 biosynthesis via inhibition of LTA_4H
- Gliotoxin blocks epoxide hydrolase but not aminopeptidase activity of LTA_4H
- Reducing conditions confer gliotoxin LTA_4H inhibitory activity

Authors

Stefanie König, Simona Pace, Helmut Pein, ..., Jana Gerstmeier, Ewgenij Proschak, Oliver Werz

Correspondence

oliver.werz@uni-jena.de

In Brief

König et al. identified leukotriene A_4 hydrolase (LTA_4H) in human leukocytes as a molecular target of gliotoxin from *Aspergillus fumigatus.* Under reducing conditions, gliotoxin inhibits leukotriene A_4 hydrolase activity leading to suppression of chemotactic leukotriene B_4 biosynthesis and neutrophil infiltration, which may underlie the neutrophil-compromising properties of this fungal toxin.

König et al., 2019, Cell Chemical Biology *26*, 1–11
April 18, 2019 © 2019 Elsevier Ltd.
https://doi.org/10.1016/j.chembiol.2019.01.001

3.3 Manuscript III (M-III)

Myxochelins target human 5-lipoxygenase

Sebastian Schieferdecker, Stefanie König, Andreas Koeberle, Hans-Martin Dahse, Oliver Werz, Markus Nett

Journal of Natural Products 2015 78(2), 335-338

Here, we described the isolation and characterization of biological activity of three myxochelins isolated from *Pyxidicoccus fallax*. While myxochelin A was already known, we identified myxochelin C and D as new structural representatives with isotopic incorporation. Besides the clarification of the structure, we performed various biological assay to clarify the mode of action of these myxochelins. We found that myxochelin A exhibits potent antiproliferative effects towards the leukemic K-562 cells, but fails to affect adherent HeLa cells. A methylation of the catechol residues reduced these antiproliferative effects. Furthermore, we identified 5-LOX as molecular target of myxochelins in cell-free assays (IC_{50}=1.9 µM) correlating to suppression of proliferation of K-562 cells. As described before, myxochelins act as siderophores thus hypothesizing 5-LOX inhibition by iron chelation. Taken together, myxochelins may targeted 5-LOX as iron-ligand agents leading to inhibition of proliferation in leukemic cells harboring 5-LOX.

Own contribution: Experimental design and performance of 5-LOX assays with purified enzyme, purification of human recombinant 5-LOX from *E. coli*; coordination of mPGES-1 activity assay; data analysis; partially writing the manuscript. **Total contribution: 30%**.

3.4 Manuscript IV (M-IV)

Melleolides induce rapid cell death in human primary monocytes and cancer cells

Markus Bohnert*, Olga Scherer*, Katja Wiechmann, Stefanie König, Hans-Martin Dahse, Dirk Hoffmeister, Oliver Werz

* contributed equally

Bioorganic & Medicinal Chemistry 2014 22(15), 3856-61

In this manuscript, we analyzed several melleolides, isolated from the basidiomycete genus *Armillaria mellea*, for their cytotoxic potential in human primary monocytes and in various cancer cell lines. Structure-activity relationship analysis revealed the importance of the α,β-unsaturated double bound for potent cytotoxicity. Interestingly, DAO displayed comparable results for monocytes and HeLa cells in contrast to other antiproliferative compounds, which were less active against primary monocytes, e.g., staurosporine, or pretubulysin. Furthermore, DAO induced an unusual rapid onset of cell death (within < 1 hr), which contrasts cell death induction for other cytotoxic compounds (> 5 hrs). Based on morphological analysis and flow cytometry experiments, we hypothesized an untypical mechanism of rapid cell death induction for melleolides with an unknown target, combining necrotic as well as apoptotic features.

Own contribution: Experimental design and performance of MTT assays with DAO and staurosporine in human primary monocytes and HeLa cells; isolation of monocytes and cell culture; data analysis; partially writing the manuscript. **Total contribution: 20%**.

3.5 Manuscript V (M-V)

Rapid cell death induction by the honey mushroom mycotoxin dehydroarmillylorsellinate through covalent reaction with membrane phosphatidylethanolamines

Stefanie König*, Konstantin Löser*, Helmut Pein*, Konstantin Neukirch, Anna Czapka, Stephanie Hoeppener, Maximilian Dörfer, Dirk Hoffmeister, Andreas Koeberle, Oliver Werz

* contributed equally

manuscript in preparation, **planned submission: 3rd quarter 2019** in *Cell Chemical Biology*

This work presents the clarification of the mode of action for the cytotoxicity of the melleolide DAO in human primary monocytes and cancer cells. DAO rapidly induced cell death within 15 min analyzed by a reduced mitochondrial reductase activity and an increased PARP cleavage. We found that these effects were caused by an interaction of the α,β-unsaturated aldehyde of DAO with the head groups of phospholipids of cell membranes, which might be the reason for the rapid loss of plasma membrane integrity and cellular viability. As result, DAO reacted covalently via an 1,4-addition with ethanolamine and PE. In addition, subcellular fractionation was used to determine a predominant accumulation of DAO within a specific cell organelle fraction. Conclusively, DAO causes cell death by membrane damage, seemingly due to covalent modification of PE with detrimental consequences for cell integrity and viability.

Own contribution: Experimental design and performance of MTT and LDH assay, Western Blot analysis of phospho-p38 MAPK, phospho-Akt, BiP, CHOP, and ATF-4 in monocytes; experimental design and performance of measurement of non-cellular and cellular DAO-PE adducts for UPLC-MS/MS analysis after treatment with phospholipase D; extraction of cellular DAO-PE adducts and their analysis by UPLC-MS/MS; experimental design, optimization, and performance of subcellular fractionation, Western Blot analysis of each fraction, extraction of cellular DAO-PE adducts and phospholipids in separated fractions and their analysis by UPLC-MS/MS; maintenance of cell culture and performance of blood cell isolation; data analysis; writing the manuscript. **Total contribution: 70%**.

4. DISCUSSION

In the last decades, several studies have described diverse biological functions of natural products in mammals biosynthesized by fungi, bacteria, or plants. Natural products are also known to interfere with the host defense as potent virulent factors, can cause cell death or possess anti-inflammatory features, but the underlying modes of action and molecular targets are still elusive. Considering the growing connection between inflammation and cancer, the present work focuses on the target identification of natural secondary metabolites to clarify interference with inflammation and their importance for pathogenicity. Here, we investigated DAO, gliotoxin, and myxochelins for their effects and underlying mechanisms in inflammatory processes and cell death induction in human cells.

We identified 5-LOX as molecular target of the myxobacterial compound myxochelin A biosynthesized by *Pyxidicoccus fallax* and of the melleolide DAO from honey mushroom *Armillaria mellea*. While myxochelin A and various derivatives chelated the ferrous iron in the enzyme´s active site by its catechol residues (**manuscript III**), DAO interfered with surface cysteines located at the substrate entrance of 5-LOX (**manuscript I**) resulting in abrogated LT formation. Besides DAO, we tested several melleolides for structure-activity relationships and identified that the α,β-unsaturated aldehyde group serves as Michael acceptor mediating 5-LOX inhibition. Michael acceptor containing compounds interact, inter alia, with cysteines located at the entrance to the catalytic center of 5-LOX and hence influencing 5-LOX activity and LT biosynthesis [15, 16]. In the case of DAO, this α,β-unsaturated aldehyde group interacts with C^{159} preventing 5-LOX/FLAP interaction without prejudicing nuclear 5-LOX translocation in intact neutrophils but failed to selectively target C^{159} in cell homogenates. Instead, DAO affected two or more cysteines (C^{159}, C^{300}, C^{416}, C^{418}) in lysed cells that results in an equally abrogated LT formation, indicating two distinct mode of actions in neutrophils (**manuscript I**) with minimal impairment of cell viability (unpublished data). Furthermore, DAO exhibited potent and similar cytotoxic properties in human monocytes as well as in various cancer cells with an untypical rapid onset of cell death compared to various antiproliferative and cytotoxic compounds. However, we revealed apoptotic as well as necrotic cell death characteristics of DAO by flow cytometry and light microscopy analysis including an abrogated metabolic activity of mitochondria (**manuscript IV**). Subsequently, we identified a covalent binding of the reactive α,β-unsaturated aldehyde group to the ethanolamine head group of the membrane phospholipid PE. Hence, we confirmed our previous hypothesis of a composed cell death process by showing simultaneously PARP cleavage and membrane rupture, measured by LDH release, correlating with increased DAO-ethanolamine adducts. Moreover, DAO manipulated mitochondrial functions and caused impaired autophagic processes with enhanced lysosomal rupture and decreased intracellular pH value leading to the assumption that DAO-induced cell death linked several dysfunctional cellular processes (**manuscript V**).

Another fungal toxin, gliotoxin, plays an important role in several inflammatory processes, e.g., inducing cell death in primary immune cells [175, 207] or inducing IA as potent virulence factor of *Aspergillus fumigatus* [1, 2]. Various theories exist for cell death induction and triggering IA with its indications [160], whereby only target identification of gliotoxin for IA plays a central role in this thesis. Our data show that gliotoxin abrogates the biosynthesis of the important neutrophil chemoattractant LTB_4 by covalent binding to LTA_4H. Furthermore, we found that gliotoxin chelates the zinc ion in the epoxide hydrolase center by its reduced free thiol groups but failed to inhibit LTA_4H under non-cellular conditions. An inhibition of the aminopeptidase activity and an abrogation of other epoxide hydrolases could be excluded. Moreover, we confirmed our results *in vivo* and verified gliotoxin as virulence factor of *A. fumigatus* responsible for neutropenia and the resulting host resistance to *A. fumigatus* (**manuscript II**).

4.1 Natural compounds and their effect on inflammatory key processes

During the early phase of inflammation, pro-inflammatory signaling molecules, e.g., cytokines, chemokines, and several eicosanoids are produced by tissue resident macrophages or mast cells. These inflammatory mediators initiate the recruitment of leukocytes, mainly neutrophils, to the site of infection or injury for host protection. In the case of dysregulation, inflammation becomes persistent, which ultimately can even lead to cancer [21, 29, 208]. We tested the secondary metabolites DAO, myxochelin A, and gliotoxin in human primary immune cells to clarify their role in inflammatory processes and to reveal their modes of action.

The metabolism of AA is one important pathway mediating initiation and resolution of inflammation depending on particular enzyme activity and LM formation. 5-LOX is part of the AA pathway and responsible for the biosynthesis of pro-inflammatory LT. The melleolide DAO abrogated 5-LOX activity in a direct and selective manner by interacting with C^{159} located at the catalytic entry and prevented thereby an interaction between 5-LOX and its helper protein FLAP (**manuscript I**). Indeed, the myxobacterial compound myxochelin A reduced also directly 5-LOX activity but instead of interacting with essential amino acids, myxochelin A seemingly chelated the central iron in 5-LOX by its catechol basic structure belonging to the family of iron ligand inhibitors (**manuscript III**).

In the last years, the number of investigated naturally occurring 5-LOX inhibitors increased [40, 41], harboring various modes of action to impede LT biosynthesis. While embelin acted as non-redox inhibitor for hampering 5-LOX activity [74] or the indirubin derivative 6-BIO interacted with the ATP binding site of 5-LOX [79], compounds containing a catechol residue, e.g., rosmarinic acid [209], caffeic acid, and its derivatives [210, 211] were typical natural representatives for the iron-complexing inhibitor type. Also the siderophore myxochelin A [203] contained a catechol basic structure. We analyzed myxochelin A and various derivatives for structure-activity relationships for 5-LOX inhibition (**manuscript III**, [206,

212]). In line with results from previous investigations [203], we showed that the catechol basic structure was essential for abrogated LT biosynthesis and methylation of the aromatic hydroxyl residues resulted in a completely reversed 5-LOX inhibition. We observed increased inhibition of 5-LOX activity if the second hydroxyl moiety was located in meta position [206, 212], whereas the second hydroxyl residue in para position impaired the bioactivity [206]. Interestingly, derivatives harboring the second hydroxyl group in meta position did not lose their biological activity, although the chrome azurol S assay, measuring iron affinities, was negative [212]. This supports different modes of action for 5-LOX inhibition depending on the myxochelin structure. Furthermore, a single methoxy substituent at the catechol residue is sufficient for reducing 5-LOX inhibition. However, structural modifications at the lysinol partial structure were negligible for 5-LOX inhibition [206]. Myxochelins failed to inhibit 5-LOX activity in cellular systems or exhibited only a weak activity, assuming that the high polarity of the structure was responsible for limited cellular uptake. Of interest, the myxochelins showed a structural resemblance to another natural product, that is, curcumin which is biosynthesized by the plant *Curcuma longa*. Curcumin was previously identified as potent 5-LOX and mPGES-1 inhibitor [213, 214], hypothesizing that myxochelins could also interfere with mPGES-1. However, myxochelins failed to inhibit mPGES-1 activity in cell-free assays supporting selective 5-LOX inhibition. Conceivably, myxochelins could possess antioxidant activities similar to caffeic acid and derivatives [210], which requires further investigations. In conclusion, myxochelins impeded primarily 5-LOX activity by iron-chelating effects of the catechol residue in the active center of the enzyme and represent an interesting substance class for investigation of new natural 5-LOX inhibitors.

We examined four different melleolides for structure activity relationship for 5-LOX inhibition under cellular and non-cellular conditions (**manuscript I**). The structure of melleolides can be divided in a sesquiterpene moiety and an orsellinic acid residue. Melleolides harboring an α,β-unsaturated aldehyde group at position 1 with a $\Delta^{2,3}$ or $\Delta^{2,4}$ double bond exhibited potent 5-LOX inhibition, whereby compounds with a $\Delta^{2,3}$ double bond were less active or failed to diminish LT biosynthesis, when the α,β-unsaturated aldehyde group was replaced by a hydroxyl moiety. Interestingly, the Michael acceptor functionality might be responsible for further biological activities of melleolides like antifungal activity, antimicrobial activity, and cytotoxic properties published in previous studies [186, 194]. However, structural modifications at the orsellinic residue like a hydroxyl group at position 5´ instead of methylation or a 6´-chlorine and hydroxylation at position 4 of the sesquiterpene moiety caused only a minor loss of 5-LOX inhibitory potency. We identified DAO and arnamial as most potent compounds for 5-LOX inhibition, whereby arnamial was more potent under cell-free conditions, and DAO exhibited more reducing activity in cells with 10-fold lower IC_{50}. Both structures were characterized by the α,β-unsaturated aldehyde group at position 1 with a $\Delta^{2,4}$ double bond but

arnamial contained a more liphophilic orsellinic acid residue (5´-methylation, 6´-chlorine). In fact, compounds with high lipophilicity correlated with more potent 5-LOX inhibition than less lipophilic structures [215], but this correlation explains not a 10-fold less inhibition under cell free conditions in case of DAO. All experiments were compared to the well-known 5-LOX inhibitor zileuton suppressing 5-LOX activity in comparable manner in different experimental settings (this study and others [6]). Furthermore, external supplementation of AA to intact cells reduced the inhibitory effect of DAO similarly to the potency under cell-free conditions, suggesting an additional effect of DAO on proteins/enzymes involved in the 5-LOX pathway. Indeed, several enzymes and enzyme activities participate in LT biosynthesis: (I) AA release by $cPLA_2$ from membrane phospholipids, (II) AA transfer by FLAP to 5-LOX and 5-LOX/FLAP complex assembly, (III) nuclear 5-LOX translocation, and (IV) preceding activating 5-LOX signaling pathways such as phosphorylation by MAPK and cellular Ca^{2+} mobilization [10]. By means of our data, we excluded direct $cPLA_2$ inhibition by determination of unaffected released [^{3}H]-labeled AA. Instead we observed hampered 5-LOX/FLAP complex assembly leading to impeded AA transport by FLAP or a competition between DAO and AA for the 5-LOX binding pocket without affecting the 5-LOX translocation to the nuclear membrane. In general, 5-LOX inhibition can be mediated by iron-chelating agents, redox active compounds, or AA mimetics, which compete with AA for binding at the active or allosteric site of 5-LOX [40, 41]. Based on the chemical structure, DAO possesses no fatty acid-like features excluding competition with AA. Also, redox activities and iron-chelating effects were not reported for DAO. Interestingly, compounds containing a Michael acceptor functionality like thymoquinone (TQ), U73122 or nitro fatty acids showed a high reactivity with SH-groups and exhibited LT abrogation by building covalent adducts with surface cysteines located at the catalytic entrance to the 5-LOX activity center [15, 16, 216]. The 5-LOX structure contained nine different cysteines, whereby C^{99} and C^{449} were present in 12-LOX as well as in 15-LOX [15, 19]. As DAO inhibited neither 12-LOX nor 15-LOX activity, we excluded an interaction with these two cysteines. The four cysteine residues C^{159}, C^{300}, C^{416}, and C^{418} were located closed to the substrate entry [19, 51], and as published before, they are responsible for 5-LOX dimerization [51], 5-LOX/FLAP co-localization at the nuclear envelope, and finally for influencing 5-LOX product formation without hampering 5-LOX translocation [50, 51]. We incubated stable transfected HEK cells containing cysteine mutants in which respective cysteines were replaced by serine (5-LOX_4C mutant). Interestingly, DAO failed to inhibit 5-LOX activity in intact cells as well as in cell homogenates supporting our presumption that DAO affected one or more cysteines by building a covalent bonding between the Michael acceptor group and the thiol group of cysteines. In contrast, zileuton, which is an iron-chelating agent [6], was still able to abrogate LT biosynthesis of the 5-LOX_4C mutant, as expected. We replaced the four individual cysteines by serine and the melleolide was tested in cell-free and cell-based assays. Under cell-free conditions, DAO failed

to inhibit LT formation for single cysteine mutations implying that two or more cysteines were necessary for inhibition by DAO hypothesizing that DAO might affect a 5-LOX dimerization [51] via two or more cysteines with lacking 5-LOX/FLAP interaction, since FLAP has been active only in intact cells [53]. In contrast, interaction with C^{159} played a crucial role for diminished 5-LOX activity in cells. Thus, our results indicated that DAO caused abrogated 5-LOX/FLAP complex assembly essentially via C^{159}, except a participation of C^{300}, C^{416}, and C^{418} in intact cells.

The nuclear membrane protein FLAP is essential for the LT biosynthesis as 5-LOX helper protein for AA transfer [64, 217] but exhibits no own enzymatic activity [52, 55]. Typical FLAP inhibitors showed comparable inhibitory characteristics as melleolides: active in cellular systems and reduced active or rather inactive under cell-free conditions. These compounds triggered reduced LT biosynthesis by preventing 5-LOX/FLAP assemblies without affecting 5-LOX translocation being important for LT biosynthesis [217-220]. Furthermore, FLAP belongs to the MAPEG family and possesses sequence and structure homology to LTC_4S and mPGES-1 [221, 222]. Indeed, our data revealed no interference of MAPEG family members, e.g., LTC_4S, mPGES-1, thus excluding a class effect against these proteins. In addition, cysteines (C^{159}, C^{300}, C^{416}, C^{418}) played an important role for 5-LOX/FLAP co-localization at the nuclear membrane as described before [50] and interaction with C^{416} and C^{418} by Michael acceptors impeded the entry of AA to the catalytic center of 5-LOX along with impaired LT biosynthesis [15, 216]. Along these lines, all cysteine mutants caused a strikingly lower LT formation, and interestingly the 5-LOX_4C mutant as well as the 5-LOX_C^{159}S mutant failed to form complex assemblies with FLAP indicating the importance of C^{159} in AA metabolism. Interestingly, DAO required C^{159} for direct inhibition of 5-LOX activity leading to abrogated LT formation in intact cells. In contrast to zileuton, whose 5-LOX inhibition was independent of cysteine mutants, DAO failed to inhibit 5-LOX activity, when C^{159} was replaced by serine, suggesting a direct hampered 5-LOX/FLAP interaction, or the interaction between DAO and C^{159} evoked strong conformational modifications preventing 5-LOX/FLAP interaction and/or avoiding the substrate entry to the catalytic center. Moreover, melleolides and other Michael acceptors failed to inhibit 5-LOX translocation, which is essential for LT formation [220, 223]. Hence, Michael acceptor-containing compounds evinced commonalities to classical FLAP inhibitors, e.g., MK886 [217, 219], but they differed clearly from other novel direct 5-LOX inhibitors like hyperforin [77] or indirubin [79].

Taken together, melleolides especially DAO targets 5-LOX through a covalent binding via their α,β-unsaturated aldehyde group with the thiol group of C^{159} located at the catalytic entry of 5-LOX. DAO reduces LT biosynthesis by preventing 5-LOX/FLAP interaction via C^{159} in cells, while on the enzymatic level DAO interferes with two or more cysteines leading to less

potent inhibition of 5-LOX activity. Finally, C^{159} is crucial for the 5-LOX/FLAP complex assembly at the nuclear envelope and the formation of LT.

Besides 5-LOX inhibition, suppression of LT can be also mediated by LTA_4H inhibition preventing LTB_4 biosynthesis or through hampered LTC_4S activity leading to abrogation of cysLT. LTB_4 is known as potent chemoattractant for immune cells and plays an important role in host protection against infection through the recruitment of primary immune cells, especially neutrophils to the site of infection [4, 5]. We found that the mycotoxin gliotoxin abrogated LT formation by LTA_4H inhibition *in vitro* and *in vivo* and hence causing neutrophil-mediated host resistance to IA (**manuscript II**).

We used two distinct inflammatory animal models: (I) a murine zymosan-induced peritonitis model [224], and a (II) carrageenan-induced pleurisy model in rats [225] to investigate the effects of gliotoxin on inflammation and immune cells. In comparison to the well-known 5-LOX inhibitor zileuton [6], gliotoxin reduced LTB_4 formation in murine and rat plasma and suppressed neutrophil infiltration into peritoneal and thoracic exudates at low doses. Furthermore, gliotoxin abrogated selective LTB_4 formation without inhibiting 5-LOX, 12-/15-LOX, and COX. Interestingly, tr-LTB_4 isomers and LTC_4 were increased after gliotoxin treatment, indicating further utilization of LTA_4 and thus an intact upstream LTA_4 biosynthetic pathway. These data suggest that LTA_4 was used as substrate by LTC_4S to generate LTC_4 and was non-enzymatically converted to tr-LTB_4 derivatives. Such substrate shunting was previously reported and is a typical behavior of LTA_4H inhibitors like captopril [226], SC-57461A [8], and others [99], suggesting that gliotoxin targets LTA_4H.

Gliotoxin exhibited comparable results *in vitro* in human primary neutrophils and monocytes in comparison to the 5-LOX inhibitor zileuton [6] and the LTA_4H inhibitor SC-57461A [7], while zileuton suppressed all 5-LOX products and SC-57461A showed similar results to gliotoxin implying that gliotoxin acted as a selective LTA_4H inhibitor. LTA_4H is a bifunctional metalloenzyme harboring two distinct enzyme activities: (I) an epoxide hydrolase activity hydrolyzing LTA_4 to the potent chemoattractant LTB_4 during initiation of inflammation, and (II) an aminopeptidase activity inactivating the pro-inflammatory tripeptide PGP during resolution of inflammation [13, 82, 89]. Hence, development of LTA_4H inhibitors with selective inhibition of the epoxide hydrolase activity is essential for therapeutic application interfering with the inflammatory response during a chronic inflammation [104]. Until now, only one selective epoxide hydrolase inhibitor was identified, that is, ARM-1 [107], whereas several other LTA_4H inhibitors affect both enzyme activities including chemically synthesized compounds, e.g., SC-57461A [7], bestatin [102], captopril [103] as well as natural occurring ingredients, e.g., 6-gingerol [227], resveratrol [228], or α-lipoic acid [229]. Our data revealed gliotoxin as first natural compound targeting selective epoxide hydrolase activity. Furthermore, several other enzymes involved in the AA pathway harbor an epoxide hydrolase activity like

sEH or other hepoxilin hydrolases. Apart from its N-terminal phosphatase activity, sEH contains also a C-terminal epoxide hydrolase activity [230] converting anti-inflammatory epoxy fatty acids to their corresponding diol metabolites and playing hence an important role in inflammatory diseases, e.g., cardiovascular, neuro-inflammatory, and metabolic diseases [14, 231, 232]. However, gliotoxin failed to inhibit sEH in two different cell lines A549 and HepG2 [218] as wells as under cell-free conditions (unpublished data).

Gliotoxin failed to suppress LTA_4H activity under cell-free conditions. Structurally, epidithiodioxopiperazines contain an intramolecular disulfide bridge, which is mandatory for their biological activity and can be cleaved, inter alia, by glutathione (GSH) or dithiothreitol (DTT) to its reduced dithiol form [164]. Our data revealed that the reduced dithiol form of gliotoxin is required for suppression of LTA_4H activity. Indeed, we provided exogenous GSH in cell-free experimental settings, whereas in intact cells GSH is abundant in the cytosol. Cellular treatment with the oxidizing diamide impaired the inhibitory effect of gliotoxin on LTA_4H. As expected, redox active agents, e.g., GSH or diamide, did not influence the activity of SC-57461A. Moreover, gliotoxin suppressed LTA_4H activity, when it was first incubated in intact cells followed by a cell lysis prior stimulation, which indicates irreversible LTA_4H inhibition comparable to SC-57461A. We assumed that reduced gliotoxin interacted with LTA_4H, where the free thiol moieties reacted with the active site of LTA_4H coordinating the epoxide hydrolase activity [82]. As described before, LTA_4H is a monomeric zinc metalloenzyme in which zinc connects both enzymatic binding pockets [84]. Conceivably, gliotoxin reacted with the active site Zn^{2+} forming chelate complexes by its reduced free thiol groups supported by the results that supplementation of external Zn^{2+} ions impaired the inhibitory activity of gliotoxin without affecting the potency of SC-57461A. Our data were confirmed by a recently published paper, where reduced gliotoxin inhibited the Zn^{2+}-dependent alkaline phosphatase by chelation of Zn^{2+} [233]. Along these lines, other thiodioxopiperazines exhibited similar modes of action like sporidesmin playing an important role in agriculture and veterinary medicine [234, 235] due to its interaction with thiol-disulfide oxidoreductases [236], or chaetocin being a substrate for thioredoxin reductase [237] as well as the antibiotic thiolutin harboring a dithiopyrrolone structure and inactivating JAB1/MPN/Mov34 (JAMM) metalloproteases [238]. All compounds are natural ingredients of fungi species containing an intramolecular disulfide bond and acted mostly under reducing conditions with metalloproteases harboring an active site Zn^{2+} ion. Furthermore, the inhibitory effects were avoided by external supplementation of Zn^{2+} ions [238, 239] indicating further targets of gliotoxin and a possible substance class effect for Zn^{2+}-containing metalloproteases, where previously described structures could also interact with LTA_4H except of chaetocin, which we have already tested (unpublished data).

In the last decades, the influence of mycotoxins especially ingredients of the mold *A. fumigatus* increased the triggering of allergic and respiratory diseases for humans due to the

enhanced contact with molds [240, 241]. Humans continuously inhale conidia of *A. fumigatus* that trigger the host defense leading to a recruitment of neutrophils to the site of infection [242]. Immunocompromised patients lack the efficient innate immune response and hence exhibit an increased risk for diseases [243]. One major virulence factor of *A. fumigatus* is gliotoxin [244] causing IA with high mortality rates (30-95%) of immunocompromised patients [181] particularly with neutropenic conditions [1, 170, 245]. Of interest, neutrophils were resistant to gliotoxin-mediated apoptosis [175], and neutrophil functions were not affected by gliotoxin except phagocytosis [170]. Recently, it was shown that host-derived LTB_4 played an important role in innate immunity to IA, and LTB_4 was crucial for the host resistance to *A. fumigatus* mediating the recruitment of neutrophils [246]. Furthermore, LTB_4-treated neutrophils exhibited an increased antifungal activity against *A. fumigatus* [247], and reduced LTB_4 levels led to enhanced mortality of *A. fumigatus* infected mice and raised fungal germination in lung tissue [246]. These facts and the knowledge that gliotoxin was produced during the infection process [3] supported our hypothesis that reduced LTB_4 formation by gliotoxin is the underlying mechanism for neutropenic conditions in the infected host. Furthermore, infection of mice with an *A. fumigatus* strain with an eliminated *gliP* gene (involved in the first biosynthesis step of gliotoxin (Δ*gliP*) [248]) exhibited a reduced virulence of *A. fumigatus* confirming gliotoxin as significant inducer of aspergillosis [1]. As expected, Δ*gliP*-infected mice showed an abrogated neutrophil infiltration and a lower degree of destructed neutrophils in lung tissue in comparison to lung tissue of mice infected with wild type *A. fumigatus*. Together, Δ*gliP* and thus, the reduced gliotoxin biosynthesis failed to compromise neutrophils and their functions, indicating that gliotoxin caused neutropenia by hampered LTB_4 formation due to LTA_4H inhibition in *A. fumigatus*-infected hosts and clarifying thereby the underlying virulence mechanism of *A. fumigatus*-triggered IA.

In conclusion, we identified LTA_4H as a target of gliotoxin hampering the biosynthesis of the major chemoattractant for neutrophils, namely LTB_4, which plays an important role in the innate immune response. The clarification of the mode of action of gliotoxin is of biological relevance for the pathology of *A. fumigatus* and the neutrophil-mediated host resistance against IA for the generation of clinical pictures and the development of new therapeutic approaches.

4.2 Natural compounds and their influence on cell viability in human cells

As previously described, gliotoxin and DAO play also an important role as potent fungal toxins in human cancer cells as well as in primary immune cells [186, 194, 207, 249] with partially enlightened modes of action, whereby the cytotoxicity of myxochelins have not been yet analyzed in human cells (**additional data**).

In contrast to DAO, several targets of gliotoxin are known to mediate cell death. In general, cell death can be distinguished by three main types: (I) apoptosis, (II) autophagy, and

(III) necrosis, mediated by various signaling pathways [126]. In fact, gliotoxin induced apoptosis by caspase 3 activation [207] and increased ROS formation during its redox cycle eliciting oxidative stress [250, 251]. Additionally, gliotoxin caused activation of JNK leading to Bim activation and facilitation of the pro-apoptotic Bak oligomerization resulting in cytochrome c and ROS release by mitochondria followed by caspase 9 activation [180, 252]. Furthermore, DNA was fragmented by gliotoxin after enhanced cAMP levels, which activated PKA and triggered the phosphorylation of histone 3 [179], and gliotoxin prevented NFκB activation by IκBα stabilization [177]. However, neutrophils were not affected by gliotoxin regarding apoptosis [175]. Conventionally, cytotoxic agents exhibit a higher potency to induce cell death in cancer cells than in non-transformed cells (**manuscript IV**, [253]) mediated by intensified metabolic processes with high energy turnover and stronger proliferation of cancer cells. Also myxochelins reduced the viability only of cancer cells without affecting primary immune cells (**additional data**). Interestingly, these myxobacterial compounds exhibited cytotoxic effects primarily in leukemic cells hypothesizing a correlation to 5-LOX inhibition, since 5-LOX is one key enzyme in myeloid leukemia cells [254-256], and myxochelins failed to cause cytotoxicity in 5-LOX deficient HeLa cells (**additional data**, **manuscript III**). Nevertheless, existence of further targets related to their cytotoxicity should be considered. In the case of melleolides, DAO showed similar apoptotic patterns in primary monocytes as compared to several cancer cells with an untypical rapid onset of cell death (**manuscript IV**) linking apoptosis, autophagic cell death, and necrosis by targeting the phospholipid PE of various cellular membranes, leading to a loss of several pivotal cell functions (**manuscript V**).

As described before, melleolides caused cytotoxic effects in human cells by ROS-mediated caspase activation [187], decreased DNA synthesis [194], or due to autophagy-associated cell death [195], but a specific target is still elusive. In general, most compounds mediating cell death evinced more potent cytotoxicity towards cancer cells due to their enhanced proliferation and increased metabolic processes as non-transformed cells [253, 257, 258]. It was shown that melleolides from *Armillaria mellea* reduced potently cell viability of various human cancer cell lines [186, 194] lacking the analysis of cytotoxicity of melleolides in human primary cells. Our results exhibited similar cytotoxic effects of the sesquiterpene aryl ester DAO in human primary monocytes (IC_{50}=2.3 µM) and in various cancer cells including the leukemic cell lines THP-1 (IC_{50}=3.0 µM), MM6 (IC_{50}=4.2 µM), K-562 (IC_{50}=5.0 µM), and the immortal cervix carcinoma cell line HeLa cells (IC_{50}=1.6 µM) (**manuscript IV**). Subsequently, we analyzed the structure-activity relationship of six different melleolides (including arnamial, 6´-dechloroarnamial, DAO, armillarin, armillaridin, melleolide D) to get information about the structural residues, which are actively participated in cell death induction. As a result, compounds harboring a $\Delta^{2,4}$ double bond, e.g., arnamial, 6´-dechloroarnamial, and DAO, caused a potent loss of cell viability for all tested cell types, comparable to their antifungal

activity [186]. Armillarin and armillaridin, which possess a $\Delta^{2,3}$ double bond, induced similar cytotoxic effects in monocytic THP-1 and MM6 cell lines but showed a reduced cytotoxic potency in primary monocytes, K-562, and HeLa cells. Of interest, THP-1 and MM6 cells are acute monocytic leukemia cells, whereas K-562 cells are chronic myelogenous leukemia cells, which might be the reason for the different cytotoxic impact of DAO between the leukemia cell lines. In contrast, melleolide D possesses a $\Delta^{2,3}$ double bond and a hydroxyl residue instead of the free aldehyde moiety at position 1, resulting in negligible cytotoxic properties. In fact, compounds containing a $\Delta^{2,4}$ or a $\Delta^{2,3}$ unsaturated aldehyde caused potent cytotoxicity, whereas the $\Delta^{2,3}$ unsaturated aldehyde exerted reduced effects suggesting that only an unsaturated aldehyde residue at the sesquiterpene moiety caused reduced cell viability. Contrarily to the melleolides, the well-known apoptotic pan-kinase inhibitor staurosporine [259] and the cytotoxic myxobacterial compound pretubulysin, acting as microtubule disrupting agent [258, 260], caused efficient cytotoxicity in cancer cells but not so in monocytes. Hence, we hypothesize a general target for cytotoxicity of melleolides, which might be independent from proliferation and metabolic processes. Other sesquiterpenes like acylfulvenes and their natural precursor illudin S harboring also a $\Delta^{2,4}$ unsaturated aldehyde moiety [261], which show a high reactivity with thiol residues and cysteine-containing proteins [262], exhibited a comparable cytotoxicity for non-transformed cells and cancer cells, presumably due to an interaction with DNA after a reductive activation by prostaglandin reductase 1 [261]. Acylfulvenes and melleolides harbor similar structural elements, which may result in similar mechanisms for cell death induction like impaired DNA biosynthesis [194, 261, 262].

Melleolides, especially DAO, caused rapid cytotoxic effects after about 1 hr measured by MTT assay, whereas the pan-kinase inhibitor staurosporine [259], the protein biosynthesis inhibitor cycloheximide and the DNA transcription inhibitor actinomycin [263] required more than 5 hrs to impair cell viability. We speculated that melleolides could interact with the plasma membrane to induce cell lysis. Opposed to this, morphological analysis of cells treated with DAO, staurosporine, or triton X-100 by light microscopy excluded cell lysis as possible mechanism. Thus, the detergent triton X-100 was used as positive control for cell permeabilization exhibiting contrarily modifications of cell morphology. Within the analyzed time, DAO caused typical features of necrosis such as plasma membrane rupture of the monocytes after 3 hrs exposure to DAO, whereas staurosporine induced fragmentation of the nucleus and triggered the formation of apoptotic bodies, which are characteristics of apoptosis [126, 128]. Interestingly, further investigations by flow cytometry disclosed also apoptotic signals without statistical significance in contrast to staurosporine, which clearly provoked significantly apoptosis without any necrotic patterns, as expected. Moreover, metabolic activity of mitochondria was decreased by DAO, which is also a sign of apoptosis, leading to the

hypothesis, that DAO may influence the mitochondrial membrane potential and DAO may induce various forms of cell death (**manuscript IV**).

In general, the classical apoptosis pathway is dependent on caspase activation initiated by an extrinsic or intrinsic pathway leading to the cleavage of PARP [130]. In our study, DAO affected PARP cleavage already after 15 min, while staurosporine required 5 hrs for the cleavage. Of interest, caspases were only slightly affected by DAO indicating a caspase-independent apoptosis [139], but pre-incubation with the pan-caspase inhibitor QVD prevented at least PARP cleavage [264], nevertheless reduced cell viability was available caused by DAO as well as staurosporine. Seemingly, slightly caspase 8 activation by DAO was sufficient for triggering apoptosis signaling (**manuscript V**). Furthermore, we showed by the decrease of the phosphorylation of the survival factor Akt and an increased phosphorylation of the stress factor p38 MAPK that cellular processes became disordered. However, activation of p38 MAPK was independent on ER stress and on the activation of the unfolded protein response. Of interest, besides an abrogated metabolic activity, DAO disrupted also the cell membrane within 15 min measured by LDH assay supporting initiation of necrosis with the loss of membrane integrity. As described before, DAO harbors a reactive α,β-unsaturated aldehyde residue mediating the majority of its biological activities [186, 265]. Other natural products containing a Michael acceptor residue, especially an α,β-unsaturated aldehyde, modulated membrane functions like the sesquiterpene dialdehyde polygodial triggering a membrane rupture of *Saccharomyces cerevisiae* by building covalent adducts with phospholipids of the plasma membrane [266-269]. Similar effects were reported for ophiobolin A isolated from the *Bipolaris* genus that mediated cell death by forming pyrrole-containing adducts with PE of the cellular membrane [270]. However, ophiobolin A did not affect exclusively plasma membrane phospholipids, but also mitochondrial functionality provoked by depolarized mitochondrial membrane potential, increased ROS production, and mitochondrial network fragmentation [271, 272] linking apoptosis, autophagy, and necrosis. In the case of DAO, we detected a comparable mode of action to polygodial and ophiobolin A. By pre-incubations with the phospholipids PE, PS, and PC, we demonstrated that DAO interacted with the ethanolamine head group of PE measured by UPLC-MS/MS. Furthermore, the time course of DAO-ethanolamine (DAO-EA) product formation correlated to LDH release, supporting our hypothesis that DAO-EA product formation was responsible for the early loss of membrane fluidity and functionality. Usually, PE is located at the inner leaflet of plasma membranes [273], but during the early stage of apoptosis PE as well as PS are translocated from the inner leaflet to the cell membrane surface [274], which may explain the early cytotoxic effects of DAO. Additional, PE is not only available in plasma membranes but also in other cell organelle membranes like nuclei, mitochondria, ER, or lysosomes, where a greater portion of PE is located within the outer leaflet of mitochondria in comparison to other organelles [273]. This

can be explained by the synthesis and trafficking of PE between ER and mitochondria [273]. As described before, other melleolides like armillarikin or armillaridin made a negative impact on mitochondrial transmembrane potential [187, 195], which plays an important role for ATP generation, and inducing thereby apoptosis. Consequently, mitochondrial dysfunction leads to an increased permeability of the mitochondrial membrane and a subsequent release of the proapoptotic stimulus cytochrome c into the cytosol, which initialize downstream events in the apoptotic cascade [275]. Of interest, exposure to DAO for 3 hrs enhanced strongly the release of cytochrome c into the cytosol with a simultanously decrease of non-cytosolic cytochrome c. These results were comparable to staurosporine increasing also the release of cytochrome c from mitochondria, but less pronounced as compared to DAO. Moreover, transmission electron microscopy (TEM) of monocytes after DAO treatment revealed us defects of the nuclear membrane and in particular, a disappearance of mitochondria, leading to the hypothesis that DAO induced rapid cell death by interacting with membranous PE of several cell organelles. Additional, we supported our thesis with liposome leakage assays, where DAO caused leakage of PE-composed liposomes in cell-free system, but liposomes made from PC were not affected by DAO indicating a covalent binding to the EA moiety in PE. Otherwise PE acts as anchor for autophagosomes [276] thus supporting recycling of cytoplasmic structures by autophagy leading to ATP generation [141]. Our data revealed that DAO interacted primarily with PE of the membrane fraction containing plasma membrane, lysosomes, and Golgi vesicles, and equally with mitochondria and nuclei after 15 min incubations analyzed by a subcellular fractionation. Interestingly, after 3 hrs, plasma membrane interaction of DAO was increased, whereas the accumulation in mitochondria remained unchanged and in nuclei decreased. As expected, exposure to DAO induced a reorganization of PE species, especially the most common PE species PE(18:0/18:1) and PE(18:1/18:1), in the plasma membrane fraction, which could be explained as protecting metabolic processes. Furthermore, an interaction of DAO with lysosomal PE could cause reduced PE amounts in lysosomal membranes and abrogated autophagic processes leading to apoptosis due to impaired ATP formation [276]. An enhanced amount of autophagosomes was detectable in apoptotic cells supporting autophagy as cytoprotective mechanism for elimination of toxic molecules [277, 278]. As a consequence of intensified autophagic processes, formation of lysosomes increased resulting in a strengthened intake of DAO leading to a lysosomal rupture with intracellular acidification caused by released lysosomal hydrolases and finally triggering necrosis. Additional, lysosome formation could become hyperactive to support cell functions by energy generation resulting in a breakdown of cellular organelles and proteins provoking eventually self-cannibalism [147]. This hypothesis is supported by an increased lysosomal rupture and decreased intracellular pH value caused by DAO. However, autophagy correlated also with caspase 8 activation involving autophagy protein 5 (Atg5) and LC3-PE that are

responsible for the extension of autophagosomal membrane and autophagosome formation [279-282]. Our results demonstrate that DAO influenced only slightly caspase 8 activity without affecting other apoptotic caspases. Together with the intracellular PE interaction, the decreased PE amount and the decreased intracellular pH value, we speculate that DAO additionally prevented the autophagosomal membrane formation hypothesizing that affected cells might execute appropriate countermeasures to gain energy which could result in a hyperactive autophagy leading to a loss of organized metabolic processes and finally fast cell death.

In conclusion, we studied the cytotoxic mode of action of DAO causing cell death by a covalent interaction of its α,β-unsaturated aldehyde moiety with the ethanolamine head group of PE of several cell organelles acting as non-ionic surfactant. Due to these effects, DAO linked various forms of cytotoxicity and thus leading to a destruction of metabolic processes.

4.3 Conclusion

We here characterized and clarified several biological activities and mode of actions of natural compounds from fungi and bacteria, namely DAO from *Armillaria mellea*, gliotoxin from *Aspergillus fumigatus*, and myxochelin A from *Pyxidicoccus fallax*, respectively, in human primary immune cells. The 5-LOX pathway plays a considerable role in inflammation by mediating the biosynthesis of important pro-inflammatory LM. DAO as well as myxochelins inhibited 5-LOX activity and thus prevented the formation of LT. In brief, we identified 5-LOX as a molecular target of melleolides from *A. mellea* and myxochelins from *P. fallax*. We propose that melleolides containing an α,β-unsaturated aldehyde moiety function as Michael acceptors leading to an interference of critical surface cysteines of 5-LOX. On the enzymatic level, two or more of these cysteines trigger the inhibitory effect of melleolides, whereas only C^{159} mediates the suppression of cellular 5-LOX product formation by melleolides due to the prevention of 5-LOX/FLAP complex assembly. Conclusively, our data emphasize the importance of C^{159} for 5-LOX/FLAP interaction, which is a requirement for cellular LT biosynthesis. While melleolides appear unsuitable for the therapeutic usage due to their potent cytotoxicity towards primary immune cells representing a new way for cell death induction, myxochelins constitute an interesting substance class for new 5-LOX inhibitors. However, further investigations are crucial to fulfil the characterization of 5-LOX inhibition *in vitro* and to analyze the compounds *in vivo*. Furthermore, myxochelins could be used in the therapy of acute and chronic leukemia due to their anti-proliferative effects in leukemic cells without affecting primary cells requiring further investigations to clarify the mode of action. In contrast, DAO targets the membrane PE by a covalent reaction of its α,β-unsaturated aldehyde moiety with the EA head group of the phospholipid leading to a perturbation of cellular membrane structure. Consequently, membrane integrity is impaired, which might be the reason for the unusual rapid onset of cell death in various cell types. The knowledge about the cytotoxic

mechanism of DAO can be used as tool for the analysis of cellular processes and the generation of new anti-cancer drugs. Last but not least, we reveal LTA_4H as molecular target of the mycotoxin gliotoxin from *A. fumigatus*, and thus, we suggest inhibition of the biosynthesis of the pivotal chemoattractant LTB_4 as biological relevant mode of action of gliotoxin. On the basis of these immunomodulatory effects by gliotoxin in human neutrophils, new therapeutic approaches can be developed to successfully treat IA of immunocompromised patients and thus reducing the high mortality rate. Furthermore, gliotoxin can be used as structural starting basis for the design of new LTA_4H inhibitors which affect only the pro-inflammatory epoxide hydrolase activity without influencing the aminopeptidase activity.

5. LITERATURE

1. Sugui, J.A., et al., *Gliotoxin is a virulence factor of Aspergillus fumigatus: gliP deletion attenuates virulence in mice immunosuppressed with hydrocortisone.* Eukaryot Cell, 2007. **6**(9): p. 1562-9.
2. Sutton, P., P. Waring, and A. Mullbacher, *Exacerbation of invasive aspergillosis by the immunosuppressive fungal metabolite, gliotoxin.* Immunol Cell Biol, 1996. **74**(4): p. 318-22.
3. Sugui, J.A., et al., *Host immune status-specific production of gliotoxin and bis-methyl-gliotoxin during invasive aspergillosis in mice.* Sci Rep, 2017. **7**(1): p. 10977.
4. Samuelsson, B., et al., *Leukotrienes and lipoxins: structures, biosynthesis, and biological effects.* Science, 1987. **237**(4819): p. 1171-6.
5. Afonso, P.V., et al., *LTB4 is a signal-relay molecule during neutrophil chemotaxis.* Dev Cell, 2012. **22**(5): p. 1079-91.
6. Carter, G.W., et al., *5-lipoxygenase inhibitory activity of zileuton.* J Pharmacol Exp Ther, 1991. **256**(3): p. 929-37.
7. Askonas, L.J., et al., *Pharmacological characterization of SC-57461A (3-[methyl[3-[4-(phenylmethyl)phenoxy]propyl]amino]propanoic acid HCl), a potent and selective inhibitor of leukotriene A(4) hydrolase I: in vitro studies.* J Pharmacol Exp Ther, 2002. **300**(2): p. 577-82.
8. Kachur, J.F., et al., *Pharmacological characterization of SC-57461A (3-[methyl[3-[4-(phenylmethyl)phenoxy]propyl]amino]propanoic acid HCl), a potent and selective inhibitor of leukotriene A(4) hydrolase II: in vivo studies.* J Pharmacol Exp Ther, 2002. **300**(2): p. 583-7.
9. Hillmann, F., et al., *Virulence determinants of the human pathogenic fungus Aspergillus fumigatus protect against soil amoeba predation.* Environ Microbiol, 2015. **17**(8): p. 2858-69.
10. Radmark, O., et al., *5-Lipoxygenase, a key enzyme for leukotriene biosynthesis in health and disease.* Biochim Biophys Acta, 2015. **1851**(4): p. 331-9.
11. Tholander, F., et al., *Crystal structure of leukotriene A4 hydrolase in complex with kelatorphan, implications for design of zinc metallopeptidase inhibitors.* FEBS Lett, 2010. **584**(15): p. 3446-51.
12. Snelgrove, R.J., *Leukotriene A4 hydrolase: an anti-inflammatory role for a proinflammatory enzyme.* Thorax, 2011. **66**(6): p. 550-1.
13. Haeggstrom, J.Z., F. Tholander, and A. Wetterholm, *Structure and catalytic mechanisms of leukotriene A4 hydrolase.* Prostaglandins Other Lipid Mediat, 2007. **83**(3): p. 198-202.
14. Wagner, K.M., et al., *Soluble epoxide hydrolase as a therapeutic target for pain, inflammatory and neurodegenerative diseases.* Pharmacol Ther, 2017. **180**: p. 62-76.
15. Hornig, M., et al., *Inhibition of 5-lipoxygenase by U73122 is due to covalent binding to cysteine 416.* Biochim Biophys Acta, 2012. **1821**(2): p. 279-86.
16. Maucher, I.V., et al., *Michael acceptor containing drugs are a novel class of 5-lipoxygenase inhibitor targeting the surface cysteines C416 and C418.* Biochem Pharmacol, 2017. **125**: p. 55-74.
17. Chae, H.J., et al., *Molecular mechanism of staurosporine-induced apoptosis in osteoblasts.* Pharmacol Res, 2000. **42**(4): p. 373-81.
18. Belmokhtar, C.A., J. Hillion, and E. Segal-Bendirdjian, *Staurosporine induces apoptosis through both caspase-dependent and caspase-independent mechanisms.* Oncogene, 2001. **20**(26): p. 3354-62.
19. Gilbert, N.C., et al., *The structure of human 5-lipoxygenase.* Science, 2011. **331**(6014): p. 217-9.
20. Lawrence, T., D.A. Willoughby, and D.W. Gilroy, *Anti-inflammatory lipid mediators and insights into the resolution of inflammation.* Nat Rev Immunol, 2002. **2**(10): p. 787-95.
21. Medzhitov, R., *Origin and physiological roles of inflammation.* Nature, 2008. **454**(7203): p. 428-35.

22. Basil, M.C. and B.D. Levy, *Specialized pro-resolving mediators: endogenous regulators of infection and inflammation.* Nat Rev Immunol, 2016. **16**(1): p. 51-67.
23. Levy, B.D., et al., *Lipid mediator class switching during acute inflammation: signals in resolution.* Nat Immunol, 2001. **2**(7): p. 612-9.
24. Kundu, J.K. and Y.J. Surh, *Inflammation: gearing the journey to cancer.* Mutat Res, 2008. **659**(1-2): p. 15-30.
25. Aggarwal, B.B., et al., *Inflammation and cancer: how hot is the link?* Biochem Pharmacol, 2006. **72**(11): p. 1605-21.
26. Balkwill, F. and A. Mantovani, *Inflammation and cancer: back to Virchow?* Lancet, 2001. **357**(9255): p. 539-45.
27. de Visser, K.E., A. Eichten, and L.M. Coussens, *Paradoxical roles of the immune system during cancer development.* Nat Rev Cancer, 2006. **6**(1): p. 24-37.
28. Hanahan, D. and R.A. Weinberg, *Hallmarks of cancer: the next generation.* Cell, 2011. **144**(5): p. 646-74.
29. Elinav, E., et al., *Inflammation-induced cancer: crosstalk between tumours, immune cells and microorganisms.* Nat Rev Cancer, 2013. **13**(11): p. 759-71.
30. Aggarwal, B.B., *Nuclear factor-kappaB: the enemy within.* Cancer Cell, 2004. **6**(3): p. 203-8.
31. Karin, M., *Nuclear factor-kappaB in cancer development and progression.* Nature, 2006. **441**(7092): p. 431-6.
32. Aggarwal, B.B., R.V. Vijayalekshmi, and B. Sung, *Targeting inflammatory pathways for prevention and therapy of cancer: short-term friend, long-term foe.* Clin Cancer Res, 2009. **15**(2): p. 425-30.
33. Rich, M.R., *Conformational analysis of arachidonic and related fatty acids using molecular dynamics simulations.* Biochim Biophys Acta, 1993. **1178**(1): p. 87-96.
34. Brash, A.R., *Arachidonic acid as a bioactive molecule.* J Clin Invest, 2001. **107**(11): p. 1339-45.
35. Martin, S.A., A.R. Brash, and R.C. Murphy, *The discovery and early structural studies of arachidonic acid.* J Lipid Res, 2016. **57**(7): p. 1126-32.
36. Funk, C.D., *Prostaglandins and leukotrienes: advances in eicosanoid biology.* Science, 2001. **294**(5548): p. 1871-5.
37. Samuelsson, B., *Leukotrienes: a new class of mediators of immediate hypersensitivity reactions and inflammation.* Adv Prostaglandin Thromboxane Leukot Res, 1983. **11**: p. 1-13.
38. Serhan, C.N., M. Hamberg, and B. Samuelsson, *Lipoxins: novel series of biologically active compounds formed from arachidonic acid in human leukocytes.* Proc Natl Acad Sci U S A, 1984. **81**(17): p. 5335-9.
39. Serhan, C.N., M. Hamberg, and B. Samuelsson, *Trihydroxytetraenes: a novel series of compounds formed from arachidonic acid in human leukocytes.* Biochem Biophys Res Commun, 1984. **118**(3): p. 943-9.
40. Pergola, C. and O. Werz, *5-Lipoxygenase inhibitors: a review of recent developments and patents.* Expert Opin Ther Pat, 2010. **20**(3): p. 355-75.
41. Werz, O., J. Gerstmeier, and U. Garscha, *Novel leukotriene biosynthesis inhibitors (2012-2016) as anti-inflammatory agents.* Expert Opin Ther Pat, 2017. **27**(5): p. 607-620.
42. Meirer, K., D. Steinhilber, and E. Proschak, *Inhibitors of the arachidonic acid cascade: interfering with multiple pathways.* Basic Clin Pharmacol Toxicol, 2014. **114**(1): p. 83-91.
43. Kuhn, H., S. Banthiya, and K. van Leyen, *Mammalian lipoxygenases and their biological relevance.* Biochim Biophys Acta, 2015. **1851**(4): p. 308-30.
44. Borgeat, P., M. Hamberg, and B. Samuelsson, *Transformation of arachidonic acid and homo-gamma-linolenic acid by rabbit polymorphonuclear leukocytes. Monohydroxy acids from novel lipoxygenases.* J Biol Chem, 1976. **251**(24): p. 7816-20.
45. Brash, A.R., *Lipoxygenases: occurrence, functions, catalysis, and acquisition of substrate.* J Biol Chem, 1999. **274**(34): p. 23679-82.

46. Radmark, O. and B. Samuelsson, *Regulation of the activity of 5-lipoxygenase, a key enzyme in leukotriene biosynthesis.* Biochem Biophys Res Commun, 2010. **396**(1): p. 105-10.
47. Haeggstrom, J.Z., P. Nordlund, and M.M. Thunnissen, *Functional properties and molecular architecture of leukotriene A4 hydrolase, a pivotal catalyst of chemotactic leukotriene formation.* ScientificWorldJournal, 2002. **2**: p. 1734-49.
48. Chasteen, N.D., et al., *Characterization of the non-heme iron center of human 5-lipoxygenase by electron paramagnetic resonance, fluorescence, and ultraviolet-visible spectroscopy: redox cycling between ferrous and ferric states.* Biochemistry, 1993. **32**(37): p. 9763-71.
49. Rakonjac Ryge, M., et al., *A mutation interfering with 5-lipoxygenase domain interaction leads to increased enzyme activity.* Arch Biochem Biophys, 2014. **545**: p. 179-85.
50. Hafner, A.K., et al., *Characterization of the interaction of human 5-lipoxygenase with its activating protein FLAP.* Biochim Biophys Acta, 2015. **1851**(11): p. 1465-72.
51. Hafner, A.K., et al., *Dimerization of human 5-lipoxygenase.* Biol Chem, 2011. **392**(12): p. 1097-111.
52. Dixon, R.A., et al., *Requirement of a 5-lipoxygenase-activating protein for leukotriene synthesis.* Nature, 1990. **343**(6255): p. 282-4.
53. Evans, J.F., et al., *What's all the FLAP about?: 5-lipoxygenase-activating protein inhibitors for inflammatory diseases.* Trends Pharmacol Sci, 2008. **29**(2): p. 72-8.
54. Gillard, J., et al., *L-663,536 (MK-886) (3-[1-(4-chlorobenzyl)-3-t-butyl-thio-5-isopropylindol-2-yl]-2,2 - dimethylpropanoic acid), a novel, orally active leukotriene biosynthesis inhibitor.* Can J Physiol Pharmacol, 1989. **67**(5): p. 456-64.
55. Miller, D.K., et al., *Identification and isolation of a membrane protein necessary for leukotriene production.* Nature, 1990. **343**(6255): p. 278-81.
56. Ferguson, A.D., et al., *Crystal structure of inhibitor-bound human 5-lipoxygenase-activating protein.* Science, 2007. **317**(5837): p. 510-2.
57. Newcomer, M.E. and N.C. Gilbert, *Location, location, location: compartmentalization of early events in leukotriene biosynthesis.* J Biol Chem, 2010. **285**(33): p. 25109-14.
58. Mandal, A.K., et al., *The membrane organization of leukotriene synthesis.* Proc Natl Acad Sci U S A, 2004. **101**(17): p. 6587-92.
59. Gur, Z.T., B. Caliskan, and E. Banoglu, *Drug discovery approaches targeting 5-lipoxygenase-activating protein (FLAP) for inhibition of cellular leukotriene biosynthesis.* Eur J Med Chem, 2018. **153**: p. 34-48.
60. Werz, O., et al., *Activation of 5-lipoxygenase by cell stress is calcium independent in human polymorphonuclear leukocytes.* Blood, 2002. **99**(3): p. 1044-52.
61. Radmark, O. and B. Samuelsson, *5-lipoxygenase: regulation and possible involvement in atherosclerosis.* Prostaglandins Other Lipid Mediat, 2007. **83**(3): p. 162-74.
62. Borgeat, P. and B. Samuelsson, *Arachidonic acid metabolism in polymorphonuclear leukocytes: effects of ionophore A23187.* Proc Natl Acad Sci U S A, 1979. **76**(5): p. 2148-52.
63. Ali, H., et al., *The ability of thapsigargin and thapsigargicin to activate cells involved in the inflammatory response.* Br J Pharmacol, 1985. **85**(3): p. 705-12.
64. Abramovitz, M., et al., *5-lipoxygenase-activating protein stimulates the utilization of arachidonic acid by 5-lipoxygenase.* Eur J Biochem, 1993. **215**(1): p. 105-11.
65. Werz, O. and D. Steinhilber, *Therapeutic options for 5-lipoxygenase inhibitors.* Pharmacol Ther, 2006. **112**(3): p. 701-18.
66. Maas, R.L., et al., *Stereospecific removal of the DR hydrogen atom at the 10-carbon of arachidonic acid in the biosynthesis of leukotriene A4 by human leukocytes.* J Biol Chem, 1982. **257**(22): p. 13515-9.
67. Borgeat, P. and B. Samuelsson, *Arachidonic acid metabolism in polymorphonuclear leukocytes: unstable intermediate in formation of dihydroxy acids.* Proc Natl Acad Sci U S A, 1979. **76**(7): p. 3213-7.

68. Lam, B.K. and K.F. Austen, *Leukotriene C4 synthase: a pivotal enzyme in cellular biosynthesis of the cysteinyl leukotrienes.* Prostaglandins Other Lipid Mediat, 2002. **68-69**: p. 511-20.
69. Peters-Golden, M., M.M. Gleason, and A. Togias, *Cysteinyl leukotrienes: multi-functional mediators in allergic rhinitis.* Clin Exp Allergy, 2006. **36**(6): p. 689-703.
70. Jones, T.R., et al., *Pharmacology of montelukast sodium (Singulair), a potent and selective leukotriene D4 receptor antagonist.* Can J Physiol Pharmacol, 1995. **73**(2): p. 191-201.
71. Werz, O., *Inhibition of 5-lipoxygenase product synthesis by natural compounds of plant origin.* Planta Med, 2007. **73**(13): p. 1331-57.
72. Tateson, J.E., et al., *Selective inhibition of arachidonate 5-lipoxygenase by novel acetohydroxamic acids: biochemical assessment in vitro and ex vivo.* Br J Pharmacol, 1988. **94**(2): p. 528-39.
73. Schaible, A.M., et al., *The 5-lipoxygenase inhibitor RF-22c potently suppresses leukotriene biosynthesis in cellulo and blocks bronchoconstriction and inflammation in vivo.* Biochem Pharmacol, 2016. **112**: p. 60-71.
74. Schaible, A.M., et al., *Potent inhibition of human 5-lipoxygenase and microsomal prostaglandin E(2) synthase-1 by the anti-carcinogenic and anti-inflammatory agent embelin.* Biochem Pharmacol, 2013. **86**(4): p. 476-86.
75. Kusner, E.J., et al., *The 5-lipoxygenase inhibitors ZD2138 and ZM230487 are potent and selective inhibitors of several antigen-induced guinea-pig pulmonary responses.* Eur J Pharmacol, 1994. **257**(3): p. 285-92.
76. Grimm, E.L., et al., *Substituted coumarins as potent 5-lipoxygenase inhibitors.* Bioorg Med Chem Lett, 2006. **16**(9): p. 2528-31.
77. Feisst, C., et al., *Hyperforin is a novel type of 5-lipoxygenase inhibitor with high efficacy in vivo.* Cell Mol Life Sci, 2009. **66**(16): p. 2759-71.
78. Albert, D., et al., *Hyperforin is a dual inhibitor of cyclooxygenase-1 and 5-lipoxygenase.* Biochem Pharmacol, 2002. **64**(12): p. 1767-75.
79. Pergola, C., et al., *Indirubin core structure of glycogen synthase kinase-3 inhibitors as novel chemotype for intervention with 5-lipoxygenase.* J Med Chem, 2014. **57**(9): p. 3715-23.
80. Haeggstrom, J.Z. and C.D. Funk, *Lipoxygenase and leukotriene pathways: biochemistry, biology, and roles in disease.* Chem Rev, 2011. **111**(10): p. 5866-98.
81. Brock, T.G., et al., *Co-localization of leukotriene a4 hydrolase with 5-lipoxygenase in nuclei of alveolar macrophages and rat basophilic leukemia cells but not neutrophils.* J Biol Chem, 2001. **276**(37): p. 35071-7.
82. Stsiapanava, A., B. Samuelsson, and J.Z. Haeggstrom, *Capturing LTA4 hydrolase in action: Insights to the chemistry and dynamics of chemotactic LTB4 synthesis.* Proc Natl Acad Sci U S A, 2017. **114**(36): p. 9689-9694.
83. Mueller, M.J., et al., *Leukotriene A4 hydrolase: protection from mechanism-based inactivation by mutation of tyrosine-378.* Proc Natl Acad Sci U S A, 1996. **93**(12): p. 5931-5.
84. Thunnissen, M.M., P. Nordlund, and J.Z. Haeggstrom, *Crystal structure of human leukotriene A(4) hydrolase, a bifunctional enzyme in inflammation.* Nat Struct Biol, 2001. **8**(2): p. 131-5.
85. Rudberg, P.C., et al., *Leukotriene A4 hydrolase/aminopeptidase. Glutamate 271 is a catalytic residue with specific roles in two distinct enzyme mechanisms.* J Biol Chem, 2002. **277**(2): p. 1398-404.
86. Rudberg, P.C., et al., *Leukotriene A4 hydrolase: identification of a common carboxylate recognition site for the epoxide hydrolase and aminopeptidase substrates.* J Biol Chem, 2004. **279**(26): p. 27376-82.
87. Rudberg, P.C., et al., *Leukotriene A4 hydrolase: selective abrogation of leukotriene B4 formation by mutation of aspartic acid 375.* Proc Natl Acad Sci U S A, 2002. **99**(7): p. 4215-20.
88. Haeggstrom, J.Z., *Leukotriene A4 hydrolase/aminopeptidase, the gatekeeper of chemotactic leukotriene B4 biosynthesis.* J Biol Chem, 2004. **279**(49): p. 50639-42.

89. Snelgrove, R.J., et al., *A critical role for LTA4H in limiting chronic pulmonary neutrophilic inflammation.* Science, 2010. **330**(6000): p. 90-4.
90. Weathington, N.M., et al., *A novel peptide CXCR ligand derived from extracellular matrix degradation during airway inflammation.* Nat Med, 2006. **12**(3): p. 317-23.
91. Gaggar, A., et al., *A novel proteolytic cascade generates an extracellular matrix-derived chemoattractant in chronic neutrophilic inflammation.* J Immunol, 2008. **180**(8): p. 5662-9.
92. O'Reilly, P.J., et al., *Neutrophils contain prolyl endopeptidase and generate the chemotactic peptide, PGP, from collagen.* J Neuroimmunol, 2009. **217**(1-2): p. 51-4.
93. Akthar, S., et al., *Matrikines are key regulators in modulating the amplitude of lung inflammation in acute pulmonary infection.* Nat Commun, 2015. **6**: p. 8423.
94. Abdul Roda, M., et al., *The matrikine PGP as a potential biomarker in COPD.* Am J Physiol Lung Cell Mol Physiol, 2015. **308**(11): p. L1095-101.
95. Lobos, E.A., P. Sharon, and W.F. Stenson, *Chemotactic activity in inflammatory bowel disease. Role of leukotriene B4.* Dig Dis Sci, 1987. **32**(12): p. 1380-8.
96. Chen, X., et al., *Leukotriene A4 hydrolase as a target for cancer prevention and therapy.* Curr Cancer Drug Targets, 2004. **4**(3): p. 267-83.
97. Caliskan, B. and E. Banoglu, *Overview of recent drug discovery approaches for new generation leukotriene A4 hydrolase inhibitors.* Expert Opin Drug Discov, 2013. **8**(1): p. 49-63.
98. Di Gennaro, A. and J.Z. Haeggstrom, *Targeting leukotriene B4 in inflammation.* Expert Opin Ther Targets, 2014. **18**(1): p. 79-93.
99. Rao, N.L., et al., *Anti-inflammatory activity of a potent, selective leukotriene A4 hydrolase inhibitor in comparison with the 5-lipoxygenase inhibitor zileuton.* J Pharmacol Exp Ther, 2007. **321**(3): p. 1154-60.
100. Penning, T.D., et al., *Pyrrolidine and piperidine analogues of SC-57461A as potent, orally active inhibitors of leukotriene A(4) hydrolase.* Bioorg Med Chem Lett, 2002. **12**(23): p. 3383-6.
101. Penning, T.D., et al., *Structure-activity relationship studies on 1-[2-(4-Phenylphenoxy)ethyl]pyrrolidine (SC-22716), a potent inhibitor of leukotriene A(4) (LTA(4)) hydrolase.* J Med Chem, 2000. **43**(4): p. 721-35.
102. Orning, L., G. Krivi, and F.A. Fitzpatrick, *Leukotriene A4 hydrolase. Inhibition by bestatin and intrinsic aminopeptidase activity establish its functional resemblance to metallohydrolase enzymes.* J Biol Chem, 1991. **266**(3): p. 1375-8.
103. Orning, L., et al., *Inhibition of leukotriene A4 hydrolase/aminopeptidase by captopril.* J Biol Chem, 1991. **266**(25): p. 16507-11.
104. Low, C.M., et al., *The development of novel LTA4H modulators to selectively target LTB4 generation.* Sci Rep, 2017. **7**: p. 44449.
105. Numao, S., et al., *Feasibility and physiological relevance of designing highly potent aminopeptidase-sparing leukotriene A4 hydrolase inhibitors.* Sci Rep, 2017. **7**(1): p. 13591.
106. De Oliveira, E.O., et al., *Effect of the leukotriene A4 hydrolase aminopeptidase augmentor 4-methoxydiphenylmethane in a pre-clinical model of pulmonary emphysema.* Bioorg Med Chem Lett, 2011. **21**(22): p. 6746-50.
107. Stsiapanava, A., et al., *Binding of Pro-Gly-Pro at the active site of leukotriene A4 hydrolase/aminopeptidase and development of an epoxide hydrolase selective inhibitor.* Proc Natl Acad Sci U S A, 2014. **111**(11): p. 4227-32.
108. Brandt, S.L. and C.H. Serezani, *Too much of a good thing: How modulating LTB4 actions restore host defense in homeostasis or disease.* Semin Immunol, 2017. **33**: p. 37-43.
109. Le Bel, M., A. Brunet, and J. Gosselin, *Leukotriene B4, an endogenous stimulator of the innate immune response against pathogens.* J Innate Immun, 2014. **6**(2): p. 159-68.
110. Subbarao, K., et al., *Role of leukotriene B4 receptors in the development of atherosclerosis: potential mechanisms.* Arterioscler Thromb Vasc Biol, 2004. **24**(2): p. 369-75.

111. Chen, M., et al., *Neutrophil-derived leukotriene B4 is required for inflammatory arthritis.* J Exp Med, 2006. **203**(4): p. 837-42.
112. Griffiths, R.J., et al., *Leukotriene B4 plays a critical role in the progression of collagen-induced arthritis.* Proc Natl Acad Sci U S A, 1995. **92**(2): p. 517-21.
113. Moore, G.Y. and G.P. Pidgeon, *Cross-Talk between Cancer Cells and the Tumour Microenvironment: The Role of the 5-Lipoxygenase Pathway.* Int J Mol Sci, 2017. **18**(2).
114. Yokomizo, T., *Two distinct leukotriene B4 receptors, BLT1 and BLT2.* J Biochem, 2015. **157**(2): p. 65-71.
115. Tager, A.M. and A.D. Luster, *BLT1 and BLT2: the leukotriene B(4) receptors.* Prostaglandins Leukot Essent Fatty Acids, 2003. **69**(2-3): p. 123-34.
116. Feldberg, W. and C.H. Kellaway, *Liberation of histamine and formation of lysocithin-like substances by cobra venom.* J Physiol, 1938. **94**(2): p. 187-226.
117. Murphy, R.C., S. Hammarstrom, and B. Samuelsson, *Leukotriene C: a slow-reacting substance from murine mastocytoma cells.* Proc Natl Acad Sci U S A, 1979. **76**(9): p. 4275-9.
118. Drazen, J.M. and K.F. Austen, *Leukotrienes and airway responses.* Am Rev Respir Dis, 1987. **136**(4): p. 985-98.
119. Nakamura, M. and T. Shimizu, *Leukotriene receptors.* Chem Rev, 2011. **111**(10): p. 6231-98.
120. Yokomizo, T., M. Nakamura, and T. Shimizu, *Leukotriene receptors as potential therapeutic targets.* J Clin Invest, 2018. **128**(7): p. 2691-2701.
121. Colazzo, F., et al., *Role of the Cysteinyl Leukotrienes in the Pathogenesis and Progression of Cardiovascular Diseases.* Mediators Inflamm, 2017. **2017**: p. 2432958.
122. Lynch, K.R., et al., *Characterization of the human cysteinyl leukotriene CysLT1 receptor.* Nature, 1999. **399**(6738): p. 789-93.
123. Theron, A.J., et al., *Cysteinyl leukotriene receptor-1 antagonists as modulators of innate immune cell function.* J Immunol Res, 2014. **2014**: p. 608930.
124. Heise, C.E., et al., *Characterization of the human cysteinyl leukotriene 2 receptor.* J Biol Chem, 2000. **275**(39): p. 30531-6.
125. Kanaoka, Y., A. Maekawa, and K.F. Austen, *Identification of GPR99 protein as a potential third cysteinyl leukotriene receptor with a preference for leukotriene E4 ligand.* J Biol Chem, 2013. **288**(16): p. 10967-72.
126. Clarke, P.G., *Developmental cell death: morphological diversity and multiple mechanisms.* Anat Embryol (Berl), 1990. **181**(3): p. 195-213.
127. Kroemer, G., et al., *Classification of cell death: recommendations of the Nomenclature Committee on Cell Death.* Cell Death Differ, 2005. **12 Suppl 2**: p. 1463-7.
128. Galluzzi, L., et al., *Cell death modalities: classification and pathophysiological implications.* Cell Death Differ, 2007. **14**(7): p. 1237-43.
129. Kerr, J.F., A.H. Wyllie, and A.R. Currie, *Apoptosis: a basic biological phenomenon with wide-ranging implications in tissue kinetics.* Br J Cancer, 1972. **26**(4): p. 239-57.
130. Taylor, R.C., S.P. Cullen, and S.J. Martin, *Apoptosis: controlled demolition at the cellular level.* Nat Rev Mol Cell Biol, 2008. **9**(3): p. 231-41.
131. Hengartner, M.O., *The biochemistry of apoptosis.* Nature, 2000. **407**(6805): p. 770-6.
132. Thornberry, N.A., *Caspases: key mediators of apoptosis.* Chem Biol, 1998. **5**(5): p. R97-103.
133. Earnshaw, W.C., L.M. Martins, and S.H. Kaufmann, *Mammalian caspases: structure, activation, substrates, and functions during apoptosis.* Annu Rev Biochem, 1999. **68**: p. 383-424.
134. Lavrik, I., A. Golks, and P.H. Krammer, *Death receptor signaling.* J Cell Sci, 2005. **118**(Pt 2): p. 265-7.
135. Peter, M.E. and P.H. Krammer, *The CD95(APO-1/Fas) DISC and beyond.* Cell Death Differ, 2003. **10**(1): p. 26-35.
136. Korsmeyer, S.J., et al., *Pro-apoptotic cascade activates BID, which oligomerizes BAK or BAX into pores that result in the release of cytochrome c.* Cell Death Differ, 2000. **7**(12): p. 1166-73.

137. Keoni, C.L. and T.L. Brown, *Inhibition of Apoptosis and Efficacy of Pan Caspase Inhibitor, Q-VD-OPh, in Models of Human Disease.* J Cell Death, 2015. **8**: p. 1-7.
138. Yuan, S. and C.W. Akey, *Apoptosome structure, assembly, and procaspase activation.* Structure, 2013. **21**(4): p. 501-15.
139. Yang, Y., S. Zhao, and J. Song, *Caspase-dependent apoptosis and -independent poly(ADP-ribose) polymerase cleavage induced by transforming growth factor beta1.* Int J Biochem Cell Biol, 2004. **36**(2): p. 223-34.
140. Gobeil, S., et al., *Characterization of the necrotic cleavage of poly(ADP-ribose) polymerase (PARP-1): implication of lysosomal proteases.* Cell Death Differ, 2001. **8**(6): p. 588-94.
141. Levine, B. and G. Kroemer, *Autophagy in the pathogenesis of disease.* Cell, 2008. **132**(1): p. 27-42.
142. Mizushima, N., *Autophagy: process and function.* Genes Dev, 2007. **21**(22): p. 2861-73.
143. Parzych, K.R. and D.J. Klionsky, *An overview of autophagy: morphology, mechanism, and regulation.* Antioxid Redox Signal, 2014. **20**(3): p. 460-73.
144. Glick, D., S. Barth, and K.F. Macleod, *Autophagy: cellular and molecular mechanisms.* J Pathol, 2010. **221**(1): p. 3-12.
145. He, C. and D.J. Klionsky, *Regulation mechanisms and signaling pathways of autophagy.* Annu Rev Genet, 2009. **43**: p. 67-93.
146. Tsapras, P. and I.P. Nezis, *Caspase involvement in autophagy.* Cell Death Differ, 2017. **24**(8): p. 1369-1379.
147. Shimizu, S., et al., *Autophagic cell death and cancer.* Int J Mol Sci, 2014. **15**(2): p. 3145-53.
148. Karch, J., et al., *Autophagic cell death is dependent on lysosomal membrane permeability through Bax and Bak.* Elife, 2017. **6**.
149. Festjens, N., T. Vanden Berghe, and P. Vandenabeele, *Necrosis, a well-orchestrated form of cell demise: signalling cascades, important mediators and concomitant immune response.* Biochim Biophys Acta, 2006. **1757**(9-10): p. 1371-87.
150. Edinger, A.L. and C.B. Thompson, *Death by design: apoptosis, necrosis and autophagy.* Curr Opin Cell Biol, 2004. **16**(6): p. 663-9.
151. Brojatsch, J., et al., *A proteolytic cascade controls lysosome rupture and necrotic cell death mediated by lysosome-destabilizing adjuvants.* PLoS One, 2014. **9**(6): p. e95032.
152. Golstein, P. and G. Kroemer, *Cell death by necrosis: towards a molecular definition.* Trends Biochem Sci, 2007. **32**(1): p. 37-43.
153. Zong, W.X. and C.B. Thompson, *Necrotic death as a cell fate.* Genes Dev, 2006. **20**(1): p. 1-15.
154. Bergsbaken, T., S.L. Fink, and B.T. Cookson, *Pyroptosis: host cell death and inflammation.* Nat Rev Microbiol, 2009. **7**(2): p. 99-109.
155. Chen, D., J. Yu, and L. Zhang, *Necroptosis: an alternative cell death program defending against cancer.* Biochim Biophys Acta, 2016. **1865**(2): p. 228-36.
156. Kool, M., et al., *Alum adjuvant boosts adaptive immunity by inducing uric acid and activating inflammatory dendritic cells.* J Exp Med, 2008. **205**(4): p. 869-82.
157. Jacobson, L.S., et al., *Cathepsin-mediated necrosis controls the adaptive immune response by Th2 (T helper type 2)-associated adjuvants.* J Biol Chem, 2013. **288**(11): p. 7481-91.
158. Lima, H., Jr., et al., *Role of lysosome rupture in controlling Nlrp3 signaling and necrotic cell death.* Cell Cycle, 2013. **12**(12): p. 1868-78.
159. Waring, P. and J. Beaver, *Gliotoxin and related epipolythiodioxopiperazines.* Gen Pharmacol, 1996. **27**(8): p. 1311-6.
160. Scharf, D.H., A.A. Brakhage, and P.K. Mukherjee, *Gliotoxin--bane or boon?* Environ Microbiol, 2016. **18**(4): p. 1096-109.
161. Bell, M.R., et al., *The Structure of Gliotoxin.* Journal of the American Chemical Society, 1958. **80**(4): p. 1001-1001.

162. Waring, P., A. Sjaarda, and Q.H. Lin, *Gliotoxin inactivates alcohol dehydrogenase by either covalent modification or free radical damage mediated by redox cycling.* Biochem Pharmacol, 1995. **49**(9): p. 1195-201.
163. Tamiya, H., et al., *Secondary metabolite profiles and antifungal drug susceptibility of Aspergillus fumigatus and closely related species, Aspergillus lentulus, Aspergillus udagawae, and Aspergillus viridinutans.* J Infect Chemother, 2015. **21**(5): p. 385-91.
164. Trown, P.W. and J.A. Bilello, *Mechanism of action of gliotoxin: elimination of activity by sulfhydryl compounds.* Antimicrob Agents Chemother, 1972. **2**(4): p. 261-6.
165. Larin, N.M., et al., *Antiviral activity of gliotoxin.* Chemotherapy, 1965. **10**(1): p. 12-23.
166. Ben-Ami, R., et al., *Aspergillus fumigatus inhibits angiogenesis through the production of gliotoxin and other secondary metabolites.* Blood, 2009. **114**(26): p. 5393-9.
167. Mullbacher, A. and R.D. Eichner, *Immunosuppression in vitro by a metabolite of a human pathogenic fungus.* Proc Natl Acad Sci U S A, 1984. **81**(12): p. 3835-7.
168. Mullbacher, A., et al., *Structural relationship of epipolythiodioxopiperazines and their immunomodulating activity.* Mol Immunol, 1986. **23**(2): p. 231-5.
169. Shah, D.T., et al., *Effect of gliotoxin on human polymorphonuclear neutrophils.* Infect Dis Obstet Gynecol, 1998. **6**(4): p. 168-75.
170. Comera, C., et al., *Gliotoxin from Aspergillus fumigatus affects phagocytosis and the organization of the actin cytoskeleton by distinct signalling pathways in human neutrophils.* Microbes Infect, 2007. **9**(1): p. 47-54.
171. Jordan, T.W. and J.S. Pedersen, *Sporidesmin and gliotoxin induce cell detachment and perturb microfilament structure in cultured liver cells.* J Cell Sci, 1986. **85**: p. 33-46.
172. Schlam, D., et al., *Gliotoxin Suppresses Macrophage Immune Function by Subverting Phosphatidylinositol 3,4,5-Trisphosphate Homeostasis.* MBio, 2016. **7**(2): p. e02242.
173. Tsunawaki, S., et al., *Fungal metabolite gliotoxin inhibits assembly of the human respiratory burst NADPH oxidase.* Infect Immun, 2004. **72**(6): p. 3373-82.
174. Yoshida, L.S., S. Abe, and S. Tsunawaki, *Fungal gliotoxin targets the onset of superoxide-generating NADPH oxidase of human neutrophils.* Biochem Biophys Res Commun, 2000. **268**(3): p. 716-23.
175. Orciuolo, E., et al., *Effects of Aspergillus fumigatus gliotoxin and methylprednisolone on human neutrophils: implications for the pathogenesis of invasive aspergillosis.* J Leukoc Biol, 2007. **82**(4): p. 839-48.
176. Kroll, M., et al., *The secondary fungal metabolite gliotoxin targets proteolytic activities of the proteasome.* Chem Biol, 1999. **6**(10): p. 689-98.
177. Pahl, H.L., et al., *The immunosuppressive fungal metabolite gliotoxin specifically inhibits transcription factor NF-kappaB.* J Exp Med, 1996. **183**(4): p. 1829-40.
178. Fitzpatrick, L.R., J. Wang, and T. Le, *In vitro and in vivo effects of gliotoxin, a fungal metabolite: efficacy against dextran sodium sulfate-induced colitis in rats.* Dig Dis Sci, 2000. **45**(12): p. 2327-36.
179. Waring, P., T. Khan, and A. Sjaarda, *Apoptosis induced by gliotoxin is preceded by phosphorylation of histone H3 and enhanced sensitivity of chromatin to nuclease digestion.* J Biol Chem, 1997. **272**(29): p. 17929-36.
180. Pardo, J., et al., *The mitochondrial protein Bak is pivotal for gliotoxin-induced apoptosis and a critical host factor of Aspergillus fumigatus virulence in mice.* J Cell Biol, 2006. **174**(4): p. 509-19.
181. Arias, M., et al., *Preparations for Invasion: Modulation of Host Lung Immunity During Pulmonary Aspergillosis by Gliotoxin and Other Fungal Secondary Metabolites.* Front Immunol, 2018. **9**: p. 2549.
182. Lewis, R.E., et al., *Detection of gliotoxin in experimental and human aspergillosis.* Infect Immun, 2005. **73**(1): p. 635-7.
183. Baumgartner, K., M.P. Coetzee, and D. Hoffmeister, *Secrets of the subterranean pathosystem of Armillaria.* Mol Plant Pathol, 2011. **12**(6): p. 515-34.
184. Donnelly, D.M., et al., *Antibacterial sesquiterpene aryl esters from Armillaria mellea.* J Nat Prod, 1985. **48**(1): p. 10-6.

185. Lackner, G., et al., *Assembly of melleolide antibiotics involves a polyketide synthase with cross-coupling activity.* Chem Biol, 2013. **20**(9): p. 1101-6.
186. Bohnert, M., et al., *Cytotoxic and antifungal activities of melleolide antibiotics follow dissimilar structure-activity relationships.* Phytochemistry, 2014. **105**: p. 101-8.
187. Chen, Y.J., C.C. Chen, and H.L. Huang, *Induction of apoptosis by Armillaria mellea constituent armillarikin in human hepatocellular carcinoma.* Onco Targets Ther, 2016. **9**: p. 4773-83.
188. Yang, J.S., et al., *Chemical constituents of Armillaria mellea mycelium. I. Isolation and characterization of armillarin and armillaridin.* Planta Med, 1984. **50**(4): p. 288-90.
189. Lung, M.Y. and Y.C. Chang, *Antioxidant properties of the edible Basidiomycete Armillaria mellea in submerged cultures.* Int J Mol Sci, 2011. **12**(10): p. 6367-84.
190. Momose, I., et al., *Melleolides K, L and M, new melleolides from Armillariella mellea.* J Antibiot (Tokyo), 2000. **53**(2): p. 137-43.
191. Obuchi, T., et al., *Armillaric acid, a new antibiotic produced by Armillaria mellea.* Planta Med, 1990. **56**(2): p. 198-201.
192. Kim, S.K., et al., *Armillariella mellea induces maturation of human dendritic cells without induction of cytokine expression.* J Ethnopharmacol, 2008. **119**(1): p. 153-9.
193. Sun, Y., et al., *Structural elucidation and immunological activity of a polysaccharide from the fruiting body of Armillaria mellea.* Bioresour Technol, 2009. **100**(5): p. 1860-3.
194. Bohnert, M., et al., *In vitro cytotoxicity of melleolide antibiotics: structural and mechanistic aspects.* Bioorg Med Chem Lett, 2011. **21**(7): p. 2003-6.
195. Chang, W.H., et al., *Armillaridin induces autophagy-associated cell death in human chronic myelogenous leukemia K562 cells.* Tumour Biol, 2016. **37**(10): p. 14291-14300.
196. Chi, C.W., C.C. Chen, and Y.J. Chen, *Therapeutic and radiosensitizing effects of armillaridin on human esophageal cancer cells.* Evid Based Complement Alternat Med, 2013. **2013**: p. 459271.
197. Misiek, M., et al., *Structure and cytotoxicity of arnamial and related fungal sesquiterpene aryl esters.* J Nat Prod, 2009. **72**(10): p. 1888-91.
198. Schieferdecker, S., et al., *Structure and biosynthetic assembly of gulmirecins, macrolide antibiotics from the predatory bacterium Pyxidicoccus fallax.* Chemistry, 2014. **20**(48): p. 15933-40.
199. Surup, F., et al., *Disciformycins A and B: 12-membered macrolide glycoside antibiotics from the myxobacterium Pyxidicoccus fallax active against multiresistant staphylococci.* Angew Chem Int Ed Engl, 2014. **53**(49): p. 13588-91.
200. Schieferdecker, S., et al., *Myxochelins target human 5-lipoxygenase.* J Nat Prod, 2015. **78**(2): p. 335-8.
201. Nett, M. and G.M. Konig, *The chemistry of gliding bacteria.* Nat Prod Rep, 2007. **24**(6): p. 1245-61.
202. Schaberle, T.F., et al., *Antibiotics from myxobacteria.* Nat Prod Rep, 2014. **31**(7): p. 953-72.
203. Kunze, B., et al., *Myxochelin A, a new iron-chelating compound from Angiococcus disciformis (Myxobacterales). Production, isolation, physico-chemical and biological properties.* J Antibiot (Tokyo), 1989. **42**(1): p. 14-7.
204. Miyanaga, S., et al., *Absolute configuration and antitumor activity of myxochelin A produced by Nonomuraea pusilla TP-A0861.* J Antibiot (Tokyo), 2006. **59**(11): p. 698-703.
205. Miyanaga, S., et al., *Synthesis and evaluation of myxochelin analogues as antimetastatic agents.* Bioorg Med Chem, 2009. **17**(7): p. 2724-32.
206. Schieferdecker, S., et al., *Myxochelin-Inspired 5-Lipoxygenase Inhibitors: Synthesis and Biological Evaluation.* ChemMedChem, 2017. **12**(1): p. 23-27.
207. Stanzani, M., et al., *Aspergillus fumigatus suppresses the human cellular immune response via gliotoxin-mediated apoptosis of monocytes.* Blood, 2005. **105**(6): p. 2258-65.
208. Schottenfeld, D. and J. Beebe-Dimmer, *Chronic inflammation: a common and important factor in the pathogenesis of neoplasia.* CA Cancer J Clin, 2006. **56**(2): p. 69-83.

209. Petersen, M. and M.S. Simmonds, *Rosmarinic acid.* Phytochemistry, 2003. **62**(2): p. 121-5.
210. Koshihara, Y., et al., *Caffeic acid is a selective inhibitor for leukotriene biosynthesis.* Biochim Biophys Acta, 1984. **792**(1): p. 92-7.
211. Boudreau, L.H., et al., *New Hydroxycinnamic Acid Esters as Novel 5-Lipoxygenase Inhibitors That Affect Leukotriene Biosynthesis.* Mediators Inflamm, 2017. **2017**: p. 6904634.
212. Korp, J., et al., *Harnessing Enzymatic Promiscuity in Myxochelin Biosynthesis for the Production of 5-Lipoxygenase Inhibitors.* Chembiochem, 2015. **16**(17): p. 2445-50.
213. Koeberle, A., et al., *SAR studies on curcumin's pro-inflammatory targets: discovery of prenylated pyrazolocurcuminoids as potent and selective novel inhibitors of 5-lipoxygenase.* J Med Chem, 2014. **57**(13): p. 5638-48.
214. Koeberle, A., H. Northoff, and O. Werz, *Curcumin blocks prostaglandin E2 biosynthesis through direct inhibition of the microsomal prostaglandin E2 synthase-1.* Mol Cancer Ther, 2009. **8**(8): p. 2348-55.
215. Werz, O., *5-lipoxygenase: cellular biology and molecular pharmacology.* Curr Drug Targets Inflamm Allergy, 2002. **1**(1): p. 23-44.
216. Awwad, K., et al., *Electrophilic fatty acid species inhibit 5-lipoxygenase and attenuate sepsis-induced pulmonary inflammation.* Antioxid Redox Signal, 2014. **20**(17): p. 2667-80.
217. Gerstmeier, J., et al., *Time-resolved in situ assembly of the leukotriene-synthetic 5-lipoxygenase/5-lipoxygenase-activating protein complex in blood leukocytes.* FASEB J, 2016. **30**(1): p. 276-85.
218. Garscha, U., et al., *Pharmacological profile and efficiency in vivo of diflapolin, the first dual inhibitor of 5-lipoxygenase-activating protein and soluble epoxide hydrolase.* Sci Rep, 2017. **7**(1): p. 9398.
219. Garscha, U., et al., *BRP-187: A potent inhibitor of leukotriene biosynthesis that acts through impeding the dynamic 5-lipoxygenase/5-lipoxygenase-activating protein (FLAP) complex assembly.* Biochem Pharmacol, 2016. **119**: p. 17-26.
220. Mandal, A.K., et al., *The nuclear membrane organization of leukotriene synthesis.* Proc Natl Acad Sci U S A, 2008. **105**(51): p. 20434-9.
221. Jakobsson, P.J., et al., *Membrane-associated proteins in eicosanoid and glutathione metabolism (MAPEG). A widespread protein superfamily.* Am J Respir Crit Care Med, 2000. **161**(2 Pt 2): p. S20-4.
222. Martinez Molina, D., S. Eshaghi, and P. Nordlund, *Catalysis within the lipid bilayer-structure and mechanism of the MAPEG family of integral membrane proteins.* Curr Opin Struct Biol, 2008. **18**(4): p. 442-9.
223. Gerstmeier, J., et al., *5-Lipoxygenase-activating protein rescues activity of 5-lipoxygenase mutations that delay nuclear membrane association and disrupt product formation.* FASEB J, 2016. **30**(5): p. 1892-900.
224. Rao, T.S., et al., *In vivo characterization of zymosan-induced mouse peritoneal inflammation.* J Pharmacol Exp Ther, 1994. **269**(3): p. 917-25.
225. Cuzzocrea, S., et al., *5-Lipoxygenase knockout mice exhibit a resistance to pleurisy and lung injury caused by carrageenan.* J Leukoc Biol, 2003. **73**(6): p. 739-46.
226. Shindo, K., et al., *Captopril inhibits neutrophil synthesis of leukotriene B4 in vitro and in vivo.* J Immunol, 1994. **153**(12): p. 5750-9.
227. Jeong, C.H., et al., *[6]-Gingerol suppresses colon cancer growth by targeting leukotriene A4 hydrolase.* Cancer Res, 2009. **69**(13): p. 5584-91.
228. Oi, N., et al., *Resveratrol, a red wine polyphenol, suppresses pancreatic cancer by inhibiting leukotriene A(4)hydrolase.* Cancer Res, 2010. **70**(23): p. 9755-64.
229. Torres, M.J., et al., *Effect of alpha lipoic acid on leukotriene A4 hydrolase.* Eur J Pharmacol, 2017. **799**: p. 41-47.
230. Harris, T.R. and B.D. Hammock, *Soluble epoxide hydrolase: gene structure, expression and deletion.* Gene, 2013. **526**(2): p. 61-74.
231. Morisseau, C. and B.D. Hammock, *Impact of soluble epoxide hydrolase and epoxyeicosanoids on human health.* Annu Rev Pharmacol Toxicol, 2013. **53**: p. 37-58.

232. Hu, J., et al., *Inhibition of soluble epoxide hydrolase prevents diabetic retinopathy.* Nature, 2017. **552**(7684): p. 248-252.
233. Saleh, A.A., et al., *Systems impact of zinc chelation by the epipolythiodioxopiperazine dithiol gliotoxin in Aspergillus fumigatus: a new direction in natural product functionality.* Metallomics, 2018. **10**(6): p. 854-866.
234. Ferguson, L.R., et al., *In vitro and in vivo mutagenicity studies on sporidesmin, the toxin associated with facial eczema in ruminants.* Mutat Res, 1992. **268**(2): p. 199-210.
235. Collett, M.G., et al., *Chronic sporidesmin toxicosis and photosensitisation in an alpaca (Vicugna pacos) in New Zealand.* N Z Vet J, 2016. **64**(5): p. 314-6.
236. Srinivasan, U., et al., *Selective inactivation of glutaredoxin by sporidesmin and other epidithiopiperazinediones.* Biochemistry, 2006. **45**(29): p. 8978-87.
237. Tibodeau, J.D., et al., *The anticancer agent chaetocin is a competitive substrate and inhibitor of thioredoxin reductase.* Antioxid Redox Signal, 2009. **11**(5): p. 1097-106.
238. Lauinger, L., et al., *Thiolutin is a zinc chelator that inhibits the Rpn11 and other JAMM metalloproteases.* Nat Chem Biol, 2017. **13**(7): p. 709-714.
239. Duncan, E.J., M.P. Thompson, and S.H. Phua, *Zinc protection of HepG2 cells from sporidesmin toxicity does not require de novo gene transcription.* Toxicol Lett, 2005. **159**(2): p. 164-72.
240. Schutze, N., et al., *Exposure to mycotoxins increases the allergic immune response in a murine asthma model.* Am J Respir Crit Care Med, 2010. **181**(11): p. 1188-99.
241. Bossou, Y.M., et al., *Impact of Mycotoxins Secreted by Aspergillus Molds on the Inflammatory Response of Human Corneal Epithelial Cells.* Toxins (Basel), 2017. **9**(7).
242. Schneemann, M. and A. Schaffner, *Host defense mechanism in Aspergillus fumigatus infections.* Contrib Microbiol, 1999. **2**: p. 57-68.
243. Park, S.J. and B. Mehrad, *Innate immunity to Aspergillus species.* Clin Microbiol Rev, 2009. **22**(4): p. 535-51.
244. Lamoth, F., *Aspergillus fumigatus-Related Species in Clinical Practice.* Front Microbiol, 2016. **7**: p. 683.
245. Heinekamp, T., et al., *Interference of Aspergillus fumigatus with the immune response.* Semin Immunopathol, 2015. **37**(2): p. 141-52.
246. Caffrey-Carr, A.K., et al., *Host-Derived Leukotriene B4 Is Critical for Resistance against Invasive Pulmonary Aspergillosis.* Front Immunol, 2017. **8**: p. 1984.
247. Jones, C.N., et al., *Human Neutrophils Are Primed by Chemoattractant Gradients for Blocking the Growth of Aspergillus fumigatus.* J Infect Dis, 2016. **213**(3): p. 465-75.
248. Cramer, R.A., Jr., et al., *Disruption of a nonribosomal peptide synthetase in Aspergillus fumigatus eliminates gliotoxin production.* Eukaryot Cell, 2006. **5**(6): p. 972-80.
249. Nguyen, V.T., et al., *Gliotoxin isolated from marine fungus Aspergillus sp. induces apoptosis of human cervical cancer and chondrosarcoma cells.* Mar Drugs, 2013. **12**(1): p. 69-87.
250. Eichner, R.D., et al., *Gliotoxin causes oxidative damage to plasmid and cellular DNA.* J Biol Chem, 1988. **263**(8): p. 3772-7.
251. Suen, Y.K., et al., *Gliotoxin induces apoptosis in cultured macrophages via production of reactive oxygen species and cytochrome c release without mitochondrial depolarization.* Free Radic Res, 2001. **35**(1): p. 1-10.
252. Geissler, A., et al., *Apoptosis induced by the fungal pathogen gliotoxin requires a triple phosphorylation of Bim by JNK.* Cell Death Differ, 2013. **20**(10): p. 1317-29.
253. Tretiakova, I., et al., *Myrtucommulone from Myrtus communis induces apoptosis in cancer cells via the mitochondrial pathway involving caspase-9.* Apoptosis, 2008. **13**(1): p. 119-31.
254. Chen, Y., et al., *Loss of the Alox5 gene impairs leukemia stem cells and prevents chronic myeloid leukemia.* Nat Genet, 2009. **41**(7): p. 783-92.
255. Chen, Y., D. Li, and S. Li, *The Alox5 gene is a novel therapeutic target in cancer stem cells of chronic myeloid leukemia.* Cell Cycle, 2009. **8**(21): p. 3488-92.
256. Roos, J., et al., *5-Lipoxygenase is a candidate target for therapeutic management of stem cell-like cells in acute myeloid leukemia.* Cancer Res, 2014. **74**(18): p. 5244-55.

257. Braig, S., et al., *Pretubulysin: a new option for the treatment of metastatic cancer.* Cell Death Dis, 2014. **5**: p. e1001.
258. Kubisch, R., et al., *Simplified pretubulysin derivatives and their biological effects on cancer cells.* J Nat Prod, 2014. **77**(3): p. 536-42.
259. Tamaoki, T., et al., *Staurosporine, a potent inhibitor of phospholipid/Ca++dependent protein kinase.* Biochem Biophys Res Commun, 1986. **135**(2): p. 397-402.
260. Ullrich, A., et al., *Pretubulysin, a potent and chemically accessible tubulysin precursor from Angiococcus disciformis.* Angew Chem Int Ed Engl, 2009. **48**(24): p. 4422-5.
261. Kelner, M.J., et al., *Preclinical evaluation of illudins as anticancer agents.* Cancer Res, 1987. **47**(12): p. 3186-9.
262. McMorris, T.C., et al., *Preparation and biological activity of amino acid and peptide conjugates of antitumor hydroxymethylacylfulvene.* J Med Chem, 2000. **43**(19): p. 3577-80.
263. Searle, J., et al., *An electron-microscope study of the mode of cell death induced by cancer-chemotherapeutic agents in populations of proliferating normal and neoplastic cells.* J Pathol, 1975. **116**(3): p. 129-38.
264. Caserta, T.M., et al., *Q-VD-OPh, a broad spectrum caspase inhibitor with potent antiapoptotic properties.* Apoptosis, 2003. **8**(4): p. 345-52.
265. Bohnert, M., et al., *Melleolides induce rapid cell death in human primary monocytes and cancer cells.* Bioorg Med Chem, 2014. **22**(15): p. 3856-61.
266. Fujita, K. and I. Kubo, *Multifunctional action of antifungal polygodial against Saccharomyces cerevisiae: involvement of pyrrole formation on cell surface in antifungal action.* Bioorg Med Chem, 2005. **13**(24): p. 6742-7.
267. Kubo, I., K. Fujita, and S.H. Lee, *Antifungal mechanism of polygodial.* J Agric Food Chem, 2001. **49**(3): p. 1607-11.
268. Kubo, I., et al., *Antibacterial activity of polygodial.* Phytother Res, 2005. **19**(12): p. 1013-7.
269. Kubo, I. and M. Taniguchi, *Polygodial, an antifungal potentiator.* J Nat Prod, 1988. **51**(1): p. 22-9.
270. Chidley, C., et al., *The anticancer natural product ophiobolin A induces cytotoxicity by covalent modification of phosphatidylethanolamine.* Elife, 2016. **5**.
271. Rodolfo, C., et al., *Ophiobolin A Induces Autophagy and Activates the Mitochondrial Pathway of Apoptosis in Human Melanoma Cells.* PLoS One, 2016. **11**(12): p. e0167672.
272. Morrison, R., et al., *Ophiobolin A, a sesterpenoid fungal phytotoxin, displays different mechanisms of cell death in mammalian cells depending upon the cancer cell origin.* Int J Oncol, 2017. **50**(3): p. 773-786.
273. Vance, J.E., *Phospholipid synthesis and transport in mammalian cells.* Traffic, 2015. **16**(1): p. 1-18.
274. Emoto, K., et al., *Exposure of phosphatidylethanolamine on the surface of apoptotic cells.* Exp Cell Res, 1997. **232**(2): p. 430-4.
275. Green, D.R. and G. Kroemer, *The pathophysiology of mitochondrial cell death.* Science, 2004. **305**(5684): p. 626-9.
276. Rockenfeller, P., et al., *Phosphatidylethanolamine positively regulates autophagy and longevity.* Cell Death Differ, 2015. **22**(3): p. 499-508.
277. Gozuacik, D. and A. Kimchi, *Autophagy as a cell death and tumor suppressor mechanism.* Oncogene, 2004. **23**(16): p. 2891-906.
278. Thorburn, A., *Apoptosis and autophagy: regulatory connections between two supposedly different processes.* Apoptosis, 2008. **13**(1): p. 1-9.
279. Yu, L., et al., *Regulation of an ATG7-beclin 1 program of autophagic cell death by caspase-8.* Science, 2004. **304**(5676): p. 1500-2.
280. Hou, W., et al., *Autophagic degradation of active caspase-8: a crosstalk mechanism between autophagy and apoptosis.* Autophagy, 2010. **6**(7): p. 891-900.
281. Young, M.M., et al., *Autophagosomal membrane serves as platform for intracellular death-inducing signaling complex (iDISC)-mediated caspase-8 activation and apoptosis.* J Biol Chem, 2012. **287**(15): p. 12455-68.

282. Kabeya, Y., et al., *LC3, a mammalian homologue of yeast Apg8p, is localized in autophagosome membranes after processing.* EMBO J, 2000. **19**(21): p. 5720-8.

APPENDIX 1: ADDITIONAL DATA

A.1 Effects of natural products on cancer cell proliferation

The prevalence of cancer increases dictated due to our lifestyle, thus initiating 90% to 95% of cancer by lifestyle factors, for instance, tobacco smoke, obesity, stress, UV, or environmental pollutants [32]. Hence, it is of prime interest to search for additional compounds enabling new therapeutic approaches and to improve cancer therapy with reduced side effects. Several natural products exhibit, besides their anti-inflammatory potential, also antiproliferative effects on human cancer cells without affecting human primary immune cells suggesting a beneficial therapy option, e.g., pretubulysin [265], or myxochelin A.

A.1.1 Myxochelin A reduces primarily cell viability of leukemic cancer cells

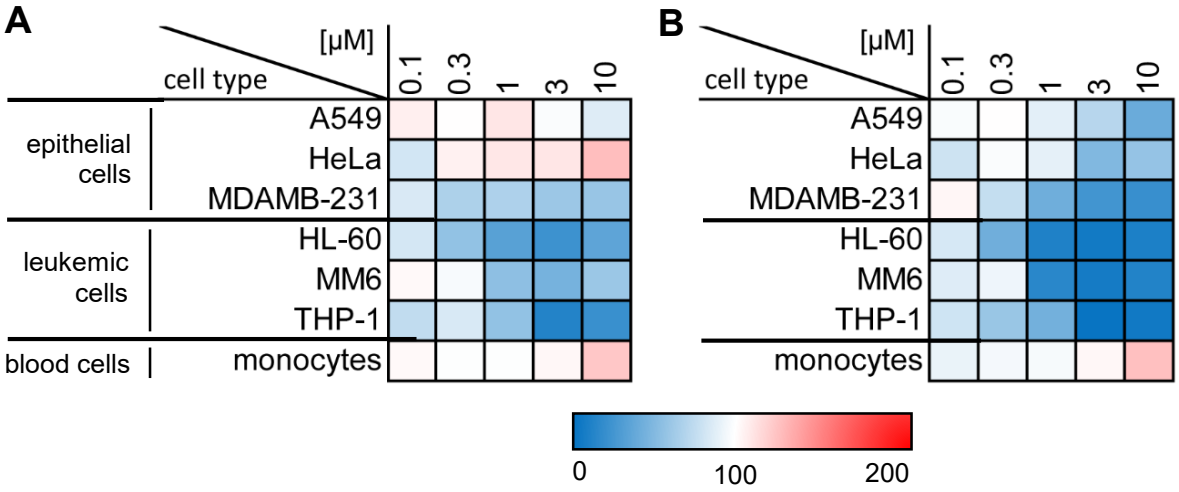

Fig. A1 Effect by myxochelin A on cell viability of human cells. *Various epithelial and leukemic cancer cells were treated with myxochelin A at indicated concentrations for (A) 24 hrs or (B) 48 hrs in comparison to human primary monocytes. Cell viability was analyzed by MTT assay after 24 hrs. Data are given as mean + S.E, n = 3.*

As published before, predatory myxobacteria generate a variety of antibiotics and anti-cancer agents [201, 202], e.g., myxochelin A. Moreover, myxochelin A and its derivatives were also described as antimetastatic agents analyzed in murine colon 26L-5 cells [204, 205], supporting their use as anti-cancer drugs. We analyzed the cytotoxic effect of myxochelin A in various cancer cells: (I) epithelial cancer cells including A549, HeLa, and MDAMB-231 cells, (II) leukemic cells consisting of HL-60, MM6, and THP-1 cells in comparison to freshly isolated human monocytes. Cells were treated with myxochelin A for 24 hrs or 48 hrs followed by addition of MTT (5 mg/mL PBS, as described in **manuscript IV, V**). As control, we used the well-known pan-kinase inhibitor staurosporine (1 µM) [259]. After 24 h (**Fig. A1 A**), myxochelin A reduced the cell viability of leukemic cells much more potent than the viability of endothelial

cancer cells except the breast cancer cells MDAMB-231. Interestingly, MDAMB-231 cells are derived from metastatic side hypothesizing comparable characteristics to systemic cancer cells like HL-60, MM6, or THP-1 cells. As expected, after 48 hrs (**Fig. A1 B**), cytotoxic effects towards cancer cells increased, and again, leukemic cells were more affected by myxochelin A than epithelial cells. In contrast, cell viability of human primary monocytes was not impaired after 24 hrs neither 48 hrs.

APPENDIX 2: MANUSCRIPTS

M-I: Melleolides from honey mushroom inhibit 5-lipoxygenase via C159

Please cite this article in press as: König et al., Melleolides from Honey Mushroom Inhibit 5-Lipoxygenase via Cys159, Cell Chemical Biology (2018), https://doi.org/10.1016/j.chembiol.2018.10.010

Cell Chemical Biology
Article

CellPress

Melleolides from Honey Mushroom Inhibit 5-Lipoxygenase via Cys159

Stefanie König,[1] Erik Romp,[1] Verena Krauth,[1] Michael Rühl,[2] Maximilian Dörfer,[3] Stefanie Liening,[1] Bettina Hofmann,[2] Ann-Kathrin Häfner,[2] Dieter Steinhilber,[2] Michael Karas,[2] Ulrike Garscha,[1] Dirk Hoffmeister,[3] and Oliver Werz[1,4,*]
[1]Department of Pharmaceutical/Medicinal Chemistry, Institute of Pharmacy, Friedrich-Schiller-University Jena, 07743 Jena, Germany
[2]Institute of Pharmaceutical Chemistry, Goethe University Frankfurt, 60438 Frankfurt, Germany
[3]Department of Pharmaceutical Microbiology at the Hans Knöll Institute, Friedrich-Schiller-University Jena, 07745 Jena, Germany
[4]Lead Contact
*Correspondence: oliver.werz@uni-jena.de
https://doi.org/10.1016/j.chembiol.2018.10.010

SUMMARY

5-Lipoxygenase (5-LO) initiates the biosynthesis of pro-inflammatory leukotrienes from arachidonic acid, which requires the nuclear membrane-bound 5-LO-activating protein (FLAP) for substrate transfer. Here, we identified human 5-LO as a molecular target of melleolides from honey mushroom (*Armillaria mellea*). Melleolides inhibit 5-LO via an α,β-unsaturated aldehyde serving as Michael acceptor for surface cysteines at the substrate entrance that are revealed as molecular determinants for 5-LO activity. Experiments with 5-LO mutants, where select cysteines had been replaced by serine, indicated that the investigated melleolides suppress 5-LO product formation via two distinct modes of action: (1) by direct interference with 5-LO activity involving two or more of the cysteines 159, 300, 416, and 418, and (2) by preventing 5-LO/FLAP assemblies involving selectively Cys159 in 5-LO. Interestingly, replacement of Cys159 by serine prevented 5-LO/FLAP assemblies as well, implying Cys159 as determinant for 5-LO/FLAP complex formation at the nuclear membrane required for leukotriene biosynthesis.

INTRODUCTION

Natural products are discovered at a rapid rate, and bioactivities are extensively screened for in routine assays. However, the knowledge on the modes of action and molecular targets of these bioactive compounds is severely lagging behind. In the arena of mushroom toxins, the mode of action is understood only for very few compounds, among them the amanitins, psilocybin, muscarine, coprine, and ibotenic acid. The melleolides (Figure 1A) are natural products of the basidiomycete *Armillaria mellea* (honey mushroom), a globally distributed mushroom that also represents an important plant pathogen (Baumgartner et al., 2011). Bioactivities include antimicrobial and antifungal effects, as well as cytotoxicity against human monocytes and cancer cells (Bohnert et al., 2011, 2014b; Misiek et al., 2009; Momose et al., 2000). Intriguingly, these activities follow dissimilar structure-activity relationships (SARs) (Bohnert et al., 2014a). With more than 60 published members, melleolides rank among the largest and most diverse classes of fungal natural products. Structurally, they are composed of an orsellinic acid moiety esterified to a protoilludene-type sesquiterpene secondary alcohol. Many melleolides feature an α,β-unsaturated aldehyde moiety that may act as Michael acceptor, but molecular targets of the melleolides are thus far unknown. We previously showed that Michael acceptor-containing drugs such as thymoquinone (TQ) (Maucher et al., 2017) or nitro fatty acids (Awwad et al., 2014) are direct covalent inhibitors of human 5-lipoxygenase (5-LO) by targeting Cys416 and Cys418.

5-LO is the key enzyme in the biosynthesis of pro-inflammatory leukotrienes (LTs) from arachidonic acid (AA) that play important roles in disorders such as asthma, rheumatoid arthritis, allergic rhinitis, neurodegenerative and cardiovascular diseases, and cancer (Radmark et al., 2015). LT biosynthesis is mainly restricted to leukocytes where the cytosolic phospholipase A_2 ($cPLA_2$) and 5-LO translocate to the nuclear envelope upon cell activation. $cPLA_2$ releases AA from membrane phospholipids (Leslie, 2015), and AA is then transferred by the nuclear membrane-bound 5-LO-activating protein (FLAP) to 5-LO, which assembles a complex with FLAP. 5-LO oxygenates AA to yield the intermediate 5(S)-hydroperoxyeicosatetraenoic acid (5-HPETE) and then dehydrates 5-HPETE to LTA_4, again aided by FLAP (Radmark et al., 2015). LTA_4 can be enzymatically converted to the chemoattractant LTB_4 or to cysteinyl-LTs (LTC_4, D_4, or E_4) that contract smooth muscles in the airways and microcirculation (Haeggstrom and Funk, 2011). FLAP binds AA and is essential for 5-LO activity in intact cells, seemingly by accomplishing appropriate substrate access for 5-LO (Evans et al., 2008). The 5-LO/FLAP complex assembly at the nuclear membrane requires AA, and FLAP inhibitors prevent 5-LO/FLAP interactions and 5-LO product formation in an AA-competitive fashion (Bair et al., 2012; Gerstmeier et al., 2014, 2016b). Recently, we showed that the cysteines 159, 300, 416, and 418, located on the 5-LO protein surface close to the AA entry site, are important for co-localization with FLAP (Hafner et al., 2015).

The poor knowledge on the pharmacology behind mushroom toxins, and the fact that honey mushrooms are considered edible and collected in many regions prompted us to investigate the mode of action of the melleolides. To explore their molecular

Please cite this article in press as: König et al., Melleolides from Honey Mushroom Inhibit 5-Lipoxygenase via Cys159, Cell Chemical Biology (2018), https://doi.org/10.1016/j.chembiol.2018.10.010

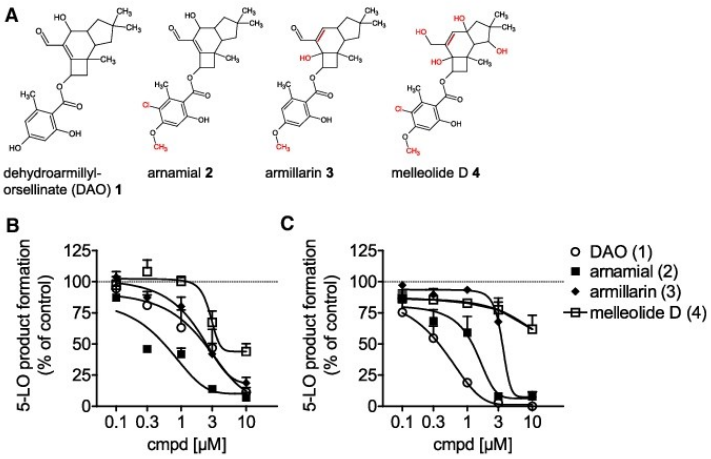

Figure 1. Melleolides Inhibit 5-LO Activity in Cell-Free and Cell-Based Systems

(A) Chemical structures of melleolides **1–4**.

(B) Effect of **1–4** on 5-LO product formation in a cell-free assay. Purified human recombinant 5-LO (0.5 μg/mL) was pre-incubated with compounds or vehicle (0.1% DMSO) at 4°C for 10 min. Samples were pre-warmed for 30 s at 37°C and incubated with 2 mM $CaCl_2$ and 20 μM AA for another 10 min. The reaction was terminated and 5-LO products were then analyzed by reverse-phase high-performance liquid chromatography (RP-HPLC).

(C) Effect of **1–4** on 5-LO product formation in a cell-based system. Neutrophils (5×10^6/mL) were pre-incubated with compounds or 0.1% DMSO (vehicle) for 10 min at 37°C prior to stimulation with 2.5 μM A23187 for 10 min at 37°C, and 5-LO product formation was determined. Data are expressed as percentage of vehicle control (100%), means ± SEM, n = 3.

targets in mammalian cells, we investigated four structurally different representatives (Figure 1A) for interference with human 5-LO. We identified 5-LO as a molecular target for those melleolides that possess an α,β-unsaturated aldehyde with thiol-reactive Michael acceptor functionality. These melleolides mediate their 5-LO-inhibitory effects via surface cysteines of 5-LO. Our data suggest that melleolides interact with Cys159 at the entrance of the catalytic center of 5-LO, which prevents the complex assembly with FLAP and thus abrogates 5-LO activity. We conclude that Cys159 of 5-LO is critical for the assembly of the 5-LO/FLAP complex, whereas cysteines 300, 416, and 418 do not contribute.

RESULTS

Melleolides Inhibit 5-LO Activity in Cell-Free and Cell-Based Systems

We investigated the effects of four structurally related melleolides isolated from *Armillaria mellea* (Figure 1A) on the activity of 5-LO in a cell-based model using Ca^{2+}-ionophore A23187-stimulated human neutrophils, and in a cell-free assay using purified human recombinant 5-LO as enzyme source. The investigated compounds included dehydroarmillylorsellinate (DAO) (**1**), arnamial (**2**), armillarin (**3**), and melleolide D (**4**). Concentration-response experiments with these melleolides in the cell-free assay revealed **2** as most potent derivative with a half maximal inhibitory concentration (IC_{50}) of 0.3 ± 0.02 μM, followed by **3** (IC_{50} = 2.5 ± 0.4 μM) and **1** (IC_{50} = 2.8 ± 0.9 μM, Figure 1B). Compound **4** was much less efficient (IC_{50} > 10 μM). Of interest, in neutrophils, **1** was the most efficient derivative against 5-LO (IC_{50} = 0.3 ± 0.1 μM, Figure 1C), with 10-fold higher potency versus cell-free assay conditions. Melleolides **2** (IC_{50} = 1.0 ± 0.2 μM) and **3** (IC_{50} = 5.2 ± 1.4 μM) showed comparable efficiency as in the cell-free test system. Again, **4** caused only moderate inhibition of 5-LO activity in neutrophils (IC_{50} > 10 μM). Cell viability analysis (trypan blue and light microscopy) exclude detrimental effects of **1–4** during the 10 min pre-incubation period of neutrophils (data not shown).

DAO (1) Potently Inhibits 5-LO Activity in Intact Neutrophils and Monocytes

To explore 5-LO inhibition by melleolides, we focused on **1**, which was the most potent derivative in neutrophils. First, we analyzed the effect of **1** against 5-LO in neutrophil homogenates, another cell-free test system for assessment of 5-LO activity (Werz and Steinhilber, 2005). Compared with its high potency in neutrophils, **1** was less active against 5-LO in corresponding homogenates (IC_{50} = 1.1 ± 0.2 μM), similar as for isolated 5-LO (Figure 2A). In contrast, the 5-LO inhibitor zileuton was equally effective for isolated 5-LO and cellular 5-LO activity ($IC_{50} \sim 0.8$ μM, Figure 2B). This suggested that **1** may interact with other enzyme(s) or factors involved in cellular 5-LO product formation such as $cPLA_2$ or FLAP. Analysis of AA release using [^{3}H]AA-labeled neutrophils indicated weak suppression of AA liberation by **1** (at 1 μM), which was much less pronounced as compared with RSC-3388, a specific $cPLA_2$ inhibitor (Table S1). We next supplemented neutrophils with exogenous AA (20 μM), to overcome potential deficiencies in endogenous AA supply due to potential $cPLA_2$ or FLAP inhibition (Werz and Steinhilber, 2005). The strong potency of **1** in absence of exogenous AA (i.e., IC_{50} = 0.3 μM) was about 7-fold decreased upon AA supplementation (IC_{50} = 2.1 μM, Figure 2C), suggesting that **1** may interfere with AA-related action(s). We also tested whether **1** may interfere with signaling processes important for 5-LO activation, such as its activation by mitogen-activated protein kinases (MAPKs) (Radmark et al., 2015). However, up to 10 μM, **1** failed to suppress the phosphorylation of p38 MAPK and extracellular signal-regulated kinase-1/2, and thus of $cPLA_2$ in neutrophils (Figure S1). Moreover, **1** did not cause strong inhibition of other enzymes in LT or eicosanoid biosynthesis such as LTC_4 synthase, cyclooxygenase-1/2, or microsomal prostaglandin E2 synthase-1 (Table S1), indicating a certain selectivity against 5-LO.

Besides neutrophils, also monocytes have high capacities to biosynthesize 5-LO products (Surette et al., 1993). Melleolide **1** inhibited 5-LO activity also in human monocytes stimulated with A23187, with comparable efficiency (IC_{50} = 0.8 μM), as in neutrophils (Figure 2D). A more detailed analysis showed that **1**

Please cite this article in press as: König et al., Melleolides from Honey Mushroom Inhibit 5-Lipoxygenase via Cys159, Cell Chemical Biology (2018), https://doi.org/10.1016/j.chembiol.2018.10.010

CellPress

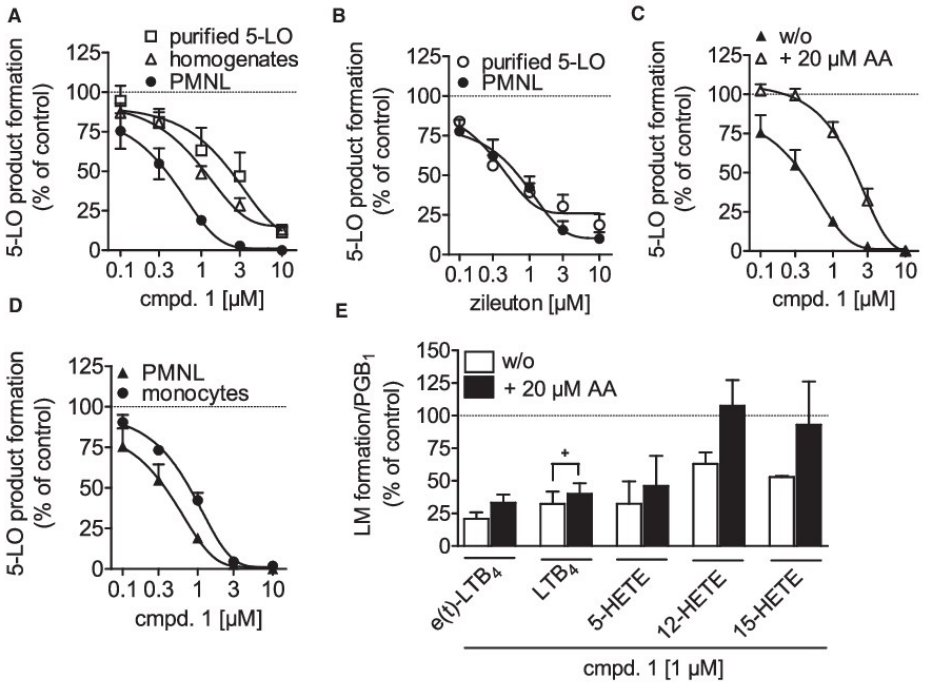

Figure 2. DAO (1) Potently Inhibits 5-LO Activity in Intact Neutrophils and Monocytes

(A) Purified human recombinant 5-LO, intact human neutrophils (5×10^6/mL), or neutrophil homogenates (corresponding to 5×10^6 cells/mL) were incubated with **1** or vehicle (0.1% DMSO) for 10 min at 37°C (neutrophils) or 4°C (5-LO, homogenates) prior to addition of 2.5 μM A23187 (neutrophils) or 2 mM $CaCl_2$ and 20 μM AA (5-LO, homogenates).

(B) Neutrophils or purified human recombinant 5-LO were pre-incubated for 10 min with zileuton or vehicle (0.1% DMSO) prior to addition of 2.5 μM A23187 (neutrophils) or 2 mM $CaCl_2$ and 20 μM AA (5-LO).

(C) Neutrophils were pre-incubated for 10 min with **1** or vehicle (0.1% DMSO) prior to addition of 2.5 μM A23187 with or without 20 μM AA.

(D) Effect of **1** on 5-LO product formation in neutrophils and monocytes. Cells (5×10^6/mL) were pre-treated with **1** or vehicle (0.1% DMSO) for 10 min. 5-LO product formation was started by 2.5 μM A23187.

(E) Effect of **1** (1 μM) on eicosanoid biosynthesis in intact monocytes stimulated with 2.5 μM A23187 in the presence or absence of 20 μM AA. All incubations (A–E) were performed for 10 min at 37°C, and then 5-LO product formation was determined by RP-HPLC and eicosanoids in (E) were analyzed by ultra-performance liquid chromatography-MS/MS. Data are expressed as percentage of uninhibited control (100%), means ± SEM, n = 3, +$p < 0.05$ versus vehicle control, paired t test.

See also Figure S1 and Table S1.

(at 1 μM) decreased all lipid mediators formed by 5-LO (i.e., tr-LTB_4 isomers, LTB_4, and 5-hydroxyeicosatetraenoic acid [HETE]) to a similar degree, which again was less pronounced when exogenous AA was supplemented (Figure 2E). Formation of 12- and 15-HETE was less affected by **1**, and, in the presence of exogenous AA (20 μM), **1** lost its inhibitory potency to suppress the biosynthesis of these lipid mediators.

Characterization of 5-LO Inhibition by Melleolides and Interaction with Cysteine

We characterized 5-LO inhibition by **1** in more detail. Washout experiments with isolated 5-LO revealed that **1** acts in a partially irreversible manner (Figure 3A), since the suppressive effect of **1** against 5-LO was hardly reversed upon 10-fold dilution. 5-LO activity studies with increasing AA concentrations (3–60 μM) in the cell-free assay revealed that the inhibitory potency of **1** is markedly improved at higher AA concentrations (IC_{50} = 7 μM at 3 μM AA versus IC_{50} = 0.3 μM at 60 μM AA, Figure 3B, left panel), even though the absolute activities of 5-LO strongly differ at the various AA concentrations (Figure 3B, right panel). Note that in intact neutrophils, exogenous supplementation of 20 μM AA gave the opposite effect and decreased the potency of **1** to inhibit 5-LO product formation, suggesting that the molecular mechanisms for suppression of 5-LO activity differ between intact cells and cell-free assays.

Compounds featuring a Michael acceptor, such as TQ or nitro fatty acids, were shown to act as direct covalent enzyme inhibitors that target the catalytically relevant Cys416 and Cys418 in 5-LO (Awwad et al., 2014; Maucher et al., 2017). It appeared reasonable that the α,β-unsaturated aldehyde in **1**, **2**, and **3** may function as Michael acceptors and react with these cysteines. Incubation of melleolides with glutathione (GSH) for

Please cite this article in press as: König et al., Melleolides from Honey Mushroom Inhibit 5-Lipoxygenase via Cys159, Cell Chemical Biology (2018), https://doi.org/10.1016/j.chembiol.2018.10.010

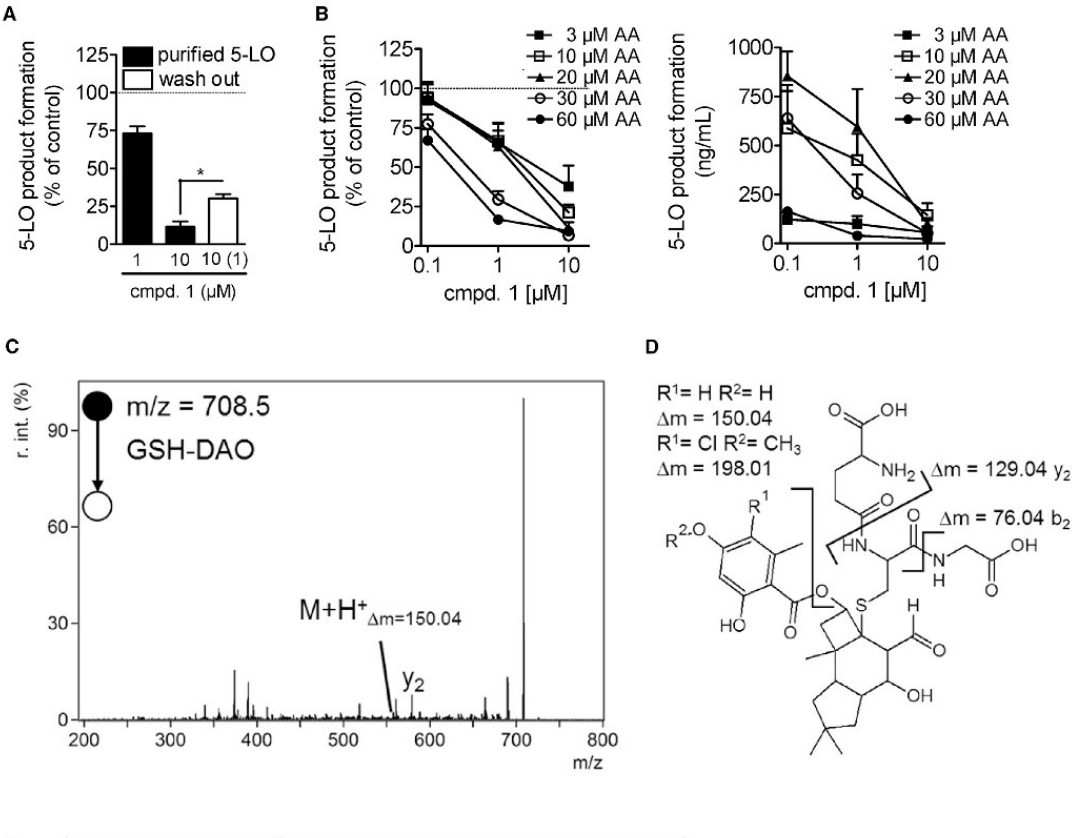

E

		Amino acid/Peptide terminus				
		Cys	His	Lys	Ser	N-Term
cmpd.	1	X**	X**	X**	-	X*
	2	X**	X**	X**	-	X*

Figure 3. Characterization of 5-LO Inhibition by Melleolides and Interaction with Cysteine

(A) Reversibility of 5-LO inhibition by **1**. Purified 5-LO (0.5 μg/mL) was pre-incubated with **1** (1 or 10 μM) or vehicle (0.1% DMSO) at 4°C for 10 min, pre-warmed at 37°C for 30 s, and 2 mM $CaCl_2$ and 20 μM AA were added. "Wash out" samples had been diluted 10-fold with assay buffer prior to addition of 2 mM $CaCl_2$ and 20 μM AA. After 10 min at 37°C, 5-LO products were analyzed by RP-HPLC. Data are expressed as percentage of control (100%), means ± SEM, n = 3, *$p < 0.05$ versus control, paired t test.

(B) Effect of various AA concentrations on 5-LO inhibition by **1**. Purified 5-LO (0.5 μg/mL) was pre-incubated with **1** or vehicle (0.1% DMSO) at 4°C for 10 min. Samples were pre-warmed at 37°C for 30 s, and 2 mM $CaCl_2$ and the indicated concentrations of AA were added and then incubated for 10 min at 37°C. Data are expressed as percentage of control (100%, left panel) or as ng/mL 5-LO products formed (right panel) and are given as means ± SEM, n = 3.

(C) MS^2 spectrum of **1** (DAO)-modified glutathione.

(D) Schematic fragmentation reactions with expected mass shifts.

(E) Results of specificity analysis with standard peptides. X, modification observed; –, no modification observed. *Indicates the detection of imine-formation in mass spectrum (side reaction), **Indicates the modification of peptide confirmed in MS^2 and/or MS^3.

See also Figures S2 and S3.

60 min at 37°C and subsequent analysis of the reaction mixture by tandem mass spectrometry (MS/MS) showed that **1** (Figures 3C and 3D) and **2** (Figure S2) reacted with the thiol group of GSH. The spectra revealed the expected signals for the resulting GSH-melleolide adducts (708.5 Da for **1**, Figure 3C, and 756.7 Da for **2**, Figure S2).

Please cite this article in press as: König et al., Melleolides from Honey Mushroom Inhibit 5-Lipoxygenase via Cys159, Cell Chemical Biology (2018), https://doi.org/10.1016/j.chembiol.2018.10.010

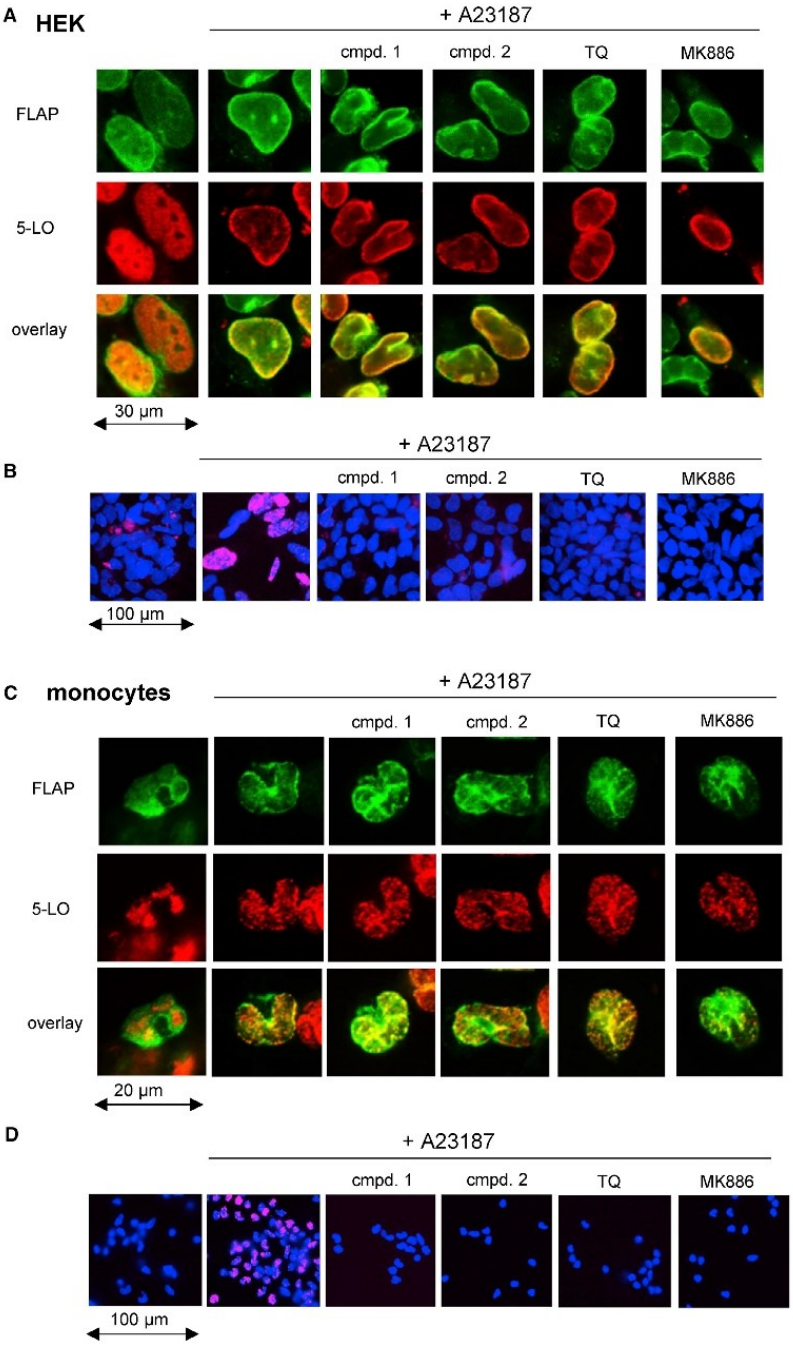

(legend on next page)

Please cite this article in press as: König et al., Melleolides from Honey Mushroom Inhibit 5-Lipoxygenase via Cys159, Cell Chemical Biology (2018), https://doi.org/10.1016/j.chembiol.2018.10.010

We next performed an amino acid residue specificity analysis (Figure 3E) to study binding of the melleolides to cysteine, histidine, serine, or lysine residues. These residues react in a Michael-like reaction but can also yield a semi-thioacetal or a semi-aminal. High-resolution MS spectra display the predicted masses of the reaction products that show the modification of cysteine, histidine, and lysine by **1** and **2**. MS/MS spectra displayed one main peak, which indicated the loss of chloroorsellinic acid or orsellenic acid, depending on the used melleolide. MS^3-spectra then showed the expected peptide fragment ion spectra and pointed out the binding side of the reactive sesquiterpene (Figure S3). The reaction of the melleolides with 5-LO displayed the mass of the modified peptide of **2** containing Cys159. MS/MS spectra yielded poor fragment ion abundance, so the exact modification site could not be confirmed.

Modulation of 5-LO Translocation and 5-LO/FLAP Interaction by Melleolides

5-LO translocation to the nuclear envelope and interaction with FLAP is a determinant for cellular 5-LO product formation (Gerstmeier et al., 2016a; Mandal et al., 2008). The superior potency of **1** against 5-LO activity in intact cells versus isolated enzyme led us to investigate if melleolides could block 5-LO translocation and/or interaction with FLAP. A convenient model based on HEK293 cells, stably transfected with 5-LO and FLAP, as well as human primary monocytes, were used. Immunofluorescence (IF) microscopy was performed to visualize the localization of the target proteins in the cell (Gerstmeier et al., 2014, 2016a). In agreement with previous data, 5-LO in resting HEK cells or human monocytes was mainly nucleosolic but co-localized with FLAP at the nuclear envelope upon A23187 stimulation (Figures 4A and 4C). However, neither **1** or **2** nor the Michael acceptor TQ or the FLAP inhibitor MK886 blocked A23187-induced 5-LO translocation (Figures 4A and 4C). Of interest, **1** and **2** (3 μM, each) as well as TQ (10 μM) impeded A23187-induced 5-LO/FLAP complex assembly in HEK cells (Figure 4B) and in monocytes (Figure 4D) that was monitored by *in situ* proximity ligation assay (PLA). The FLAP inhibitor MK886 (0.3 μM, used as control) blocked 5-LO/FLAP complex formation (Figures 4B and 4D), while the 5-LO inhibitor zileuton failed in this respect (not shown), as reported previously (Gerstmeier et al., 2016b). Taken together, the melleolides **1** and **2** as well as TQ impede the assembly of the LT-biosynthetic 5-LO/FLAP complex at the nuclear membrane, yet without blocking 5-LO translocation. This effect may be causative for superior inhibition of 5-LO product formation in intact cells.

Mutation of 5-LO Cysteines Affects Product Formation and Susceptibility for Melleolides

Previous studies suggested a role of the four surface cysteines 159, 300, 416, and 418 in 5-LO for cellular product formation (Hafner et al., 2015). Michael acceptors can act at either at Cys416 or Cys418 causing inhibition of 5-LO (Maucher et al., 2017). Thus, we studied if melleolides require these critical cysteines (Figure 5A) for inhibition of 5-LO. HEK cells were co-transfected with FLAP and with wild-type 5-LO (5-LO_WT) or with 5-LO mutants in which all four cysteines (5-LO_4C) or single cysteines had been replaced by serine. The mutated 5-LO proteins were expressed in HEK cells to a similar (5-LO_4C) or somewhat minor degree (5-LO_C159S, 5-LO_C300S, 5-LO_C416S, and 5-LO_C418S) versus 5-LO_WT (Figure 5B). Along these lines, the enzymatic capacities of corresponding HEK cell homogenates containing these 5-LO mutants were about 2- to 4-fold lower versus 5-LO_WT (Table 1). In HEK cell homogenates, **1** (Figure 5C, Table 1) and **2** (Figure S4) blocked 5-LO_WT activity, whereas 5-LO_4C was not affected at all. As for 5-LO_WT, the enzymatic activities of the mutants 5-LO_C159S, 5-LO_C300S, 5-LO_C416S, or 5-LO_C418S were also inhibited by **1** (Figure 5C, Table 1) and **2** (Figure S4). In contrast, zileuton inhibited 5-LO_WT and all mutated 5-LOs about equally well (Figure 5D).

Next, we analyzed cellular 5-LO product formation in intact HEK cells. Since previous data showed that 5-LO/FLAP-expressing HEK cells require exogenous AA for significant 5-LO product formation (Gerstmeier et al., 2014, 2016a), the cells were stimulated with A23187 plus 3 μM AA. In contrast to 5-LO activity in homogenates, all mutated 5-LOs formed much less amounts of products versus 5-LO_WT in intact cells (approximately 5- to 10-fold lower), in particular 5-LO_C159S (Table 1). Of interest, while product formation of 5-LO_WT was efficiently inhibited by **1** (10 μM), in HEK cells expressing 5-LO_4C but also 5-LO_C159S, melleolide **1** (or **2**, Figure S4) failed to markedly inhibit 5-LO product formation (Figure 5E, Table 1). Note that in cells expressing either 5-LO_C300S, 5-LO_C416S, or 5-LO_C418S, treatment with **1** (or **2**, Figure S4) caused efficient and concentration-dependent inhibition of 5-LO product formation comparable with cells expressing 5-LO_WT (Figure 5E). In contrast, zileuton consistently inhibited 5-LO activity in HEK cells regardless of the 5-LO mutations (Figure 5F). Hence, **1** and **2** may inhibit 5-LO product formation in intact cells via Cys159.

Role of Cysteines in 5-LO for Translocation and 5-LO/FLAP Interaction

In agreement with previous data (Hafner et al., 2015), the strikingly reduced capacities of the cysteine-mutated 5-LOs in intact HEK cells versus the moderately decreased activity of the 5-LO mutants in homogenates implied that cysteine mutations could affect 5-LO translocation and/or interaction with FLAP. Analysis of 5-LO translocation and co-localization with FLAP by IF microscopy revealed no impact of the cysteine mutations. That is, the subcellular localization of 5-LO_WT and all 5-LO mutants in resting HEK cells was comparable, and, upon A23187

Figure 4. Modulation of 5-LO Translocation and 5-LO/FLAP Interaction by Melleolides

Stably transfected HEK293 cells expressing 5-LO and FLAP (A and B) or human monocytes (C and D) were pre-incubated with compounds or vehicle (0.1% DMSO) for 10 min at 37°C, and subsequently incubated with 2.5 μM A23187 for 10 min. Images show single staining for FLAP (green), 5-LO (red), and overlay of 5-LO and FLAP (bottom lane). Results are representative for 100 individual cells of three independent experiments. (B and D) Proximity ligation assay (PLA) for assessing cellular *in situ* 5-LO/FLAP complex assembly. Stably transfected HEK293 cells expressing 5-LO and FLAP (B) or human monocytes (D) were pre-incubated with compounds or vehicle (0.1% DMSO) for 10 min at 37°C, and subsequently incubated with 2.5 μM A23187 for 10 min. DAPI (blue) was used to stain the nucleus and PLA signals (magenta dots) visualize 5-LO/FLAP interactions. Results are representative for 100 individual cells analyzed in three independent experiments.

Please cite this article in press as: König et al., Melleolides from Honey Mushroom Inhibit 5-Lipoxygenase via Cys159, Cell Chemical Biology (2018), https://doi.org/10.1016/j.chembiol.2018.10.010

CellPress

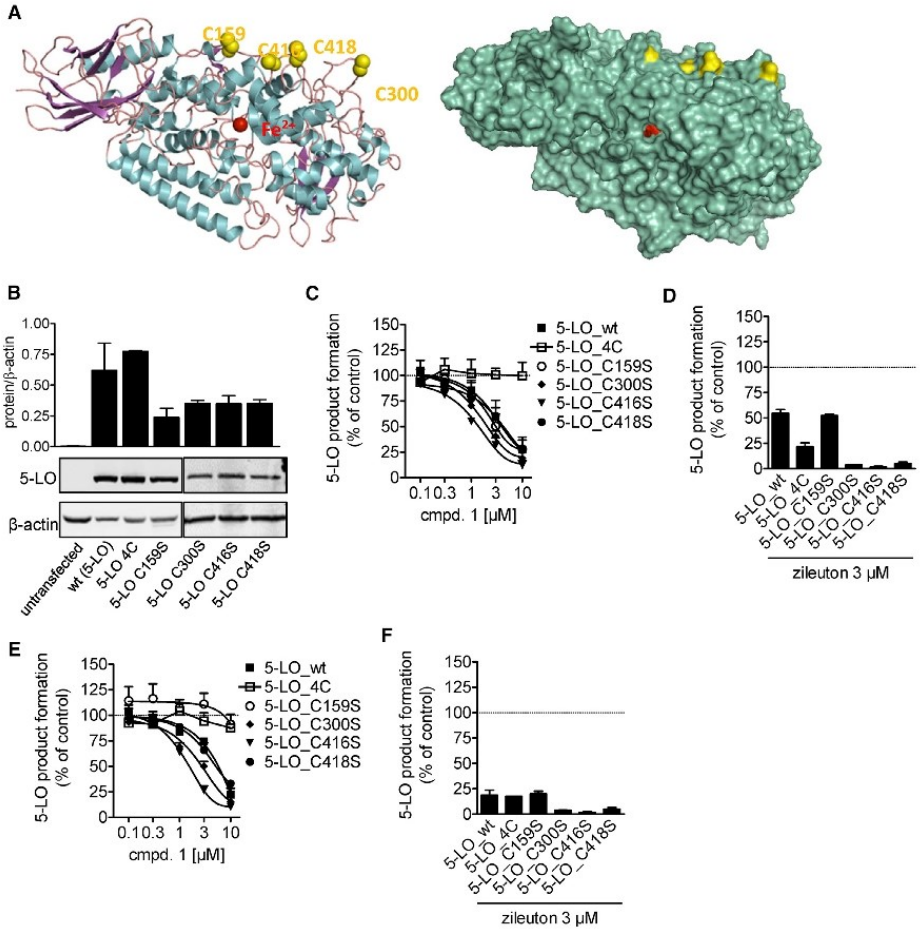

Figure 5. Mutation of 5-LO Cysteines Affects Product Formation and the Susceptibility for Melleolides

(A) Computational model of human 5-LO highlighting cysteine residues 159, 300, 416, and 418. The active site iron is highlighted in red.

(B) Western blot analysis of 5-LO protein expression in stably transfected HEK293 cells expressing FLAP and various 5-LO proteins (5-LO_WT and the mutants 5-LO_4C, 5-LO_C159S, 5-LO_C300S, 5-LO_C416S, and 5-LO_C418S). Results are representative for three independent experiments. Densitometric protein analysis: correlation of 5-LO density to β-actin density, means ± SEM, n = 3.

(C and D) Inhibition of 5-LO product formation in homogenates of HEK cells expressing FLAP and 5-LO (WT or mutants) by **1** at the indicated concentrations (C) and by 3 μM zileuton (D). HEK cells were sonicated on ice and pre-incubated with compounds or vehicle (0.1% DMSO) at 4°C for 10 min. Samples were pre-warmed for 30 s at 37°C and incubated with 2 mM $CaCl_2$ and 20 μM AA for another 10 min.

(E and F) Inhibition of 5-LO product formation in intact HEK cells expressing FLAP and 5-LO (WT or mutants) by **1** at the indicated concentrations (E) and by 3 μM zileuton (F). HEK cells (1 × 10^6/mL) were pre-incubated with **1**, zileuton, or vehicle (0.1% DMSO) for 10 min at 37°C and then stimulated with 2.5 μM A23187 and 3 μM AA for 10 min. Data are expressed as percentage of vehicle control (100%), means ± SEM, n = 4.

See also Figure S4.

stimulation, they all translocated to FLAP at the nuclear envelope (Figure 6A). Of interest, Cys159 seems to be instrumental for the 5-LO/FLAP interaction which was visualized by *in situ* PLA (Figure 6B). Thus, in HEK cells expressing 5-LO_WT, 5-LO_C300S, 5-LO_C416S, or 5-LO_C418S, stimulation with A23187 led to 5-LO/FLAP complex assembly. However, in HEK cells expressing 5-LO_4C or 5-LO_C159S, challenge with A23187 failed in this respect, implying a critical role of Cys159 in 5-LO/FLAP interaction.

DISCUSSION

Here, we identified human 5-LO as a molecular target of melleolides from honey mushroom. Exploiting **1** and **2** as the most

Please cite this article in press as: König et al., Melleolides from Honey Mushroom Inhibit 5-Lipoxygenase via Cys159, Cell Chemical Biology (2018), https://doi.org/10.1016/j.chembiol.2018.10.010

Table 1. Formation of 5-LO Products of Wild-Type and Mutated 5-LOs in HEK Cells and Corresponding Homogenates; Effects of Compound 1

	5-LO Product Formation			
	HEK Homogenates (ng/10^6 Cells)		Intact HEK Cells (ng/10^6 Cells)	
Enzyme	w/o	+ Compound **1** (% Inhibition)	w/o	+ Compound **1** (% Inhibition)
5-LO_WT	919.4 ± 40.0	243.0 ± 80.0 (72.6%)	346.8 ± 97.2	101.9 ± 23.3 (77.7%)
5-LO_4C	484.3 ± 58.8	477.7 ± 74.0 (0.4%)	48.1 ± 7.1	42.1 ± 6.3 (12.4%)
5-LO_C159S	456.9 ± 177.5	76.5 ± 11.9 (72.6%)	31.2 ± 12.4	24.6 ± 6.5 (9.8%)
5-LO_C300S	374.5 ± 29.7	71.6 ± 12.2 (81.0%)	71.5 ± 8.9	11.8 ± 4.5 (87.6%)
5-LO_C416S	223.1 ± 18.3	28.3 ± 12.0 (88.1%)	48.9 ± 9.5	5.0 ± 0.8 (89.6%)
5-LO_C418S	465.3 ± 22.8	124.9 ± 5.2 (73.2%)	66.6 ± 23.1	23.0 ± 9.5 (66.7%)

For analysis of 5-LO product formation in intact cells, HEK cells (1 × 10^6/mL) stably expressing FLAP and 5-LO enzymes (wild-type or mutants) were pre-incubated with 10 μM of **1** or vehicle (0.1% DMSO), and then stimulated with 2.5 μM A23187 and 3 μM AA for 10 min at 37°C. For analysis of 5-LO product formation in homogenates, the HEK cells (1 × 10^6/mL) were sonicated, the resulting homogenates were pre-incubated with 10 μM of **1** or vehicle (0.1% DMSO) and then incubated with 20 μM AA for 10 min at 37°C. Data are expressed as ng 5-LO products formed per 10^6 cells; means ± SEM, n = 4. w/o, without.

potent melleolide representatives revealed Cys159 in 5-LO as a crucial moiety for functional interaction of 5-LO with FLAP in LT biosynthesis. Our data suggest that melleolides suppress 5-LO product formation by two distinct modes of action: (1) by direct interference with the 5-LO enzyme activity involving two or more of the cysteines 159, 300, 416, and 418, and (2) by a more efficient mechanism that selectively involves Cys159 and prevents cellular 5-LO/FLAP complex assembly without affecting 5-LO translocation. Thus, our results shed light on the catalytic and regulatory role of cysteines at the substrate entrance of the 5-LO active site for the cellular capacity to biosynthesize LTs.

Melleolides were shown to exhibit antimicrobial activity and cytotoxic properties for cancer cells and primary human monocytes (Bohnert et al., 2011, 2014b), but interference with LT biosynthesis is thus far unexplored. With 5-LO, we identified a molecular target for these bioactive natural products. The efficient 5-LO-inhibitory melleolides possess a reactive aldehyde group at position 1 and a $\Delta^{2,4}$ (i.e., **1** and **2**) or $\Delta^{2,3}$ (i.e., **3**) double bond in the sesquiterpene moiety. Our SAR analysis indicates that the Michael acceptor functionality impacts 5-LO inhibitory activity, but also minor structural arrangements in the sesquiterpene moiety (α,β double bond at $\Delta^{2,4}$ versus $\Delta^{2,3}$ position, and the 4-OH moiety) and in the orsellinic acid residue (5′-OH methylation, 6′-chlorine). Strong potencies of 5-LO inhibitors often correlate with high lipophilicity (Werz, 2002), which may explain the superior effect of **2** with 5′-methoxy and 6′-chlorine residues over **1** in the cell-free assay.

Unexpectedly, the SARs for 5-LO inhibition by melleolides in intact neutrophils differ and reveal **1** as the most potent compound with a 10-fold lower IC_{50} value compared with interference with 5-LO in cell-free assays. Such superior potency in intact cells was not observed for the 5-LO inhibitor zileuton (this study and others [Carter et al., 1991]) and implies that additional factors that govern cellular 5-LO activity might be affected by melleolides. In fact, cellular regulation of 5-LO is complex, and several points of attack are conceivable that eventually cause or potentiate suppression of 5-LO product formation including interference with (1) AA release, (2) AA transfer via FLAP, (3) 5-LO translocation, and (4) upstream 5-LO signaling pathways such as MAPK and Ca^{2+}, and other 5-LO-activating processes (Radmark et al., 2015; Werz and Steinhilber, 2005). Our data show that melleolides, in addition to directly inhibiting 5-LO activity, prevent the 5-LO/FLAP complex assembly and, thus, could interfere with the AA transfer from FLAP to 5-LO. This may explain why excess of AA (20 μM) in intact cells diminishes the 5-LO-inhibitory potency of melleolides, although inhibition of 5-LO activity in cell-free assays is favored by high AA concentrations.

Most direct 5-LO inhibitors comprise lipophilic redox-active and/or iron-chelating compounds as well as AA mimetics that reversibly block AA conversion at the active or allosteric sites of 5-LO (Werz, 2002; Werz and Steinhilber, 2005). Based on the chemical structures of melleolides, fatty acid-like features are not readily apparent, and iron-chelating or redox properties have not been reported. Of interest, structurally different compounds containing SH-reactive groups such as the Michael acceptors TQ (Maucher et al., 2017), nitro fatty acids (Awwad et al., 2014), unsubstituted aminophenols (Kretschmer et al., 2017), or the maleimide-featured inhibitor U73122 (Feisst et al., 2005; Hornig et al., 2012) were shown to form covalent adducts with the surface cysteines 159, 416, and/or 418 and thereby potently and irreversibly inhibit 5-LO activity. The 5-LO structure exposes nine cysteine residues on the surface (Gilbert et al., 2011). We previously identified four cysteines (cysteines 159, 300, 416, and 418) located on the 5-LO surface in the region around the substrate entrance of the catalytic center that mediate dimerization of 5-LO (Hafner et al., 2011) and are important for the co-localization of 5-LO with FLAP at the nuclear membrane (Hafner et al., 2015). In our present study, melleolides failed to inhibit the activity of the 5-LO_4C mutant in cell-free and cell-based assays, suggesting that one or more of these cysteines are necessary to confer the 5-LO suppressive effect. In contrast, zileuton, which chelates the active site iron in 5-LO (Carter et al., 1991), suppressed the activity of this mutant, as expected. Note that 5-LO single mutants, with only one of the cysteines 159, 300, 416, or 418 being replaced by serine, were still effectively inhibited by melleolides in cell-free assays, implying that at least two of these cysteines are involved. This contrasts the suppressive effect of melleolides on 5-LO activity in intact

Please cite this article in press as: König et al., Melleolides from Honey Mushroom Inhibit 5-Lipoxygenase via Cys159, Cell Chemical Biology (2018), https://doi.org/10.1016/j.chembiol.2018.10.010

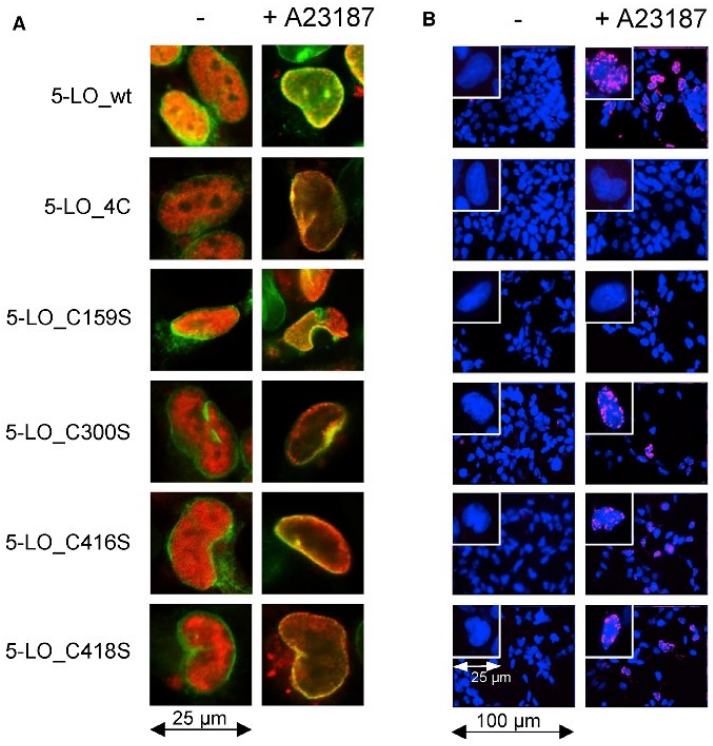

Figure 6. Role of Cysteines in 5-LO for Translocation and 5-LO/FLAP Interaction

(A) Immunofluorescence microscopy analysis of 5-LO translocation and co-localization with FLAP. Images show overlay of 5-LO (red) and FLAP (green).

(B) PLA for analysis of cellular *in situ* 5-LO/FLAP complex assembly. DAPI (blue) was used to stain the nucleus and *in situ* PLA signals (magenta dots) visualize 5-LO/FLAP complexes. Scale bars, 25 μm (insets) and 100 μm (overview). For both (A) and (B), stably transfected HEK cells expressing FLAP and 5-LO (WT or mutants) were incubated with 2.5 μM A23187 or vehicle (0.1% DMSO) for 10 min at 37°C. Results are representative for 100 individual cells of three independent experiments.

cells, where Cys159 emerged as a crucial residue required to mediate inhibition of 5-LO product formation. Thus, our results suggest that melleolides act via Cys159 to prevent the 5-LO/FLAP complex assembly while cysteines 300, 416, and 418 do not contribute.

FLAP, a nuclear membrane protein without any known enzymatic activity, is essential for 5-LO product formation in intact cells (Miller et al., 1990) by enabling AA substrate transfer to 5-LO for conversion to LTA_4 (Ferguson et al., 2007). Accordingly, FLAP inhibitors efficiently inhibit cellular LT biosynthesis by preventing 5-LO/FLAP assemblies (Garscha et al., 2016; Gerstmeier et al., 2016b) but they fail to inhibit 5-LO activity in cell-free assays where FLAP is dispensable for 5-LO to convert AA (Evans et al., 2008). Along these lines, mutation of cysteines 159, 300, 416, or 418, which were postulated to be important for 5-LO/FLAP co-localization (Hafner et al., 2015), hardly affected 5-LO activity in cell-free homogenates, but strikingly in intact cells. Moreover, 5-LO_C159S or 5-LO_4C failed to form complex assemblies with FLAP, in contrast to 5-LOs possessing Cys159. Interestingly, **1** and **2** (but not zileuton) required Cys159 to inhibit 5-LO product formation in intact cells. However, when this cysteine was replaced by serine, these mutants were not susceptible to the tested melleolides. Therefore, Cys159 is of major importance for 5-LO to interact with FLAP and as such mediates suppression of cellular 5-LO product formation by melleolides.

5-LO translocation to the nuclear envelope is mediated by elevated intracellular Ca^{2+} that binds to the C2-like domain of 5-LO (Kulkarni et al., 2002), and is essential for product biosynthesis (Gerstmeier et al., 2016b; Mandal et al., 2008; Radmark et al., 2015). The prenylated acylphloroglucinol hyperforin binds to the 5-LO C2-like domain and blocks 5-LO translocation and activity (Feisst et al., 2009), while FLAP inhibitors primarily prevent 5-LO/FLAP interaction without definite blockade of 5-LO movement (Garscha et al., 2016; Gerstmeier et al., 2016b). In analogy to MK886, **1** and **2** as well as TQ failed to block 5-LO translocation but they clearly inhibited the 5-LO/FLAP interaction.

Taken together, we identified human 5-LO as a molecular target of melleolides from the honey mushroom. We propose that melleolides containing an α,β-unsaturated aldehyde function as Michael acceptors that interfere with critical surface cysteines of 5-LO. While two or more of these cysteines mediate the direct inhibitory effects of melleolides on the enzymatic level, Cys159 confers suppression of cellular 5-LO product formation by melleolides via preventing the 5-LO/FLAP complex assembly. Finally, our data highlight the importance of Cys159 for 5-LO to interact with FLAP, a prerequisite for the biosynthesis of LTs in the cellular context.

SIGNIFICANCE

Only for very few mushroom toxins is the pharmacological mode of action understood and the molecular targets known. Melleolides are a family of sesquiterpene aryl esters of the globally distributed plant pathogenic and edible honey mushroom (*Armillaria mellea*). This family of natural products comprises >60 published members and represents one of the largest family of fungal small bioactive molecules. We discovered human 5-lipoxygenase (5-LO), the key enzyme in leukotriene biosynthesis, as a molecular target for those melleolides that possess an α,β-unsaturated aldehyde with thiol-reactive Michael acceptor functionality. Since leukotrienes are potent bioactive mediators with pivotal functions in inflammation and in the immune

Please cite this article in press as: König et al., Melleolides from Honey Mushroom Inhibit 5-Lipoxygenase via Cys159, Cell Chemical Biology (2018), https://doi.org/10.1016/j.chembiol.2018.10.010

response, their formation needs to be tightly controlled, for example, by temporal assembly of the biosynthetic protein complex of 5-LO with its helper protein FLAP. We provide evidence that melleolides mediate 5-LO inhibition via critical surface cysteines of the enzyme by two distinct modes of action: (1) by direct interference with the 5-LO catalytic activity involving two or more of the cysteines 159, 300, 416, and 418, and (2) by a more efficient cellular mechanism involving selectively Cys159, which prevents assembly of the 5-LO/FLAP complex in leukotriene biosynthesis. In conclusion, identification of 5-LO as a target for melleolides represents a basis for further investigations that will help evaluate the bioactions of this mushroom and its ingredients in view of the use for culinary purposes. By exploiting these melleolides as chemical tools we shed light on the catalytic and regulatory role of cysteines of 5-LO at the substrate entrance of the active site for the cellular capacity to generate bioactive mediators. Therefore, our study also unravels Cys159 in 5-LO as a crucial residue for accomplishing the functional interaction of 5-LO with FLAP in leukotriene biosynthesis, which offers a potential site for novel small-molecule inhibitors to intervene with 5-LO-related disorders.

STAR★METHODS

Detailed methods are provided in the online version of this paper and include the following:

- KEY RESOURCES TABLE
- CONTACT FOR REAGENT AND RESOURCE SHARING
- EXPERIMENTAL MODEL AND SUBJECT DETAILS
  - Human Cells
- METHODS DETAILS
  - Expression and Purification of Human Recombinant 5-LO
  - Determination of 5-LO Product Formation in Intact Cells and Homogenates
  - Determination of Release of [^{3}H]-Labeled Arachidonic Acid
  - LTC_4 Synthase Activity Assay
  - Determination of Isolated COX-1 and -2 Activity
  - Determination of PGE_2 Synthase Activity in a Cell-Free Assay
  - SDS PAGE and Western Blot
  - GSH Incubation
  - Standard Peptide Incubation
  - MALDI-MS Measurement and Data Analysis
  - Analysis of Subcellular Localization of 5-LO by Immunofluorescence Microscopy
  - In Situ Analysis of 5-LO/FLAP Interaction by Proximity Ligation Assay
- QUANTIFICATION AND STATISTICAL ANALYSIS

SUPPLEMENTAL INFORMATION

Supplemental Information includes four figures and one table and can be found with this article online at https://doi.org/10.1016/j.chembiol.2018.10.010.

ACKNOWLEDGMENTS

We thank Sven George for expert technical assistance and Dr. Michael Hörnig for mutation of 5-LO plasmids. The study was supported by Else Kröner-Fresenius-Stiftung (Else Kröner-Graduiertenkolleg), LOEWE TMP and Fraunhofer-Projektgruppe für Translationale Medizin und Pharmakologie (TMP), Deutsche Forschungsgemeinschaft (DFG; SFB 1039). Work in the groups of O.W. and D.H. is supported by the Collaborative Research Center ChemBioSys (SFB1127) of the DFG and by the DFG-funded excellence graduate school Jena School for Microbial Communication (JSMC).

AUTHOR CONTRIBUTIONS

S.K., B.H., D.S., M.K., U.G., D.H., and O.W. designed the research, gave advice, and planed the study. S.K., E.R., V.K., M.R., S.L., A.-K.H., M.D., and U.G., performed the experiments and analyzed the data. S.K. and O.W. wrote the manuscript.

DECLARATION OF INTERESTS

The authors declare no competing interests.

Received: May 28, 2018
Revised: July 25, 2018
Accepted: October 5, 2018
Published: November 8, 2018

REFERENCES

Albert, D., Zundorf, I., Dingermann, T., Muller, W.E., Steinhilber, D., and Werz, O. (2002). Hyperforin is a dual inhibitor of cyclooxygenase-1 and 5-lipoxygenase. Biochem. Pharmacol. *64*, 1767–1775.

Awwad, K., Steinbrink, S.D., Fromel, T., Lill, N., Isaak, J., Hafner, A.K., Roos, J., Hofmann, B., Heide, H., Geisslinger, G., et al. (2014). Electrophilic fatty acid species inhibit 5-lipoxygenase and attenuate sepsis-induced pulmonary inflammation. Antioxid. Redox Signal. *20*, 2667–2680.

Bair, A.M., Turman, M.V., Vaine, C.A., Panettieri, R.A., Jr., and Soberman, R.J. (2012). The nuclear membrane leukotriene synthetic complex is a signal integrator and transducer. Mol. Biol. Cell *23*, 4456–4464.

Baumgartner, K., Coetzee, M.P., and Hoffmeister, D. (2011). Secrets of the subterranean pathosystem of Armillaria. Mol. Plant Pathol. *12*, 515–534.

Bohnert, M., Miethbauer, S., Dahse, H.M., Ziemen, J., Nett, M., and Hoffmeister, D. (2011). In vitro cytotoxicity of melleolide antibiotics: structural and mechanistic aspects. Bioorg. Med. Chem. Lett. *21*, 2003–2006.

Bohnert, M., Nutzmann, H.W., Schroeckh, V., Horn, F., Dahse, H.M., Brakhage, A.A., and Hoffmeister, D. (2014a). Cytotoxic and antifungal activities of melleolide antibiotics follow dissimilar structure-activity relationships. Phytochemistry *105*, 101–108.

Bohnert, M., Scherer, O., Wiechmann, K., Konig, S., Dahse, H.M., Hoffmeister, D., and Werz, O. (2014b). Melleolides induce rapid cell death in human primary monocytes and cancer cells. Bioorg. Med. Chem. *22*, 3856–3861.

Carter, G.W., Young, P.R., Albert, D.H., Bouska, J., Dyer, R., Bell, R.L., Summers, J.B., and Brooks, D.W. (1991). 5-Lipoxygenase inhibitory activity of zileuton. J. Pharmacol. Exp. Ther. *256*, 929–937.

Evans, J.F., Ferguson, A.D., Mosley, R.T., and Hutchinson, J.H. (2008). What's all the FLAP about?: 5-lipoxygenase-activating protein inhibitors for inflammatory diseases. Trends Pharmacol. Sci. *29*, 72–78.

Feisst, C., Albert, D., Steinhilber, D., and Werz, O. (2005). The aminosteroid phospholipase C antagonist U-73122 (1-[6-[[17-beta-3-methoxyestra-1,3,5(10)-trien-17-yl]amino]hexyl]-1H-pyrrole-2,5- dione) potently inhibits human 5-lipoxygenase in vivo and in vitro. Mol. Pharmacol. *67*, 1751–1757.

Feisst, C., Pergola, C., Rakonjac, M., Rossi, A., Koeberle, A., Dodt, G., Hoffmann, M., Hoernig, C., Fischer, L., Steinhilber, D., et al. (2009). Hyperforin is a novel type of 5-lipoxygenase inhibitor with high efficacy in vivo. Cell Mol. Life Sci. *66*, 2759–2771.

Please cite this article in press as: König et al., Melleolides from Honey Mushroom Inhibit 5-Lipoxygenase via Cys159, Cell Chemical Biology (2018), https://doi.org/10.1016/j.chembiol.2018.10.010

Ferguson, A.D., McKeever, B.M., Xu, S., Wisniewski, D., Miller, D.K., Yamin, T.T., Spencer, R.H., Chu, L., Ujjainwalla, F., Cunningham, B.R., et al. (2007). Crystal structure of inhibitor-bound human 5-lipoxygenase-activating protein. Science *317*, 510–512.

Fischer, L., Poeckel, D., Buerkert, E., Steinhilber, D., and Werz, O. (2005). Inhibitors of actin polymerisation stimulate arachidonic acid release and 5-lipoxygenase activation by upregulation of Ca2+ mobilisation in polymorphonuclear leukocytes involving Src family kinases. Biochim. Biophys. Acta *1736*, 109–119.

Fischer, L., Szellas, D., Radmark, O., Steinhilber, D., and Werz, O. (2003). Phosphorylation- and stimulus-dependent inhibition of cellular 5-lipoxygenase activity by nonredox-type inhibitors. FASEB J. *17*, 949–951.

Garscha, U., Voelker, S., Pace, S., Gerstmeier, J., Emini, B., Liening, S., Rossi, A., Weinigel, C., Rummler, S., Schubert, U.S., et al. (2016). BRP-187: a potent inhibitor of leukotriene biosynthesis that acts through impeding the dynamic 5-lipoxygenase/5-lipoxygenase-activating protein (FLAP) complex assembly. Biochem. Pharmacol. *119*, 17–26.

Gerstmeier, J., Newcomer, M.E., Dennhardt, S., Romp, E., Fischer, J., Werz, O., and Garscha, U. (2016a). 5-Lipoxygenase-activating protein rescues activity of 5-lipoxygenase mutations that delay nuclear membrane association and disrupt product formation. FASEB J. *30*, 1892–1900.

Gerstmeier, J., Weinigel, C., Barz, D., Werz, O., and Garscha, U. (2014). An experimental cell-based model for studying the cell biology and molecular pharmacology of 5-lipoxygenase-activating protein in leukotriene biosynthesis. Biochim. Biophys. Acta *1840*, 2961–2969.

Gerstmeier, J., Weinigel, C., Rummler, S., Radmark, O., Werz, O., and Garscha, U. (2016b). Time-resolved in situ assembly of the leukotriene-synthetic 5-lipoxygenase/5-lipoxygenase-activating protein complex in blood leukocytes. FASEB J. *30*, 276–285.

Gilbert, N.C., Bartlett, S.G., Waight, M.T., Neau, D.B., Boeglin, W.E., Brash, A.R., and Newcomer, M.E. (2011). The structure of human 5-lipoxygenase. Science *331*, 217–219.

Haeggstrom, J.Z., and Funk, C.D. (2011). Lipoxygenase and leukotriene pathways: biochemistry, biology, and roles in disease. Chem. Rev. *111*, 5866–5898.

Hafner, A.K., Cernescu, M., Hofmann, B., Ermisch, M., Hornig, M., Metzner, J., Schneider, G., Brutschy, B., and Steinhilber, D. (2011). Dimerization of human 5-lipoxygenase. Biol. Chem. *392*, 1097–1111.

Hafner, A.K., Gerstmeier, J., Hornig, M., George, S., Ball, A.K., Schroder, M., Garscha, U., Werz, O., and Steinhilber, D. (2015). Characterization of the interaction of human 5-lipoxygenase with its activating protein FLAP. Biochim. Biophys. Acta *1851*, 1465–1472.

Hornig, M., Markoutsa, S., Hafner, A.K., George, S., Wisniewska, J.M., Rodl, C.B., Hofmann, B., Maier, T., Karas, M., Werz, O., et al. (2012). Inhibition of 5-lipoxygenase by U73122 is due to covalent binding to cysteine 416. Biochim. Biophys. Acta *1821*, 279–286.

Koeberle, A., Northoff, H., and Werz, O. (2009). Curcumin blocks prostaglandin E2 biosynthesis through direct inhibition of the microsomal prostaglandin E2 synthase-1. Mol. Cancer Ther. *8*, 2348–2355.

Koeberle, A., Siemoneit, U., Buhring, U., Northoff, H., Laufer, S., Albrecht, W., and Werz, O. (2008). Licofelone suppresses prostaglandin E2 formation by interference with the inducible microsomal prostaglandin E2 synthase-1. J. Pharmacol. Exp. Ther. *326*, 975–982.

Kretschmer, S.B., Woltersdorf, S., Vogt, D., Lillich, F.F., Ruhl, M., Karas, M., Maucher, I.V., Roos, J., Hafner, A.K., Kaiser, A., et al. (2017). Characterization of the molecular mechanism of 5-lipoxygenase inhibition by 2-aminothiazoles. Biochem. Pharmacol. *123*, 52–62.

Kulkarni, S., Das, S., Funk, C.D., Murray, D., and Cho, W. (2002). Molecular basis of the specific subcellular localization of the C2-like domain of 5-lipoxygenase. J. Biol. Chem. *277*, 13167–13174.

Leslie, C.C. (2015). Cytosolic phospholipase A(2): physiological function and role in disease. J. Lipid Res. *56*, 1386–1402.

Liening, S., Scriba, G.K., Rummler, S., Weinigel, C., Kleinschmidt, T.K., Haeggstrom, J.Z., Werz, O., and Garscha, U. (2016). Development of smart cell-free and cell-based assay systems for investigation of leukotriene C4 synthase activity and evaluation of inhibitors. Biochim. Biophys. Acta *1861*, 1605–1613.

Mandal, A.K., Jones, P.B., Bair, A.M., Christmas, P., Miller, D., Yamin, T.T., Wisniewski, D., Menke, J., Evans, J.F., Hyman, B.T., et al. (2008). The nuclear membrane organization of leukotriene synthesis. Proc. Natl. Acad. Sci. U S A *105*, 20434–20439.

Maucher, I.V., Ruhl, M., Kretschmer, S.B., Hofmann, B., Kuhn, B., Fettel, J., Vogel, A., Flugel, K.T., Manolikakes, G., Hellmuth, N., et al. (2017). Michael acceptor containing drugs are a novel class of 5-lipoxygenase inhibitor targeting the surface cysteines C416 and C418. Biochem. Pharmacol. *125*, 55–74.

Miller, D.K., Gillard, J.W., Vickers, P.J., Sadowski, S., Leveille, C., Mancini, J.A., Charleson, P., Dixon, R.A., Ford-Hutchinson, A.W., Fortin, R., et al. (1990). Identification and isolation of a membrane protein necessary for leukotriene production. Nature *343*, 278–281.

Misiek, M., Williams, J., Schmich, K., Huttel, W., Merfort, I., Salomon, C.E., Aldrich, C.C., and Hoffmeister, D. (2009). Structure and cytotoxicity of arnamial and related fungal sesquiterpene aryl esters. J. Nat. Prod. *72*, 1888–1891.

Momose, I., Sekizawa, R., Hosokawa, N., Iinuma, H., Matsui, S., Nakamura, H., Naganawa, H., Hamada, M., and Takeuchi, T. (2000). Melleolides K, L and M, new melleolides from *Armillariella mellea*. J. Antibiot. (Tokyo) *53*, 137–143.

Pace, S., Rossi, A., Krauth, V., Dehm, F., Troisi, F., Bilancia, R., Weinigel, C., Rummler, S., Werz, O., and Sautebin, L. (2017). Sex differences in prostaglandin biosynthesis in neutrophils during acute inflammation. Sci. Rep. *7*, 3759.

Pergola, C., Gerstmeier, J., Monch, B., Caliskan, B., Luderer, S., Weinigel, C., Barz, D., Maczewsky, J., Pace, S., Rossi, A., et al. (2014). The novel benzimidazole derivative BRP-7 inhibits leukotriene biosynthesis in vitro and in vivo by targeting 5-lipoxygenase-activating protein (FLAP). Br. J. Pharmacol. *171*, 3051–3064.

Radmark, O., Werz, O., Steinhilber, D., and Samuelsson, B. (2015). 5-Lipoxygenase, a key enzyme for leukotriene biosynthesis in health and disease. Biochim. Biophys. Acta *1851*, 331–339.

Scherer, O., Steinmetz, H., Kaether, C., Weinigel, C., Barz, D., Kleinert, H., Menche, D., Muller, R., Pergola, C., and Werz, O. (2014). Targeting V-ATPase in primary human monocytes by archazolid potently represses the classical secretion of cytokines due to accumulation at the endoplasmic reticulum. Biochem. Pharmacol. *91*, 490–500.

Soderberg, O., Gullberg, M., Jarvius, M., Ridderstrale, K., Leuchowius, K.J., Jarvius, J., Wester, K., Hydbring, P., Bahram, F., Larsson, L.G., et al. (2006). Direct observation of individual endogenous protein complexes in situ by proximity ligation. Nat. Methods *3*, 995–1000.

Steinhilber, D., Herrmann, T., and Roth, H.J. (1989). Separation of lipoxins and leukotrienes from human granulocytes by high-performance liquid chromatography with a Radial-Pak cartridge after extraction with an octadecyl reversed-phase column. J. Chromatogr. *493*, 361–366.

Surette, M.E., Palmantier, R., Gosselin, J., and Borgeat, P. (1993). Lipopolysaccharides prime whole human blood and isolated neutrophils for the increased synthesis of 5-lipoxygenase products by enhancing arachidonic acid availability: involvement of the CD14 antigen. J. Exp. Med. *178*, 1347–1355.

Werz, O. (2002). 5-Lipoxygenase: cellular biology and molecular pharmacology. Curr. Drug Targets Inflamm. Allergy *1*, 23–44.

Werz, O., and Steinhilber, D. (2005). Development of 5-lipoxygenase inhibitors – lessons from cellular enzyme regulation. Biochem. Pharmacol. *70*, 327–333.

Please cite this article in press as: König et al., Melleolides from Honey Mushroom Inhibit 5-Lipoxygenase via Cys159, Cell Chemical Biology (2018), https://doi.org/10.1016/j.chembiol.2018.10.010

STAR★METHODS

KEY RESOURCES TABLE

REAGENT or RESOURCE	SOURCE	IDENTIFIER
Antibodies		
p-ERK1/2 (Thr202/Tyr204)	Cell Signaling Technology	9106S; RRID: AB_331768
ERK1/2	Cell Signaling Technology	9102S; RRID: AB_330744
p-cPLA$_2$ (Ser505)	Cell Signaling Technology	2831S; RRID: AB_2164445
p-p38 (Thr180/Tyr182)	Cell Signaling Technology	9211S; RRID: AB_331641
β-actin	Cell Signaling Technology	3700S; RRID: AB_2242334
GAPDH	Santa Cruz	Sc-47724; RRID: AB_627678
IRDye 800CW Goat anti-Mouse IgG (H+L)	LI-COR	[P/N 925-32210]; RRID: AB_2687825
IRDye 680LT Goat anti-Rabbit IgG (H+L)	LI-COR	[P/N 925-68020]; RRID: AB_2687826
FLAP	Abcam	ab85227; RRID: AB_10673941
Alexa Fluor 488 goat anti-rabbit IgG (H+L)	Invitrogen	A11034; RRID: AB_2576217
Alexa Fluor 555 goat anti-mouse IgG (H+L)	Invitrogen	A21424; RRID: AB_141780
Chemicals, Peptides, and Recombinant Proteins		
DMSO	VWR	1029500500
bovine serum albumin	AppliChem	A1391.0500
penicillin/streptomycin	GE Healthcare Life Sciences	A2213
RPMI-1640	GE Healthcare Life Sciences	R8758-6
fetal calf serum	Sigma	F7524
Histopaque®-1077	Sigma	10771-500ML
Thymoquinone	Sigma	03416-100MG
Celecoxib	Sigma	PZ0008
N-Formyl-Met-Leu-Phe (fMLP)	Sigma	F3506-10MG
Duolink® insitu PLA probe anti-mouse minus	Sigma	DUO92004-100RXN
Duolink® insitu PLA probe anti-rabbit plus	Sigma	DUO92002-100RXN
Duolink® insitu detection reagents far red	Sigma	DUO92013
Duolink® insitu PLA wash buffers fluorescence	Sigma	DUO82049-4L
Rotiszint® eco plus	Carl Roth	0016.4
ovine COX-1	Cayman Chemicals	60100
human recombinant COX-2	Cayman Chemicals	60122
LTA$_4$ methyl ester	Cayman Chemicals	20010.25 μg
LTC$_4$ methyl ester d$_5$	Cayman Chemicals	9001287-50
MK886	Cayman Chemicals	10133-5
arachidonic acid	Cayman Chemicals	90010
Zileuton	Sequoia Research Products	SRP01100z
Critical Commercial Assays		
DC protein assay kit	Biorad	5000111
Experimental Models: Cell Lines		
HEK293	ATCC	CRL-153
HEK293_5-LO	Hafner et al., 2015	N/A
HEK293_5-LO_C159S	Hornig et al., 2012	N/A
HEK293_5-LO_C300S	Hornig et al., 2012	N/A
HEK293_5-LO_C416S	Hornig et al., 2012	N/A
HEK293_5-LO_C418S	Hornig et al., 2012	N/A
HEK293_5-LO_C159S_C300S_C416S_C418S	Hafner et al., 2015	N/A
A549	ATCC	CCL-185

(Continued on next page)

Please cite this article in press as: König et al., Melleolides from Honey Mushroom Inhibit 5-Lipoxygenase via Cys159, Cell Chemical Biology (2018), https://doi.org/10.1016/j.chembiol.2018.10.010

Continued

REAGENT or RESOURCE	SOURCE	IDENTIFIER
Experimental Models: Organisms/Strains		
Escherichia coli BL21 (DE3)	New England Biolabs	C2525I
Software and Algorithms		
GraphPad InStat 3	GraphPad Software Inc	https://www.graphpad.com/scientific-software/instat/
Odyssey 3.0 software	LI-COR	https://www.licor.com/bio/products/software/image_studio/index.html
Xcalibur Qual Browser Software 2.0.7	Thermo Fisher Scientific	http://www.thermofisher.com/order/catalog/product/OPTON-30487
mMass version 5.5.0	open source mass spectometry	http://www.mmass.org/download/
AxioVision Se64 Rel. 4.9	Carl Zeiss	https://www.zeiss.de/mikroskopie/downloads/axiovision-downloads.html

CONTACT FOR REAGENT AND RESOURCE SHARING

Further information and requests for resources and reagents should be directed to and will be fulfilled by the Lead Contact, Oliver Werz (oliver.werz@uni-jena.de)

EXPERIMENTAL MODEL AND SUBJECT DETAILS

Human Cells

Neutrophils and monocytes were isolated from peripheral human blood of adult healthy male and female volunteers (18-65 years) as described (Pace et al., 2017; Scherer et al., 2014) and with consent obtained from the Institute of Transfusion Medicine, University Hospital Jena. Individual blood samples provided and used for leukocyte isolation were blinded and thus, the exact age and the sex of the donor was unknown. The protocols for experiments with human neutrophils and monocytes were approved by the ethical commission of the Friedrich-Schiller-University Jena (approval no. 4025-02/14). All methods were performed in accordance with the relevant guidelines and regulations. Leukocyte concentrates were prepared by centrifugation (4000×g, 20 min, 20°C) and erythrocytes were removed by dextran sedimentation, followed by centrifugation on lymphocyte separation medium (Histopaque®-1077, Sigma-Aldrich) to obtain peripheral blood mononuclear cells (PBMC) and neutrophils. Resulting neutrophils were finally resuspended in PBS pH 7.4 containing 1 mg/mL glucose and 1 mM $CaCl_2$ (PGC buffer). PBMC were seeded in RPMI 1640 (Sigma-Aldrich) containing 10% (v/v) heat inactivated fetal calf serum (FCS), 100 U/mL penicillin, and 100 μg/mL streptomycin in cell culture flasks (Greiner Bio-one, Frickenhausen, Germany) for 1.5 h at 37°C and 5% CO_2. Adherent monocytes were washed twice with PBS and were resuspended in PGC buffer. HEK (human embryonic kidney, female fetus)293 cells stably transfected with FLAP and 5-LO or 5-LO mutants (Hornig et al., 2012; Hafner et al., 2015) were cultured in monolayers in DMEM High Glucose (4.5 g/L) medium supplemented with heat-inactivated FCS (10%, v/v), 100 U/mL penicillin, and 100 μg/mL streptomycin at 37°C in a 5% CO_2 incubator.

METHODS DETAILS

Expression and Purification of Human Recombinant 5-LO

Escherichia coli (BL21) cells were transformed with plasmid pT3-5-LO, and human recombinant 5-LO protein was expressed overnight at 30°C as previously described (Fischer et al., 2003). Cells were lysed in 50 mM triethanolamine/HCl pH 8.0, 5 mM EDTA, 1 mM phenylmethanesulphonyl fluoride (PMSF), soybean trypsin inhibitor (STI, 60 μg/mL), and lysozyme (1 mg/mL), homogenized by sonication (3 × 20 s), and centrifuged at 40,000×g for 20 min at 4°C. For purification of 5-LO, ATP affinity chromatography was used and the 40,000×g supernatant (S40) was applied to an ATP agarose column (Sigma-Aldrich). Aliquots of semi-purified 5-LO were diluted with ice-cold PBS containing 1 mM EDTA. Samples were pre-incubated with the test compounds or vehicle (0.1% DMSO). After 10 min at 4°C, samples were stimulated with 2 mM $CaCl_2$ plus the indicated concentrations of AA to start 5-LO product formation. The reaction was stopped after 10 min by addition of one volume of ice-cold methanol, and the formed metabolites were analyzed by RP-HPLC as described (Pergola et al., 2014; Steinhilber et al., 1989). 5-LO products include the all-trans isomers of LTB_4 as well as 5-HPETE and its corresponding alcohol 5-HETE.

Determination of 5-LO Product Formation in Intact Cells and Homogenates

For activity assays with intact cells, 5 × 10^6 freshly isolated neutrophils or monocytes, or 1 × 10^6 HEK293 cells stably producing the indicated recombinant proteins, were resuspended in 1 mL PGC buffer. After pre-incubation with compounds **1-4** (10 min, 37°C), 5-LO product formation was started by addition of 2.5 μM A23187 with or without 20 μM AA (neutrophils, monocytes) or 3 μM AA (HEK cells). After 10 min at 37°C, the reaction was stopped with 1 mL of ice-cold methanol. Formed 5-LO metabolites were extracted

Please cite this article in press as: König et al., Melleolides from Honey Mushroom Inhibit 5-Lipoxygenase via Cys159, Cell Chemical Biology (2018), https://doi.org/10.1016/j.chembiol.2018.10.010

CellPress

and analyzed by RP-HPLC using a C18 RP Radial PAK column (Waters, Eschborn, Germany) (Pergola et al., 2014; Steinhilber et al., 1989) or optionally by UPLC-MS/MS as described (Pace et al., 2017).

To determine 5-LO product formation in homogenates, neutrophils (5×10^6) or HEK293 cells (1×10^6) were resuspended in 1 mL PBS containing 1 mM EDTA. Cells were lysed on ice by sonication (3 × 20 s) and resulting cell homogenates were pre-incubated with compounds or vehicle (0.1% DMSO) for 10 min on ice. 5-LO product formation was started by addition of 2 mM $CaCl_2$ and 20 μM AA (neutrophils) or 10 μM AA (HEK cells). After 10 min at 37°C, reaction was stopped by 1 mL ice-cold methanol. 5-LO product formation was analyzed as described above for intact cells.

Determination of Release of [^{3}H]-Labeled Arachidonic Acid

Release of [^{3}H]-labeled AA from human neutrophils was analyzed as described (Fischer et al., 2005). In brief, freshly isolated neutrophils were immediately resuspended at 10^7 cells/mL RPMI 1640 medium containing 5 nM [^{3}H]AA (corresponding to 0.5 μCi/mL, specific activity 200 Ci/mmol) and incubated for 120 min at 37°C in 5% CO_2 atmosphere. Cells were then washed twice with PBS containing 1 mg/mL glucose and 2 mg/mL fatty acid-free bovine albumin, to remove unincorporated [^{3}H]AA. Labelled neutrophils (2×10^7) were resuspended in 1 mL PGC containing 2 mg/mL fatty acid-free bovine albumin and pre-incubated with 0.1% DMSO or test compounds (15 min, 37°C) and then stimulated with 2.5 μM A23187 for 10 min. The samples were then placed on ice, centrifuged and aliquots (300 μL) of the supernatants were assayed for radioactivity by scintillation counting (Micro Beta Trilux, Perkin Elmer, Waltham, MA, USA).

LTC_4 Synthase Activity Assay

Preparation of HEK293 cells stably expressing LTC_4 synthase and generation of microsomes were performed as described (Liening et al., 2016). Microsomes were pre-incubated with compounds or vehicle (0.1% DMSO) for 10 min at 4°C prior stimulation with 1 μM LTA_4 methyl ester (Cayman, Ann Harbor, MI) for 10 min. The reaction was stopped by 1 vol ice-cold methanol and acidified PBS, and the internal standard LTC_4 methyl ester-d_5 was added prior to solid phase extraction. LTC_4 methyl ester formation was analyzed by UPLC-MS/MS as described previously (Liening et al., 2016).

Determination of Isolated COX-1 and -2 Activity

Purified COX-1 (ovine, 50 units) or COX-2 (human recombinant, 20 units) were pre-incubated with compounds or vehicle (0.1% DMSO) for 5 min at 4°C in 1 mL reaction buffer containing 100 mM Tris buffer pH 8, 5 mM GSH, 5 μM hemoglobin, and 100 μM EDTA prior 1 min at 37°C to prewarm samples. COX product formation was started by adding AA (COX-1: 5 μM, COX-2: 2 μM) which resulted in generation of 12-HHT (12(*S*)-hydroxy-5-*cis*-8,10-*trans*-heptadecatrienoic acid) non-enzymatically formed from COX-derived PGH_2. 12-HHT was measured by RP-HPLC as previously reported (Albert et al., 2002).

Determination of PGE_2 Synthase Activity in a Cell-Free Assay

Preparation of A549 cells, induction of mPGES-1 by IL-1β, generation of microsomes, and analysis of mPGES-1 activity was performed exactly as described previously (Koeberle et al., 2008, 2009).

SDS PAGE and Western Blot

Neutrophils (1×10^7/100 μL ice-cold PGC buffer) were pre-incubated for 10 min at 37°C with test compounds at 37°C, stimulated with 1 μM *N*-formyl-methionyl-leucyl-phenylalanine (fMLP) for 1.5 min at 37°C. The reaction was stopped by addition of 100 μL ice-cold 2 × SDS loading buffer (20 mM Tris-HCl pH 8, 2 mM EDTA, 5% (m/v) SDS, 10% (v/v) β-mercaptoethanol, 10 μg/mL leupeptin, 60 μg/mL STI, 1 mM PMSF, 40 μL glycerol and 0.1% bromophenol blue (1:1, v/v). Samples were boiled for 5 min at 96°C, sonicated (3 × 10 sec, 4°C) and proteins were separated and analyzed by SDS–PAGE and Western Blotting.

To control stable expression of transfected enzymes, HEK cells (1×10^6/100 μL) were washed and lysed with Triton X-100 lysis buffer (20 mM Tris-HCl pH 7.4, 150 mM NaCl, 2 mM EDTA, 1% (v/v) Triton X-100, 0.5% (v/v) NP-40, 10 μg/mL leupeptin, 60 μg/mL STI, 1 mM PMSF) for 15 min on ice with occasional vortexing. Lysates were centrifuged (21,000×g, 10 min, 4°C) and the supernatant was mixed with 4 × Laemmli buffer (50 mM Tris-HCl pH 6.8, 12.5 mM EDTA, 2% (m/v) SDS, 10% (v/v) glycerol, 1% (v/v) β-mercaptoethanol, 0.02% (m/v) bromophenol blue) and samples were boiled for 5 min at 96°C.

Correct protein loading on the gels and transfer of proteins to nitrocellulose membrane (Amersham PROTRAN® supported 0.45 NC, GE Healthcare, Freiburg, Germany) were confirmed by Ponceau staining. Antibodies recognizing phosphorylated ERK1/2 (Thr202/Tyr204), ERK1/2, p-$cPLA_2$ (Ser505), p-p38 (Thr180/Tyr182) or β-actin were from Cell Signaling Technology (Boston, MA) and used at 1:1000 dilution. The antibody against GAPDH (1:1000) was purchased from Santa Cruz (Dallas, TX) and the rabbit FLAP (1:1000) antibody was obtained from Abcam (Cambridge, UK). The rabbit 5-LO antiserum (1551, AK7, 1:8 dilution) was kindly provided by Dr. Olof Rådmark, Karolinska Institutet, Stockholm, Sweden. Infrared-labeled secondary antibody IRDye 800CW goat anti-mouse was from LI-COR Biosciences (Lincoln, NE). For detection, the Odyssey Infrared Imaging System (LI-COR Bioscience, Lincoln, NE) and for analysis the Odyssey application software (version 3.0.25) were used.

GSH Incubation

Glutathione (GSH) adduct formation tests were carried out directly on the MALDI-target in a total volume of 2 μL. 1 μL of 2 mM GSH in PBS pH 7.4 and 1 μL of 20 μM compound or vehicle in PBS pH 7.4 were mixed on the target to obtain a final concentration of 1 mM

Please cite this article in press as: König et al., Melleolides from Honey Mushroom Inhibit 5-Lipoxygenase via Cys159, Cell Chemical Biology (2018), https://doi.org/10.1016/j.chembiol.2018.10.010

CellPress

GSH and 10 μM compound. The reaction mixture was kept humid for 30 min at 37°C using a SunDigest digestion chamber (SunChrom, Friedrichsdorf, Germany). The reaction was stopped after 30 min of incubation with 1 μL CHCA-solution (3 mg/mL CHCA (α-cyano-4-hydroxy-cinnamic acid) in 70/30/0.1 acetonitrile/water/trifluoroacetic acid (TFA)). After matrix crystallization, we used chilled 5%-formic acid to remove salt contaminations from the matrix crystals and recrystallized the sample with acetonitrile/water (80/20, v/v) mixture containing 0.1% TFA to obtain a homogeneous crystallization.

Standard Peptide Incubation

Binding assays using the standard peptides AAAACAAAAR, AAAAHAAAAR, AAAAKAAAAR, AAAASAAAAR (JPT Peptide technology, Berlin, Germany) were also directly carried out on the MALDI-target. Peptides were diluted in PBS pH 7.4 to a concentration of 20 μM and mixed separately with each compound at a concentration of 20 μM in a total volume of 2 μL to obtain a final concentration of 10 μM peptide and 10 μM compound. Incubation was performed using the SunDigest system for 1 h at 37°C. The reaction was stopped using the same matrix solution as described above. Washing and recrystallization of the formed spots were performed as previously described (Kretschmer et al., 2017).

MALDI-MS Measurement and Data Analysis

MALDI-MS measurements were carried out using a MALDI-Duo ion source coupled to an Orbitrap LTQ XL mass spectrometer (Thermo Fisher Scientific, Bremen, Germany). MS measurements were carried out on an Orbitrap mass analyzer. For GSH adducts, the mass was recorded from m/z 200.00 to 800.00 and for standard peptide assay, the mass range was between m/z 800.00 and 2000.00. 50 subspectra were accumulated for data analysis. Mass resolution was set to 30,000 (FWHM at m/z: 400), laser energy was adjusted to optimize MS spectra quality. MS/MS spectra of reaction products and peptides were recorded using the ion trap mass analyzer. 100 subspectra were accumulated for data analysis. Normalized collision energy was set to 50. Isolation of the particular reaction product was performed using an isolation width of 1 Da. MS spectra were analyzed using the Qual Browser software version 2.0.7 (Thermo Fisher Scientific). This software was also used to compare the theoretical masses. Theoretical masses of peptides, reaction products, and MS/MS ion masses were calculated using mMass version 5.5.0.

Analysis of Subcellular Localization of 5-LO by Immunofluorescence Microscopy

For analysis of 5-LO and FLAP subcellular localization in monocytes, PBMC were seeded in RPMI medium containing 2 mM L-glutamine, 100 U/ml penicillin, and 100 μg/ml streptomycin onto glass coverslips in a 12-well plate and cultured for 1.5 h. The 5-LO/FLAP subcellular localization was also analyzed using HEK293 cells stably transfected with 5-LO enzymes and FLAP. Cells (0.45×10^6/mL) were seeded on poly-D-lysine-coated coverslips and cultured at 37°C, 5% CO_2 until 60% confluence. Cells were washed with PGC buffer and pre-incubated with test compounds or vehicle (0.1% DMSO) 10 min at 37°C in PGC buffer prior to activation. Cells were then stimulated for 10 min with 2.5 μM A23187 and stopped by fixation with 4% paraformaldehyde solution. Ice-cold acetone (5 min, 4°C) was used for permeabilization prior to blocking with non-immune goat serum. Samples were incubated with mouse monoclonal anti-5-LO antibody (1:300; made in-house, Goethe University Frankfurt, Germany) (Gerstmeier et al., 2014; Pergola et al., 2014) and rabbit polyclonal anti-FLAP antibody (1:500; Abcam, Cambridge, UK) at 4°C overnight. 5-LO and FLAP were stained with the fluorophore-labeled secondary antibodies; Alexa Fluor 488 goat anti-rabbit (1:1000) and Alexa Fluor 555 goat anti-mouse (1:1000, Invitrogen, Darmstadt, Germany). Nuclear DNA was stained with DAPI (Invitrogen). Samples were analyzed with a Zeiss Axiovert 200 M microscope, and a Plan Neofluar ×100/1.30 Oil (DIC III) objective (Zeiss, Jena, Germany). A Zeiss AxioCam MR camera was used for image acquisition.

In Situ Analysis of 5-LO/FLAP Interaction by Proximity Ligation Assay

To analyze the *in situ* interaction of 5-LO with FLAP in monocytes and HEK293 cells, an *in situ* proximity ligation assay (PLA) was performed, according to the manufacturers' protocol (Soderberg et al., 2006) and as described (Gerstmeier et al., 2016b). Samples were treated, fixed and incubated with primary antibody as described for IF microscopy above. Cells were then incubated with species specific secondary antibodies conjugated with oligonucleotides (PLA probe anti-mouse MINUS and anti-rabbit PLUS) for 1 h at 37°C. By addition of two other circleforming DNA oligonucleotides and a ligase (30 min at 37°C) the antibody-bound oligonucleotides form a DNA circle when the target proteins are less than 40 nm distant from each other. The newly generated DNA circle was amplified by rolling circle amplification and visualized by hybridization with fluorescently labeled oligonucleotides. Nuclear DNA was stained with DAPI. The PLA interaction signal appears as a fluorescent spot and was analyzed using the above described microscope and equipment.

QUANTIFICATION AND STATISTICAL ANALYSIS

Results are presented as means ± standard error of the mean (SEM) of *n* independent observations, where *n* represents the number of performed experiments at different days or with different donors. Statistical analysis of the data was performed by one-way ANOVA using GraphPad InStat (Graphpad Software Inc., San Diego, CA) followed by a Bonferroni post-hoc test for multiple or student t-test for single comparisons, respectively. P-values < 0.05 were considered as significant.

Cell Chemical Biology, Volume *26*

Supplemental Information

Melleolides from Honey Mushroom Inhibit 5-Lipoxygenase via Cys159

Stefanie König, Erik Romp, Verena Krauth, Michael Rühl, Maximilian Dörfer, Stefanie Liening, Bettina Hofmann, Ann-Kathrin Häfner, Dieter Steinhilber, Michael Karas, Ulrike Garscha, Dirk Hoffmeister, and Oliver Werz

Supporting Information

Melleolides from honey mushroom inhibit 5-lipoxygenase via Cys159

Stefanie König, Erik Romp, Verena Krauth, Michael Rühl, Maximilian Dörfer, Stefanie Liening, Bettina Hofmann, Ann-Kathrin Häfner, Dieter Steinhilber, Michael Karas, Ulrike Garscha, Dirk Hoffmeister, and Oliver Werz

Content:

Supplemental Table 1

Supplemental Figures 1 - 4

Supplemental Table 1

assay / enzyme	**cmpd. 1** (% remaining activity)	**control inhibitor** (% remaining activity)
[^{3}H]AA release (neutrophils)	75.2 ± 3.1	48.8 ± 2.6 (RSC-3388, 10 μM)
LTC_4 synthase	83.7 ± 14.5	3.5 ± 0.7 (MK886, 10 μM)
COX-1	89.7 ± 5.7	26.2 ± 7.2 (indomethacin, 10 μM)
COX-2	114.3 ± 8.2	59.1 ± 0.8 (celecoxib, 5 μM) 25.4 ± 1.7 (indomethacin, 10 μM)
mPGES-1	79.8 ± 2.9	18.1 ± 3.2 (MK886, 10 μM)

Table S1. **Effects of 1 on various enzymes involved in eicosanoid biosynthesis, related to Figure 2.** Melleolide **1** (1 μM) or control inhibitors (as indicated) were added to the respective enzymes or isolated neutrophils 10 min prior starting the reaction. Data are expressed as percentage of control (vehicle, 100%), mean ± SEM, n = 3.

Supplemental Figure 1

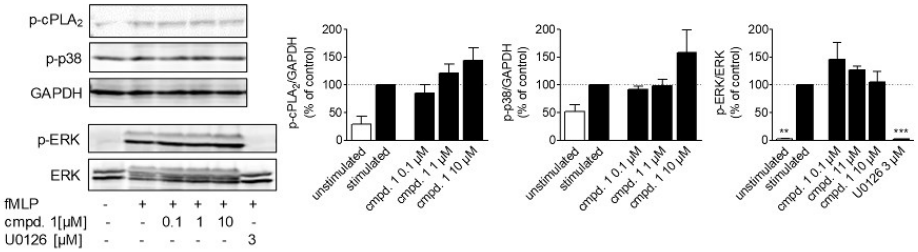

Fig. S1. Effects of 1 on the phosphorylation of p38 MAPK, ERK-1/2 and cPLA$_2$ in neutrophils, related to Figure 2. Neutrophils were pre-incubated with **1**, reference inhibitor U0126 (3 µM), or vehicle (0.1% DMSO) for 10 min at 37 °C prior stimulation with 1 µM *N*-formyl-methionyl-leucyl-phenylalanine (fMLP) for 1.5 min. The amounts of phospho-ERK-1/2 and ERK1/-2 (for normalization), phospho-p38 MAPK, phospho-cPLA$_2$ and GAPDH (for normalization) were analyzed by Western blot. Data, obtained by densitometry (bar charts, mean + S.E.M.; $n = 3$), are expressed as percentage of fMLP-stimulated control.

Supplemental Figure 2

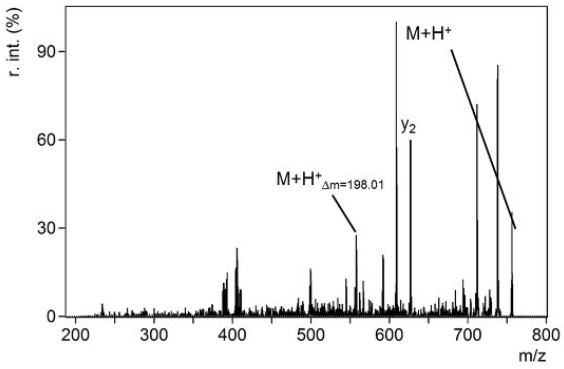

Fig. S2. MS²-spectra of modified cmpd. 2-modified GSH indicate covalent binding of cmpd. 2 to GSH, related to Figure 3.

Supplemental Figure 3

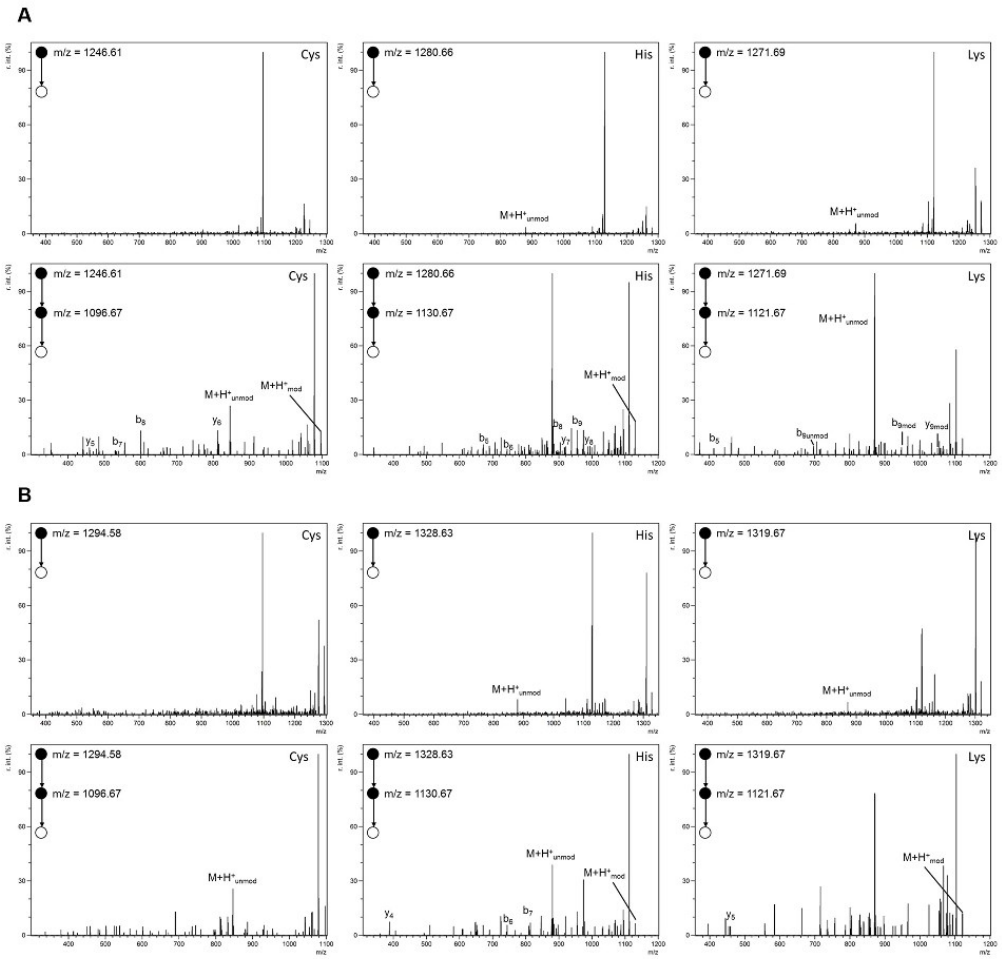

Fig. S3. MS²-spectra covalent binding of cmpd. 1 and cmpd. 2 to synthetic peptides, related to Figure 3. (A) Modification of standard peptides by compd. **1**. Upper panel shows MS² spectra of modified AAAACAAAAR (left row), AAAAHAAAAR (middle row) and AAAAKAAAAR (right row). Lower panel shows MS³ spectra of the main fragments m/z = 1096.67, 1130.67 and 1121.67. (B) Modification of standard peptides by cmpd. **2**. Upper panel shows MS² spectra of modified AAAACAAAAR (left row), AAAAHAAAAR (middle row) and AAAAKAAAAR (right row). Lower panel shows MS³ spectra of the main fragments m/z = 1096.67, 1130.67 and 1121.67.

Supplemental Figure 4

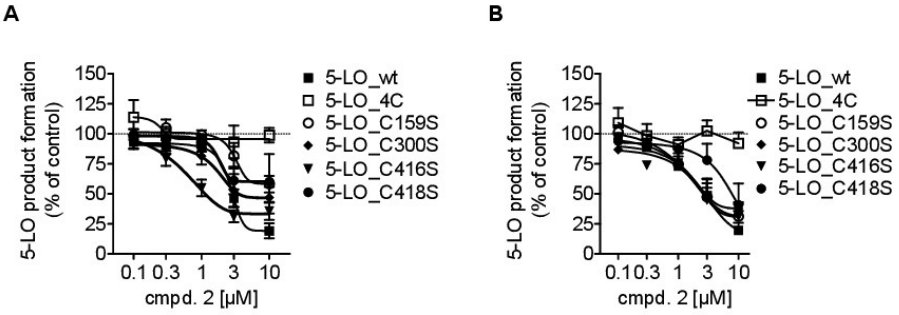

Fig. S4. Inhibition of 5-LO by cmpd. 2, related to Figure 5. (A) Intact HEK cells. (B) HEK homogenates. HEK cells (10^6/ml) expressing 5-LO_FLAP, 4C_FLAP, C159S_FLAP, C300S_FLAP, C416S_FLAP or C418S_FLAP mutant were pretreated with compd. **2** or 0.1% DMSO (vehicle) for 10 min at 37 °C. Cells were stimulated with 2.5 µM A23187 and 3 µM AA for 10 min at 37 °C. Data are expressed as percentage of control (100%), mean ± SEM, n = 4, * $p<0.05$, ** $p< 0.01$, *** $p< 0.001$ versus vehicle control.

M-II: Gliotoxin from *Aspergillus fumigatus* abrogates leukotriene B_4 formation through inhibition of leukotriene A_4 hydrolase

Please cite this article in press as: König et al., Gliotoxin from *Aspergillus fumigatus* Abrogates Leukotriene B_4 Formation through Inhibition of Leukotriene A_4 Hydrolase, Cell Chemical Biology (2019), https://doi.org/10.1016/j.chembiol.2019.01.001

Cell Chemical Biology
Article

CellPress

Gliotoxin from *Aspergillus fumigatus* Abrogates Leukotriene B_4 Formation through Inhibition of Leukotriene A_4 Hydrolase

Stefanie König,[1] Simona Pace,[1] Helmut Pein,[1] Thorsten Heinekamp,[2] Jan Kramer,[3] Erik Romp,[1] Maria Straßburger,[4] Fabiana Troisi,[1] Anna Proschak,[3] Jan Dworschak,[5] Kirstin Scherlach,[5] Antonietta Rossi,[6] Lidia Sautebin,[6] Jesper Z. Haeggström,[7] Christian Hertweck,[5,8] Axel A. Brakhage,[2,8] Jana Gerstmeier,[1] Ewgenij Proschak,[3] and Oliver Werz[1,9,*]

[1]Department of Pharmaceutical/Medicinal Chemistry, Institute of Pharmacy, Friedrich-Schiller-University Jena, 07743 Jena, Germany
[2]Department of Molecular and Applied Microbiology, Leibniz Institute for Natural Product Research and Infection Biology, Hans Knoell Institute (HKI), 07745 Jena, Germany
[3]Institute of Pharmaceutical Chemistry, Goethe University Frankfurt, 60438 Frankfurt, Germany
[4]Transfer Group Antiinfectives, Leibniz Institute for Natural Product Research and Infection Biology, Hans Knoell Institute (HKI), 07745 Jena, Germ
[5]Dep for Natural Product Research and Infection Biology, Hans Knoell Institute (HKI), 07745 Jena, Germany
[6]Department of Pharmacy, School of Medicine, University of Naples Federico II, 80131 Naples, Italy
[7]Division of Physiological Chemistry II, Department of Medical Biochemistry and Biophysics, Karolinska Institutet, 17177 Stockholm, Sweden
[8]Friedrich-Schiller-University Jena, 07743 Jena, Germany
[9]Lead Contact
*Correspondence: oliver.werz@uni-jena.de
https://doi.org/10.1016/j.chembiol.2019.01.001

SUMMARY

The epidithiodioxopiperazine gliotoxin is a virulence factor of *Aspergillus fumigatus*, the most important airborne fungal pathogen of humans. Gliotoxin suppresses innate immunity in invasive aspergillosis, particularly by compromising neutrophils, but the underlying molecular mechanisms remain elusive. Neutrophils are the first responders among innate immune cells recruited to sites of infection by the chemoattractant leukotriene (LT)B_4 that is biosynthesized by 5-lipoxygenase and LTA_4 hydrolase (LTA_4H). Here, we identified gliotoxin as inhibitor of LTA_4H that selectively abrogates LTB_4 formation in human leukocytes and in distinct animal models. Gliotoxin failed to inhibit the formation of other eicosanoids and the aminopeptidase activity of the bifunctional LTA_4H. Suppression of LTB_4 formation by gliotoxin required the cellular environment and/or reducing conditions, and only the reduced form of gliotoxin inhibited LTA_4H activity. Conclusively, gliotoxin suppresses the biosynthesis of the potent neutrophil chemoattractant LTB_4 by direct interference with LTA_4H thereby impairing neutrophil functions in invasive aspergillosis.

INTRODUCTION

Aspergillus fumigatus is a ubiquitous fungus and the most common cause of invasive aspergillosis (IA), which affects primarily immunocompromised patients with a mortality rate of 30%–95% (Segal, 2009). During IA, *A. fumigatus* produces toxic secondary metabolites with gliotoxin as an important mycotoxin (Scharf et al., 2016). Gliotoxin is considered as a virulence factor contributing to IA due to its immunosuppressive properties (Park and Mehrad, 2009; Sutton et al., 1996), particularly in neutrophils (Comera et al., 2007; Spikes et al., 2008; Sugui et al., 2007). A variety of bioactivities were demonstrated for gliotoxin, such as induction of apoptosis, inhibition of nuclear factor κB (NF-κB) by preventing proteasome-mediated degradation of IκBα, inhibition of reactive oxygen species generation by phagocytes, and inhibition of angiogenesis (Scharf et al., 2016; Waring and Beaver, 1996), as well as changes in cell morphology and cell adhesion of neutrophils (Comera et al., 2007). So far, the underlying mechanism of how gliotoxin contributes to IA and compromises neutrophils is incompletely understood.

Leukotrienes are bioactive lipid mediators (LMs) involved in innate and adaptive immune responses, inflammation, and in several diseases such as asthma and atherosclerosis (Haeggstrom and Funk, 2011; Radmark et al., 2015). LTB_4 is one of the most potent chemoattractants for neutrophils (Afonso et al., 2012; Lammermann et al., 2013), with crucial roles in host defense against infections and inflammation by triggering the recruitment and activation of innate immune cells (Brandt and Serezani, 2017; Haeggstrom and Funk, 2011; Radmark et al., 2015). Neutrophils and monocytes possess high capacities to generate LTB_4 and are considered as major sources for LTB_4 in the blood and at sites of inflammation (Lammermann et al., 2013; Surette et al., 1993). In LT biosynthesis (Figure 1A), arachidonic acid (AA) is released by cytosolic phospholipase A_2 ($cPLA_2$) and then converted by 5-lipoxygenase (5-LO) in a two-step reaction: first dioxygenation to 5-hydroperoxyeicosatetraenoic acid (5-HPETE) and then dehydration to the instable

Please cite this article in press as: König et al., Gliotoxin from *Aspergillus fumigatus* Abrogates Leukotriene B_4 Formation through Inhibition of Leukotriene A_4 Hydrolase, Cell Chemical Biology (2019), https://doi.org/10.1016/j.chembiol.2019.01.001

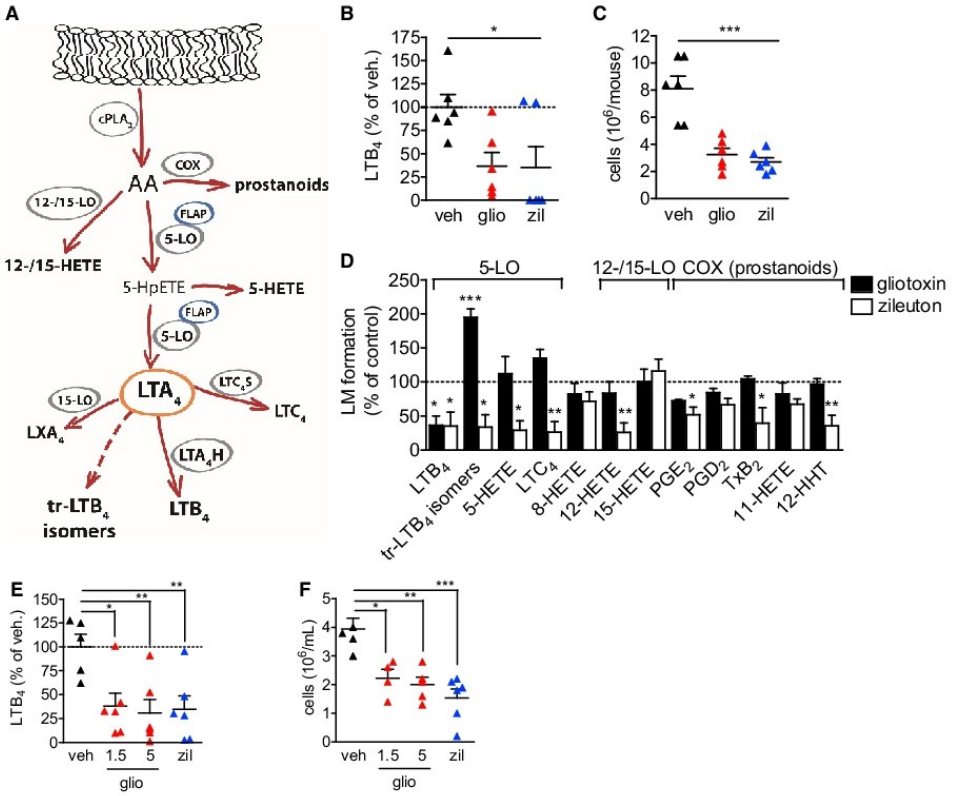

Figure 1. Gliotoxin Selectively Suppresses LTB_4 Biosynthesis and Blocks Neutrophil Recruitment *In Vivo*

(A) Simplified scheme of the eicosanoid biosynthetic pathway with focus on LTA_4 metabolism. AA, arachidonic acid; $cPLA_2$, cytosolic phospholipase A_2; COX, cyclooxygenase; LO, lipoxygenase; FLAP, 5-LO-activating protein; LT, leukotriene; LTA_4H, leukotriene A_4 hydrolase; LTC_4S, leukotriene C_4 synthase; LXA_4, lipoxin A_4; 5-HETE, 5-hydroxy-eicosatetraenoic.

(B–D) Zymosan-induced peritonitis in mice. Male mice (n = 6 per group) were pre-treated i.p. with 5 mg/kg gliotoxin, 10 mg/kg zileuton, or vehicle (4%, v/v, DMSO), 30 min before i.p. injection of zymosan. Analysis was performed 4 h after zymosan injection. Data are means ± SEM, n = 6. *$p < 0.05$; **$p < 0.01$; ***$p < 0.001$ versus vehicle (Student's t test). (B) Circulating LTB_4 levels in murine plasma measured by ELISA. (C) Neutrophil infiltration in peritoneal exudates. (D) Circulating LM levels in murine plasma measured by UPLC-MS/MS.

(E and F) Carrageenan-induced pleurisy in rats. Male rats (n = 6) were pre-treated i.p. with 1.5 or 5 mg/kg gliotoxin, 10 mg/kg zileuton, or vehicle (4% DMSO), 30 min before intrathoracic injection of carrageenan. Analysis was performed 2 h after carrageenan injection. (E) Circulating LTB_4 levels in rat plasma measured by ELISA. (F) Neutrophil infiltration in thoracic exudates. Data are means ± SEM, n = 6. *$p < 0.05$; **$p < 0.01$; ***$p < 0.001$ versus vehicle (Student's t test).

See also Figure S1.

epoxide leukotriene A_4 (LTA_4) (Radmark et al., 2015). LTA_4 can be hydrolyzed by LTA_4 hydrolase (LTA_4H) to LTB_4 or conjugated with glutathione (GSH) by LTC_4 synthase (LTC_4S) to LTC_4 (Figure 1A). Moreover, LTA_4 may degrade non-enzymatically to *trans* (tr)-LTB_4 isomers, and the intermediate 5-HPETE can be reduced to 5-HETE (Haeggstrom and Funk, 2011; Radmark et al., 2015). LTA_4H is a ubiquitously expressed, soluble Zn^{2+} metalloenzyme that harbors two distinct enzymatic activities with overlapping active sites: (1) an epoxide hydrolase activity that converts LTA_4 to the pro-inflammatory chemoattractant LTB_4 and (2) an aminopeptidase activity that, for instance, hydrolyses the pro-inflammatory tripeptide Pro-Gly-Pro (PGP) (Haeggstrom et al., 2007; Snelgrove et al., 2010; Stsiapanava et al., 2017).

Recently, host-derived LTB_4 was shown to be critical for neutrophil recruitment and resistance to pulmonary *A. fumigatus* challenge in mice (Caffrey-Carr et al., 2017). Here, we identified gliotoxin as a potent and selective inhibitor of the epoxide hydrolase activity of LTA_4H. We show that pre-treatment of mice and rats with gliotoxin effectively blocked agonist-induced neutrophil recruitment along with reduced levels of circulating LTB_4, while other LMs were not suppressed. Our data propose that abrogating chemotactic LTB_4 formation through inhibition of LTA_4H might be one crucial mode of action of how gliotoxin

Please cite this article in press as: König et al., Gliotoxin from *Aspergillus fumigatus* Abrogates Leukotriene B_4 Formation through Inhibition of Leukotriene A_4 Hydrolase, Cell Chemical Biology (2019), https://doi.org/10.1016/j.chembiol.2019.01.001

CellPress

exerts its neutrophil-compromising properties during establishment of IA.

RESULTS

Gliotoxin Selectively Suppresses LTB_4 Biosynthesis and Blocks Neutrophil Recruitment *In Vivo*

Since 5-LO and LTB_4 are critical for neutrophil recruitment and defense against *A. fumigatus* (Caffrey-Carr et al., 2017), we hypothesized that the neutrophil-compromising properties of gliotoxin could be due to interference with LTB_4 biosynthesis. To study the effects of gliotoxin on LT formation and on neutrophil recruitment *in vivo,* we used two distinct (agonist, species, organ) LT/neutrophil-driven models of acute inflammation, i.e., (1) zymosan-induced mouse peritonitis (Rao et al., 1994) and (2) carrageenan-induced rat pleurisy (Cuzzocrea et al., 2003). Since in *A. fumigatus*-infected murine lungs, gliotoxin was locally found at ~4 mg/kg of lung tissue (Lewis et al., 2005), we here used a dose of 5 mg/kg gliotoxin. The clinically used LT biosynthesis blocker zileuton (a 5-LO inhibitor) was applied as reference drug (10 mg/kg). In zymosan-induced peritonitis, a well-established experimental *in vivo* model for evaluation of inhibitors of LT biosynthesis and LTB_4-mediated neutrophil chemotaxis, intraperitoneal (i.p.) pre-treatment of mice with gliotoxin (5 mg/kg, 30 min) suppressed circulating LTB_4 plasma levels 4 h after zymosan injection to 36.6% ± 13.4% versus vehicle control (=100%) with similar efficacy as zileuton (10 mg/kg; 35.4% ± 20.3%) (Figure 1B). In parallel, gliotoxin blocked neutrophil infiltration into the peritoneal cavity, comparable with zileuton (Figure 1C). However, zileuton also caused significant suppression of all other 5-LO-derived products (i.e., tr-LTB_4 isomers, 5-HETE, and LTC_4), and to a minor extent also reduced 12-LO- and cyclooxygenase-derived eicosanoids. In contrast, gliotoxin exclusively suppressed LTB_4 formation but enhanced the levels of tr-LTB_4 isomers (194.9% ± 12.7% versus vehicle control), probably by redirection to non-enzymatic LTA_4 hydrolysis (Figure 1D).

Comparable results were obtained with rats using carrageenan-induced pleurisy, which represents a model of lung inflammation. Thus, pre-treatment with gliotoxin (5 mg/kg, i.p., 30 min) as well as zileuton (10 mg/kg, i.p., 30 min) efficiently reduced circulating LTB_4 plasma levels 2 h after intrathoracic carrageenan injection (Figure 1E), and neutrophil recruitment in the thoracic cavity was markedly reduced (Figure 1F). Similar effects of gliotoxin were evident at the lower dose of only 1.5 mg/kg (Figures 1E and 1F). Again, tr-LTB_4 isomer levels were elevated and other 5-LO-derived LMs or detectable eicosanoids were not impaired by gliotoxin (Figure S1). Together, gliotoxin selectively impaired the levels of chemotactic LTB_4 among various LMs, accompanied by potent suppression of neutrophil infiltration, suggesting LTA_4H as potential point of attack.

Gliotoxin Potently and Selectively Inhibits LTB_4 Biosynthesis in Human Neutrophils and Monocytes

Next, we studied the LTB_4-suppressive effects of gliotoxin in isolated human primary leukocytes side-by-side with the structurally distinct but selective LTA_4H inhibitor SC-57461A (Askonas et al., 2002). Pre-incubation of neutrophils with gliotoxin and subsequent stimulation with Ca^{2+}-ionophore A23187 inhibited LTB_4 formation (half maximal inhibitory concentration [IC_{50}] = 1.5 ± 0.5 μM) with concomitant increase of the tr-LTB_4 isomers, but without alteration of 5-HETE production (Figure 2A). Short-term incubations of neutrophils for 0.5–2 h with gliotoxin (0.3–10 μM) revealed no cytotoxic effects (MTT assay, not shown). In sharp contrast, zileuton inhibited the formation of all 5-LO products, as expected, while the LTA_4H inhibitor SC-57461A modulated 5-LO product biosynthesis in the same way as gliotoxin, that is, inhibition of LTB_4 formation with moderate impairment of 5-HETE but strong elevation of tr-LTB_4 isomers (Figure 2A).

Besides neutrophils, monocytes possess high capacities to generate LTB_4 and in addition also express LTC_4S and, thus, substantially produce LTC_4 from LTA_4 (Lam and Austen, 2002; Surette et al., 1993). Like in neutrophils, gliotoxin potently suppressed A23187-induced LTB_4 formation in human monocytes (IC_{50} = 0.8 ± 0.1 μM) with concomitant increase of LTC_4 (Figure 2B). In contrast, zileuton blocked the formation of all 5-LO products, while SC-57461A, in analogy to gliotoxin, inhibited only LTB_4 formation but not the formation of other 5-LO-derived products (Figure 2B). Finally, we analyzed the eicosanoid profiles in neutrophils and monocytes more comprehensively to learn about modulation of other biosynthetic enzymes and redirection of substrates for LM formation. Gliotoxin caused only moderate or non-significant suppression of 5-, 12-, and 15-HETE formation in both cell types, but, interestingly, increased (besides tr-LTB_4 isomers and LTC_4) also lipoxin (LX) A_4 formation (Figures 2C and 2D), which is another LTA_4 hydrolysis product that requires 5-LO and 15-LO activity for its biosynthesis but not LTA_4H (Serhan and Samuelsson, 1988). Increased LXA_4 formation was also evident with SC-57461A but not with zileuton, which blocked LXA_4 formation as expected. Collectively, gliotoxin potently and selectively inhibited LTB_4 formation with concomitant increase of other LTA_4 hydrolysis products, thus sharing pharmacodynamic profiles with the LTA_4H inhibitor SC-57461A.

Gliotoxin Represents the Virulence Factor of *A. fumigatus* that Inhibits LTB_4 Formation

We aimed to investigate if products secreted by *A. fumigatus* would mimic the LTB_4-suppressive effects of gliotoxin. In analogy to gliotoxin, supernatants from *A. fumigatus* cultures suppressed LTB_4 biosynthesis in neutrophils along with elevated levels of tr-LTB_4 isomers (Figure 3A). To trace this effect back to gliotoxin, we made use of an *A. fumigatus* strain unable to produce gliotoxin due to a mutation of the nonribosomal peptide synthetase GliP involved in gliotoxin biosynthesis (Δ*gliP* strain) (Hillmann et al., 2015). Supernatants from the Δ*gliP* strain failed to suppress LTB_4 formation and to elevate tr-LTB_4 isomers. Of interest, neutrophils in the lesions of lungs infected with gliotoxin-producing *A. fumigatus* (wild-type) displayed extensive nuclear fragmentation as a sign for apoptosis and/or necrosis (Figure 3B), suggesting direct neutrophil killing by gliotoxin (in agreement with Comera et al., 2007 and Spikes et al., 2008), whereas neutrophils infiltrated around Δ*gliP* hyphae appeared intact (Figure 3C). These data indicate that gliotoxin as part of the secretome of *A. fumigatus* is causative for inhibition of LTB_4 biosynthesis in neutrophils and support this

Please cite this article in press as: König et al., Gliotoxin from *Aspergillus fumigatus* Abrogates Leukotriene B_4 Formation through Inhibition of Leukotriene A_4 Hydrolase, Cell Chemical Biology (2019), https://doi.org/10.1016/j.chembiol.2019.01.001

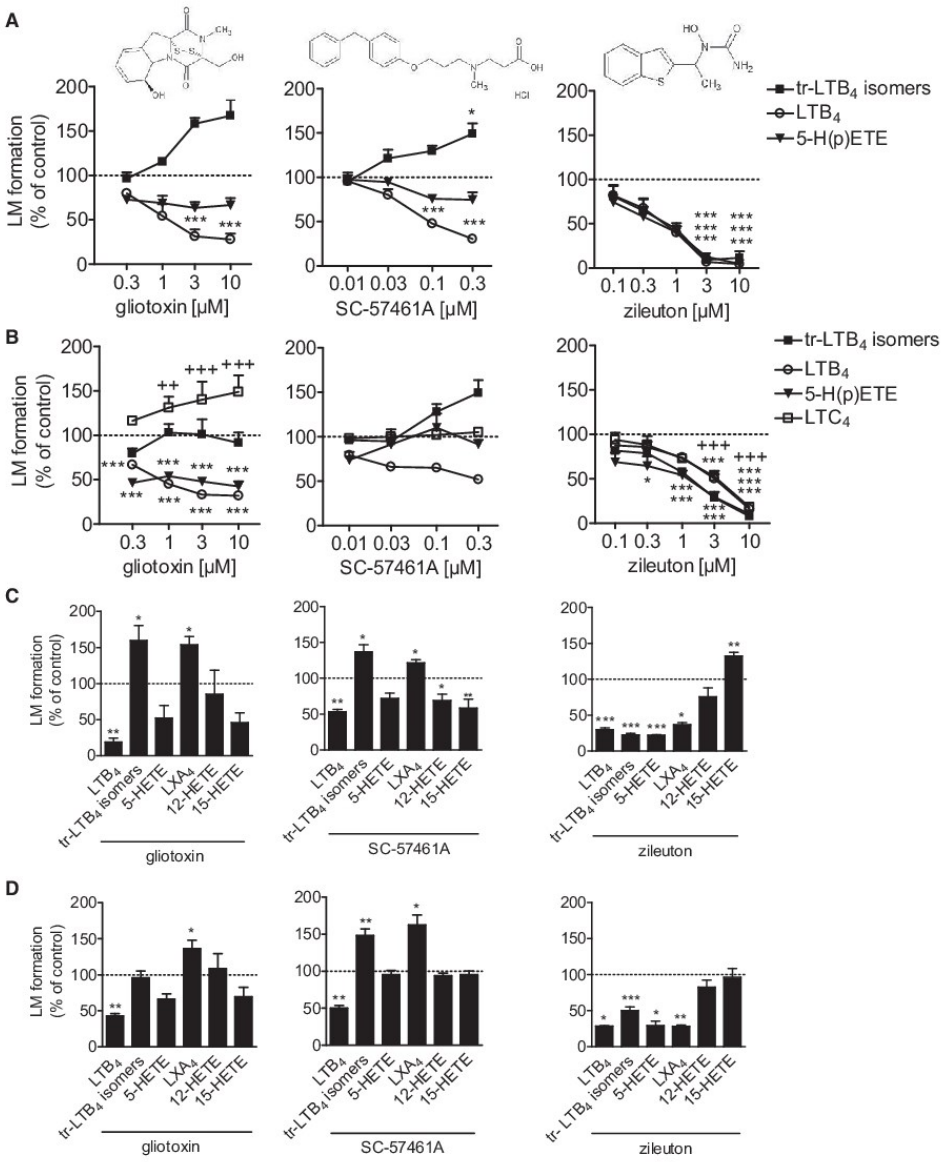

Figure 2. Gliotoxin Potently and Selectively Inhibits LTB_4 Biosynthesis in Human Neutrophils and Monocytes

(A and B) Inhibition of 5-LO product formation in intact human neutrophils (A) and in human monocytes (B). Cells were pre-incubated with gliotoxin, SC-57461A, zileuton, or 0.1% (v/v) DMSO (vehicle) for 10 min at 37°C prior stimulation with 2.5 μM A23187. Formation of tr-LTB_4 isomers, LTB_4, and 5-HETE was analyzed after 10 min by reversed-phase high-performance liquid chromatography (RP-HPLC). LTC_4 formation in monocytes was evaluated by ELISA. Data are means ± SEM; n = 4, ***$p < 0.001$; **$p < 0.01$; *$p < 0.05$; inhibitor versus vehicle control (100%), one-way ANOVA plus Bonferroni *post hoc* test.

(C and D) Effect of gliotoxin on eicosanoid formation in human neutrophils (C) and in human monocytes (D). Cells were pre-incubated with 1 μM gliotoxin, 3 μM zileuton, 0.1 μM SC-57461A, or 0.1% (v/v) DMSO (vehicle) for 10 min at 37°C prior stimulation with 2.5 μM A23187 for another 10 min. Formed eicosanoids were analyzed by UPLC-MS/MS. Data are means ± SEM; n = 4, duplicates. ***$p < 0.001$; **$p < 0.01$; *$p < 0.05$; inhibitor versus vehicle control, Student's t test.

Please cite this article in press as: König et al., Gliotoxin from *Aspergillus fumigatus* Abrogates Leukotriene B_4 Formation through Inhibition of Leukotriene A_4 Hydrolase, Cell Chemical Biology (2019), https://doi.org/10.1016/j.chembiol.2019.01.001

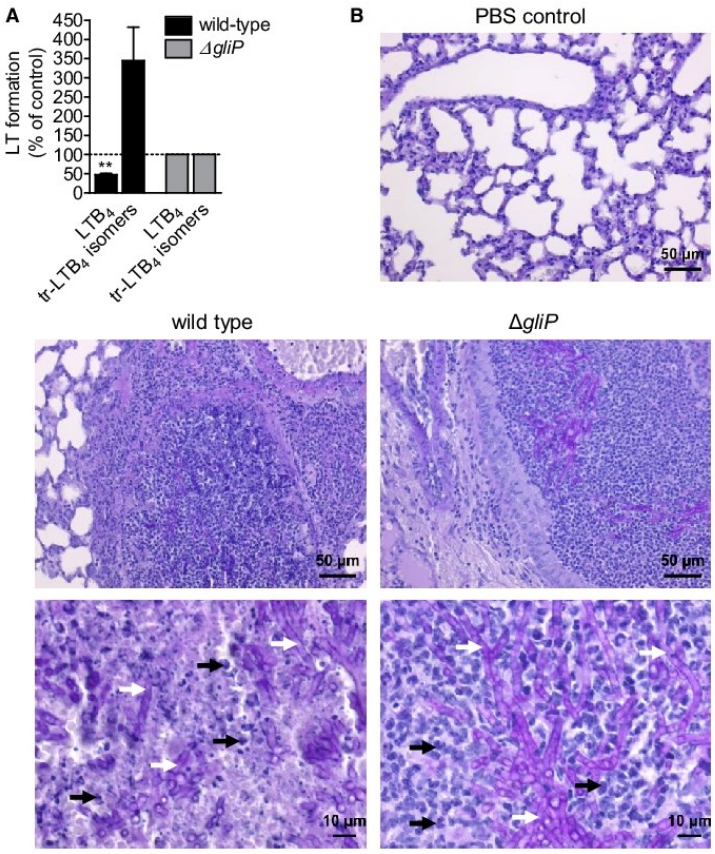

Figure 3. Gliotoxin Represents the Virulence Factor of *A. fumigatus* that Inhibits LTB_4 Formation

(A) Effect of crude extracts obtained from supernatants of *A. fumigatus* wild-type or *A. fumigatus* Δ*gliP* mutant cultures on LT formation in intact human neutrophils. After pre-incubation of neutrophils with the extracts for 15 min at 37°C, cells were stimulated with 2.5 μM A23187 for 10 min. Formed LT were analyzed by RP-HPLC. Data are means ± SEM; n = 3, **$p < 0.01$; inhibitor versus vehicle control, Student's t test.

(B) Histopathology of lungs of corticosteroid-treated mice 4 days after infection with *A. fumigatus* wild-type or Δ*gliP* conidia showing representative areas of bronchopneumonia; similar results were obtained in three additional mice, each. Non-neutropenic female CD-1 mice were infected intranasally with 2×10^5 conidia. For histopathology, 4-μm sections of lungs were stained with periodic acid-Schiff (hyphae stain pink, neutrophils stain blue). Hyphae are surrounded by inflammatory tissue; details are presented in the lower panels; white arrows indicate filamentous hyphae and black arrows point to neutrophils. As control, a lung section of a PBS-treated mouse is shown.

action as potential virulence mechanism of *A. fumigatus* triggering IA.

Gliotoxin Selectively Inhibits the Epoxide Hydrolase Activity of the Bifunctional LTA_4H

Next, we investigated whether gliotoxin, apart from the epoxide hydrolase function, also inhibits the aminopeptidase activity of LTA_4H. SC-57461A (Askonas et al., 2002) and captopril (Orning et al., 1991) inhibit both enzyme activities, while ARM1 is a selective epoxide hydrolase inhibitor and does not affect the aminopeptidase activity (Stsiapanava et al., 2014). The target peptide PGP was added to human neutrophils, and its enzymatic degradation was recorded by liquid chromatography-tandem mass spectrometry (LC-MS/MS) analysis. Pre-treatment with gliotoxin efficiently reduced LTB_4 formation but failed to inhibit the aminopeptidase activity up to 10 μM (Figure 4A). Captopril and SC-57461A suppressed both LTA_4H activities, whereas ARM1 inhibited LTB_4 formation but not PGP degradation (Figure 4A), as expected (Stsiapanava et al., 2014). We then investigated if gliotoxin could affect also other relevant epoxide hydrolases involved in eicosanoid biosynthesis, such as the soluble epoxide hydrolase (sEH), which converts epoxy-eicosatrienoic acids (EETs) into di-hydroxy-eicosatrienoic acids (di-HETrEs) (Morisseau and Hammock, 2013). A549 and HepG2 cells express sEH, which converts exogenously added 14,15-EET to the corresponding 14,15-diHETrE (Garscha et al., 2017). Gliotoxin (and SC-57461A) failed to inhibit 14,15-diHETE formation in either cell type up to 10 μM, whereas the sEH inhibitor 12-(3-adamantan-1-yl-ureido) dodecanoic acid (AUDA, 5 μM) inhibited this reaction (Figure 4B), as expected.

The Cellular Environment Confers Gliotoxin LTA_4H-Inhibitory Activity

To demonstrate direct interference with LTA_4H activity in a cell-free assay, we analyzed gliotoxin (and SC-57461A as control) against crude LTA_4H in neutrophil homogenates. To these homogenates, gliotoxin, SC-57461A, or vehicle were added, and after 10 min, 20 μM AA was provided for 5-LO to generate LTA_4 as substrate for LTA_4H *in situ*. Interestingly, in contrast to intact neutrophils, LTB_4 formation under these cell-free conditions was only moderately inhibited by gliotoxin and tr-LTB_4 isomers were not elevated, while SC-57461A efficiently blocked LTB_4 formation and elevated tr-LTB_4 isomers as expected (Figure 5A). We then first pre-incubated intact neutrophils for 10 min with gliotoxin and subsequently prepared homogenates to assay LTA_4H activity as described above. Under these conditions, gliotoxin efficiently inhibited LTB_4 biosynthesis in homogenates with $IC_{50} = 0.6 \pm 0.1$ μM and elevated tr-LTB_4 isomers (Figure 5B). These data imply that gliotoxin may (1) require the cellular environment for bioactivation to enable interference

Please cite this article in press as: König et al., Gliotoxin from *Aspergillus fumigatus* Abrogates Leukotriene B_4 Formation through Inhibition of Leukotriene A_4 Hydrolase, Cell Chemical Biology (2019), https://doi.org/10.1016/j.chembiol.2019.01.001

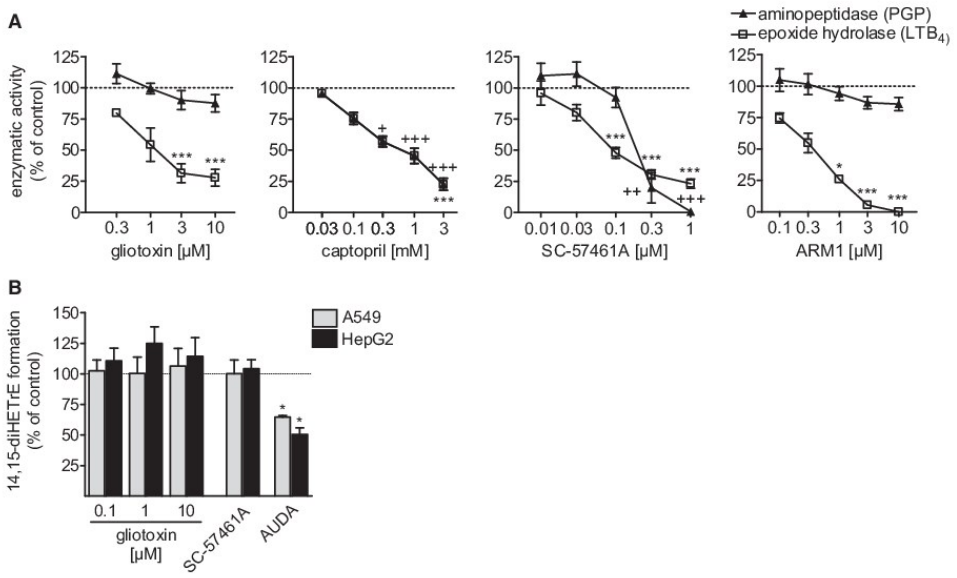

Figure 4. Gliotoxin Selectively Inhibits the Epoxide Hydrolase Activity of the Bifunctional LTA_4H

(A) Effect of gliotoxin and other LTA_4H inhibitors on the epoxide hydrolase activity (LTB_4 formation) and on the aminopeptidase activity (PGP degradation) of LTA_4H in intact human neutrophils. Neutrophils were pre-incubated with test compounds or 0.1% DMSO (vehicle) for 10 min at 37°C. For analysis of epoxide hydrolase activity, cells were stimulated with 2.5 μM A23187 for 10 min at 37°C and formed LTB_4 was analyzed by RP-HPLC. For analysis of aminopeptidase activity, 1 μM PGP plus 1 μM N-acetyl-PGP was added, and after 2 h PGP degradation was assessed by UPLC-MS/MS. Data are provided as means ± SEM; n = 3–4, ***p < 0.001; **p < 0.01; *p < 0.05; inhibitor versus vehicle control, ANOVA plus Bonferroni test.

(B) A549 or HepG2 cells were pre-incubated with gliotoxin, 0.3 μM SC-57461A, 5 μM AUDA, or 0.1% DMSO (vehicle) for 15 min at 37°C. Then, cells were incubated with 1.5 μM 14,15-EET for 30 min at 37°C. Formed 14,15-DiHETrE was measured by UPLC-MS/MS. Data are provided as means ± SEM; n = 3, *p < 0.05; inhibitor versus vehicle control, ANOVA plus Bonferroni test.

with LTA_4H and (2) may act in an irreversible fashion with the enzyme. In fact, pre-incubation of neutrophils with gliotoxin and subsequent wash-out retained the ability to inhibit LTB_4 formation in homogenates without any loss of potency (Figure 5C), supporting persistent/irreversible interaction.

Reducing Conditions Activate Gliotoxin for Inhibition of LTA_4H

Based on the proposed redox-cycling mechanism of gliotoxin (Scharf et al., 2016), we assumed that reduction of the disulfide of gliotoxin to the dithiol form inside the cell (e.g., by GSH) is a prerequisite for inhibition of LTA_4H. In fact, when the oxidative status of neutrophils was elevated by diamide (Jakobsson et al., 1992), the strong LTA_4-inhibitory potency of gliotoxin (but not of SC-57461A) was lost (Figure 6A). In a cell-free assay, gliotoxin only moderately inhibited LTB_4 formation by isolated LTA_4H from *in-situ*-generated LTA_4 (by isolated 5-LO from exogenous AA), while SC-57461A was fully active in this respect, and zileuton blocked formation of all 5-LO products (Figure 6B). Similarly, gliotoxin hardly inhibited the hydrolysis of L-arginine-7-amido-4-methylcoumarine, a suitable substrate for both the aminopeptidase and the epoxide hydrolase activity (Wittmann et al., 2016), by isolated human recombinant LTA_4H (Figure 6C). However, pre-treatment of gliotoxin with 5 mM GSH) restored LTA_4H inhibition in the cell-free assay, while in the presence of oxidized glutathione (GSSG) gliotoxin failed in this respect (Figure 6C). Analysis of gliotoxin from these incubations by ultra-performance liquid chromatography (UPLC)-MS confirmed that in the presence of GSH the disulfide was cleaved to the dithiol, while with GSSG or in absence of GSH gliotoxin was in the disulfide form (Figure 6D). LTA_4H is a Zn^{2+} metalloenzyme and it appeared possible that gliotoxin may act by complexing the catalytic Zn^{2+} ion in the active site of LTA_4H. Interestingly, inclusion of 100 μM $ZnCl_2$ in the cell-free assay (in the presence of GSH) abolished the inhibitory effect of gliotoxin on isolated LTA_4H (Figure 6C), suggesting that gliotoxin could interact with Zn^{2+}. Similarly, when neutrophils were pre-incubated with gliotoxin prior to sonication and subsequent incubation of the homogenates in the presence of 200 μM $ZnCl_2$, inhibition of LTB_4 formation by gliotoxin was strongly impaired (Figure 6E). Notably, LTA_4H inhibition by SC-57461A was not affected by $ZnCl_2$ addition (Figure 6E). These data support the hypothesis that the disulfide of gliotoxin becomes cleaved within the reducing milieu (≈5 mM GSH) in intact cells and that the dithiol form then acts in the active site of the epoxide hydrolase center of LTA_4H. In this respect, among various gliotoxin derivatives isolated from *A. fumigatus*, only compound **1**, a biosynthetic intermediate with an intramolecular

Please cite this article in press as: König et al., Gliotoxin from *Aspergillus fumigatus* Abrogates Leukotriene B_4 Formation through Inhibition of Leukotriene A_4 Hydrolase, Cell Chemical Biology (2019), https://doi.org/10.1016/j.chembiol.2019.01.001

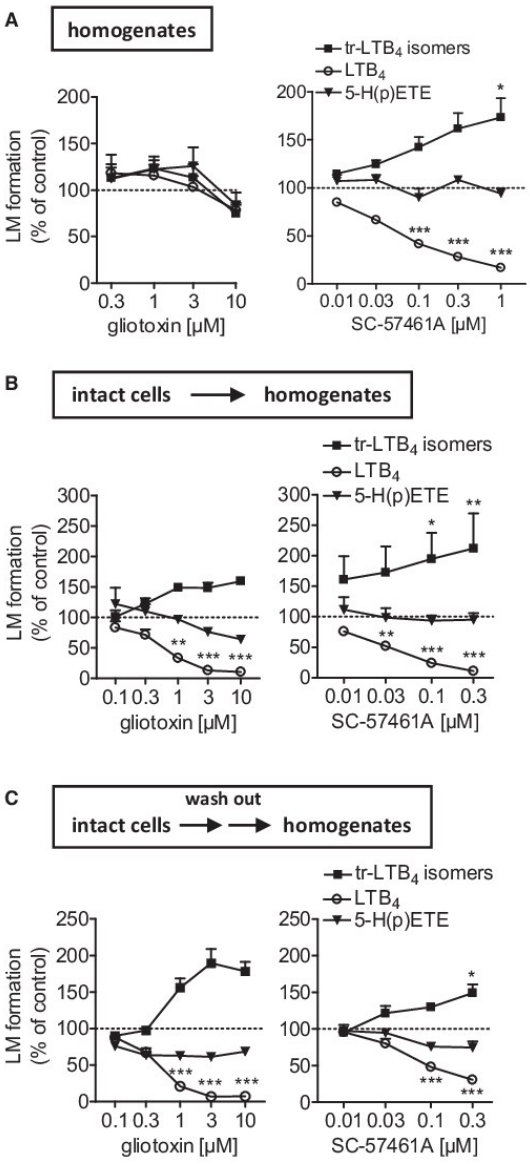

Figure 5. The Cellular Environment Confers Gliotoxin LTA_4H-Inhibitory Activity

(A) Effects of gliotoxin and SC-57461A on LT formation in cell-free neutrophil homogenates. Neutrophil homogenates were pre-incubated with test compounds or vehicle (0.1% DMSO) for 10 min on ice, pre-warmed for 30 s at 37°C, and then 20 μM AA plus 2 mM $CaCl_2$ was added. After 10 min, formation of tr-LTB_4 isomers, LTB_4, and 5-H(p)ETE was analyzed by RP-HPLC.

(B) Intact human neutrophils were first pre-incubated with test compounds or vehicle (0.1% DMSO) for 10 min at 37°C, placed on ice and sonicated. Then, the resulting homogenates were pre-warmed for 30 s at 37°C, 20 μM AA plus 2 mM $CaCl_2$ was added, and after 10 min formation of tr-LTB_4 isomers, LTB_4, and 5-H(p)ETE was analyzed by RP-HPLC.

(C) Intact human neutrophils were pre-incubated with test compounds or vehicle (0.1% DMSO) for 10 min at 37°C, centrifuged, resuspended in fresh PG buffer, sonicated, and the resulting homogenates were pre-warmed for 30 s at 37°C. Then, 20 μM AA plus 2 mM $CaCl_2$ was added, and after 10 min formation of tr-LTB_4 isomers, LTB_4, and 5-HETE was analyzed by RP-HPLC.

Data are means ± SEM; n = 3–4, ***p < 0.001; **p < 0.01; *p < 0.05; inhibitor versus vehicle control (100%), one-way ANOVA plus Bonferroni.

disulfide bond, inhibited LTB_4 formation and tr-LTB_4 isomers as gliotoxin did (Figure S2).

DISCUSSION

We show here that gliotoxin causes specific suppression of LTB_4 biosynthesis without inhibiting the formation of additional products from the same substrate (i.e., LTA_4) or related LMs generated by other enzymatic eicosanoid pathways. These LTB_4-suppressing properties of gliotoxin are directly related to selective inhibition of the epoxide hydrolase activity of LTA_4H, which either requires the cellular environment and/or reducing conditions. Our data suggest that the inactive disulfide form of gliotoxin is reduced into the bioactive dithiol, which may then target the Zn^{2+} within the active site in LTA_4H. Because LTB_4 is one of the most potent and relevant chemoattractants for neutrophils (Afonso et al., 2012; Lammermann et al., 2013) and critical for neutrophil-mediated host resistance against IA (Caffrey-Carr et al., 2017), suppression of neutrophil infiltration by gliotoxin could be the consequence of abrogated LTB_4 generation. Therefore, our data provide a molecular basis for the neutrophil-compromising properties of *A. fumigatus* during infections.

To assess LTB_4 formation and related neutrophil recruitment we used two different LT-driven *in vivo* models, i.e., zymosan-induced peritonitis in mice (Rao et al., 1994) and carrageenan-induced pleurisy in rats (Cuzzocrea et al., 2003). Both, gliotoxin and the 5-LO inhibitor zileuton strongly suppressed LTB_4 formation in these models, along with marked inhibition of neutrophil infiltration at sites of injury. Suppression of LTB_4 levels in intact cells or *in vivo* may generally be achieved via diverse modes of actions, such as direct inhibition of $cPLA_2$, 5-LO, FLAP, or LTA_4H, by interference with upstream signaling pathways of these enzymes, or by promoting LTB_4 metabolism (Werz et al., 2017). While zileuton reduced the levels of all 5-LO-derived products to a comparable degree, as expected, gliotoxin selectively suppressed LTB_4 formation without lowering any other LMs. Of interest, gliotoxin increased the amounts of tr-LTB_4 isomers and LTC_4 at the expense of LTB_4, seemingly due to redirection of LTA_4 as substrate, excluding $cPLA_2$, 5-LO, or FLAP as targets, but instead favoring LTA_4H as point of attack. Such substrate shunting from LTB_4 toward tr-LTB_4 isomers or LTC_4 due to LTA_4H blockade was observed for other LTA_4H inhibitors as well (Kachur et al., 2002; Rao et al., 2007; Shindo et al., 1994). Inhibition of LTB_4 formation by gliotoxin, accompanied by an increase of alternative LTA_4 hydrolysis products (e.g., tr-LTB_4 isomers, LTC_4, and LXA_4), was also observed in A23187-stimulated neutrophils or monocytes, effects that were shared with the LTA_4H inhibitor SC-57461A but not with zileuton, which inhibited the formation of all 5-LO-derived products. Elevated levels of the

Please cite this article in press as: König et al., Gliotoxin from *Aspergillus fumigatus* Abrogates Leukotriene B_4 Formation through Inhibition of Leukotriene A_4 Hydrolase, Cell Chemical Biology (2019), https://doi.org/10.1016/j.chembiol.2019.01.001

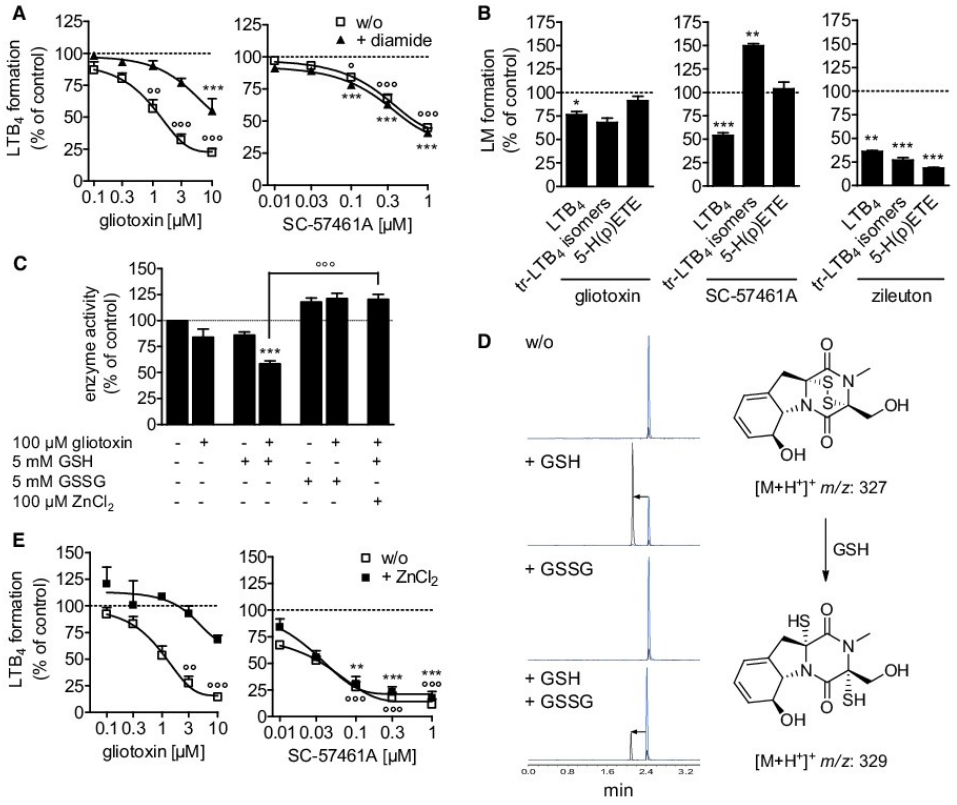

Figure 6. Reducing Conditions Activate Gliotoxin for Inhibition of LTA_4H

(A) Intact human neutrophils were pre-incubated with 50 μM diamide or vehicle (PBS) for 3 min at room temperature. Then, neutrophils were incubated with test compounds or vehicle (0.1% DMSO) for 10 min and stimulated with 2.5 μM A23187 plus 20 μM AA for 10 min at 37°C. LTB_4 formation was analyzed by RP-HPLC.

(B) Inhibition of 5-LO/LTA_4H-coupled LTB_4 formation from *in-situ*-generated LTA_4 by gliotoxin (10 μM), zileuton (3 μM), SC-57461A (0.1 μM), or vehicle (0.1% DMSO) in a cell-free assay. Purified 5-LO and LTA_4H were pre-incubated with test compounds or 0.1% DMSO (vehicle) for 10 min on ice, pre-warmed for 30 s at 37°C, and 20 μM AA plus 2 mM $CaCl_2$ was added. After 10 min at 37°C, formation of tr-LTB_4 isomers, LTB_4, and 5-H(p)ETE was analyzed by RP-HPLC.

(C and D) Glutathione confers inhibition of LTA_4H activity by gliotoxin in a cell-free assay; effects of Zn^{2+} ions. Gliotoxin was pre-incubated with GSH or GSSG (5 mM, each), in the presence or absence of $ZnCl_2$ (100 μM) at 37°C for 2 h. (C) Purified LTA_4H and substrate were added. Reaction was monitored for 60 min to determine LTA_4H activity. (D) In parallel, aliquots of these incubations were analyzed by UPLC-MS/MS for gliotoxin in reduced (dithiol) or oxidized (disulfide, blue) form.

(E) Neutrophils were pre-incubated with test compounds for 10 min at 37°C, placed on ice, and sonicated. The resulting homogenates were supplemented with 200 μM $ZnCl_2$ or vehicle (water), pre-incubated for 30 s at 37°C, and then incubated with 20 μM AA plus 2 mM $CaCl_2$ for 10 min at 37°C. LTB_4 formation was analyzed by RP-HPLC.

Data are means ± SEM; n = 3–4, ***p < 0.001; **p < 0.01 inhibitor versus vehicle control (100%), one-way ANOVA plus Bonferroni. See also Figure S2.

anti-inflammatory LXA_4 may counter-regulate the inflammatory response and sustain chemotaxis and migration of neutrophils (Serhan and Samuelsson, 1988).

A remarkable characteristic of gliotoxin as an LTA_4H inhibitor is its apparent selectivity against epoxide hydrolase function without affecting aminopeptidase activity, a feature that was shared with ARM1 (Stsiapanava et al., 2014). Most of the known LTA_4H inhibitors including SC-57461A and captopril block both activities (Caliskan and Banoglu, 2013). As aminopeptidase activity degrades the chemoattractant peptide PGP, implying anti-inflammatory properties of LTA_4H, inhibition of the aminopeptidase activity might be detrimental, and selective interference with epoxide hydrolase function is favored (Caliskan and Banoglu, 2013; Stsiapanava et al., 2014). Since the epoxide hydrolase activity of sEH, which hydrolyses structurally related eicosanoid epoxides (Wagner et al., 2017), was not affected by gliotoxin, promiscuous interference with epoxide hydrolases in eicosanoid metabolism in general is unlikely.

Please cite this article in press as: König et al., Gliotoxin from *Aspergillus fumigatus* Abrogates Leukotriene B_4 Formation through Inhibition of Leukotriene A_4 Hydrolase, Cell Chemical Biology (2019), https://doi.org/10.1016/j.chembiol.2019.01.001

CellPress

Several molecular targets of gliotoxin have been proposed before, including IκBα/NF-κB (Pahl et al., 1996), alcohol dehydrogenase (Waring et al., 1995), creatine kinase (Hurne et al., 2000), farnesyl transferase (Van der Pyl et al., 1992), chymotrypsin-like activities of the 20S proteasome (Kroll et al., 1999), the flavocytochrome b558 of NAPH oxidase (Nishida et al., 2005), and X-linked neuroligin 4 (Scafuri et al., 2017). Gliotoxin contains an internal disulfide bridge, and, interestingly, either the oxidized disulfide form or the reduced dithiol form was shown to be the active moiety depending on the target enzyme studied (Scharf et al., 2012). For inhibition of LTA_4H, the reduced dithiol form of gliotoxin was required. Cleavage of the disulfide can be achieved by treatment with excess of thiols such as GSH or dithiothreitol (Trown and Bilello, 1972). Indeed, gliotoxin inhibited LTA_4H activity in the cell-free assays only when exogenous GSH was provided, and gliotoxin blocked LTA_4H activity in intact leukocytes where abundant cytosolic GSH is present. On the other hand, intracellular GSH depletion in neutrophils by diamide impaired the potency of gliotoxin but not that of SC-57461A. We propose that the free thiol moieties of reduced gliotoxin interferes with the active site in LTA_4H that coordinates the epoxide moiety of LTA_4 (Stsiapanava et al., 2017). Possibly, gliotoxin chelates the active site Zn^{2+}, supported by the finding that excess of Zn^{2+} ions abolished the inhibitory activities of gliotoxin but not of SC-57461A, probably by capturing gliotoxin's thiol groups. Along these lines, the disulfide-containing antibiotic thiolutin acts as a Zn^{2+} chelator under reducing conditions (presence of dithiothreitol) thereby inhibiting JAMM metalloproteases, an effect that was abrogated by exogenous addition of Zn^{2+} ions as well (Lauinger et al., 2017). Attempts to demonstrate binding of gliotoxin to LTA_4H using MS-based proteomics failed to yield experimental support for covalent modification of the enzyme (data not shown).

Humans are continuously exposed to inhaled *A. fumigatus* conidia and healthy hosts can clear the organism without antibody- or cell-mediated acquired immunity (Park and Mehrad, 2009). Thus, innate immunity appears to be sufficient to resist against *A. fumigatus* for healthy humans, while for immunocompromised patients who lack efficient innate immune responses, *A. fumigatus* infections cause severe pulmonary diseases along with substantial mortality (Park and Mehrad, 2009; Segal, 2009). Neutrophils are key effector cells required for resistance against *A. fumigatus* infection (Comera et al., 2007; Heinekamp et al., 2015; Spikes et al., 2008; Sugui et al., 2007), and neutropenia is a key risk factor for patients who develop IA (Park and Mehrad, 2009; Sugui et al., 2007). Recent data demonstrate a crucial role of host-derived LTB_4 for neutrophil recruitment and innate immunity against *A. fumigatus* infection in murine lungs (Caffrey-Carr et al., 2017). These facts further support the hypothesis that suppression of LTB_4 formation by gliotoxin is a crucial mechanism underlying its neutrophil-compromising properties in the infected host. In this respect, gliotoxin is a virulence factor of *A. fumigatus* that mediates immunocompromising properties by primarily targeting neutrophils (Comera et al., 2007; Spikes et al., 2008; Sugui et al., 2007; Sutton et al., 1996). Thus, abrogation of gliotoxin production in *A. fumigatus* by deletion of *gliP* impaired the virulence in mice immunosuppressed with cortisone that still have residual neutrophil activity (Spikes et al., 2008), but not in neutropenic mice basically lacking neutrophils (Kupfahl et al., 2006; Spikes et al., 2008). This finding confirms the requirement of neutrophils for gliotoxin's immunosuppressive actions. Our present data showing that the Δ*gliP* strain failed to suppress LTB_4 formation and to compromise neutrophils, indicate that gliotoxin as part of the secretome of *A. fumigatus* is the primary mycotoxin that is causative for inhibition of LTB_4 formation, and support this action as a potential virulence mechanism of gliotoxin in IA. Apparently, reduced chemotaxis and direct neutrophil killing are causative for gliotoxin's detrimental effects on neutrophils during *A. fumigatus* infection.

Together, we reveal LTA_4H as molecular target of gliotoxin and, thus, propose inhibition of LTB_4 biosynthesis as biological relevant mode of action of this mycotoxin from *A. fumigatus*. Because LTB_4 is a major chemoattractant for neutrophils with crucial roles in neutrophil-mediated host resistance against IA, suppression of LTB_4 formation by gliotoxin may underlie its neutrophil-compromising properties.

SIGNIFICANCE

The fungal pathogen *Aspergillus fumigatus* is the most common cause of invasive aspergillosis which affects primarily immunocompromised patients with a mortality rate of 30%–95%. Humans are continuously exposed to inhaled *A. fumigatus* conidia, and healthy hosts can clear the organism without antibody- or cell-mediated acquired immunity. The epidithiodioxopiperazine gliotoxin is well recognized as one of the virulence factors of *A. fumigatus* that suppresses innate immunity in humans, particularly by compromising neutrophils. A variety of bioactivities were reported for gliotoxin, such as induction of apoptosis and angiogenesis, inhibition of NF-κB, suppression of reactive oxygen species generation by phagocytes, and induction of changes in cell morphology and cell adhesion of neutrophils. However, the molecular mechanisms underlying the immunosuppressing properties of gliotoxin remain elusive. Recently, the host-derived chemoattractant leukotriene (LT) B_4 was shown to be critical for neutrophil recruitment and resistance to pulmonary *A. fumigatus* challenge in mice. Here, we show that gliotoxin specifically abrogates the biosynthesis of LTB_4, an arachidonic acid-derived lipid mediator that is among the most potent and relevant chemoattractants for neutrophils. Thus, pre-treatment of mice and rats with gliotoxin effectively blocked agonist-induced neutrophil recruitment along with reduced levels of circulating LTB_4, while other lipid mediators were not suppressed. These LTB_4-suppressing properties of gliotoxin are mediated through selective inhibition of leukotriene A_4 hydrolase (LTA_4H), the key enzyme in LTB_4 biosynthesis. Since LTB_4 is critical for neutrophil-mediated host resistance against invasive aspergillosis, we suggest that the immunosuppressive properties of gliotoxin are directly related to abrogated LTB_4 generation. Based on the unmet medical need for efficient therapeutics to intervene with *A. fumigatus* immunopathology, understanding of the mechanisms underlying its virulence factors is of utmost importance. Therefore, our data provide a molecular basis for the neutrophil-compromising properties of *A. fumigatus* during infections, and reveal LTA_4H as a functional, molecular target of gliotoxin.

Please cite this article in press as: König et al., Gliotoxin from *Aspergillus fumigatus* Abrogates Leukotriene B_4 Formation through Inhibition of Leukotriene A_4 Hydrolase, Cell Chemical Biology (2019), https://doi.org/10.1016/j.chembiol.2019.01.001

STAR★METHODS

Detailed methods are provided in the online version of this paper and include the following:

- KEY RESOURCES TABLE
- CONTACT FOR REAGENT AND RESOURCE SHARING
- EXPERIMENTAL MODEL AND SUBJECT DETAILS
  - Animals
  - Human Cells
- METHODS DETAILS
  - Murine Infection Model
  - Murine Peritonitis Model
  - Carrageenan-Induced Pleurisy in Rats
  - Cultivation of *A. fumigatus*, Preparation of Culture Supernatants
  - 5-LO Product Formation in Neutrophils or Monocytes and in Corresponding Homogenates
  - Expression and Purification of Human Recombinant 5-LO and LTA_4H
  - Determination of the Epoxide Hydrolase Activity of LTA_4H Activity from *In-Situ* Generated LTA_4
  - Determination of the Epoxide Hydrolase Activity of LTA_4H in a Cell-free Fluorescence-Based Assay
  - Analysis of Gliotoxin by UPLC-MS-MS
  - Determination of the Aminopeptidase Activity of LTA_4H
  - Determination of Cellular sEH Activity
- QUANTIFICATION AND STATISTICAL ANALYSIS

SUPPLEMENTAL INFORMATION

Supplemental Information includes two figures and can be found with this article online at https://doi.org/10.1016/j.chembiol.2019.01.001.

ACKNOWLEDGMENTS

The financial support by the German Research Council SFB1127 ChemBioSys and SFB/TR 124 FungiNet, the DFG-funded excellence graduate school Jena School for Microbial Communication (JSMC), the Free State of Thuringa, Pro-Excellence Initiative 2 ("RegenerAging"), and the Swedish Research Council 10350 is acknowledged. J.G. received a Carl-Zeiss stipend.

AUTHOR CONTRIBUTIONS

S.P., T.H., A.R., L.S., J.Z.H., C.H., A.A.B., J.G., E.P., and O.W. designed the research, gave advice, and planed the study. S.K., S.P., H.P., T.H., J.K., E.R., M.S., F.T., A.P., J.D., K.S., and J.G. performed the experiments and analyzed the data. S.K. and O.W. wrote the manuscript.

DECLARATION OF INTERESTS

The authors declare no competing interests.

Received: April 24, 2018
Revised: August 23, 2018
Accepted: January 2, 2019
Published: February 7, 2019

REFERENCES

Afonso, P.V., Janka-Junttila, M., Lee, Y.J., McCann, C.P., Oliver, C.M., Aamer, K.A., Losert, W., Cicerone, M.T., and Parent, C.A. (2012). LTB4 is a signal-relay molecule during neutrophil chemotaxis. Dev. Cell *22*, 1079–1091.

Askonas, L.J., Kachur, J.F., Villani-Price, D., Liang, C.D., Russell, M.A., and Smith, W.G. (2002). Pharmacological characterization of SC-57461A (3-[methyl [3-[4-(phenylmethyl)phenoxy]propyl]amino]propanoic acid HCl), a potent and selective inhibitor of leukotriene A(4) hydrolase I: in vitro studies. J. Pharmacol. Exp. Ther. *300*, 577–582.

Brandt, S.L., and Serezani, C.H. (2017). Too much of a good thing: how modulating LTB4 actions restore host defense in homeostasis or disease. Semin. Immunol. *33*, 37–43.

Caffrey-Carr, A.K., Hilmer, K.M., Kowalski, C.H., Shepardson, K.M., Temple, R.M., Cramer, R.A., and Obar, J.J. (2017). Host-derived leukotriene B4 is critical for resistance against invasive pulmonary aspergillosis. Front. Immunol. *8*, 1984.

Caliskan, B., and Banoglu, E. (2013). Overview of recent drug discovery approaches for new generation leukotriene A4 hydrolase inhibitors. Expert Opin. Drug Discov. *8*, 49–63.

Comera, C., Andre, K., Laffitte, J., Collet, X., Galtier, P., and Maridonneau-Parini, I. (2007). Gliotoxin from *Aspergillus fumigatus* affects phagocytosis and the organization of the actin cytoskeleton by distinct signalling pathways in human neutrophils. Microbes Infect. *9*, 47–54.

Cuzzocrea, S., Rossi, A., Serraino, I., Mazzon, E., Di Paola, R., Dugo, L., Genovese, T., Calabro, B., Caputi, A.P., and Sautebin, L. (2003). 5-Lipoxygenase knockout mice exhibit a resistance to pleurisy and lung injury caused by carrageenan. J. Leukoc. Biol. *73*, 739–746.

Fischer, L., Szellas, D., Radmark, O., Steinhilber, D., and Werz, O. (2003). Phosphorylation- and stimulus-dependent inhibition of cellular 5-lipoxygenase activity by nonredox-type inhibitors. FASEB J. *17*, 949–951.

Garscha, U., Romp, E., Pace, S., Rossi, A., Temml, V., Schuster, D., Konig, S., Gerstmeier, J., Liening, S., Werner, M., et al. (2017). Pharmacological profile and efficiency in vivo of diflapolin, the first dual inhibitor of 5-lipoxygenase-activating protein and soluble epoxide hydrolase. Sci. Rep. *7*, 9398.

Haeggstrom, J.Z., and Funk, C.D. (2011). Lipoxygenase and leukotriene pathways: biochemistry, biology, and roles in disease. Chem. Rev. *111*, 5866–5898.

Haeggstrom, J.Z., Tholander, F., and Wetterholm, A. (2007). Structure and catalytic mechanisms of leukotriene A4 hydrolase. Prostaglandins Other Lipid Mediat. *83*, 198–202.

Heinekamp, T., Schmidt, H., Lapp, K., Pahtz, V., Shopova, I., Koster-Eiserfunke, N., Kruger, T., Kniemeyer, O., and Brakhage, A.A. (2015). Interference of *Aspergillus fumigatus* with the immune response. Semin. Immunopathol. *37*, 141–152.

Hillmann, F., Novohradska, S., Mattern, D.J., Forberger, T., Heinekamp, T., Westermann, M., Winckler, T., and Brakhage, A.A. (2015). Virulence determinants of the human pathogenic fungus *Aspergillus fumigatus* protect against soil amoeba predation. Environ. Microbiol. *17*, 2858–2869.

Hurne, A.M., Chai, C.L., and Waring, P. (2000). Inactivation of rabbit muscle creatine kinase by reversible formation of an internal disulfide bond induced by the fungal toxin gliotoxin. J. Biol. Chem. *275*, 25202–25206.

Jakobsson, P.J., Steinhilber, D., Odlander, B., Radmark, O., Claesson, H.E., and Samuelsson, B. (1992). On the expression and regulation of 5-lipoxygenase in human lymphocytes. Proc. Natl. Acad. Sci. U S A *89*, 3521–3525.

Kachur, J.F., Askonas, L.J., Villani-Price, D., Ghoreishi-Haack, N., Won-Kim, S., Liang, C.D., Russell, M.A., and Smith, W.G. (2002). Pharmacological characterization of SC-57461A (3-[methyl[3-[4-(phenylmethyl)phenoxy]propyl] amino]propanoic acid HCl), a potent and selective inhibitor of leukotriene A(4) hydrolase II: in vivo studies. J. Pharmacol. Exp. Ther. *300*, 583–587.

Kroll, M., Arenzana-Seisdedos, F., Bachelerie, F., Thomas, D., Friguet, B., and Conconi, M. (1999). The secondary fungal metabolite gliotoxin targets proteolytic activities of the proteasome. Chem. Biol. *6*, 689–698.

Kupfahl, C., Heinekamp, T., Geginat, G., Ruppert, T., Hartl, A., Hof, H., and Brakhage, A.A. (2006). Deletion of the gliP gene of *Aspergillus fumigatus* results in loss of gliotoxin production but has no effect on virulence of the fungus in a low-dose mouse infection model. Mol. Microbiol. *62*, 292–302.

Please cite this article in press as: König et al., Gliotoxin from *Aspergillus fumigatus* Abrogates Leukotriene B_4 Formation through Inhibition of Leukotriene A_4 Hydrolase, Cell Chemical Biology (2019), https://doi.org/10.1016/j.chembiol.2019.01.001

Lam, B.K., and Austen, K.F. (2002). Leukotriene C4 synthase: a pivotal enzyme in cellular biosynthesis of the cysteinyl leukotrienes. Prostaglandins Other Lipid Mediat. *68-69*, 511–520.

Lammermann, T., Afonso, P.V., Angermann, B.R., Wang, J.M., Kastenmuller, W., Parent, C.A., and Germain, R.N. (2013). Neutrophil swarms require LTB4 and integrins at sites of cell death in vivo. Nature *498*, 371–375.

Lauinger, L., Li, J., Shostak, A., Cemel, I.A., Ha, N., Zhang, Y., Merkl, P.E., Obermeyer, S., Stankovic-Valentin, N., Schafmeier, T., et al. (2017). Thiolutin is a zinc chelator that inhibits the Rpn11 and other JAMM metalloproteases. Nat. Chem. Biol. *13*, 709–714.

Lewis, R.E., Wiederhold, N.P., Chi, J., Han, X.Y., Komanduri, K.V., Kontoyiannis, D.P., and Prince, R.A. (2005). Detection of gliotoxin in experimental and human aspergillosis. Infect. Immun. *73*, 635–637.

Morisseau, C., and Hammock, B.D. (2013). Impact of soluble epoxide hydrolase and epoxyeicosanoids on human health. Annu. Rev. Pharmacol. Toxicol. *53*, 37–58.

Moser, D., Wittmann, S.K., Kramer, J., Blocher, R., Achenbach, J., Pogoryelov, D., and Proschak, E. (2015). PENG: a neural gas-based approach for pharmacophore elucidation. Method design, validation, and virtual screening for novel ligands of LTA4H. J. Chem. Inf. Model. *55*, 284–293.

Nishida, S., Yoshida, L.S., Shimoyama, T., Nunoi, H., Kobayashi, T., and Tsunawaki, S. (2005). Fungal metabolite gliotoxin targets flavocytochrome b558 in the activation of the human neutrophil NADPH oxidase. Infect. Immun. *73*, 235–244.

Orning, L., Krivi, G., Bild, G., Gierse, J., Aykent, S., and Fitzpatrick, F.A. (1991). Inhibition of leukotriene A4 hydrolase/aminopeptidase by captopril. J. Biol. Chem. *266*, 16507–16511.

Pace, S., Pergola, C., Dehm, F., Rossi, A., Gerstmeier, J., Troisi, F., Pein, H., Schaible, A.M., Weinigel, C., Rummler, S., et al. (2017a). Androgen-mediated sex bias impairs efficiency of leukotriene biosynthesis inhibitors in males. J. Clin. Invest. *127*, 3167–3176.

Pace, S., Rossi, A., Krauth, V., Dehm, F., Troisi, F., Bilancia, R., Weinigel, C., Rummler, S., Werz, O., and Sautebin, L. (2017b). Sex differences in prostaglandin biosynthesis in neutrophils during acute inflammation. Sci. Rep. *7*, 3759.

Pahl, H.L., Krauss, B., Schulze-Osthoff, K., Decker, T., Traenckner, E.B., Vogt, M., Myers, C., Parks, T., Warring, P., Muhlbacher, A., et al. (1996). The immunosuppressive fungal metabolite gliotoxin specifically inhibits transcription factor NF-kappaB. J. Exp. Med. *183*, 1829–1840.

Park, S.J., and Mehrad, B. (2009). Innate immunity to *Aspergillus* species. Clin. Microbiol. Rev. *22*, 535–551.

Radmark, O., Werz, O., Steinhilber, D., and Samuelsson, B. (2015). 5-Lipoxygenase, a key enzyme for leukotriene biosynthesis in health and disease. Biochim. Biophys. Acta *1851*, 331–339.

Rao, N.L., Dunford, P.J., Xue, X., Jiang, X., Lundeen, K.A., Coles, F., Riley, J.P., Williams, K.N., Grice, C.A., Edwards, J.P., et al. (2007). Anti-inflammatory activity of a potent, selective leukotriene A4 hydrolase inhibitor in comparison with the 5-lipoxygenase inhibitor zileuton. J. Pharmacol. Exp. Ther. *321*, 1154–1160.

Rao, T.S., Currie, J.L., Shaffer, A.F., and Isakson, P.C. (1994). In vivo characterization of zymosan-induced mouse peritoneal inflammation. J. Pharmacol. Exp. Ther. *269*, 917–925.

Scafuri, B., Varriale, A., Facchiano, A., D'Auria, S., Raggi, M.E., and Marabotti, A. (2017). Binding of mycotoxins to proteins involved in neuronal plasticity: a combined in silico/wet investigation. Sci. Rep. *7*, 15156.

Scharf, D.H., Brakhage, A.A., and Mukherjee, P.K. (2016). Gliotoxin – bane or boon? Environ. Microbiol. *18*, 1096–1109.

Scharf, D.H., Heinekamp, T., Remme, N., Hortschansky, P., Brakhage, A.A., and Hertweck, C. (2012). Biosynthesis and function of gliotoxin in *Aspergillus fumigatus*. Appl. Microbiol. Biotechnol. *93*, 467–472.

Segal, B.H. (2009). Aspergillosis. N. Engl. J. Med. *360*, 1870–1884.

Serhan, C.N., and Samuelsson, B. (1988). Lipoxins: a new series of eicosanoids (biosynthesis, stereochemistry, and biological activities). Adv. Exp. Med. Biol. *229*, 1–14.

Shindo, K., Baker, J.R., Munafo, D.A., and Bigby, T.D. (1994). Captopril inhibits neutrophil synthesis of leukotriene B4 in vitro and in vivo. J. Immunol. *153*, 5750–5759.

Snelgrove, R.J., Jackson, P.L., Hardison, M.T., Noerager, B.D., Kinloch, A., Gaggar, A., Shastry, S., Rowe, S.M., Shim, Y.M., Hussell, T., et al. (2010). A critical role for LTA4H in limiting chronic pulmonary neutrophilic inflammation. Science *330*, 90–94.

Spikes, S., Xu, R., Nguyen, C.K., Chamilos, G., Kontoyiannis, D.P., Jacobson, R.H., Ejzykowicz, D.E., Chiang, L.Y., Filler, S.G., and May, G.S. (2008). Gliotoxin production in *Aspergillus fumigatus* contributes to host-specific differences in virulence. J. Infect. Dis. *197*, 479–486.

Stsiapanava, A., Olsson, U., Wan, M., Kleinschmidt, T., Rutishauser, D., Zubarev, R.A., Samuelsson, B., Rinaldo-Matthis, A., and Haeggstrom, J.Z. (2014). Binding of Pro-Gly-Pro at the active site of leukotriene A4 hydrolase/aminopeptidase and development of an epoxide hydrolase selective inhibitor. Proc. Natl. Acad. Sci. U S A *111*, 4227–4232.

Stsiapanava, A., Samuelsson, B., and Haeggstrom, J.Z. (2017). Capturing LTA4 hydrolase in action: insights to the chemistry and dynamics of chemotactic LTB4 synthesis. Proc. Natl. Acad. Sci. U S A *114*, 9689–9694.

Sugui, J.A., Pardo, J., Chang, Y.C., Zarember, K.A., Nardone, G., Galvez, E.M., Mullbacher, A., Gallin, J.I., Simon, M.M., and Kwon-Chung, K.J. (2007). Gliotoxin is a virulence factor of *Aspergillus fumigatus*: gliP deletion attenuates virulence in mice immunosuppressed with hydrocortisone. Eukaryot. Cell *6*, 1562–1569.

Surette, M.E., Palmantier, R., Gosselin, J., and Borgeat, P. (1993). Lipopolysaccharides prime whole human blood and isolated neutrophils for the increased synthesis of 5-lipoxygenase products by enhancing arachidonic acid availability – involvement of the CD14 antigen. J. Exp. Med. *178*, 1347–1355.

Sutton, P., Waring, P., and Mullbacher, A. (1996). Exacerbation of invasive aspergillosis by the immunosuppressive fungal metabolite, gliotoxin. Immunol. Cell Biol. *74*, 318–322.

Trown, P.W., and Bilello, J.A. (1972). Mechanism of action of gliotoxin: elimination of activity by sulfhydryl compounds. Antimicrob. Agents Chemother. *2*, 261–266.

Van der Pyl, D., Inokoshi, J., Shiomi, K., Yang, H., Takeshima, H., and Omura, S. (1992). Inhibition of farnesyl-protein transferase by gliotoxin and acetylgliotoxin. J. Antibiot. (Tokyo) *45*, 1802–1805.

Wagner, K.M., McReynolds, C.B., Schmidt, W.K., and Hammock, B.D. (2017). Soluble epoxide hydrolase as a therapeutic target for pain, inflammatory and neurodegenerative diseases. Pharmacol. Ther. *180*, 62–76.

Waring, P., and Beaver, J. (1996). Gliotoxin and related epipolythiodioxopiperazines. Gen. Pharmacol. *27*, 1311–1316.

Waring, P., Sjaarda, A., and Lin, Q.H. (1995). Gliotoxin inactivates alcohol dehydrogenase by either covalent modification or free radical damage mediated by redox cycling. Biochem. Pharmacol. *49*, 1195–1201.

Werz, O., Gerstmeier, J., and Garscha, U. (2017). Novel leukotriene biosynthesis inhibitors (2012-2016) as anti-inflammatory agents. Expert Opin. Ther. Pat. *27*, 607–620.

Werz, O., Gerstmeier, J., Libreros, S., De la Rosa, X., Werner, M., Norris, P.C., Chiang, N., and Serhan, C.N. (2018). Human macrophages differentially produce specific resolvin or leukotriene signals that depend on bacterial pathogenicity. Nat. Commun. *9*, 59.

Wittmann, S.K., Kalinowsky, L., Kramer, J.S., Bloecher, R., Knapp, S., Steinhilber, D., Pogoryelov, D., Proschak, E., and Heering, J. (2016). Thermodynamic properties of leukotriene A4 hydrolase inhibitors. Bioorg. Med. Chem. *24*, 5243–5248.

Please cite this article in press as: König et al., Gliotoxin from *Aspergillus fumigatus* Abrogates Leukotriene B_4 Formation through Inhibition of Leukotriene A_4 Hydrolase, Cell Chemical Biology (2019), https://doi.org/10.1016/j.chembiol.2019.01.001

STAR★METHODS

KEY RESOURCES TABLE

REAGENT or RESOURCE	SOURCE	IDENTIFIER
Chemicals, Peptides, and Recombinant Proteins		
DMSO	VWR	1029500500
bovine serum albumin	AppliChem	A1391.0500
penicillin/streptomycin	GE Healthcare Life Sciences	A2213
RPMI-1640	GE Healthcare Life Sciences	R8758-6
fetal calf serum	Sigma	F7524
Histopaque®-1077	Sigma	10771-500ML
cortisone acetate	Sigma	C3130-1G
SC-57461A	Sigma	PZ0110-5MG
diamide	Sigma	D3684-1G
zymosan A from *Saccharomyces cerevisiae*	Sigma	Z4250-1G
L-arginine-7-amido-4-methylcoumarine	Sigma	C8022-50MG
gliotoxin	Sigma	G9893-5MG
λ-carrageenan type IV	Sigma	C3889
captopril	Sigma	C4042-5G
zinc chloride	Sigma	229997-10G
AUDA	Cayman Chemicals	CAY10007927-5
ARM-1	Cayman Chemicals	15865-10MG
leukotriene A_4 methylester	Cayman Chemicals	CAY20010-25
Prolyl-glycyl-proline Peptide	Cayman Chemicals	11188.5
N-acetyl-Pro-Gly-Pro Peptide	Cayman Chemicals	11189.5
14,15-EET	Cayman Chemicals	CAY50651.100
d_8-5(S)-HETE	Cayman Chemicals	334230-100μg
d_4-LTB_4	Cayman Chemicals	320110-100μg
arachidonic acid	Cayman Chemicals	90010
Ca-ionophore (A23187)	Cayman Chemicals	11016-10
zileuton	Sequoia Research Products	SRP01100z
Czapek Dox medium	BD biosciences	BD233810
Critical Commercial Assays		
DC protein assay kit	Biorad	5000111
LTB_4 ELISA kit	ENZO Life Sciences	ADI-901-068
cysLT ELISA kit	ENZO Life Sciences	ADI-901-070
periodic acid Schiff (PAS) kit	Sigma	395B-1KT
Experimental Models: Cell Lines		
A549	ATCC	CCL-185
HepG2	ATCC	HB-8065
Experimental Models: Organisms/Strains		
Escherichia coli BL21 (DE3)	New England Biolabs	C2525I
Escherichia coli BL21(DE3)RIPL-Codon Plus cells	Invitrogen	NC9122855
Aspergillus fumigatus strain CEA17Δ*akuB*	Hillmann et al. (2015)	N/A
female/male CD-1 mice	Charles River	N/A
Wistar Han rats	Harlan	N/A

(*Continued on next page*)

Please cite this article in press as: König et al., Gliotoxin from *Aspergillus fumigatus* Abrogates Leukotriene B_4 Formation through Inhibition of Leukotriene A_4 Hydrolase, Cell Chemical Biology (2019), https://doi.org/10.1016/j.chembiol.2019.01.001

Continued

REAGENT or RESOURCE	SOURCE	IDENTIFIER
Software and Algorithms		
GraphPad InStat 3	GraphPad Software Inc	https://www.graphpad.com/scientific-software/instat/
Empower 3 software	Waters	http://www.waters.com/waters/de_DE/Empower-3-Chromatography-Data-Software/nav.htm?cid=513188&locale=de_DE
Analyst software 1.6	AB Sciex	https://sciex.com/products/software/analyst-software
AxioVision Se64 Rel. 4.9.1	Carl Zeiss	https://www.zeiss.de/mikroskopie/downloads/axiovision-downloads.html

CONTACT FOR REAGENT AND RESOURCE SHARING

Further information and requests for resources and reagents should be directed to and will be fulfilled by the Lead Contact, Oliver Werz (oliver.werz@uni-jena.de).

EXPERIMENTAL MODEL AND SUBJECT DETAILS

Animals

For the murine infection model, specific-pathogen-free female outbreed CD-1 mice (18-20 g) were supplied by Charles River (Sulzfeld, Germany). Animals were housed under standard conditions in individually ventilated cages und fed with normal mouse chow and water ad libitum. All animals were cared for in accordance with the European animal welfare regulation and approved by the responsible federal/state authority and ethics committee in accordance with the German animal welfare act (permit no. 03-001/12).

Male adult CD-1 mice (6-8 weeks, Charles River Laboratories, Calco, Italy) for the peritonitis model and Male Wistar Han rats (200-240 g, Harlan, San Pietro al Natisone, Italy) for the pleurisy model, were housed in a controlled environment and provided with standard rodent chow and water. The experimental procedures were approved by the Italian Ministry according to the guidelines of Italian (N. 26/2014) and European Council law (N.63/2010/UE) for animal care.

Human Cells

Monocytes and neutrophils were isolated from peripheral blood of human adult healthy male and female volunteers (18-65 years) as described (Pace et al., 2017b) and with consent obtained from the Institute of Transfusion Medicine, University Hospital Jena. Individual blood samples provided and used for isolation of the leukocytes were blinded and the exact age and the sex of the donor was unknown. The protocols for experiments with human neutrophils and monocytes were approved by the ethical commission of the Friedrich-Schiller-University Jena (approval no. 4025-02/14). All methods were performed in accordance with the relevant guidelines and regulations. Leukocyte concentrates were prepared by centrifugation (4000×g, 20 min, 20°C). Venous blood was collected in heparinized tubes (16 I.E. heparin/mL blood). Peripheral blood mononuclear cells (PBMCs) and neutrophils were freshly isolated by dextran sedimentation and centrifugation on lymphocyte separation medium (Histopaque®-1077, Sigma Aldrich). Remaining erythrocytes were removed by hypotonic lysis using water, and resulting neutrophils were resuspended in PBS containing 0.1% (w/v) glucose (PG buffer) or PBS containing 0.1% (w/v) glucose plus 1 mM $CaCl_2$ (PGC buffer) as indicated. PBMCs were seeded in RPMI 1640 (Sigma Aldrich) supplemented with 10% heat inactivated fetal calf serum (FCS), 100 U/mL penicillin and 100 μg/mL streptomycin in cell culture flasks (Greiner Bio-one, Frickenhausen, Germany) for 1.5 hrs at 37°C, 5% CO_2. Adherent monocytes were washed twice with PBS, and finally resuspended in PG or PGC buffer as indicated.

A549 cells (ATCC CCL-185, obtained from a 58 years male human donor) were cultured in monolayers at 37°C and 5% CO_2 in DMEM supplemented with 10% (v/v) FCS, 100 U/mL penicillin and 100 μg/mL streptomycin. HepG2 cells (ATCC HB-8065, obtained from a 15 years male human donor) were cultured at 37°C and 5% CO_2 in RPMI 1640 containing 10% (v/v) FCS, 100 U/mL penicillin and 100 μg/mL streptomycin.

METHODS DETAILS

Murine Infection Model

CD-1 mice were immunosuppressed with two single doses of 25 mg cortisone acetate (Sigma-Aldrich, Taufkirchen, Germany), which were injected intraperitoneally (i.p.) three days before and immediately prior to infection (day 0). Mice were anesthetized by an i.p. anesthetic combination of midazolam, fentanyl, and medetomidine. Conidia (2×10^5 in 20 μL PBS) were applied to the nares of the mice. Deep anesthesia ensured inhalation of the conidia. Anesthesia was terminated by subcutaneous injection of flumazenil, naloxon and atipamezol. Infected animals were monitored at least twice daily and humanely sacrificed if moribund (defined by severe lethargy, severe dyspnea, hypothermia, or substantial weight loss). For histopathological analyses lungs from sacrificed animals

Please cite this article in press as: König et al., Gliotoxin from *Aspergillus fumigatus* Abrogates Leukotriene B_4 Formation through Inhibition of Leukotriene A_4 Hydrolase, Cell Chemical Biology (2019), https://doi.org/10.1016/j.chembiol.2019.01.001

were removed, fixed in formalin and paraffin-embedded according to standard protocols. 4 μm sections were stained with Periodic Acid-Schiff (PAS) using standard protocols. Sections were analyzed with a Zeiss Axio Imager.M2 microscope (Carl Zeiss, Jena, Germany). Images were taken with an AxioCam 105 color and analyzed by AxioVision SE64 Rel. 4.9.1 Imaging-Software (Carl Zeiss).

Murine Peritonitis Model

CD-1 mice were treated with i.p. injections of gliotoxin (5 mg/kg), zileuton (10 mg/kg) or vehicle (0.9% saline solution containing 2% (v/v) DMSO) 30 min prior induction of peritonitis by zymosan i.p. injection (0.5 mL, 2 mg/mL in 0.9% saline solution). Four hrs after zymosan injection, mice were euthanized by CO_2 inhalation. For analysis of infiltrated cells, 2 mL peritoneal exudates were collected by lavage of the peritoneal cavity with PBS. Infiltrated cells were stained with trypan blue and counted using a Burker chamber under a light microscope.

For the analysis of lipid mediators in the plasma, blood (approximately 0.7–0.9 mL) was collected by intracardiac puncture using citrate as anticoagulant. Plasma was obtained by centrifugation of the blood at 800×g at 4°C for 10 min and immediately frozen at –80°C. Plasma samples were used to analyze LTB_4 levels by ELISA (ENZO life sciences, Lörrach, Germany), and other lipid mediators by UPLC-MS-MS. For preparation of samples for UPLC-MS-MS analysis, plasma samples were centrifuged (400 × g, 10 min, 4°C), and 400 μL supernatant were mixed with 1 mL methanol containing 200 ng of PGB_1. After 1 hr at -20°C, precipitated proteins were removed by centrifugation (1200 × g, 10 min, 4°C) and lipid mediators were purified by C18 RP solid phase extraction prior to measurement by UPLC-MS-MS as reported before (Pace et al., 2017a).

Carrageenan-Induced Pleurisy in Rats

Rats were treated i.p. with gliotoxin (1.5 mg/kg and 5 mg/kg), zileuton (10 mg/kg) or vehicle (4% DMSO) 30 min before intrathoracic injection of λ-carrageenan type IV (1%, w/v, 0.2 mL). For injection of carrageenan, rats were narcotized with 4% (v/v) enfluran mixed with 0.5 L/min O_2, 0.5 L/min N_2 and applied to a skin incision at the level of the left skin intercostal space. The skin incision was closed and rats were allowed to recover. After 2 hrs of pleurisy induction, rats were sacrificed by CO_2 inhalation prior to obtaining 2 mL thoracic exudate by lavage of the cavity with 2 mL PBS. The number of infiltrated neutrophils was determined by light microscopy using a Burker chamber and vital trypan blue staining (Pace et al., 2017a). Collected plasma was used to determine circulating LTB_4 by ELISA (Enzo life sciences) and lipid mediators by UPLC-MS-MS as described for murine peritonitis above.

Cultivation of *A. fumigatus*, Preparation of Culture Supernatants

A. fumigatus strain CEA17Δ*akuB* derives from the sequenced clinical isolate A1163 and was used to generate the Δ*gliP* mutant by targeted gene deletion as previously described (Hillmann et al., 2015). Fungal strains were cultivated from frozen conidia stock solutions for 5 days at 37°C on malt-extract agar plates. Conidia were harvested in PBS and filtrated through a 30 μm MACS SmartStrainer (Miltenyi Biotec, Bergisch Gladbach, Germany) to remove mycelial debris. Conidia were counted with a CASY cell counter. 6 × 10^7 conidia of the Δ*gliP* mutant or the wild type were cultivated in 30 ml Czapek Dox medium (BD Biosciences, Heidelberg, Germany) for six days at 28°C and shaking at 220 rpm. The supernatant was filtrated using miracloth gaze and sterilized by passing through a 0.2 μm filter. The filtrate was vacuum dried for 36 hrs and the precipitate was resuspended in sterile PBS.

5-LO Product Formation in Neutrophils or Monocytes and in Corresponding Homogenates

Human neutrophils or monocytes (5 × 10^6/mL) were resuspended in PGC buffer and pre-incubated with test compounds, precipitates from *A. fumigatus* cultures, or 0.1% (v/v) vehicle for 10 min at 37°C prior stimulation with 2.5 μM A23187. In some set of experiments, neutrophils were first pre-incubated with or without 50 μM diamide for 3 min prior to addition of test compounds or vehicle. After 10 min at 37°C, 5-LO product formation was stopped on ice. An aliquot (100 μL) of the monocyte suspension was removed and used for measuring cysLT by ELISA. To the remaining monocyte suspension and the entire neutrophil suspension, one volume of ice-cold methanol was added. Then, 530 μL acidified PBS and 200 ng of PGB_1 as internal standard were added and samples were purified by RP18 solid phase extraction. 5-LO products were eluted with methanol and subsequently measured with RP-HPLC using a C18 RP Radial PAK column (Waters, Eschborn, Germany) or optionally by UPLC-MS-MS as described (Pace et al., 2017a).

To determine 5-LO product formation in cell homogenates, neutrophils were resuspended in PBS containing 1 mM EDTA (5 × 10^6 cells/mL). Cells were lysed on ice by sonication (3 × 20 sec). Cell homogenates were pre-incubated with compounds or 0.1% (v/v) vehicle for 10 min on ice, pre-warmed for 30 sec at 37°C, and 20 μM AA and 2 mM $CaCl_2$ was added. After 10 min at 37°C, the reaction was stopped by addition of 1 mL ice-cold methanol and 5-LO products were analyzed as described above for intact cells. In some experiments, neutrophils were first pre-incubated with the test compounds or 0.1% (v/v) vehicle for 10 min at 37°C, the samples were placed on ice, homogenates were prepared by sonication (3 × 20 sec), and then 5-LO activity in the cell homogenates was determined as described above. For wash out experiments, neutrophils were first pre-incubated with compounds or 0.1% (v/v) vehicle for 10 min at 37°C, then spun down at 1200 rpm, resuspended in PBS containing 1 mM EDTA, and homogenates were prepared.

Expression and Purification of Human Recombinant 5-LO and LTA_4H

Human recombinant 5-LO was expressed overnight in *Escherichia coli* BL21 cells transformed with the pT3-5-LO vector as described previously (Fischer et al., 2003), followed by sonication (3 × 20 sec) on ice. For purification of 5-LO, ATP affinity chromatography was used. Homogenates were centrifuged at 40,000 × g (20 min, 4°C) and the supernatant was loaded on an ATP-agarose

Please cite this article in press as: König et al., Gliotoxin from *Aspergillus fumigatus* Abrogates Leukotriene B_4 Formation through Inhibition of Leukotriene A_4 Hydrolase, Cell Chemical Biology (2019), https://doi.org/10.1016/j.chembiol.2019.01.001

CellPress

(Sigma-Aldrich) column, washed with 50 mM phosphate buffer (PB) containing 1 mM EDTA and eluted with PB supplemented with 1 mM EDTA and 20 mM ATP. Isolated 5-LO was immediately used for activity assays together with isolated LTA_4H.

Human recombinant LTA_4H was expressed and purified according to Moser et al. (2015). In brief, LTA_4H was expressed in *E. coli* BL21(DE3)RIPL-Codon Plus cells (Invitrogen, Darmstadt, Germany) transformed with pET24(+)-LTA4H expression-plasmid. Cells were lysed and recombinant LTA_4H was purified by immobilized metal ion affinity chromatography (5 mL HisTrap HP column, GE Healthcare Life Science, Freiburg, Germany). LTA_4H was subsequently purified by size exclusion chromatography (Superdex200 column, GE Healthcare Life Science) with running buffer containing 50 mM Tris-HCl, 50 mM NaCl at pH 8. Pure protein was stored as glycerol stocks (20% (v/v) glycerol) at -80°C.

Determination of the Epoxide Hydrolase Activity of LTA_4H Activity from *In-Situ* Generated LTA_4

To assay the epoxide hydrolase activity of LTA_4H with *in situ* generated LTA_4, 0.5 μg purified 5-LO and 5 μg human recombinant LTA_4H were incubated with compounds or 0.1% (v/v) vehicle in 1 mL PBS containing 1 mM EDTA on ice. Samples were pre-warmed at 37°C for 30 sec, and 20 μM AA plus 2 mM $CaCl_2$ were added to start the reaction. After 10 min at 37°C, 1 mL ice-cold methanol was added and the formed lipid mediators were as analyzed by RP-HPLC as described above.

Determination of the Epoxide Hydrolase Activity of LTA_4H in a Cell-free Fluorescence-Based Assay

The epoxide hydrolase activity of recombinant LTA_4H using L-arginine-7-amido-4-methylcoumarine as substrate for both functionalities, the aminopeptidase and the epoxide hydrolase activity, was determined as described before (Wittmann et al., 2016) with some minor modifications. 10 μL of the premixes of assay buffer (50 mM Tris-HCl, 50 mM NaCl, pH 8) with or without $ZnCl_2$ (100 μM), GSH (5 mM) or GSSG (5 mM) were incubated with gliotoxin or vehicle (1%, v/v, DMSO) at 37°C for 2 hrs in a sealed black polystyrol 96 well plate (Greiner Bio-one, Frickenhausen, Germany). Then, isolated LTA_4H (145 nM) in assay buffer with Triton X-100 (0.01%, v/v) were added, and the plate was incubated at room temperature (RT) for 30 min. The reaction was started by the addition of 300 μM of non-fluorescent L-arginine-7-amido-4-methylcoumarine hydrochloride (Merck, Darmstadt, Germany) solution to a total volume of 100 μL. The change of the fluorescence intensity was measured (excitation at 370 nm and emission at 460 nm) for 60 min (one point per minute) at RT in a Tecan fluorescence plate reader (Infinite F200 pro). For the evaluation of the reaction, the slope in the linear phase was determined.

Analysis of Gliotoxin by UPLC-MS-MS

Samples from the cell-free LTA_4H assay were mixed with 79 μL acetonitrile instead of adding master mix. Analysis of gliotoxin was carried out on an Acquity UPLC with TUV detector (Waters, Eschborn, Germany) coupled to a single quadrupole mass detector (QDa, Waters). 2 μL of the sample were injected. Separation was achieved on a UPLC BEH C18 (1.7 μm, 2.1 × 50 mm) RP column (Waters) with a column temperature of 45°C. Acetonitrile and H_2O with 0.1% (v/v) formic acid were used as eluents following the gradient range from 5 to 95% in 5 min at a flow rate of 0.5 mL/min. Gliotoxin (m/z = 327.2) as well as its reduced dithiol form (m/z = 329.2) were analyzed in positive single ion mode $[M+H]^+$ using the Selected Ion Monitoring (SIM) approach. The obtained ion chromatograms were analyzed with Empower 3 software (Waters).

Determination of the Aminopeptidase Activity of LTA_4H

Neutrophils (5×10^6/mL in PG buffer) were pre-incubated with compounds or 0.1% (v/v) vehicle for 10 min at 37°C prior incubation with 1 μM Pro-Gly-Pro (PGP) and 0.1 μM N-acetyl-PGP (Cayman, Biomol, Hamburg, Germany) for 2 hrs at 37°C. The reaction was stopped on ice with 1.5 mL methanol and PGP was extracted in 60% (v/v) methanol after 1 hr at -20°C. N-acetyl-PGP (12 pmol) was used as internal standard. The extracted tripeptides were centrifuged at 2,000 rpm, 4°C for 10 min and applied to UPLC-MS-MS.

UPLC-MS-MS analysis of PGP was carried out on an Acquity UPLC BEH C_{18} column (1.7 μM, 2.1 × 100 mm) using an Acquity UPLC system (Waters). A linear gradient was used at a flow rate of 0.8 mL/min at 45°C from 100% mobile phase A (water, 0.07% (v/v) formic acid)/0% mobile phase B (acetonitrile, 0.07% (v/v) formic acid) to 60% mobile phase A/40% mobile phase B within 5 min. Quantification was performed by multiple reaction monitoring (MRM) in the positive ion mode using a QTRAP 5500 Mass Spectrometer (Sciex, Darmstadt, Germany). The ion spray voltage was set to 4500 V, the heated capillary temperature to 550°C, the curtain gas pressure to 35 psi, the sheath gas pressure to 50 psi, the auxiliary gas pressure to 80 psi, the declustering potential to 52 V, the entrance potential to 9 V, and the collision energy to 21 (PGP) and 27 V (acPGP). Under optimized ESI conditions, PGP $[M + H]^+$ ion, *m/z* 270.1, generated ions at *m/z* 173.1 and acPGP $[M + H]^+$ ion, *m/z* 312.3, generated ions at *m/z* 112 as its major product ions which were selected for quantification. Analyst software 1.6 was used for the processing of analytical data.

Determination of Cellular sEH Activity

To assay the activity of sEH in a cell-based assay, HepG2 or A549 cells were harvested and resuspended in PGC buffer (1.5×10^6 cells/mL). Cells were pre-incubated with test compounds or 0.1% (v/v) DMSO at 37°C for 15 min, and incubated with 1.5 μM 14,15-EET (Cayman Chemical/Biomol, Hamburg, Germany) for 30 min at 37°C. The reactions were stopped with one volume of ice-cold methanol, 1.31 ng d_8-5(S)-HETE and 1.36 ng d_4-LTB_4 (Cayman Chemical/Biomol) were added as internal standards, and samples were subjected to solid phase extraction on Waters Sep-Pak® Vac 6cc columns (Waters, Milford, MA, USA), washed once with water and *n*-hexane, and eluted with methylformiate (Werz et al., 2018). The nitrogen-dried samples were dissolved in 50% (v/v) methanol, and 14,15-DiHETrE formation was measured by UPLC-MS-MS using an Acquity UPLC system (Waters, Milford,

Please cite this article in press as: König et al., Gliotoxin from *Aspergillus fumigatus* Abrogates Leukotriene B_4 Formation through Inhibition of Leukotriene A_4 Hydrolase, Cell Chemical Biology (2019), https://doi.org/10.1016/j.chembiol.2019.01.001

MA, USA) and a QTRAP 5500 Mass Spectrometer (Sciex) equipped with a Turbo V™ Source and electrospray ionization (ESI) as reported previously (Garscha et al., 2017).

QUANTIFICATION AND STATISTICAL ANALYSIS

Results are presented as means ± SEM of *n* independent observations, where *n* represents the number of performed experiments at different days or with different donors/animals. Analyses of data were conducted using GraphPad Prism software (Graphpad Software Inc., San Diego, CA). IC_{50} values were determined by linear interpolation and validated with the GraphPad Instat program. Data fit was obtained using the sigmoidal concentration-response equation (variable slope) or the linear regression (GraphPad Prism software). Statistical evaluations were performed by one-way ANOVA followed by a Bonferroni post-hoc test for multiple or student t-test for single comparisons, respectively. P-values < 0.05 were considered as significant.

Supporting Information

Gliotoxin from *Aspergillus fumigatus* abrogates leukotriene B_4 formation through inhibition of leukotriene A_4 hydrolase

Stefanie König, Simona Pace, Helmut Pein, Thorsten Heinekamp, Jan Kramer, Erik Romp, Maria Straßburger, Fabiana Troisi, Anna Proschak, Jan Dworschak, Kirstin Scherlach, Antonietta Rossi, Lidia Sautebin, Jesper Z. Haeggström, Christian Hertweck, Axel A. Brakhage, Jana Gerstmeier, Ewgenij Proschak, and Oliver Werz

Content:

Supplemental Figures 1 and 2

Supplemental Figure 1

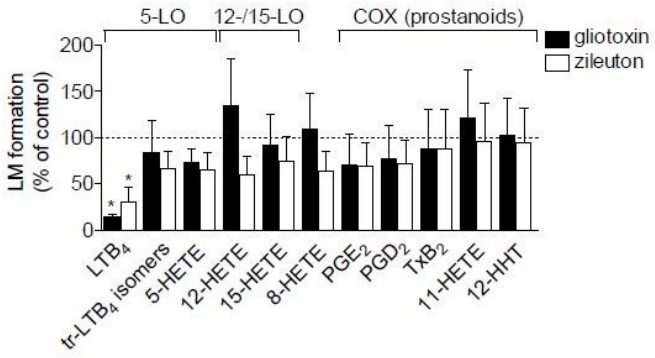

Fig. S1. Effects of gliotoxin and zileuton on circulating eicosanoid levels in rat plasma during carrageenan-induced pleurisy. Male rats (n = 6) were treated i.p. with 5 mg/kg gliotoxin, 10 mg/kg zileuton or vehicle (4% DMSO = 100%), 30 min before intrapleural injection of carrageenan. Circulating eicosanoids in the plasma were measured by UPLC-MS/MS. Data are means ± SEM, n = 6. *P < 0.05; **P < 0.01; ***P < 0.001 versus vehicle control (students t-test).

Supplemental Figure 2

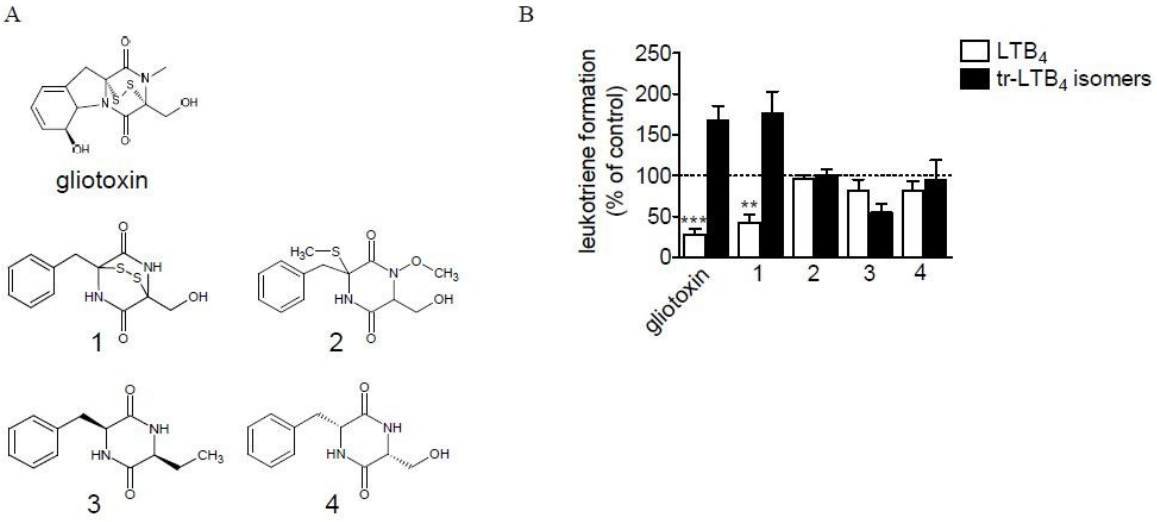

Fig. S2. Effect of gliotoxin and its derivatives on LTB_4 production in neutrophils. (A) Gliotoxin and structural derivatives synthesized or isolated from *Aspergillus fumigatus*. The synthesis or isolation of compounds **1 - 4** is described in a manuscript that is currently in preparation. (B) Effects of gliotoxin and its derivatives on LTB_4 and trans-LTB_4 isomers levels. Intact human neutrophils were pre-incubated with the test compounds for 10 min at 37 °C before stimulation with 2.5 µM A23187 for 10 min at 37 °C. Formed lipid mediators were analyzed by RP-HPLC. Data are means ± SEM; n = 3-4, duplicates. ***$p < 0.001$;**$p < 0.01$; inhibitor vs. vehicle control (100%), students t-test (gliotoxin), one way ANOVA + Bonferroni (cmpd. **1- 4**).

M-III: Myxochelins target human 5-lipoxygenase

JOURNAL OF NATURAL PRODUCTS

Note

pubs.acs.org/jnp

Myxochelins Target Human 5-Lipoxygenase

Sebastian Schieferdecker,[†] Stefanie König,[‡] Andreas Koeberle,[‡] Hans-Martin Dahse,[§] Oliver Werz,[‡] and Markus Nett*[,†]

[†]Junior Research Group Secondary Metabolism of Predatory Bacteria and [§]Department of Infection Biology, Leibniz Institute for Natural Product Research and Infection Biology, Hans Knöll Institute, Beutenbergstrasse 11a, 07745 Jena, Germany

[‡]Chair of Pharmaceutical and Medicinal Chemistry, Institute of Pharmacy, Friedrich-Schiller-University, Jena, Germany

Supporting Information

ABSTRACT: Extracts of the predatory myxobacterium *Pyxidicoccus fallax* HKI 727 showed antiproliferative effects on leukemic K-562 cells. Bioactivity-guided fractionation led to the isolation of the bis-catechol myxochelin A and two new congeners. The biosynthetic origin of myxochelins C and D was confirmed by feeding studies with isotopically labeled precursors. Pharmacological testing revealed human 5-lipoxygenase (5-LO) as a molecular target of the myxochelins. In particular, myxochelin A efficiently inhibited 5-LO activity with an IC_{50} of 1.9 μM and reduced the proliferation of K-562 cells at similar concentrations.

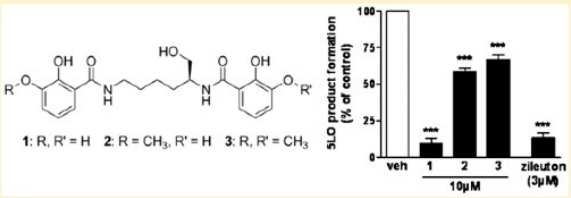

The myxobacteria are Gram-negative bacteria, which thrive in soil and in marine environments. They have been recognized as a rich source of antibiotics and anticancer agents.[1−3] Similar to other microbial producers of secondary metabolites, a single myxobacterium harbors the potential for the biosynthesis of multiple natural products.[4,5] The bioactive molecules that can be produced by a myxobacterium may foster its predatory lifestyle, facilitating the lysis of different prey organisms.[6,7] An illustrative example is *Pyxidicoccus fallax*, which secretes diverse macrolide antibiotics, including the gulmirecins and the disciformycins.[8,9] Although the activity spectrum of these molecules correlates quite well with the bacterial prey spectrum of *P. fallax*, it does not explain the observed predation of eukaryotic microorganisms. In consideration of the metabolic versatility of myxobacteria, we hence decided to expand the bioactivity testing of the gulmirecin-producing *P. fallax* strain HKI 727 and to search for compounds with antiproliferative or cytotoxic effects. This approach led to the isolation of three metabolites belonging to the myxochelin family (Figure 1).[10,11] The biosynthetic origin of the two new representatives myxochelin C (**2**) and myxochelin D (**3**) was verified in feeding studies with isotopically labeled L-methionine. Structural resemblance to the plant-derived natural product curcumin (**4**), which had previously been identified as an inhibitor of 5-lipoxygenase (5-LO),[12−14] suggested that the myxochelins might exert similar pharmacological effects. Here, we provide experimental evidence for this assumption.

Extracts of screening cultures from *P. fallax* HKI 727 grown in MD1 medium inhibited cell proliferation of K-562 cells. Since the activity could not be traced to the previously described gulmirecins,[8] the fermentation was repeated on a larger scale (30 L) in order to isolate and identify the active compound(s). The resulting culture broth was exhaustively extracted with ethyl acetate after the cell biomass had been removed by filtration. A preliminary fractionation was accomplished by ODS flash chromatography using increasing concentrations of methanol in water as eluant. All fractions were tested for their antiproliferative properties on K-562 cells, and the active ones were combined and subjected to HPLC separation. Final purification was achieved on a reversed-phase HPLC column, yielding 4.2 mg of **1**, 2.7 mg of **2**, and 2.1 mg of **3**.

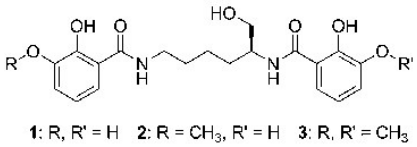

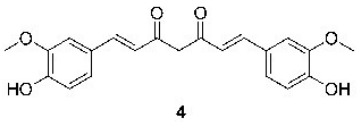

4

Figure 1. Structures of myxochelin A (**1**), myxochelin C (**2**), myxochelin D (**3**), and curcumin (**4**).

The isolated compound **1** was identified as the known natural product myxochelin A by comparison of its spectroscopic data with literature values.[15] Compound **2**, which eluted after **1** from the reversed-phase HPLC column, possessed almost identical NMR spectra. A unique singlet at 3.86 ppm in the ^{1}H NMR spectrum together with an additional carbon signal at 56.7 ppm suggested that an aromatic hydroxy

Received: November 14, 2014
Published: February 16, 2015

ACS Publications © 2015 American Chemical Society and American Society of Pharmacognosy

DOI: 10.1021/np500909b
J. Nat. Prod. 2015, 78, 335−338

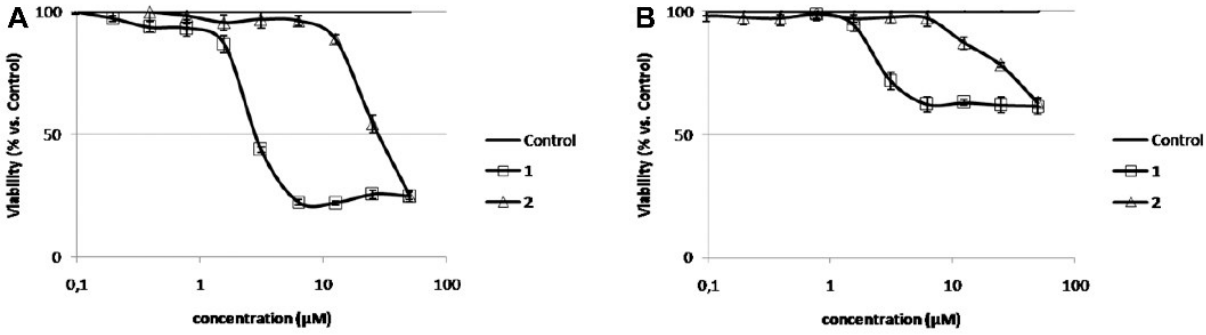

Figure 2. Inhibitory effects of **1** and **2** on K-562 (A) and HeLa cells (B).

of myxochelin A is replaced by a methoxy group in **2**. Consistent with this assumption, a molecular formula of $C_{21}H_{26}N_2O_7$ was deduced for **2** by HRESIMS. The exact position of the methoxy group could be assigned by HMBC measurement, thereby establishing the planar structure of myxochelin C. The remaining compound **3** was retained even longer on the reversed-phase HPLC column than **2**. Its pseudomolecular ion peak at m/z 433.1968 $[M + H]^+$ indicated a mass increase by 28 Da in comparison to myxochelin A. Interpretation of the NMR data led to the identification of two methoxy groups, which were allocated on the basis of heteronuclear long-range correlations to give the gross structure of myxochelin D. The configuration of the single chiral centers in **2** and **3** was determined as *S* by comparison of their optical rotation with that of myxochelin A.[15]

The myxochelins are assumed to act as siderophores, securing the iron supply of the producing bacterium.[10] Since methoxylation of the catechol residues in myxochelin A was anticipated to interfere with the coordination properties, the isolated compounds were tested in the chrome azurol S assay.[16] The poor or absent color changes confirmed that **2** and **3** are much weaker ligands than myxochelin A (Figure S1), challenging a siderophore function for the former two molecules. To exclude an abiotic origin (e.g., from methanol as a result of the chromatographic workup conditions),[17] [*methyl*-^{13}C]-L-methionine was fed to a culture of *P. fallax* HKI 727 grown in MD1 medium. Subsequently, myxochelin C was isolated and the incorporation of label was analyzed by NMR spectroscopy. While a strong enrichment of the methoxy carbon was detected, the signals of the other carbons in **2** provided no indication of specific labeling (Figure S2). This result strongly supported a biosynthetic origin for the methoxy groups in myxochelins C and D.

All isolated myxochelins were evaluated against K-562 and HeLa cells for their inhibitory effects. While myxochelin A and **2** reduced the proliferation of K-562 cells in the micromolar range in a concentration-dependent manner, **3** exerted only negligible effects on the human leukemic cell line (data not shown). In contrast, the effects on HeLa cells, which are epithelial cells from a human cervical carcinoma, were relatively weak (Figure 2). In the case of myxochelin A, the activity was significantly lower, with IC_{50} values of 305.2 μM compared to 3.9 μM for K-562 cells (Table 1). Although myxochelin A had previously been described as an antimetastatic agent and a series of synthetic analogues had been prepared for SAR studies,[15,18] the basis for its preferential activity against leukemic cells was not clear. Intrigued by the structural relatedness to curcumin (**4**), it appeared possible that curcumin

Table 1. IC_{50} Values of Myxochelins for the Inhibitory Effects on K-562 and HeLa Cells

	HeLa IC_{50} [μM]	K-562 IC_{50} [μM]
myxochelin A (**1**)	305.2 (±19.5)	3.9 (±0.1)
myxochelin C (**2**)	424.0 (±51.9)	53.5 (±5.8)
myxochelin D (**3**)	>500	>500

and myxochelin A share the same molecular targets. The anticarcinogenic properties of curcumin are due to an inhibition of 5-LO and microsomal prostaglandin E_2 synthase (mPGES)-1,[13,19] which not only are key enzymes for the progression of inflammatory processes but have also been associated with tumorigenesis.[20] The enzyme 5-LO was shown to be critically involved in chronic myeloid leukemia and was proposed to be a candidate target for therapeutic management of stem-cell-like cells in acute myeloid leukemia.[21,22] Similarly, mPGES-1 inhibitors were proposed to be promising candidates for leukemia treatment.[23] Therefore, inhibition of 5-LO and/or mPGES-1 could provide a plausible explanation for the marked antiproliferative effects of myxochelin A in K-562 cells, in particular since various 5-LO inhibitors were found to induce cell death of K-562 cells.[24] Subsequent testing in a cell-free assay confirmed that 5-LO is inhibited by myxochelin A. The natural product blocked 5-LO activity at 10 μM, comparable to the reference inhibitor zileuton at 3 μM (Figure 3A). More detailed analysis revealed concentration-dependent inhibition of 5-LO activity by myxochelin A with an IC_{50} of 1.9 μM (Figure 3B). For comparison, curcumin suppressed 5-LO activity in this cell-free assay with only slightly better efficiency, with an IC_{50} value of 0.5 μM.[13] The new myxochelins **2** and **3** were less active (IC_{50} > 10 μM) and reduced 5-LO activity at 10 μM by only 41 ± 4.1% and 33 ± 5.2%, respectively. Since 5-LO is a nonheme iron-dependent enzyme,[25] it is possible that the varying iron-binding capabilities of **1**−**3** account for the differences in 5-LO inhibition. As a matter of fact, many known 5-LO inhibitors act by chelation of ferrous iron in the enzyme's active site.[26] In contrast to curcumin and the synthetic reference inhibitor MK-886, compounds **1**−**3** failed to inhibit mPGES-1 activity up to 100 μM in a routine cell-free assay (data not shown).

In summary, myxochelin A was identified as a potent inhibitor of 5-LO. The bis-catechol natural product efficiently suppresses the proliferation of leukemic K-562 cells, whereas it has much less activity against HeLa cells. Increasing evidence suggests 5-LO is a key enzyme in myeloid leukemia.[21,22] Actually, several 5-LO inhibitors were found to induce cell death of K-562 cells but not of 5-LO-deficient HeLa cells.[24,27]

DOI: 10.1021/np500909b
J. Nat. Prod. 2015, 78, 335−338

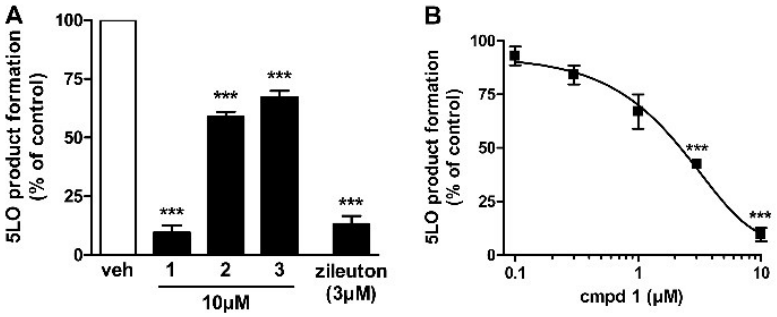

Figure 3. Effects of myxochelin A (**1**), myxochelin C (**2**), and myxochelin D (**3**) on 5-LO activity. (A) Myxochelins inhibit 5-LO. (B) Concentration−response curves of myxochelin A (**1**) for inhibition of 5-LO. Purified 5-LO (0.5 μg/mL) was incubated with the indicated test compounds at the indicated concentrations or with vehicle (DMSO, 0.1%; "veh") at 4 °C for 15 min. Samples were prewarmed for 30 s at 37 °C, 2 mM $CaCl_2$ and 20 μM arachidonic acid were added, and 5-LO product formation was determined after 10 min. Data are expressed as percentage of control (100%), means ± SE, n = 3−6, ***p < 0.001; ANOVA + Tukey HSD *post-hoc* tests.

Our findings support the assumed correlation between 5-LO inhibition and antileukemic activity, even though additional leukemia-associated targets cannot be excluded for myxochelin A. The two methylated derivatives **2** and **3** are much weaker 5-LO inhibitors than myxochelin A. At 10 μM neither compound showed significant 5-LO inhibition or antiproliferative effects against K-562 cells. At higher concentrations **2** reduced the growth of the leukemic cells, while **3** remained inactive. Therefore, the weak 5-LO inhibition of **2** or **3** seems to be irrelevant to their effect on K-562 cells. Unlike curcumin, the myxochelins do not target mPGES-1. This finding indicates discrete structural requirements for 5-LO and mPGES-1 inhibition and is consistent with previous investigations, in which a 1,3-diketone motif was proposed to be essential for affinity to mPGES-1.[13]

■ EXPERIMENTAL SECTION

General Experimental Procedures. Optical rotation was measured using a 0.5 dm cuvette with a JASCO P-1020 polarimeter at 25 °C. UV spectra were recorded on a Varian UV−visible Cary spectrophotometer. IR spectra were recorded on a Bruker FT-IR (IFS 55) spectrometer. High-resolution mass determination was carried out using an Exactive mass spectrometer (Thermo-Scientific). NMR spectra were measured at 300 K on a Bruker Avance III 500 MHz spectrometer with methanol-d_4 as solvent and internal standard. Preparative HPLC was conducted on a Shimadzu HPLC system (LC-20AT, SPD-M20A).

Production and Isolation of Myxochelins. Fermentation of *P. fallax* strain HKI 727 was carried out at 30 °C in 5 L Erlenmeyer flasks containing 3 L of MD1 medium, as previously described.[8] After 7 days of shaking at 130 rpm, the culture broth was exhaustively extracted with ethyl acetate. The organic layers were combined, and residual water was removed through the addition of anhydrous sodium sulfate (30 g/L) and filtration. Subsequently, the organic extract was concentrated to dryness under reduced pressure. The residue was suspended in a small amount of methanol and subjected to flash column chromatography using Polygoprep 60-50 C_{18} (Macherey-Nagel) as a stationary phase. Elution started with 20% methanol. The concentration of the organic solvent in the eluent was gradually increased up to 100%. All fractions that were obtained from this initial chromatographic separation were tested for their antiproliferative effects on K-562 cells. Active fractions were combined and further purified on a Nucleodur PFP column (250 × 10 mm, 5 μm; Macherey-Nagel) using a linear gradient of methanol in water (+0.1% trifluoroacetic acid). After a second round of bioactivity testing, the isolation of myxochelins was achieved on a Nucleodur C_{18} HTec column (250 × 10 mm, 5 μm; Macherey-Nagel) under isocratic conditions (70% methanol in water + 0.1% TFA) with a flow rate of 2 mL/min. The elution of compounds was detected by wavelength monitoring at 210 and 280 nm.

*Myxochelin C (**2**):* $[\alpha]^{25}_{D}$ −17.6 (*c* 0.75, MeOH); UV (MeOH) λ_{max} (log ε) 210 (4.70), 245 (4.30), 310 (3.70) nm; IR (film) ν_{max} 3360, 2935, 1637, 1586, 1543, 1458, 1343, 1250, 1075, 740 cm^{-1}; ^{1}H NMR (MeOD, 500 MHz) δ 7.32 (1H, dd, J = 8.2, 1.4 Hz, H-6″), 7.26 (1H, dd, J = 8.1, 1.4 Hz, H-6′), 7.06 (1H, dd, J = 8.0, 1.4 Hz, H-4″), 6.91 (1H, dd, J = 7.8, 1.4 Hz, H-4′), 6.81 (1H, t, J = 8.2, 8.0 Hz, H-5″), 6.69 (1H, t, J = 8.1, 7.8 Hz, H-5′), 4.16 (2H, m, H-2), 3.86 (3H, s, H-8″), 3.64 (1H, dd, J = 11.2, 5.3 Hz, H-1a), 3.61 (1H, dd, J = 11.2, 5.3 Hz, H-1b), 3.40 (2H, t, J = 7.0 Hz, H-6), 1.74 (1H, m, H-3a), 1.68 (2H, m, H-5), 1.63 (1H, m, H-3b), 1.49 (2H, m, H-4); ^{13}C NMR (MeOD, 125 MHz) δ 171.4 (C, C-7′), 170.6 (C, C-7″), 150.5 (C, C-2″), 150.0 (C, C-2′), 149.8 (C, C-3″), 147.2 (C, C-3′), 120.5 (CH, C-6″), 119.7 (CH, C-5″), 119.6 (CH, C-5′), 119.5 (CH, C-4′), 119.0 (CH, C-6′), 117.6 (C, C-1″), 117.1 (C, C-1′), 116.0 (CH, C-4″), 65.0 (CH_2, C-1), 56.7 (CH_3, C-8″), 52.6 (CH, C-2), 40.3 (CH_2, C-6), 31.6 (CH_2, C-3), 30.3 (CH_2, C-5), 24.6 (CH_2, C-4); HRESIMS m/z 441.1632 (calcd for $C_{21}H_{26}O_7N_2Na$, 441.1638).

*Myxochelin D (**3**):* $[\alpha]^{25}_{D}$ −15.8 (*c* 0.82, MeOH); UV (MeOH) λ_{max} (log ε) 210 (4.71), 248 (4.20), 309 (3.80) nm; IR (film) ν_{max} 2930, 1636, 1586, 1541, 1461, 1361, 1248, 1056, 740 cm^{-1}; ^{1}H NMR (MeOD, 500 MHz) δ 7.41 (1H, dd, J = 8.1, 1.4 Hz, H-6′), 7.32 (1H, dd, J = 8.1, 1.4 Hz, H-6″), 7.07 (1H, dd, J = 8.1, 1.4 Hz, H-4′), 7.06 (1H, dd, J = 8.1, 1.4 Hz, H-4″), 6.83 (1H, t, J = 8.1 Hz, H-5′), 6.81 (1H, t, J = 8.1 Hz, H-5″), 4.15 (2H, m, H-2), 3.87 (3H, s, H-8′), 3.86 (3H, s, H-8″), 3.65 (1H, dd, J = 11.2, 5.2 Hz, H-1a), 3.62 (1H, dd, J = 11.2, 5.1 Hz, H-1b), 3.40 (2H, t, J = 7.0 Hz, H-6), 1.75 (1H, m, H-3a), 1.68 (2H, m, H-5), 1.64 (1H, m, H-3b), 1.50 (2 H, m, H-4); ^{13}C NMR (MeOD, 125 MHz) δ 170.6 (C, C-7″), 170.2 (C, C-7′), 150.6 (C, C-2″), 150.1 (C, C-2′), 149.8 (C, C-3″), 149.7 (C, C-3′), 121.1 (CH, C-6′), 120.5 (CH, C-6″), 119.7 (CH, C-5″), 119.7 (CH, C-5′), 118.1 (C, C-1′), 117.6 (C, C-1″), 116.0 (CH, C-4″), 116.0 (CH, C-4′), 64.9 (CH_2, C-1), 56.7 (CH_3, C-8″), 56.7 (CH_3, C-8′), 52.7 (CH, C-2), 40.4 (CH_2, C-6), 31.7 (CH_2, C-3), 30.3 (CH_2, C-5), 24.5 (CH_2 C-4); HRESIMS m/z 433.1968 (calcd for $C_{22}H_{29}O_7N_2$, 433.1975).

Isotope Incorporation into Myxochelin C. For the labeling study, *P. fallax* HKI 727 was grown in MD1 medium. The production culture (5 × 3 L of medium dispensed in 5 L Erlenmeyer flasks) was amended with a filter-sterilized aqueous solution of [*methyl*-^{13}C]-L-methionine to give a final concentration of 0.44 mM. Subsequently, the culture was shaken at 130 rpm and 30 °C for 7 days. Extraction and isolation of **2** were carried out as previously described. ^{13}C NMR spectra were recorded using the inverse-gated decoupling pulse sequence.

Biological Assays. Inhibitory effects were evaluated against K-562 (DSM ACC 10) and HeLa cells (DSM ACC 57), which had been grown in RPMI 1640 medium. The adherent cells were harvested

DOI: 10.1021/np500909b
J. Nat. Prod. 2015, 78, 335−338

during the logarithmic growth phase after soft trypsinization using 0.25% trypsin in phosphate-buffered saline (PBS) containing 0.02% EDTA. For each experiment, approximately 10 000 cells were seeded with 0.1 mL of culture medium per well of the 96-well microplates. Test substances and fractions were dissolved in methanol before being diluted in RPMI 1640. Incubation was then conducted in a humidified atmosphere at 37 °C and 5% CO_2 for 72 h. In the case of K-562 cells, the number of viable cells in every well was determined using the CellTiter-Blue assay.[28] The adherent HeLa cells were fixed by glutaraldehyde and stained with a 0.05% solution of methylene blue for 5 min. After gently washing, the stain was eluted with 0.2 mL of 0.33 N HCl in the wells. The optical densities were measured at 660 nm in a Sunrise microplate reader (TECAN).

Expression, Purification, and Activity Assay of Human Recombinant 5-LO. Human recombinant 5-LO was expressed in *E. coli* BL21 (DE3), which were transformed with pT3-5LO plasmid as reported.[29] Cells were lysed in 50 mM triethanolamine/HCl pH 8.0, 5 mM EDTA, soybean trypsin inhibitor (60 μg/mL), 1 mM phenylmethanesulfonyl fluoride, dithiothreitol (1 mM), and lysozyme (1 mg/mL) and then sonified (3 × 15 s). The homogenate was centrifuged at 10000*g* for 15 min, and the remaining supernatant at 40000*g* for 70 min at 4 °C. 5-LO in the supernatant was partially purified by affinity chromatography on an ATP-agarose column. Semipurified 5-LO was diluted in PBS containing EDTA (1 mM) plus freshly added ATP (1 mM). Samples were preincubated with the test compounds for 10 min at 4 °C and prewarmed for 30 s at 37 °C. 5-LO product formation was initiated by addition of 2 mM $CaCl_2$ and 20 μM arachidonic acid. After 10 min at 37 °C, the reaction was terminated by addition of 1 mL of ice-cold methanol. Formed 5-LO metabolites including all-*trans* isomers of LTB_4 and 5*S*-hydro(pero)xy-6-*trans*-8,11,14-*cis*-eicosatetraenoic acid (5-HETE) were analyzed by RP-HPLC as previously described.[30]

Cell-Free mPGES-1 Activity Assay. Preparations of A549 cells, induction of mPGES-1, and determination of mPGES-1 activity was performed exactly as described previously.[19]

■ ASSOCIATED CONTENT

Supporting Information

Chrome azurole S assay; HRESIMS, and ^{1}H and ^{13}C NMR spectra of myxochelins C and D. This material is available free of charge via the Internet at http://pubs.acs.org.

■ AUTHOR INFORMATION

Corresponding Author

*Tel: + 49 3641 5321297. Fax: +49 3641 5320811. E-mail: Markus.Nett@hki-jena.de.

Notes

The authors declare no competing financial interest.

■ ACKNOWLEDGMENTS

Financial support was provided by Deutsche Forschungsgemeinschaft (DFG) within the SFB1127: Chemical Mediators in Complex Biosystems and by the DFG-funded graduate school JSMC. We thank A. Perner and H. Heinecke (Hans-Knöll-Institute Jena, Department of Biomolecular Chemistry) for recording high-resolution mass and IR spectra, and K. Fischer for technical assistance with mPGES-1 activity studies.

■ REFERENCES

(1) Wenzel, S. C.; Müller, R. *Curr. Opin. Drug Discovery Dev.* **2009**, *12*, 220−230.
(2) Schäberle, T. F.; Lohr, F.; Schmitz, A.; König, G. M. *Nat. Prod. Rep.* **2014**, *31*, 953−972.
(3) Nett, M.; König, G. M. *Nat. Prod. Rep.* **2007**, *24*, 1245−1261.
(4) Nett, M. In *Progress in Chemistry of Organic Natural Products*; Kinghorn, D. A.; Falk, H.; Kobayashi, J., Eds.; Springer: Switzerland, 2014; Vol. *99*, pp 199−246.
(5) Wenzel, S. C.; Müller, R. *Nat. Prod. Rep.* **2009**, *26*, 1385−1407.
(6) Xiao, Y.; Wei, X.; Ebright, R.; Wall, D. *J. Bacteriol.* **2011**, *193*, 4626−4633.
(7) Schieferdecker, S.; Exner, T. E.; Gross, H.; Roth, M.; Nett, M. *J. Antibiot.* **2014**, *67*, 519−525.
(8) Schieferdecker, S.; König, S.; Weigel, C.; Dahse, H.-M.; Werz, O.; Nett, M. *Chem.—Eur. J.* **2014**, *20*, 15933−15940.
(9) Surup, F.; Viehrig, K.; Mohr, K. I.; Herrmann, J.; Jansen, R.; Müller, R. *Angew. Chem., Int. Ed.* **2014**, *53*, 13588−13591.
(10) Kunze, B.; Bedorf, N.; Kohl, W.; Höfle, G.; Reichenbach, H. *J. Antibiot.* **1989**, *42*, 14−17.
(11) Silakowski, B.; Kunze, B.; Nordsiek, G.; Blöcker, H.; Höfle, G.; Müller, R. *Eur. J. Biochem.* **2000**, *267*, 6476−6485.
(12) Hong, J.; Bose, M.; Ju, J.; Ryu, J.-H.; Chen, X.; Sang, S.; Lee, M.-J.; Yang, C. S. *Carcinogenesis* **2004**, *25*, 1671−1679.
(13) Koeberle, A.; Muñoz, E.; Appendino, G. B.; Minassi, A.; Pace, S.; Rossi, A.; Weinigel, C.; Barz, D.; Sautebin, L.; Caprioglio, D.; Collado, J. A.; Werz, O. *J. Med. Chem.* **2014**, *57*, 5638−5648.
(14) Werz, O. *Planta Med.* **2007**, *73*, 1331−1357.
(15) Miyanaga, S.; Obata, T.; Onaka, H.; Fujita, T.; Saito, N.; Sakurai, H.; Saiki, I.; Furumai, T.; Igarashi, Y. *J. Antibiot.* **2006**, *59*, 698−703.
(16) Schwyn, B.; Neilands, J. B. *Anal. Biochem.* **1987**, *160*, 47−56.
(17) Wijeratne, E. M. K.; Bashyal, B. P.; Gunatilaka, M. K.; Arnold, A. E.; Gunatilaka, A. A. L. *J. Nat. Prod.* **2010**, *73*, 1156−1159.
(18) Miyanaga, S.; Sakurai, H.; Saiki, I.; Onaka, H.; Igarashi, Y. *Bioorg. Med. Chem.* **2009**, *17*, 2724−2732.
(19) Koeberle, A.; Northoff, H.; Werz, O. *Mol. Cancer Ther.* **2009**, *8*, 2348−2355.
(20) Rådmark, O.; Samuelsson, B. *J. Int. Med.* **2010**, *268*, 5−14.
(21) Chen, Y.; Hu, Y.; Zhang, H.; Peng, C.; Li, S. *Nat. Genet.* **2009**, *41*, 783−792.
(22) Roos, J.; Oancea, C.; Heinssmann, M.; Khan, D.; Held, H.; Kahnt, A. S.; Capelo, R.; la Buscato, E.; Proschak, E.; Puccetti, E.; Steinhilber, D.; Fleming, I.; Maier, T. J.; Ruthardt, M. *Cancer Res.* **2014**, *18*, 5244−5255.
(23) Li, Y.; Yin, S.; Nie, D.; Xie, S.; Ma, L.; Wang, X.; Wu, Y.; Xiao, J. *Int. J. Hematol.* **2011**, *5*, 472−478.
(24) Ogmundsdóttir, H. M.; Zoëga, G. M.; Gissurarson, S. R.; Ingólfsdóttir, K. *J. Pharm. Pharmacol.* **1998**, *50*, 107−115.
(25) Gilbert, N. C.; Bartlett, S. G.; Waight, M. T.; Neau, D. B.; Boeglin, W. E.; Brash, A. R.; Newcomer, M. E. *Science* **2011**, *331*, 217−219.
(26) Ford-Hutchinson, A. W.; Gresser, M.; Young, R. N. *Annu. Rev. Biochem.* **1994**, *63*, 383−417.
(27) Hostanska, K.; Daum, G.; Saller, R. *Anticancer Res.* **2002**, *22*, 2853−2862.
(28) Krauth, F.; Dahse, H.-M.; Rüttinger, H.-H.; Frohberg, P. *Bioorg. Med. Chem.* **2010**, *18*, 1816−1821.
(29) Fischer, L.; Szellas, D.; Rådmark, O.; Steinhilber, D.; Werz, O. *FASEB J.* **2003**, *8*, 949−951.
(30) Werz, O.; Bürkert, E.; Samuelsson, B.; Rådmark, O.; Steinhilber, D. *Blood* **2002**, *3*, 1044−1052.

DOI: 10.1021/np500909b
J. Nat. Prod. 2015, 78, 335−338

M-IV: Melleolides induce rapid cell death in human primary monocytes and cancer cells

Bioorganic & Medicinal Chemistry 22 (2014) 3856–3861

Contents lists available at ScienceDirect

Bioorganic & Medicinal Chemistry

journal homepage: www.elsevier.com/locate/bmc

Melleolides induce rapid cell death in human primary monocytes and cancer cells

Markus Bohnert [a,†], Olga Scherer [b,†], Katja Wiechmann [b], Stefanie König [b], Hans-Martin Dahse [c], Dirk Hoffmeister [a,*], Oliver Werz [b,*]

[a] Department of Pharmaceutical Microbiology at the Hans-Knöll-Institute, Friedrich-Schiller-Universität Jena, Beutenbergstrasse 11a, 07745 Jena, Germany
[b] Chair of Pharmaceutical/Medicinal Chemistry, Institute of Pharmacy, Friedrich-Schiller-Universität Jena, Philosophenweg 14, 07743 Jena, Germany
[c] Department of Infection Biology, Leibniz Institute for Natural Product Research and Infection Biology—Hans-Knöll-Institute, Beutenbergstrasse 11a, 07745 Jena, Germany

ARTICLE INFO

Article history:
Received 26 April 2014
Revised 6 June 2014
Accepted 17 June 2014
Available online 25 June 2014

Keywords:
Natural products
Structure activity relationship
Monocytes
Cell death
Cytotoxicity

ABSTRACT

The melleolides are structurally unique and bioactive natural products of the basidiomycete genus *Armillaria*. Here, we report on cytotoxic effects of melleolides from *Armillaria mellea* towards non-transformed human primary monocytes and human cancer cell lines, respectively. In contrast to staurosporine or pretubulysin that are less cytotoxic for monocytes, the cytotoxic potency of the active melleolides in primary monocytes is comparable to that in cancer cells. The onset of the cytotoxic effects of melleolides was rapid (within <1 h), as compared to the apoptosis inducer staurosporine, the protein biosynthesis inhibitor cycloheximide, and the DNA transcription inhibitor actinomycin D (>5 h, each). Side-by-side comparison with the detergent triton X-100 and staurosporine in microscopic and flow cytometric analysis studies as well as analysis of the viability of mitochondria exclude cell lysis and apoptosis as relevant or primary mechanisms. Our results rather point to necrotic features of cell death mediated by an as yet elusive but rapid mechanism.

© 2014 Elsevier Ltd. All rights reserved.

1. Introduction

The melleolides, made by the basidiomycete genus *Armillaria* (honey mushrooms), are a structurally unique family of natural products as they combine orsellinic acid, or a derivative thereof, with a protoilludene-type secondary alcohol.[1,2] The melleolide backbone represents a metabolic hybrid, as both a sesquiterpene cyclase[3] and a polyketide synthase mediate biosynthesis, with the latter cross-linking the building blocks through esterification.[4] Some, but not all melleolides are regioselectively chlorinated at C-6′, as exemplified by arnamial **1** and its 6′-dechloro derivative **2**.

Initially, the melleolides were recognized as antimicrobially active compounds.[5,6] Subsequently, cytotoxic activity against human cancer cell lines was described for **1**[7] which showed an IC_{50} of 3.9 μM for Jurkat cells. First insight into the structure–activity relationship came from a subsequent study which included Jurkat, K-562, HeLa, and MCF-7 cancer cells.[8] The more hydrophilic compounds did not affect cell viability implying that primarily terpene hydroxylation at positions 10, 13, and 14 is critical for cytotoxicity. Consequently, dehydroarmillylorsellinate (**3**) which does not carry an alcohol functionality at any of these positions, was found to be active against K-562 cells (IC_{50} = 5.0 μM).

For antifungal activity, the double bond position ($\Delta^{2,4}$) of the sesquiterpene moiety of melleolides was shown to be critical for antifungal activity. An absent or shifted double bond ($\Delta^{2,3}$), like in armillarin (**4**), armillaridin (**5**), and melleolide D (**6**), leads to a loss of antifungal activity but does not impact cytotoxicity against human cells.[9]

In our present study we compared the cytotoxic activity of melleolides towards proliferating cancer cells and non-transformed primary monocytes. We hypothesized that monocytes would be less susceptible, due to their non-proliferating character and the fact that they are generally less sensitive to most cytotoxic/anti-proliferative agents, as compared to cancer cells. In fact, primary monocytes or peripheral blood mononuclear cells (i.e., monocytes and lymphocytes) are often utilized as models in order to demonstrate cancer cell selectivity of proposed anti-cancer agents. For example, we previously showed that induction of cell death of primary human monocytes by the microtubule-disrupting agent pretubulysin and the apoptosis inducer myrtucommulone required 20- to >100-fold higher concentrations, respectively, as compared to various cancer cell lines.[10,11] Conversely, agents that target specific cell receptors of leukocytes such as leukotoxin from

* Corresponding authors.
E-mail address: oliver.werz@uni-jena.de (O. Werz).
† Equal contribution.

http://dx.doi.org/10.1016/j.bmc.2014.06.032
0968-0896/© 2014 Elsevier Ltd. All rights reserved.

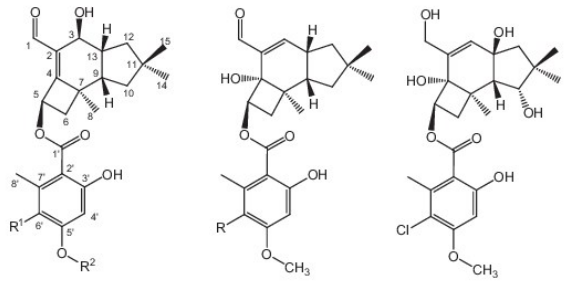

Figure 1. Structures of the melleolides **1**–**6** from *A. mellea*.

Aggregatibacter actinomycetemcomitans may cause selective cytotoxicity against leukocytes without affecting cancer cells.[12–14]

In the present study we screened a set of six melleolides (Fig. 1) with (**1**–**3**) or without (**4**–**6**) antifungal activity for their cytotoxic effects on primary monocytes from human whole blood. Consistent with our previous results for cancer cell lines,[8] we found that the α,β-unsaturated aldehyde and absence of hydroxy groups at the cyclopentene primarily correlated with potent cytotoxic properties towards various cancer cells, but also against primary monocytes.

Intriguingly, we observed an unusually rapid onset of cell death (<1–2 h) for the cytotoxic melleolides, which has not been reported for other well-recognized cytotoxic agents such as staurosporine, cycloheximide, or actinomycin D. Our data suggest a unique mode of action of melleolides regarding their cytotoxicity that warrants further attempts to identify the respective molecular target(s) in future studies.

2. Results and discussion

2.1. Structure–activity relationship of melleolides for induction of cell death

A set of six previously described melleolides (**1**–**6**, Fig. 1)[8,9] was analyzed for cytotoxicity properties against freshly isolated human primary monocytes and a set of cancer cells (i.e., THP-1, Mono Mac 6 (MM6), K-562 and HeLa cells). Employing the MTT (3-(4,5-dimethylthiazol-2-yl)-2,5-diphenyltetrazolium bromide) assay, we determined the lowest EC_{50} of 2.3 μM for **3** regarding the loss of monocyte viability, which is comparable or even lower than the EC_{50} values (1.6–5.0 μM) analyzed for transformed cancer cell lines in this respect (Table 1). Similar results were obtained for **1** and **2**, which share the important structural feature for anti-fungal activity, that is, the $\Delta^{2,4}$-double bond. Melleolides **4** and **5**, which are characterized by a $\Delta^{2,3}$ double bond, were equally active against THP-1 and MM6 cells (EC_{50} values between 4.5 and 6.6 μM), but exerted lower cytotoxic effects against monocytes, HeLa, and K-562 cells (8.9–43.2 μM). Melleolide D (**6**), which features a hydroxy group at C-1, instead of the aldehyde, is essentially inactive (Table 1, Fig. 2A).

The high cytotoxic potential of selected melleolides observed in primary monocytes was also evident in the human leukemia cell lines THP-1 and MM6, implying the presence of a common cellular target in primary monocytes and cancer cells as being responsible for the cytotoxic effects.

Next, we verified the induction of monocytic cell death by measuring LDH levels as marker for loss of membrane integrity in melleolide-treated supernatants. As shown in Figure 2B, marked cytotoxic effects of **3** with the $\Delta^{2,4}$-double bond, but not for the antifungally inactive **6** with its tetrahydroxylated sesquiterpene moiety were evident; staurosporine and triton X-100 were used as reference controls that caused LDH release, as expected.

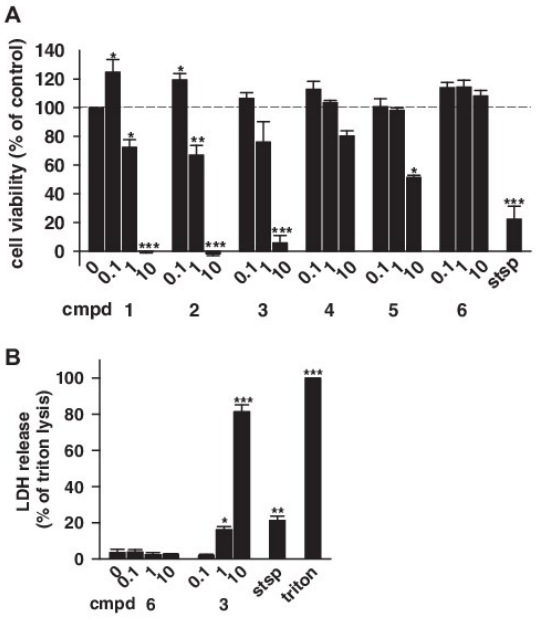

Figure 2. Reduction of monocyte viability by melleolides. (A) Monocytes were incubated with melleolides **1**–**6** at the indicated concentrations (μM) or staurosporine (stsp, 3 μM). Cell viability was analyzed by the MTT assay after 24 h. (B) Monocytes were treated with melleolides **3** and **6** at the indicated concentrations (μM), staurosporine (stsp, 3 μM), and triton X-100 (0.2%), respectively. After 4 h the release of LDH was analyzed. Data are given as mean + SE, $n = 3$. $^{*}p < 0.05$, $^{**}p < 0.01$, $^{***}p < 0.001$ versus vehicle control; ANOVA + Bonferroni.

Table 1
Cytotoxic effects of melleolides

Compd	THP-1 EC_{50} (μM)	MM6 EC_{50} (μM)	monoc. EC_{50} (μM)	K-562 EC_{50} (μM)	HeLa EC_{50} (μM)	
1	2.9 (±0.4)	3.2 (±0.4)	3.8 (±0.5)	2.3 (±0.3)	4.9 (±0.2)	$\Delta^{2,4}$-Double bond
2	2.4 (±0.7)	2.9 (±0.7)	3.1 (±0.7)	4.1 (±0.1)	12.3 (±0.3)	
3	3.0 (±0.5)	4.2 (±1.9)	2.3 (±0.4)	5.0 (±0.3)	1.6 (±0.1)	
4	4.8 (±0.5)	6.6 (±0.7)	43.2 (±2.4)	23.7 (±1.5)	16.7 (±2.1)	$\Delta^{2,3}$-Double bond
5	4.5 (±0.1)	5.6 (±0.3)	12.3 (±2.2)	8.9 (±1.3)	9.2 (±1.7)	
6	>100	48.6 (±1.0)	60.7 (±0.7)	>100	>100	

EC_{50} values for induction of cell death of THP-1, Mono Mac 6 (MM6), monocytes (monoc.), K-562, and HeLa cells within 24 h. Data are given as mean ± SE, $n = 3$.

In contrast to the melleolide **3** that was about equally potent against monocytes and HeLa cells, the multiple protein kinase inhibitor staurosporine was much more potent in cancer cells (HeLa) as compared to primary monocytes (Fig. 3). Similarly, the microtubule disrupting agent pretubulysin, a highly cytotoxic myxobacterial compound against cancer cells[15] also failed to reduce the viability of primary monocytes up to 1 μM but clearly caused cell death of transformed MM6 cells (EC_{50} = 0.03 μM, Fig. 3). As outlined above, such reduced susceptibility of primary monocytes towards cell death induction is usually the case with (potential) anti-cancer agents, for example, myrtucommulone, hyperforin, boswellic acids, and others.

2.2. Rapid onset of cytotoxicity by melleolides

We performed time-course experiments in order to investigate the timing of the cell death. In parallel to the melleolide **3** we analyzed (I) staurosporine, a well-recognized inducer of the mitochondrial pathway of apoptosis,[16] (II) cycloheximide, an inhibitor of protein biosynthesis, and (III) actinomycin D, an inhibitor of DNA transcription, which all are known to be cytotoxic for cancer cells.[17]

To assess the rapid onset of cell death by **3** (<5 h) more accurately, the MTT assay was modified. In fact, the first significant reduction of cell viability (approx. 40%) was observed 2 h after exposure to compound **3** in monocytes and HeLa cells (Fig. 4). None of the other agents caused a comparably rapid onset of cell

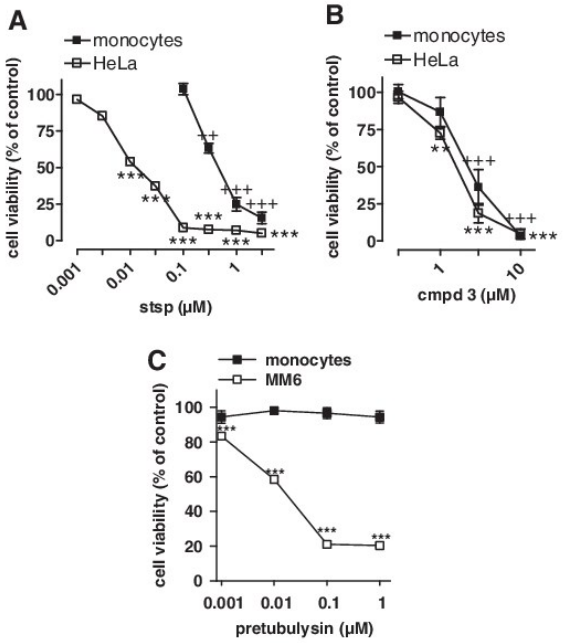

Figure 3. Effects of staurosporine (A), melleolide **3** (B), and pretubulysin (C) on primary monocytes and transformed HeLa or MM6 cells. Monocytes, HeLa or MM6 cells were treated with staurosporine, compound **3** or pretubulysin at the indicated concentrations. Cell viability was analyzed by the MTT assay after 24 h. Data are given as mean ± SE, $n = 3$. $^{**}p$ <0.01, $^{***}p$ <0.001 versus vehicle control; ANOVA + Bonferroni.

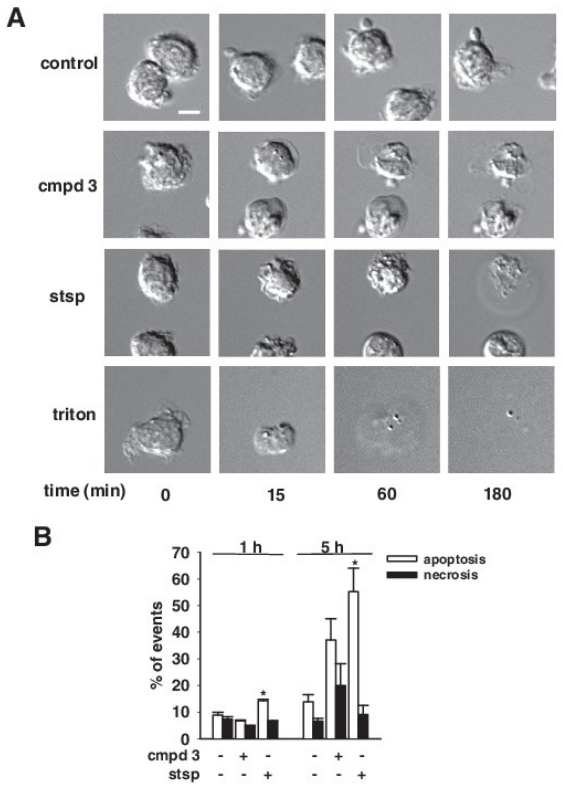

Figure 5. (A) Morphological analysis of monocytes. Cells were treated with the given agents (5 μM compound **3**, 3 μM staurosporine, 0.2% triton X-100) for the indicated periods of time, and analyzed by light microscopy. Pictures shown are representatives out of three independent experiments. (B) Flow cytometric analysis of PE Annexin V and 7-amino-actinomycin staining for apoptotic and necrotic cells, respectively. Data are means + SE, $n = 3$–4. $^{*}p$ <0.05, versus vehicle control; ANOVA + Bonferroni.

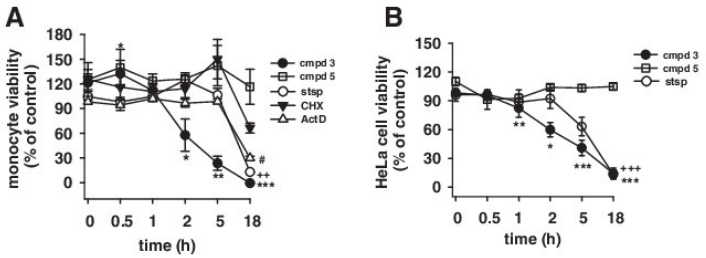

Figure 4. Time course of cell death induction in (A) primary monocytes and (B) HeLa cells. Cells were treated with compounds **3** and **5** (5 μM each), staurosporine (3 μM), cycloheximide (CHX, 25 μM), actinomycin D (Act D, 1 μM) or vehicle (0.3% DMSO) for the indicated times and cell viability was analyzed by the inverse MTT assay. Data are means ± SE, $n = 3$. $^{*}p$ <0.05, $^{**}p$ <0.01, $^{***}p$ <0.001 versus vehicle control; ANOVA + Bonferroni.

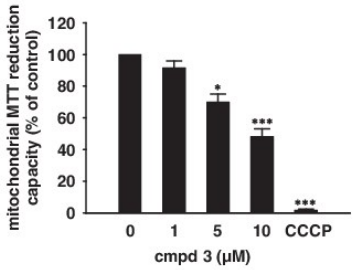

Figure 6. Effects of melleolide **3** on the viability of mitochondria. Mitochondria, isolated from MM6 cells, were treated with compound **3**, carbonyl cyanide 3-chlorophenyl-hydrazone (CCCP 10 μM), or 0.3% DMSO (vehicle control) for 3 h at 4 °C. MTT solution was added and after blue staining of the vehicle control, formazan formation was stopped and were analyzed. Data are given as means + SE; $n = 3$; $^{*}p < 0.05$, $^{***}p < 0.001$ versus vehicle control, ANOVA + Bonferroni.

death. A significant effect of staurosporine (3 μM) was observed after about 18 h. Similarly, CHX (25 μM) and actinomycin reduced cell viability only after 18, but not after 5 h of monocyte exposure (Fig. 4A).

2.3. Effects of melleolide on cell morphology and mitochondrial functionality

The rapid onset of cell death induction by **3** suggested that the melleolides may cause cell lysis. Within 1–3 h, morphological analysis of primary monocytes by light microscopy revealed typical features of necrosis after treatment with **3**. Thus, after 15 min cells started to form blebs devoid of organelles. Marked effects were observed after 1 h. After 3 h the plasma membrane was ruptured (Fig. 5). In contrast, after 3 h staurosporine caused signs of apoptosis, i.e., fragmentation of the nucleus and formation of apoptotic bodies. Also, a different pattern was evident for monocytes treated with the detergent triton X-100 that rapidly permeabilized the cells with subsequent structural collapse (Fig. 5).

Based on the comparative morphological analysis, our data suggest that **3**, unlike triton X-100, does not permeabilize monocytes, and unlike staurosporine, does not induce apoptosis, but instead may eventually cause necrosis. Attempts to study induction of necrosis and apoptosis of monocytes by **3** using flow cytometric analysis and PE Annexin V and 7-amino-actinomycin (7-AAD) staining revealed a tendency towards necrosis (i.e., 7-AAD positive) but also some apoptotic features (i.e., PE Annexin V positive) were evident, without reaching statistical significances, whereas staurosporine clearly caused apoptosis without any significant increased necrosis pattern (Fig. 5B).

Finally, we also investigated whether mitochondria are affected by the melleolide **3** by analysis of their metabolic activity using the MTT assay. Incubation of isolated mitochondria with **3** (up to 10 μM) caused about 50% reduction of metabolic activity, while carbonyl cyanide 3-chlorophenyl-hydrazone (CCCP), used as a control that abolishes mitochondrial membrane potential, completely reduced mitochondrial activity, as expected (Fig. 6).

3. Conclusion

We showed that cytotoxic melleolides rapidly induce cell death in human primary monocytes and transformed cells by a yet undefined destructive mechanism. Intriguingly, in contrast to other cytotoxic agents such as staurosporine, pretubulysin or myrtucommulone,[10,11,16] the melleolides seemingly affect non-transformed cells equally well as hyperproliferative cancer cells. Therefore, our findings may be relevant in view of the function of melleolides as molecular probes for yet unknown target(s), rather than as potential drug leads. Moreover, in contrast to other cytotoxic agents, induction of cell death by **3** is rapid, and our data do not support apoptotic or lytic effects by **3** as primary mode of cell death. Some indications (morphological pattern and 7-AAD staining) point to necrotic features. Therefore, and as isolated mitochondria were hardly affected by **3** in the MTT assay, we suggest that modulation of a specific target protein on the plasma membrane might be responsible for cell death induction by bioactive melleolides. Notably, the vicinally unsaturated aldehyde function could readily react with the SH-group of cysteines within active sites of proteins. Thus, multiple targets might be addressed by the reactive aldehydes. Contrasting the melleolides' potent bioactivity, the fruiting bodies of *Armillaria* species are considered edible mushrooms which are traditionally used for nutrition. This is consistent with our own observations that fruiting bodies contain melleolides only in traces, if at all, whereas all published work describes that melleolides were isolated from cultures of undifferentiated asexual mycelium.

4. Experimental section

4.1. General and microbiological procedures

Seed cultures of *Armillaria mellea* FR-P 75[7] were routinely grown in potato dextrose broth shaken at 24 °C and 120 rpm in the dark, for 18–20 days. The mycelium was homogenized using an Ultraturrax disperser prior to inoculation of the production culture. For melleolide production glucose minimal medium[18] was used. The total culture volume was 12 L, dispensed into 2 L Erlenmeyer flasks. The fungus was incubated for about four weeks, at 25 °C and 120 rpm. Chemicals, solvents, and media components were purchased from Roth, Sigma–Aldrich, and VWR.

4.2. Isolation of melleolides

To procure melleolides from liquid fungal cultures, the biomass was separated from the broth and extracted three times with an equal volume of a cyclohexane ethyl acetate (3:1, v/v) mixture. The extract was dried over Na_2SO_4 and then successively concentrated under reduced pressure using a rotary evaporator. Subsequent lyophilization yielded a greyish amorphous powder. Small aliquots were dissolved in methanol for initial preparative HPLC (method I, below) which resulted in nine fractions. Fractions six and seven were identified as pure compounds **4** and **5**, respectively. Three fractions were rechromatographed using methods II, III and IV which resulted in pure melleolides **1**, **2** and **3**, respectively. To analyze extracts and purification steps by HPLC and LC–MS, analytical methods V and VI were applied. Melleolide D (**6**) was isolated as described previously.[8] The isolation yields were: **1**, 6 mg/L; **2**, 0.6 mg/L, **3**, 5 mg/L; **4** and **5**, 1 mg/L; **6**, 2 mg/L.

For preparative HPLC an Agilent 1260 series instrument equipped with a Phenomenex Luna C18 column (250 × 21.2 mm, 10 μm particle size) was used. Analytical HPLC was run on an Agilent 1200 instrument with a Zorbax Eclipse XDB C-18 column 150 × 4.6 mm, 3.5 μm particle size. For LC–MS runs an Agilent 1100 instrument with a Zorbax Eclipse XDB C-8 column (150 × 4.6 mm, 5 μm particle size) fitted to a 1100 MSD Trap was used. All chromatograms were recorded at $\lambda = 254$ nm, the respective diode array detectors covered the wavelength range from $\lambda = 190$–700 nm. The preparative methods (I–IV) used water (A) and 83% acetonitrile in water (B) as solvents, the flow rate was 21.0 mL/min.

Method I (gradient): 50% B, held for 1 min, then linear increase to 85% within 2 min and within 10.5 min to 100% B.

Method II (gradient): 80% B, held for 1 min, then increased to 100% B within 19 min.

Method III (gradient): solvent B increased from 85% to 100% B within 10 min.

Method IV (gradient): 45% B, held for 1 min, followed by a linear increase to 83% within 4 min. Then, B was increased to 95% within 8 min.

Method V: Solvents were water (A) and acetonitrile (B). The gradient was 2 min held at 15% B, then linear increase to 95% B within 31 min, at a flow of 0.6 mL/min.

Method VI: Solvents were 0.1% (v/v) formic acid in water (A) and 0.1% (v/v) formic acid in MeOH (B). The gradient was 10% B, held for 30 s, followed by a linear increase to 90% B within 14.5 min, and held at 90% B for 2 min, at a flow of 1 mL/min.

4.3. Isolation of primary monocytes and cell lines

Leukocyte concentrates were obtained from the Institute of Transfusion Medicine at the University Hospital Jena, Germany. The concentrates were prepared from the blood of healthy adult human donors who had not taken any anti-inflammatory medication for the 10 days prior to blood donation, as described.[19] In brief, freshly withdrawn peripheral blood was pretreated with citrate-phosphate-dextrose solution as anticoagulant and processed with the 2C+ protocol of the Atreus Whole Blood Processing System (Terum BCT, Lakewood, CO). Peripheral blood mononuclear cells (PBMC) were isolated by dextran sedimentation and centrifugation on LSM 1077 lymphocyte separation medium (PAA Laboratories, Pasching, Austria). For isolation of monocytes, the PBMC were washed twice with ice-cold phosphate-buffered saline (PBS) and plated (density 2×10^7 cells/ml) in culture flasks (Greiner Bio-One, Frickenhausen, Germany) containing PBMC medium (RPMI 1640 medium supplemented with 100 U/ml penicillin, 100 μg/ml streptomycin and 2 mM L-glutamine) for 1.5 h at 37 °C, 5% CO_2. Non-adherent cells were removed; adherent monocytes were scraped, washed with ice-cold PBS and resuspended in ice-cold PBS with a purity of >85%, defined by forward- and side-light scatter properties and detection of the CD14 surface molecule by flow cytometry (BD FACS Calibur, Heidelberg, Germany). Monocytes were cultured in monocyte medium (RPMI 1640 supplemented with 2% human serum, L-glutamine (2 mM), penicillin (100 U/ml), and streptomycin (100 μg/ml)).

The human monocytic cell line MM6 (kindly provided by Dr. Thorsten Maier, University of Frankfurt, Germany) was cultured in RPMI 1640 medium supplemented with heat-inactivated fetal calf serum (FCS, 10%, v/v), penicillin (100 U/ml), streptomycin (100 μg/ml), insulin (10 μg/ml), oxaloacetic acid (1 mM), sodium pyruvate (1 mM), and 1 × non-essential amino acids at 37 °C and 5% CO_2. HeLa cells were cultured in Dulbecco's Modified Eagle's Medium (DMEM) supplemented with heat-inactivated FCS (10%, v/v), penicillin (100 U/ml), and streptomycin (100 μg/ml) at 37 °C and 5% CO_2. THP-1 and K-562 cells were cultured in RPMI 1640 medium supplemented with heat-inactivated FCS (10%, v/v), 2 mM L-glutamine, penicillin (100 U/ml), and streptomycin (100 μg/ml) at 37 °C and 5% CO_2.

4.4. MTT assay

Cells (3×10^4 MM6, THP-1, and K-562, 1×10^4 HeLa, or 2×10^5 monocytes per well) were seeded in a 96-well plate in the respective medium (100 μl/well). Monocytes were allowed to adhere for 1.5 h (37 °C, 5% CO_2) prior to treatment. Test compounds (0.3% DMSO as vehicle) were added to each well and samples were incubated for the indicated time. Then, 20 μl of thiazolyl blue tetrazolium bromide (MTT, 5 mg/ml PBS) were added, and the incubation was continued at 37 °C, 5% CO_2 until blue staining of the vehicle control. Formazan formation was stopped by adding 100 μl of lysis buffer (SDS, 10%, w/v in 20 mM HCl) and samples were shaken overnight. Absorbance of each well was measured at 570 nm in a Multiskan™ microplate spectrophotometer (Thermo Scientific, Ulm, Germany).

4.5. Inverse MTT assay

Cells were seeded in a 96-well plate (10^4 (HeLa) or 2×10^5 cells (monocytes) per well) in the respective medium (100 μl/well). HeLa cells were allowed to adhere for 24 h, monocytes for 1.5 h (37 °C, 5% CO_2). 20 μl of MTT (5 mg/ml PBS) were added 2 h prior to cell lysis. In contrast to the conventional MTT assay, test compounds (0.3% DMSO as vehicle) were added at the indicated time points prior to cell lysis to avoid a prolonged exposure time during incubation with MTT. Termination of formazan formation, as well as sample analysis, was performed as described in 4.4.

4.6. LDH release assay

Monocytes (1.5×10^6/ml) were resuspended in monocyte medium and seeded into 96-well plates (duplicates). Cells were incubated for 1.5 h, 37 °C and 5% CO_2 for adhesion. Subsequently, compounds, vehicle (DMSO) or 0.2% triton X-100 as lysis control were added. After 4 h at 37 °C and 5% CO_2, cells were removed by centrifugation (600g, 4 °C) and the resulting supernatant was pipetted into a 96-well plate. Reaction buffer (containing, 0.3 mM NADH and 1.5 mM sodium pyruvate in 75 mM Tris/HCl, pH 7.4) was added and absorbance of NADH was immediately measured at 340 nm, 25 °C.

4.7. Life cell imaging

Monocytes (2.5×10^5/ml) were plated into glass bottom dishes (MatTek Corporation, MA) containing RPMI 1640 supplemented with FCS (10%, v/v), 100 U/ml penicillin, 100 μg/ml streptomycin and 2 mM L-glutamine. Cells were allowed to adhere for 1.5 h at 37 °C and 5% CO_2. Then, cells were washed with pre-warmed PBS and PBS plus 0.1% (w/v) glucose, 1 mM $CaCl_2$, and 1 mM $MgCl_2$ was added. Compounds were added and images of the monocytes were taken after indicated times using an AxioCam MR3 camera (Zeiss, Jena, Germany) and were acquired, cut, linearly adjusted in the overall brightness and contrast, and exported to TIF by the AxioVision 4.8 software. The microscope incubator (Axio Observer Z1 inverted microscope, LCI Plan-Neofluar 63x/1.3 Imm Corr DIC M27 objective, Carl Zeiss, Jena, Germany) was kept at 37 °C and 5% CO_2.

4.8. Determination of mitochondrial MTT reduction capacity

MM6 cells were washed in PBS (450 × g, 10 min, 4 °C), resuspended in ice-cold isolation buffer[19] and homogenized on ice with 4 × 10 strokes in a dounce homogenizer. Disrupted cells were centrifuged (750g, 20 min, 4 °C) and the resulting supernatant containing mitochondria was spun down (10,000 × g, 15 min, 4 °C). Pelleted mitochondria were washed in ice-cold isolation buffer (10,000 × g, 15 min, 4 °C) and resuspended in ice-cold respiratory buffer.[20] Mitochondrial protein concentration was determined using the DC Protein Assay (Bio-Rad, Munich, Germany). Mitochondria (2.5 μg/μl, 100 μl/sample) were exposed to the test compounds (0.3% DMSO as vehicle) for 1 h at 4 °C. Then, 20 μl of MTT (5 mg/ml PBS) were added and mitochondria were incubated at 30 °C until blue staining of the vehicle control. Further steps were performed as described in 4.4.

4.9. Flow cytometric analysis of PE Annexin V and 7-amino-actinomycin staining

Monocytes (1.0×10^6/ml) were isolated and cultured in monocyte medium overnight. Then, cells were incubated with the test compounds for 1 or 5 h, respectively. After detachment with Accutase I (PAA Laboratories, Pasching, Austria), monocytes were stained with phycoerythrin (PE)-conjugated Annexin V and the intercalator 7-amino-actinomycin (7-AAD). For staining, the Annexin V PE apoptosis detection Kit I (BD Biosciences) was used according to manufacturer instructions. Flow cytometric analysis was performed on Attune Acoustic Focusing Cytometer (Life Technologies).

Acknowledgments

M.B. and S.K. gratefully acknowledge doctoral fellowships by the Excellence Graduate School Jena School for Microbial Communication (JSMC). We thank Katrin Schubert and Marius Melzer (Friedrich-Schiller-University Jena) and Andrea Perner (Hans-Knöll-Institute Jena) for expert technical assistance and recording mass spectra, respectively. This study was also supported by the Deutsche Forschungsgemeinschaft (DFG) FOR1406, WE 2260/11-1.

References and notes

1. Arnone, A.; Cardillo, R.; Nasini, G. *Phytochemistry* **1986**, *25*, 471.
2. Midland, S. L.; Izac, R. R.; Wing, R. M.; Zaki, A. I.; Munnecke, D. E.; Sims, J. J. *Tetrahedron Lett.* **1982**, *23*, 2515.
3. Engels, B.; Heinig, U.; Grothe, T.; Stadler, M.; Jennewein, S. *J. Biol. Chem.* **2011**, *286*, 6871.
4. Lackner, G.; Bohnert, M.; Wick, J.; Hoffmeister, D. *Chem. Biol.* **2013**, *20*, 1101.
5. Donnelly, D.; Sanada, S.; Oreilly, J.; Polonsky, J.; Prange, T.; Pascard, C. *J. Chem. Soc., Chem. Commun.* **1982**, 135.
6. Momose, I.; Sekizawa, R.; Hosokawa, N.; Iinuma, H.; Matsui, S.; Nakamura, H.; Naganawa, H.; Hamada, M.; Takeuchi, T. *J. Antibiot.* **2000**, *53*, 137.
7. Misiek, M.; Williams, J.; Schmich, K.; Huttel, W.; Merfort, I.; Salomon, C. E.; Aldrich, C. C.; Hoffmeister, D. *J. Nat. Prod.* **2009**, *72*, 1888.
8. Bohnert, M.; Miethbauer, S.; Dahse, H. M.; Ziemen, J.; Nett, M.; Hoffmeister, D. *Bioorg. Med. Chem. Lett.* **2011**, *21*, 2003.
9. Bohnert, M.; Nützmann, H.-W.; Schroeckh, V.; Horn, F.; Dahse, H.-M.; Brakhage, A.A.; Hoffmeister, D. *Phytochemistry*. **2014**, in press; http://dx.doi.org/10.1016/j.phytochem.2014.05.009.
10. Kubisch, R.; von Gamm, M.; Braig, S.; Ullrich, A.; Burkhart, J. L.; Colling, L.; Hermann, J.; Scherer, O.; Muller, R.; Werz, O.; Kazmaier, U.; Vollmar, A. M. *J. Nat. Prod.* **2014**, *77*, 536.
11. Tretiakova, I.; Blaesius, D.; Maxia, L.; Wesselborg, S.; Schulze-Osthoff, K.; Cinatl, J., Jr.; Michaelis, M.; Werz, O. *Apoptosis* **2008**, *13*, 119.
12. Kachlany, S. C. *J. Dent. Res.* **2010**, *89*, 561.
13. Strathdee, C. A.; Lo, R. Y. C. *J. Bacteriol.* **1989**, *171*, 916.
14. Taichman, N. S.; Dean, R. T.; Sanderson, C. J. *Infect. Immun.* **1980**, *28*, 258.
15. Ullrich, A.; Chai, Y.; Pistorius, D.; Elnakady, Y. A.; Herrmann, J. E.; Weissman, K. J.; Kazmaier, U.; Muller, R. *Angew. Chem., Int. Ed.* **2009**, *48*, 4422.
16. Sanchez, V.; Lucas, M.; Sanz, A.; Goberna, R. *Biosci. Rep.* **1992**, *12*, 199.
17. Searle, J.; Lawson, T. A.; Abbott, P. J.; Harmon, B.; Kerr, J. F. *J. Pathol.* **1975**, *116*, 129.
18. Schneider, P.; Weber, M.; Hoffmeister, D. *Fungal Genet. Biol.* **2008**, *45*, 302.
19. Pergola, C.; Rogge, A.; Dodt, G.; Northoff, H.; Weinigel, C.; Barz, D.; Radmark, O.; Sautebin, L.; Werz, O. *FASEB J.* **2011**, *25*, 3377.
20. Waldmeier, P. C.; Feldtrauer, J. J.; Qian, T.; Lemasters, J. J. *Mol. Pharmacol.* **2002**, *62*, 22.

M-V: Rapid cell death induction by the honey mushroom mycotoxin dehydroarmillylorsellinate through covalent reaction with membrane phosphatidylethanolamines

Rapid cell death induction by the honey mushroom mycotoxin dehydroarmillylorsellinate through covalent reaction with membrane phosphatidylethanolamines

Stefanie König[1*], Konstantin Löser[1*], Helmut Pein[1*], Konstantin Neukirch[1], Anna Czapka[1], Stephanie Hoeppener[2,3], Maximilian Dörfer[4], Dirk Hoffmeister[4], Andreas Koeberle[1], and Oliver Werz[1,3§]

[1] Department of Pharmaceutical/Medicinal Chemistry, Institute of Pharmacy, Friedrich Schiller University Jena, Philosophenweg 14, D-07743 Jena, Germany.

[2] Laboratory of Organic and Macromolecular Chemistry (IOMC), Friedrich Schiller University Jena, Humboldtstr. 10, D-07743 Jena, Germany

[3]Jena Center of Soft Matter (JCSM), Friedrich Schiller University Jena, Philosophenweg 7, D-07743 Jena, Germany

[4] Department of Pharmaceutical Microbiology at the Hans Knoell Institute, Friedrich Schiller University Jena, Winzerlaer Straße 2, D-07745 Jena, Germany

[*] contributed equally

§ **corresponding author**: Prof. Dr. Oliver Werz, Chair of Pharmaceutical/ Medicinal Chemistry, Institute of Pharmacy, Friedrich Schiller University Jena, Philosophenweg 14, D-07743 Jena, Germany; Phone: +49-03641-949801; Fax: +49-03641-949802;

e-mail: oliver.werz@uni-jena.de.

Abbreviations

ATP – adenosine triphosphate, DAO - dehydroarmillylorsellinate, EA – ethanolamine, ER – endoplasmic reticulum, LDH – lactate dehydrogenase, PL – phospholipid, PE – phosphatidylethanolamine, ROS – reactive oxygen species, Stsp – staurosporine.

Summary

Melleolides form a group of fungal mycotoxins of the basidiomycete genius *Armillaria mellea* that induce rapid cell death in various mammalian cells with yet unknown mode of action. Here, we show that the melleolide dehydroarmillylorsellinate (DAO) covalently binds to phosphatidylethanolamine (PE) contained in cell membranes, accompanied by rapid loss of plasma membrane integrity and cellular viability. DAO caused a remarkable rapid onset of cell death of human cancer cells and primary human monocytes (i.e. within 15 min), which was temporally accompanied by PARP cleavage and loss of membrane integrity. DAO possesses a reactive α,β-unsaturated aldehyde group as Michael acceptor and covalently reacted via 1,4-addition with ethanolamine (EA) and with PE but not with other phospholipids containing serine or choline head groups. DAO-PE adduct formation coincided with membrane damage, and excess of exogenous EA prevented DAO-induced cell death. Moreover, DAO caused leakage of artificial PE-composed liposomes in a cell-free system. Subcellular fractionation studies indicate that DAO-PE adducts accumulate in cellular membranes along with decreased PE contents. Conclusively, DAO causes cell death by membrane damage seemingly due to covalent modification of PE with detrimental consequences for cell integrity and viability.

Introduction

The honey mushroom *Armillaria mellea* produces antimicrobial and cytotoxic natural products belonging to the large group of melleolides with more than 60 elucidated members [1-5]. These secondary metabolites combine sesquiterpene arylesters with orsellinic acid residues and exhibit mainly secondary alcohols. Up to now only a few targets and mode of actions are investigated for these mushroom toxins [6, 7]. Several melleolides show antitumor and cytotoxic effects in various human cells [1, 3, 8-10]. For example, armillarikin induces ROS-mediated and caspase-dependent apoptosis by downregulation of the mitochondrial transmembrane potential in leukemia cells [9, 11], and armillaridin induces autophagy-associated apoptosis in human leukemia cells and negatively influences the mitochondrial transmembrane potential [8, 12, 13]. Furthermore, decreased DNA synthesis was observed in different human cancer cell lines for some melleolides [1].

Cell death can be classified in three major subgroups – apoptosis, autophagic cell death and necrosis [14-16]. Typical characteristics for apoptosis are caspase activation, mitochondrial outer membrane permeabilization, cell rounding, nuclear condensation, and cell fragmentation to apoptotic bodies [17]. Autophagy is also a programmed physiological process in organism required to recycle macromolecules, cytoplasmic material, and cell organelles [18] but also for ATP production [19] via a lysosomal degradation pathway. In contrast, necrosis is an uncontrolled process and is constituted by signaling- and damage-induced lesions like mitochondrial dysfunction, ATP depletion, increased reactive oxygen species (ROS) formation or early plasma membrane ruptures [20, 21].

Membrane phospholipids (PL) constitute of a phosphate-bound head group (sn-3 position) and a glycerol residue connected with two ester-linked fatty acid chains (sn-1/sn-2 position). PL are classified by the functional head group, encompassing PE, phosphatidylcholine (PC), phosphatidylserine (PS), phosphatidylinositol (PI), phosphatidylglycerol (PG), phosphatidic

acid (PA), sphingomyelins (SP), and cardiolipins (CL). Typical cellular membranes consists of 45-55% PC, 15-25% PE, 10-15% PI, and 5-10% PS, where PE and PS are mainly found in the inner membrane leaflet [22]. During the early stage of apoptosis, PE and PS are exposed to the outer leaflet of the plasma membrane [23]. PE is participating in a wide range of cellular processes like the formation of hexagonal phases within the membrane because of its cone shape [24], protein arrangement inside the membrane [25], enhancing membrane fusion [24, 26], oxidative phosphorylation [27], mitochondrial stability [28] and autophagy [29, 30] and plays a substantial role in lipid synthesis as precursor of other lipids [31].

Here we show that the melleolide dehydroarmillylorsellinate (DAO, **Fig. 1A**) interferes with PE in cellular membranes by covalent binding to the EA head group. DAO possesses an α,β-unsaturated aldehyde that functions as Michael acceptor to react with nucleophilic residues such as thiol moieties of cysteine residue in 5-lipoxygenase (5-LO) [7]. Previous data showed that in contrast to other cytotoxic cell death-inducing agents, DAO causes remarkably rapid cell death with equal effectiveness in primary human monocytes and various cancer cell lines [3]. Our data suggest that covalent binding of DAO to membranous PE is the cause for the rapid perturbation of membrane integrity and consequent induction of cell death with characteristics of apoptosis and necrosis.

Results

DAO causes rapid cell death in human cells with unique characteristics

As reported before [3], the effectiveness of DAO and of the pan kinase inhibitor staurosporine (Stsp) for induction of cell death (assessed by MTT assay) in HeLa cells and primary monocytes was strikingly different. Thus, while Stsp-induced cell death is mainly mediated by apoptosis [32], DAO might confer its cytotoxicity primarily via necrotic features [3]. Moreover, DAO was about equipotent in monocytes and HeLa cells (EC_{50} = 1.6 and 2.3 µM, respectively), while Stsp was much more (40-fold) effective in HeLa cells (EC_{50} = 0.01 µM) as compared to monocytes (EC_{50} = 0.4 µM). The onset in cell death induction by DAO was remarkably rapid. Thus, exposure to DAO for only 15 min caused significant loss of viability of monocytes which was hardly different from 1 hr or 24 hrs treatment (**Fig. 1B**). In contrast, for Stsp, exposure for more than 5 hrs was needed to cause cytotoxicity in monocytes (not shown, see [3]). Release of lactate dehydrogenase (LDH) from cells to the external space reflects the loss of plasma membrane integrity. In agreement with the loss of cell viability assessed by MTT assay, LDH release from monocytes and HeLa cells was rapidly induced by DAO with almost maximal effects after about 30 min of exposure (**Fig. 1C**).

We next studied the effects of DAO and Stsp on cell morphology using light microscopy and transmission electron microscopy (TEM). DAO (even at low concentrations such as 0.1 µM) caused morphological signs of cells death within 3 hrs, reflected by wrinkling and shriveling of the plasma membrane (PM, **Fig. 1D**), which is actually a typical feature of necrosis. In contrast, Stsp caused classical signs of apoptosis in HeLa cells such as cellular fragmentation and formation of apoptotic bodies, along with shrinkage of the cells (**Fig. 1D**). Analysis by TEM revealed typical morphological features of monocytes with bean-shaped nucleus as well as intact organelles and plasma membrane (**Fig. 1E**). Upon Stsp-treatment (3 hrs), the nucleus lost its bean shape and rendered to a round structure with seemingly intact nuclear membrane and

also intact mitochondria. In contrast, 3 hrs treatment of monocytes with DAO caused defects of the nuclear membrane and in particular, mitochondria appeared to be lost (**Fig. 1E**). Together, DAO induces a remarkable rapid onset of cell death of primary cells and cancer cells accompanied by apparent membrane damages, which are characteristics that differ from those of classical apoptotic cell death inducers like Stsp.

Contribution of apoptotic pathways in mediating cell death by DAO

In order to explore the contribution of apoptotic pathways in mediating cell death by DAO, we analyzed hallmarks of apoptosis and stress signaling on a molecular level in monocytes. In fact, the rapid cell death induction by DAO (5 µM) within 15 min coincided with cleavage of PARP to a 89 kDa fragment as marker for apoptosis in monocytes; in contrast Stsp failed to induce PARP cleavage during short term treatment (within 1 hr, **Fig. 2A**) but instead required at least 5 hrs (**Supplemental Fig. 1**). The intrinsic pathway of apoptosis is initialized by a loss of mitochondrial membrane potential ($\Delta\Psi_m$) and the release of cytochrome c from mitochondria [33]. We found that in contrast to vehicle-treated monocytes exposure to 10 µM DAO for 3 hrs caused substantial release of cytochrome c into the cytosol, while in parallel the cytochrome c levels in organelles was minute (**Fig. 2B**). Also Stsp (3 µM) induced cytochrome c release from mitochondria within 3 hrs, albeit much less pronounced as compared to DAO.

Protein kinase signaling critically regulates the initiation of apoptosis, where the survival kinase Akt counteracts apoptosis [34] while p38 MAPK rather promotes it [35]. Exposure of monocytes to DAO (5 µM) and Stsp (3 µM) suppressed phosphorylation and thus activation of Akt. In contrast, both compounds elevated phosphorylation/activation of p38 MAPK (**Fig. 2C**). Again, the effects of DAO were more rapidly apparent (15 min) as compared to Stsp (30-60 min, **Fig. 2C**). The activation of p38 MAPK was independent on endoplasmic reticulum (ER)

stress and on the activation of the unfolded protein response (UPR), reflected by the failure of DAO to induce the UPR genes immunoglobulin heavy chain-binding protein (BiP), C/EBP [CCAAT/enhancer-binding protein]-homologous protein (CHOP), and activating transcription factor 4 (ATF4), at the protein level assessed by Western blot (**Fig. 2D**). Finally, we employed the pan-caspase inhibitor QVD to block apoptotic signaling. QVD (10 μM) inhibited DAO-induced PARP cleavage in monocytes (**Fig. 2E**). In contrast, QVD failed to reverse cell death induction by DAO after 3 and 48 hrs, but also loss of cell viability in response to Stsp was not completely reversed by QVD (**Fig. 2F**), in line with the reported necroptosis induction in monocytic U937 cells [36]. Conclusively, DAO-induced cell death is accompanied by apoptotic features which are seemingly not operative but rather necrotic pathways are responsible.

DAO interacts with the ethanolamine residue of phosphatidylethanolamine

The α,β-unsaturated aldehyde of DAO functions as Michael acceptor to react with nucleophilic residues such as thiol moieties of cysteine residue in 5-lipoxygenase [7]. It appeared reasonable that the rapid induction of cell death by DAO and the associated detrimental membrane alterations could be due to reaction of the α,β-unsaturated aldehyde of DAO with amine moieties of ethanolamine (EA) or serine (Ser) head group of membrane PE and PS thereby perturbing membrane integrity. We incubated different types of phospholipids (i.e., PE, PC, PS) with DAO followed by cleavage of the PL between the phosphate and the EA, Ser or choline moiety, respectively, using exogenously added phospholipase (PL)D and UPLC-MS/MS analysis of potentially formed adducts of DAO with the head group moieties. As shown in **Fig. 3A**, two major signals at 442.4 and 485.3 m/z appeared upon incubation of DAO with PE and subsequent PLD cleavage which may represent adducts of DAO with one or two EA molecules. These DAO-EA adducts are reaction products, where (i) the primary amine of one EA molecule forms an α,β-unsaturated Schiff base with the aldehyde group of DAO (resulting in 442.4 m/z)

and/or (ii) the primary amine moieties of two EA molecules react in 1,4-addition to yield imine structures (485.3 m/z) (**Fig. 3A**). Note that only a weak signal was detectable for DAO itself (399.4 m/z), suggesting that DAO efficiently reacted with PE to form the two adducts. In contrast, when DAO was incubated in parallel with PS or PC, the signal for DAO remained pronounced, whereas peaks with 442.4 or 485.3 m/z were not detectable (**Fig. 3B**), suggesting that DAO does not react with PS or PC.

We then studied if DAO-PE adducts might be formed also from intact monocytes and HeLa cells upon exposure to DAO for 3 hrs, by analysis of DAO-EA after treatment of cell lysates with exogenous PLD. Incubation of these cells with DAO caused concentration-dependent increases in DAO-EA adducts, starting at 0.1 µM DAO (**Fig. 3C**). The cellular amount of PE was maintained/decreased (**Fig. XY**). Next, we explored if DAO-PE interactions temporally correlate with detrimental effects on membrane integrity and thus with cell death induction. Treatment of monocytes or HeLa cells with 5 µM DAO resulted in rapid formation of DAO-PE adducts already after 15 min, reaching a plateau after about 1 hr to 3 hrs (**Fig. 3D**), which resembles the kinetics for the loss of membrane integrity (**Fig. 1C**) and decrease in cell viability (**Fig. 1B**). Note that for both the loss of membrane integrity and DAE-PE adduct formation, DAO displays more pronounced effects in monocytes versus HeLa cells (**Fig. 3D** and **Fig. 1C**). Taken together, DAO-EA adduct formation proceeds in parallel to membrane damage, suggesting that the interaction of DAO with PE in the plasma membrane might be eventually causative for cell death induction. In fact, incubation of DAO (10 µM) or Stsp (3 µM) with 50 mM EA for 2 hrs prior to addition to monocytes or HeLa cells abrogated the cytotoxic effect of DAO but not of Stsp (**Fig. 3E**), assessed by MTT assay. Note that preincubation of DAO with choline failed in this respect and L-serine could only marginally restore cell viability (**Fig. 3F**). Again, Stsp-induced loss of monocyte viability was not affected by preceeding reaction with EA, serine or choline (**Fig. 3F**). Together, DAO binds to EA in PL and exogenous EA prevents

DAO-induced cell death suggesting that DAO acts by covalent modification of PE in cellular membranes.

Subcellular locales of DAO-PE interactions and consequences for PE contents

In order to explore the interaction between DAO and PE in the cellular context and to locate the subcellular PE binding sites of DAO, we performed subcellular fractionation of HeLa cells to obtain fractions enriched in nuclei, mitochondria, cytosol, and membranes. HeLa cells were preincubated with or without DAO for 15 or 180 min and cells were subjected to hypotonic lysis by passing them through a 25 G needle and subsequent differential centrifugation. Western blot for respective markers proteins confirmed correct cell fractionation and enrichment of related organelles (**Supplemental Fig. 2**). In cells treated with vehicle for 15 min, the cellular PE content was about equally distributed between fractions where nuclei, mitochondria, or membranes are enriched, while no PE was detectable in the cytosol (**Fig. 4A**). DAO did not significantly alter the subcellular distribution of PE (**Fig. 4A**). After 180 min, nuclear PE increased at the expense of membranous PE, and about 5% of the total PE was cytosolic. DAO further promoted this redistribution and increased nuclear PE at the expense of membranous PE (**Fig. 4A**). Importantly, when we analyzed the subcellular fractions for DAO-PE adducts (measured as DAO-EA after treatment of the fractions with PLD to cleave PE), we found that most of the DAO-PE (44% after 15 min and 62% after 180 min) was formed in the membrane fraction, with about equal or somewhat elevated contents in the mitochondrial as compared to the nuclear fraction (**Fig. 4B**).

Next, we analyzed whether DAO affects specific PE species in the subcellular fractions of HeLa cells after 3 hrs incubation using a targeted phospholipidomics approach (UPLC-MS/MS). In general, PE(18:0/18:1) and PE(18:1/18:1) were the most abundant species in the nuclear, mitochondrial and membrane fraction (**Fig. 4C**). However, the contents of PE species were not

markedly affected by DAO in comparison to the vehicle, the amounts of PE(18:0/18:1) and PE(18:1/18:1) were slightly increased in the nuclear fraction upon exposure to DAO after 3 hrs (**Fig. 4C**). Interestingly, after 15 min, PE(18:0/18:1) was the most common PE species in the membrane fraction closely followed by PE(18:1/18:1) (**Fig. 4D**) and after 3 hrs, these two PE species behaved exactly the other way (**Fig. 4C**). If we compared PE levels after 15 min DAO exposure with PE levels after 3 hrs DAO treatment in correlation to the total PE amount, a potent reduction of PE levels in the membrane fraction, especially PE(18:0/18:1) and PE(18:1/18:1) was obvious. Similar effects were observed also for less abundant PE species, such as PE(18:0/20:4), PE(16:0/18:1) or PE(16:1/18:1) (**Fig. 4F**). Together, DAO covalently reacts with the major PE species, preferably with those in membranes, which as a consequence leads to a subcellular rearrangement of single PE species within cell organelles.

In order to confirm that DAO reacts with PE in membranes and thus abrogates membrane integrity, we studied if DAO could cause leakage of artificial PE-composed liposomes in a cell-free system [37]. DAO caused release of the fluorescent dye 8-hydroxypyrene-1,3,6-trisulfonic acid trisodium salt (HPTS) from liposomes composed PE but not of PC indicating that it induces liposome leakage (**Fig. 4G** and **Supplemental Fig. 3**). Moreover, incubation of monocytes with DAO induced rapid (within 15 min) acidification of vesicles, starting at 1 μM DAO being comparable to the effect of the protonophore carbonyl cyanide m-chlorophenyl hydrazine (CCCP), as demonstrated by fluorescence microscopy using Lysotracker® as pH-sensitive dye for lysosomal staining (**Fig. 4H**).

Discussion

Melleolides belong to one of the largest globally distributed mycotoxin group of mushrooms. Only for a few of these mycotoxins the modes of action and targets are explored like for muscarine, coprine, psilocybin, and ibotenic acid. Since the last century, researchers have followed up with the bioactions of secondary metabolites of the basidiomycete species *Armillaria mellea* in plants and human cells [38-41]. Here, we reveal a mode of action underlying the cytotoxic properties of the melleolide DAO in human cells. We showed before [3] that DAO induces remarkably rapid cell death in human cancer cell lines and in primary immune cells, but the mode of action remained obscure. Here, we provide evidence that DAO covalently binds to PE in cellular membranes. Our data suggest, that DAO covalently reacts with the EA head group of PE thereby perturbing plasma membrane structure and integrity, eventually leading to rapid cell death.

Besides DAO, several other melleolides display cytotoxic properties [1, 2, 4, 8, 9], but the rapid onset of cell death by DAO is unique. Interestingly, in contrast to other well-known cell death-inducing agents such as Stsp or pretubulysin that are more effective in cancer cells versus normal untransformed cells, DAO is equally potent in primary monocytes and cancer cell lines, and loss of cell viability due to DAO is apparent within few minutes as compared to Stsp that needed at least 5 hrs to cause cell death [3]. As described before, DAO displayed apoptotic as well as necrotic features of cell death measured by flow cytometry with an Annexin V/7-amino-actinomycin staining, and marked apoptosis induction was only obvious after 5 hrs [3]. Here, we find that DAO causes cleavage of the classical apoptosis marker PARP in human monocytes to a 89 kDa fragment within 15 min. Furthermore, the increase of phosphorylation of the stress-regulated p38 MAPK and the simultaneous decrease of the phosphorylation of the survival factor Akt due to DAO may contribute to cell death induction. Cells treated with Stsp demonstrated classical apoptotic characteristics like apoptotic bodies and fragmentation of

nuclei [15, 17], DAO-treated cells were crumpled and shrunk along with membrane rupture, particular of mitochondrial membranes. These properties are typical characteristics of necrosis [20, 21] suggesting that both apoptotic and necrotic features of DAO-induced cell death.

Recently, the plant toxin ophiobolin A from the *Bipolaris* genus [42] was shown to react with PE and/or EA [43], accompanied by strong cytotoxic properties in various cancer cells [44-46]. Of interest also ophiobolin A possesses an α,β-unsaturated aldehyde moiety that covalently reacts with the EA moiety in one PE molecule yielding the formation of a pyrrole [43], while DAO forms first an imine (as for ophiobolin A) with PE but then couples via 1,4 addition to a second PE molecule. Our data suggest that via covalent binding to the amine moiety of EA residues DAO interacts with the head group of PE without forming adducts with PC, and seemingly also not with PS, although serine possesses a primary amine function like EA. In fact, substantial excess of exogenously added L-serine partially reverted the cytotoxic effects of DAO (Fig. 3G), while choline failed in this respect.

We suggest that DAO-PE adduct formation causes perturbances of cellular membranes resulting in loss of membrane integrity. Thus, formation of DAO-EA adducts from cells treated with DAO temporally correlated to LDH release as marker for impaired plasma membrane integrity, processes that occurred within 15 min upon cell exposure to DAO, and DAO caused disappearance of mitochondria as visualized by TEM. PE is a cone-shaped lipid and responsible for the formation of hexagonal membrane phases [24]. If DAO covalently binds to the EA moiety in PE, the arranged membrane structure might become perturbed and prone to ruptures with consequent LDH release. In fact, the cytotoxic effects of DAO were abrogated by supplementation of exogenous EA and serine, but not of choline, that may capture the reactive aldehyde moiety of DAO, and DAO cause leakage of liposomes composed of PE but not of liposomes made from PC. Therefore, we hypothesize that the interaction of DAO with membranous PE is the major cause for the rapid cell death induction.

In normal untransformed cells, PE is arranged in the inner leaflet of the plasma membrane and the mitochondrial membrane [22] but during cell death PE and also PS are translocated to the outer plasma membrane [23]. Upon treatment of HeLa cells with DAO, adducts with PE were most abundant in the membrane fraction, supporting the hypothesis that DAO acts on membranous PE. Moreover, treatment of HeLa cells with DAO caused primarily a rearrangement of various PE species (particularly PE (18:0/18:1) and PE (18:1/18:1)) in the plasma membrane fraction leading to the presumption that DAO might affect various metabolic processes.

PE is necessary for autophagosomal membranes and autophagy which is essential to gain ATP by recycling cytoplasmic compounds [19]. During apoptosis, cells increase the autophagic response to support cell functions and to eliminate toxic molecules. These effects were intensified by reduced caspase-8 levels [47, 48]. Cells become hyperactive and lysosomal resorption of DAO is enhanced. Simultaneously, DAO interacts with PE in the inner leaflet of lysosomes followed by a lysosomal membrane rupture and as consequence the pH declines, as shown in monocytes by using the pH-sensitive dye Lysotracker®, eventually inducing necrosis. Taken together, DAO causes apoptosis and necrosis by manipulating several cellular mechanisms initialized by perturbing membrane integrity.

In conclusion, we identified membrane PE as molecular target for the melleolide DAO that via the α,β-unsaturated aldehyde moiety covalently reacts with the EA headgroup of PE. These DAO-PE interactions translate into perturbation of cellular membrane structure with consequent loss of integrity which eventually causes the remarkably rapid onset of cell death in various cell types.

Materials and Methods

Materials

DAO was isolated as described before [3]. Antibodies against Lamin B1, Lamp1, and syntaxin 6, abcam (Cambridge, United Kingdom); DPX, abcr GmbH (Karlsruhe, Deutschland); bovine serum albumin (BSA), EDTA, and Tris, AppliChem (Darmstadt, Germany); DOPC, and DOPE, Avanti Polar Lipids (Alabaster, AL); L-glutamine, BioChem GmbH (Karlsruhe, Germany); AA, Cayman Chemical (Biomol, Hamburg, Germany); Antibodies against cleaved PARP (Asp214), phospho-p38 MAPK (Thr180/Tyr182), phospho-Akt (Ser473), ATF-4, CHOP, BiP, calnexin, COX IV, and β-actin were from Cell Signaling Technology (Boston, MA); phosphoplipase D from *Streptomyces chromofuscus*, ENZO life sciences (Lörrach, Germany); cytochrome c, Epitomics Inc. (Burlingame, CA); acetonitrile, Dulbecco's modified Eagle's high glucose medium with glutamine, penicillin/streptomycin-solution, sepharose and trypsin-EDTA, GE Healthcare Life Science (Freiburg, Germany); goat anti-rabbit IgG Alexa Fluor 488 antibody, and goat anti-mouse IgG Alexa Fluor 555 antibody, Invitrogen (Darmstadt, Germany); DMSO, Merck (Darmstadt, Germany); ATP, Roche (Mannheim, Germany); SDS, Roth GmbH (Karlsruhe, Germany); GAPDH, and β-tubulin, Santa Cruz Biotechnology (Heidelberg, Germany); Dulbecco´s Buffer Substance (PBS), staurosporine, and HPLC solvents, VWR (Darmstadt, Germany); dextrane, fetal calf serum (FCS), 3-(4,5-dimethylthiazol-2-yl)-2,5-diphenyltetrazolium bromide (MTT), RPMI 1640 Medium, phenylmethanesulfonyl fluoride, soybean trypsin inhibitor, lysozyme, leupeptin, HPTS, ethanolamine, choline, L-serine, triton X-100, chicken egg PE, chicken egg PC, QVD, LysoTracker® as well as other chemicals were from Sigma-Aldrich (Taufkirchen, Germany).

Cells

Monocytes were isolated from peripheral human blood of adult (18-65 years) healthy volunteers with written informed consent, obtained from the Institute of Transfusion Medicine, University

Hospital Jena, as described [49]. The experimental protocol was approved by the ethical committee of the University Hospital Jena. All methods were performed in accordance with the relevant guidelines and regulations. Leukocyte concentrates were prepared by centrifugation (4000×g, 20 min, 20 °C) and erythrocytes were removed by dextran sedimentation followed by centrifugation on lymphocyte separation medium (Histopaque®-1077, Sigma, Taufkirchen, Germany) to obtain peripheral mononuclear blood cells (PBMCs). PBMCs were seeded in RPMI 1640 (Sigma Aldrich, Taufkirchen, Germany) containing 10% (v/v) heat inactivated fetal calf serum (FCS), 100 U/mL penicillin, and 100 µg/mL streptomycin in cell culture flasks (Greiner Bio-one, Frickenhausen, Germany) for 1.5 h at 37 °C and 5% CO_2. Adherent monocytes were washed twice with PBS and were resuspended in PBS containing 1 mg/ml glucose. HeLa cells were cultured in monolayers in DMEM High Glucose (4.5 g/L) medium supplemented with heat-inactivated fetal calf serum (FCS, 10%, v v), 100 U/mL penicillin, and 100 µg/mL streptomycin at 37 °C in a 5% CO_2 incubator.

Analysis of cell viability by MTT assay

Monocytes (2 × 10^6/mL in RPMI 1640 containing 5% heat inactivated FCS, 100 U/mL penicillin and 100 µg/mL streptomycin) or 0.1 × 10^6/mL HeLa cells in DMEM High Glucose supplemented with 5% FCS, 100 U/mL penicillin and 100 µg/mL streptomycin were seeded in a 96-well plate. Monocytes were allowed to adhere for 1.5 h at 37 °C, 5% CO_2. Cell were incubated at 37 °C and 5% CO_2 with vehicle (0.5% DMSO) or compounds (i.e. DAO or Stsp) for indicated time points. In some experiments, EA, choline, L-serine or QVD were added 15 min prior to DAO or Stsp. After the times indicated, cells were incubated with thiazolyl blue tetrazolium bromide (MTT, 5 mg/mL PBS) until blue staining of the vehicle-containing control cells. Formazan formation was stopped by 100 µL SDS lysis buffer (10%, w/v in 20 mM HCl) and the well plate was shake overnight. Finally, absorbance was measured at 570 nm with a

Multiskan™ microplate spectrophotometer (Thermo Scientific, Ulm, Germany). The pan protein kinase inhibitor staurosporine (1 µM) was used as cytotoxic control inhibitor.

LDH release assay

For analysis of extracellular LDH as marker for loss of plasma membrane integrity, we used the CytoTox96® Non-Radioactive Cytotoxicity assay kit (Promega, Madison, WI, USA). Freshly prepared monocytes (0.5×10^6/mL RPMI 1640 containing 5% heat inactivated FCS, 100 U/mL penicillin and 100 µg/mL streptomycin) or 0.1×10^6/mL HeLa cells in DMEM High Glucose supplemented with 5% FCS, 100 U/mL penicillin and 100 µg/mL streptomycin were seeded in a 96-well plate. Monocytes were allowed to adhere for 1.5 h at 37 °C, 5% CO_2 prior treatment with vehicle (0.5% DMSO), triton X-100 (lysis control) or 5 µM DAO for indicated time points. After incubation, the manufactures instructions were followed and the LDH release was measured by recording the absorbance at 490 nm with a Multiskan™ microplate spectrophotometer (Thermo Scientific, Ulm, Germany).

Microscopic morphology analysis

HeLa cells (0.25×10^6/mL DMEM High Glucose supplemented with 5% FCS, 100 U/mL penicillin and 100 µg/mL streptomycin) were incubated for 3 hrs with vehicle (0.1% DMSO, v/v), DAO or Stsp. Then, cells were placed on ice, washed with PBS, and analyzed by light microscopy using an AxioCam MR3 camera (Zeiss, Jena, Germany). Images were acquired, cut, linearly adjusted in the overall brightness and contrast, and exported to TIF by the AxioVision 4.8 software. The microscope incubator (Axio Observer Z1 inverted microscope, LCI Plan-Neofluar 63x/1.3 Imm Corr DIC M27 objective, Carl Zeiss, Jena, Germany) was kept at 37 °C and 5% CO_2.

Lysotracker® analysis

For acidification analysis of monocytes by fluorescence microscopy, freshly isolated monocytes (2.5×10^5/mL RPMI 1640 containing 5% heat inactivated FCS, 100 U/mL penicillin and 100 µg/mL streptomycin) were seated in Glass Bottom Microwell Dishes (MatTek Corporation, MA). After 1.5 hr adhesion time at 37 °C and 5% CO_2, cells were treated for 1 hr with vehicle (0.1% (v/v) DMSO), 10 µM CCCP or 0.1 µM, 1 µM, 10 µM DAO at 37 °C and 5% CO_2 followed by washing with pre-warmed PBS. Cells were resuspended in PBS containing 1 mM $CaCl_2$, 1 mM $MgCl_2$ and 0.1% glucose. For the staining, 50 nM LysoTracker® Red-DND-99 (Sigma, Taufkirchen, Germany) was added to the cells and after 5 min, red fluorescence of the accumulated probe in acidic cell organelles was imaged using an Axio Observer Z1 microscope (Carl Zeiss, Jena, Germany).

For analysis by a fluorescence microplate reader (NOVOstar®, BMG Labtechnologies, Offenburg, Germany), freshly isolated monocytes (1.5×10^6/mL RPMI 1640 containing 5% heat inactivated FCS, 100 U/mL penicillin and 100 µg/mL streptomycin) were seated into a black 96-well plate with glass bottom. Monocytes were allowed to adhere for 1.5 hr at 37 °C, 5% CO_2 prior treatment with vehicle (0.1% (v/v) DMSO), 10 µM CCCP as control, and DAO as indicated concentrations for 1 hr. After washing and resuspension in PBS (0.1% glucose, 1 mM $CaCl_2$, 1 mM $MgCl_2$), cells were stained with 50 nM LysoTracker® and 0.5% (v/v) Hoechst for 5 min at 37 °C, 5% CO_2. After washing, fluorescence was excited at 577 nm (LysoTracker®) and 350 nm (Hoechst staining) and the emission was recorded at 590 nm (LysoTracker®) and 480 nm (Hoechst staining). Acidification was calculated from ratio of fluorescence intensities of LysoTracker® in relation to the fluorescence of Hoechst staining.

TEM

Monocytes, resuspended in RPMI 1640 containing 5% heat-inactivated FCS, 5 ml L-glutamine, 100 U/mL penicillin and 100 µg/mL streptomycin, were incubated with DAO, Stsp or vehicle for 3 hrs at 37 °C and 5% CO_2. Cells were washed in PBS pH 7.4, centrifuged (800×g, 5 min,

20 °C) and resuspended in 2.5% glutaraldehyde (v/v, in water) for fixation. After 20 min at RT, cells were washed by centrifugation (5000 rpm, 5 min, 4 °C) and resuspended in PBS. For the embedding process, cells were washed 3 times with PBS pH 7.4 for 5 min. After each washing step, the sample was centrifuged at 2000 rpm for 2 min. Post-fixation was performed by osmium tetroxide (1% OsO_4 in PBS pH 7.4) for 1 hr. Samples were washed again with PBS pH 7.4 and the monocytes were gradually dehydrated by a series of increasing ethanol:water mixtures (50%, 70%, 90% and 100% ethanol, 10 min for each step and centrifugation at 2000 rpm for 2 min). Resin infiltration was performed in 2 steps (Embed812: EtOH 2:1 with 18 µL per mL resin DMP-30 (for 1 hr at RT), Science Services). Samples were centrifuged at 2000 rpm for 8 min. The second infiltration step was performed in undiluted Embed812 resin (overnight at RT). After an additional centrifugation step the resin was exchanged and infiltrated for 2 hrs. Samples were subsequently transferred to BEEM capsules (Plano), centrifuged once (2000 rpm, 8 min) and cured at 60° C for 24 hrs. The embedded samples were sectioned in 80 to 100 nm thick slices utilizing an ultramicrotome (PowerTome PC, RMC Products) equipped with a diamond knife (Diatome). The slices were placed on a carbon coated TEM grid (Quantifoil) and imaged with a 200 kV FEI Tecnai G²20 (FEI Company).

Detection of DAO-PE adducts *in vitro*

For analysis of DAO-PE adduct formation, 5.2 µL solution of DAO (5 mM) and 2 µL transphosphorylated chicken egg PE (13 mM, Sigma Aldrich, Taufkirchen, Germany) were added to 44.8 µL reaction buffer containing 1 M triethylammonium acetate, $CHCl_3$ and MeOH (1:1:3, v/v/v). Vehicle and chicken egg PC (13 mM, instead of PE) were used as controls. After 3 hrs incubation at 37 °C, samples were diluted with MeOH to 500 µL, internal standard was added and 50 µL were dried under a nitrogen stream. The pellet was resuspended with 25 µL MeOH and diluted to 250 µL with PBS, following incubation with 275 U phospholipase D from *Streptomyces chromofuscus* (ENZO life sciences, Lörrach, Germany) for 16 hrs at 37 °C. DAO

adducts were extracted with 1 mL $CHCl_3$/MeOH (2:1, v/v). The lower organic phase was dried by a nitrogen stream and the pellet was resuspended with 1 mL MeOH before measuring by UPLC-MS/MS.

Isolation of cellular DAO-PE adducts

Monocytes (5×10^6 cells/mL) in RPMI 1640 containing 5% FCS, 100 U/mL penicillin and 100 µg/mL streptomycin or HeLa cells (0.25×10^6 cells/mL) in DMEM High Glucose supplemented with 5% FCS, 100 U/mL penicillin and 100 µg/mL streptomycin were incubated with vehicle (0.1% DMSO, v/v) or DAO for the indicated time points at 37 °C and 5% CO_2. Cells were placed on ice and washed twice with ice-cold PBS. The cell pellet was resuspended with ice-cold 200 µL $CHCl_3$/MeOH (2:1, v/v) supplemented with 50 mM pentyl-pyridoxamine. The cell suspension was allowed to homogenize for 20 min at RT followed by addition of internal standard and extraction with 40 µL 0.9% NaCl solution. The suspension was vortexed for 30 sec and centrifuged (4000 rpm, 5 min, 4 °C). The lower phase was dried under a stream of nitrogen and the pellet was resuspended with 50 µL MeOH by sonication. An aliquot of the solution (50 µL) was diluted with 200 µL PBS and sonicated for 2 min in an ultrasonic bath, followed by incubation of extracted phospholipids with 875 U phospholipase D from *S. chromofuscus* for 16 hrs at 37 °C. The solution was extracted with 1 mL ice-cold $CHCl_3$/MeOH mixture (2:1, v/v). The lower organic phase was dried, and the pellet was resuspended with 0.5 mL $CHCl_3$/MeOH mixture (2:1, v/v) followed by addition of 125 µL 0.9% NaCl solution and another extraction. The dried lower phase was resuspended with 100 µL MeOH and DAO-EA adducts were measured by UPLC-MS/MS.

Reversed phase liquid chromatography and mass spectrometry

Chromatography was carried out on an Acquity UPLC BEH C8 column (1.7 µm, 1 × 100 mm) using an Acquity™ Ultra Performance liquid chromatography system from Waters (Milford, MA, USA). DAO, PL's, and DAO-PE conjugates were separated at 0.75 ml/min and 45°C using

a gradient of 30% mobile phase A (acetonitrile/water, 10/90, 10 mM ammoniumacetate)/70% mobile phase B (acetonitrile/water, 95/5, 10 mM ammonium acetate) to 20% mobile phase A/80% mobile phase B within 5 min and to 100% mobile phase B within 2 min followed by isocratic elution for another 2 min. The chromatography system, controlled by Acquity UPLC Software 1.40 (Waters), was coupled to a QTRAP 5500 Mass Spectrometer (Sciex, Darmstadt, Germany) equipped with an electrospray ionization source.

For identification of DAO, the precursor-to-product ion transitions in multiple reaction monitoring were m/z 399.2 → 104.9 (collision energy: -50 eV; collision cell exit potential: -13 V), and 399.2 → 148.9 (collision energy: -24 eV; collision cell exit potential: -16 V). Quantification of DAO was based on the transition 399.2 → 148.9 using an external calibration curve, quantification of phospholipids and PL-conjugates was based on the internal standard DMPC (collision energy: -38 eV; collision cell exit potential: -12 V). Analytes with varying collision energies (CE) and collision cell exit potentials are listed below in table 1. The ion spray voltage was set to -4000 V, the heated capillary temperature to 650°C, the curtain gas pressure to 30 psi, the declustering potential to -50 V, collisionally activated dissociation (CAD) to medium, nebulizer gas (GS1) to 50, heater gas (GS2) to 60, and the entrance potential -10 V. Analyst software 1.6 (Sciex, Darmstadt, Germany) was used for the processing of analytical data.

analyt	precursor-to-product ion transition (m/z)	Collision energy (CE)	Collision cell exit potential (CXP)
DAO 1xEA T1	442.4 → 149.0	-20 → 50	-17 → 64
DAO 1xEA T2	442.4 → 105.0	-56 → 36	-7 → 2
DAO 2xEA T1	484.8 → 149.0	-41 → 46	-52
DAO 2xEA T2	484.4 → 105.0	-66 → 44	-52 → 90

DAO-PE(16:0/18:1)	1098.7 → 948.5	-52 → 35	-42 → 7
DAO-PE(16:0/18:11)	1098.7 → 281.2	-76 → 80	-42 → 7
DAO-PE(18:1/18:1)	1126.8 → 976.6	-49 → 20	-12
DAO-PE(18:0/20:4)	1148.7 → 998.5	-49 → 51	-12
DAO-PE(18:0/20:41)	1148.7 → 283.4	-79 → 33	- 12
d8-AA	311.3 → 267.1	-16	-18
d4-LTB4	339.3 → 197.2	-22	-13
d4-PGE2	355.3 → 193.2	-38	-18

Liposomal leakage assay

Solutions containing either 5 µmol dioleoyl-PC (DOPC) or 2.5 µmol dioleoyl-PE (DOPE) plus 2.5 µmol DOPC (Avanti Polar Lipids, Inc.) were prepared in $CHCl_3$. The solvent was removed using a nitrogen stream and subsequent evaporation under vacuum. Lipid films were rehydrated by vortexing in a water bath (30 °C) with 1 mL of a solution of 35 mM 8-hydroxypyrene-1,3,6-trisulfonic acid trisodium salt (HPTS, fluorophore) and 50 mM 1,1'-[1,4-phenylenebis(methylene)]-bis pyridinium dibromide (DPX, colissional quencher) in 20 mM HEPES, 150 mM NaCl, and 1 mM EDTA forming essentially heterogenous multilamellar vesicles (MLV). Then, large unilamellar vesicles (LUV) were formed by six freeze-thaw cycles. Liposome suspensions were extruded 20 times through 100 nm polycarbonate filters (LiposoFast-Basic, Avestin Inc.) to generate LUVs with HPTS/DPX encapsulated [50]. LUVs were separated from free HPTS/DPX by size exclusion chromatography using a Sepharose column and 20 mM HEPES, 150 mM NaCl, 1 mM EDTA as buffer.

A 100 µL sample of HPTS/DPX-containing liposomes diluted (1:20) in 20 mM HEPES, 150 mM NaCl, 1 mM EDTA was dispensed in 96-well-plates. Then, 10 µM DAO was added and the fluorescence of HPTS was monitored each 14 s on a NOVOstar (BMG LABTECH GmbH)

using excitation at 450 nm and emission at 520 nm over 15 min and at RT. A negative control using DMSO was used as the 0% leakage reference, and 0.2% Triton X-100 was used as positive control yielding 100% leakage. For each time point, the fluorescence data were normalized to these two reference samples.

Cytochrome c release

Cells were seeded in RPMI 1640 containing 5% FCS, 100 U/mL penicillin and 100 µg/mL streptomycin (4×10^6/ml) and incubated with the test compounds or vehicle (DMSO). After 3 hrs, cells were washed once in PBS and 10^7 cells were resuspended in 200 µl PBS. For permeabilization of the plasma membrane, 20.3 µM digitonin was added and immediately vortexed (10 sec), incubated for another 30 seconds at room temperature and centrifuged at 20,000g at 4°C for 1 min. The supernatant (cytosolic fraction) and pellet (non-cytosolic fraction) were transferred to a new tube, respectively, and mixed 1:1 (vol/vol) with 5% trichloroacetic acid. Precipitation of cytosolic proteins was performed at 4°C overnight. Proteins were pelleted by centrifugation at 20,000g at 4°C for 30 min and resuspended in 25 µl PBS. Aliquots of 5 µl were used for determination of protein concentration using Roti-Nanoquant (Roth, Karlsruhe, Germany). Equal amounts of protein were mixed 1:1 (vol/vol) with 2 × SDS/PAGE sample loading buffer and analyzed for cytochrome c by SDS-PAGE and Western Blot using an anti-cytochrome c-antibody (Epitomics Inc., Burlingam, CA).

Subcellular fractionation

HeLa cells (0.25×10^6 cells/mL, in DMEM High Glucose supplemented with 5% FCS, 100 U/mL penicillin and 100 µg/mL streptomycin) were pre-incubated with vehicle (0.1% DMSO, v/v) or DAO (5 µM) for the indicated time points at 37 °C and 5% CO_2. Cells were placed on ice and the cell pellet was washed with 500 µL PBS followed by 5 min centrifugation (4600 rpm) at 4 °C. The cell pellet was resuspended with hypotonic lysis buffer pH 7.4 (10 mM HEPES, 2 mM $MgCl_2$, 0.1 mM EDTA, 0.1 mM EGTA, 10 mM KCl, 1 mM DTT) and cells

were passed through a 25 G needle (sterican 0.5 × 40 mm, Gr 17/42, B. Braun Melsungen AG) 10 times using a 10 mL syringe. The cell suspension was kept on ice for 20 min before adding kinase inhibitor cocktail. To get nuclei, the cell suspension was centrifuged for 10 min at 550 g and 4 °C. Supernatant was used for continuing subcellular fractionation and pellet was again washed with hypotonic lysis buffer, centrifuged (550 g, 10 min, 4 °C) and frozen at -20 °C. The supernatant was centrifuged at 10,000 g and 4 °C for 10 min. The resulting mitochondrial pellet was again washed as described for the nuclear pellet and subsequently frozen at -20 °C. The supernatant was used to obtain the cytosolic and microsomal fraction by ultracentrifugation at 100,000 g and 4 °C for 1 h. The cytosolic fraction corresponds to the supernatant and was evaporated until dryness with Eppendorf® concentrator at 30 °C. The pellet corresponds to the microsomal fraction and was frozen at -20 °C.

For preparation of Western Blot samples, pellets were resuspended in 100 µL Western Blot lysis buffer and homogenized by sonification on ice. On the other hand, pellets were used for mass spectroscopy analysis. Lipids were extracted as described before by Bligh and Dyer method [51] and cellular DAO-PE adducts were analyzed as specified above.

SDS PAGE and Western Blot

Subcellular fractions (see above) or isolated monocytes were resuspended in 100 µL ice-cold 2 × SDS loading buffer (20 mM Tris-HCl pH 8, 2 mM EDTA, 5% (m/v) SDS, 10% (v/v) β-mercaptoethanol, 10 µg/mL leupeptin, 60 µg/mL soybean trypsin (STI), 1 mM PMSF, 40 µL glycerol and 0.1% bromophenol blue (1:1, v/v). Samples were heated for 5 min at 96 °C and proteins were separated by SDS-PAGE on a 10% acrylamide gel. Correct protein loading on the gels and transfer of proteins to the nitrocellulose membrane (Amersham PROTRAN® supported 0.45 NC, GE Healthcare, Freiburg; Germany) was confirmed by Ponceau staining. Antibody recognizing cleaved PARP (Asp214), phospho-p38 MAPK (Thr180/Tyr182), phosho-Akt (Ser473), ATF-4, CHOP, BiP, calnexin, syntaxin 6, COX IV and β-actin were from

Cell Signaling Technology (Boston, MA) and used at 1:1000 dilution. Antibodies against GAPDH and β-tubulin were purchased from SantaCruz (Dallas, TX) and also used at 1:1000 dilution. Antibodies against Lamin B1 (1:200), syntaxin 6 (1:1000) and Lamp1 (1:1000) were purchased from abcam (Cambridge, United Kingdom). Infrared labeled secondary antibody IRDye 800CW goat anti-mouse was from LI-COR Biosciences (Lincoln, NE). For detection, the Odyssey Infrared Imaging System (LI-COR Bioscience, Lincoln, NE) and for analysis the Odyssey application software (version 3.0.25) were used.

Statistics

Results are presented as means ± standard error of the mean (SEM) of *n* independent observations, where *n* represents the number of performed experiments at different days or with different donors. Statistical analysis of the data was performed by one-way ANOVA using GraphPad InStat (Graphpad Software Inc., San Diego, CA) followed by a Bonferroni post-hoc test for multiple or student t-test for single comparisons, respectively. P-values < 0.05 were considered as significant.

Acknowledgments

This work was supported by the Collaborative Research Centers ChemBioSys (SFB1127) and Polytarget (SFB1278) of the Deutsche Forschungsgemeinschaft (DFG) and by the DFG-funded excellence graduate school Jena School for Microbial Communication (JSMC).

Declaration of Interests

The authors declare no competing interests.

Legends for the figures

Figure 1: DAO causes rapid cell death in human cells with unique characteristics.

(A) Chemical structure of DAO. (B) Monocytes were incubated with DAO at indicated concentrations for 15 min, 60 min, and 24 hrs. Cell viability was analyzed by MTT assay. Means ± SEM, n =3. (C) Monocytes or HeLa cells were incubated with DAO (5 µM) for the indicated time points. Plasma membrane integrity was analyzed by LDH assay. Means ± SEM, n =3. *p < 0.05, **p < 0.01, ***p < 0.001 vs vehicle control; ANOVA plus Bonferroni post hoc test. (D) Morphological analysis of HeLa cells by light microscopy. Cells were treated with the compounds at indicated concentrations for 3 hrs and were then analyzed by light microscopy. Pictures shown are representatives out of three independent experiments. (E) TEM analysis of monocytes. Freshly isolated human monocytes were pretreated with 10 µM DAO, 3 µM Stsp or vehicle (0.1% DMSO) for 3 hrs. Cells were prepared for TEM analysis which was performed as described in the Method section. Arrows indicate the presence of mitochondria.

Figure 2: Contribution of apoptotic pathways in mediating cell death by DAO.

(A) Monocytes were treated with DAO (5 µM) or staurosporine (Stsp, 3 µM) for the indicated time points. Then, PARP cleavage to an 89 kDa fragment was assessed by Western Blotting (left panel) and densitometric analysis (right panel) was performed in correlation to GAPDH. Means ± SEM, n = 3. (B) Cytochrome C release from human monocytes. Intact monocytes were pretreated with 10 µM DAO, 3 µM Stsp or vehicle (0.1% DMSO) for 3 hrs. Then, cells were fractionated by mild detergent lysis and the cytosolic and the non-cytosolic fractions were analyzed by Western blot for cytochrome (Cyt) c. β-Actin and calnexin were used as marker proteins for respective fractions. (C) Monocytes were incubated with 5 µM DAO, 3 µM Stsp or vehicle. Total cell lysates were prepared after the indicated times and analyzed for phospho-p38 MAPK and phospho-Akt by Western blot (left panel). Densitometric analysis (right panel) was performed in correlation to β-actin. Means ± SEM, n = 3. (D) Protein expression of BiP, ATF-4 and CHOP in monocytes. Cells were incubated with DAO (5 µM) or vehicle (0.1% DMSO) for the indicated time points and then analyzed by Western blot (left panel). Densitometric analysis (right panel) was performed in correlation to β-actin. Means ± SEM, n = 3. (E) Monocytes were pre-incubated with the pan-caspase inhibitor QVD (10 µM) 30 min prior incubation with 5 µM DAO, 3 µM Stsp or vehicle for 3 hrs. Protein levels were analyzed by Western Blot (lower panel) and densitometric analysis (upper panel) were performed in correlation to GAPDH. (F) Monocytes were pre-incubated with the pan-caspase inhibitor QVD (10 µM) 30 min prior incubation with 10 µM DAO, 3 µM Stsp or vehicle for 3 hrs (left panel) or 48 hrs (right panel). Then, cell viability was assessed by MTT assay. Means ± SEM, n = 3. *p < 0.05, **p < 0.01, ***p < 0.001 vs vehicle control; ANOVA plus Bonferroni post hoc test.

Figure S1: Effect of staurosporine on PARP cleavage after 5 hrs incubation.

Monocytes were treated with DAO (5 µM) or staurosporine (Stsp, 3 µM) for 5 hrs. Then, PARP cleavage to a 89 kDa fragment was assessed by Western Blotting (left panel) and densitometric analysis (right panel) was performed in correlation to GAPDH. Means ± SEM, n = 3. p < 0.05, **p < 0.01, ***p < 0.001 vs vehicle control; students t-test.

Figure 3: DAO interacts with the ethanolamine (EA) residue of phosphatidylethanolamine.

(A, B) DAO (0.5 mM) was incubated with chicken egg PE (13 mM in $CHCl_3$), chicken PC (13 mM in $CHCl_3$) and bovine brain PS in reaction buffer for 3 hrs at 37 °C. Then, phospholipids were cleaved by exogenously added phospholipase D for 16 hrs at 37 °C (insert panel A). DAO-EA, -choline or –serine adducts were analyzed by UPLC-MS/MS. (C) Monocytes and HeLa cells were incubated with DAO at the indicated concentrations for 3 hrs. DAO-PE adducts were extracted with $CHCl_3$/MeOH (3:1) and cleaved by phospholipase D treatment for analysis of DAO-EA adducts by UPLC-MS/MS. Means ± SEM, n = 3. (D) Monocytes and HeLa cells were incubated with 5 µM DAO for the indicated periods. DAO-PE adducts were extracted and analyzed by UPLC-MS/MS. Means ± SEM, n = 3. (E) DAO (5 µM), Stsp (1 µM) or vehicle (0.1% DMSO) were incubated with 50 mM EA for 2 hrs at 37 °C and subsequently extracted using MeOH/$CHCl_3$ (1:2, vol:vol) as described in the Method section. Extracts containing EA-adducts or unreacted DAO or Stsp were resolved in ethanol (vehicle) and added to monocytes (left panel) or HeLa cells (right panel) for 3 hrs, and cell viability was assessed by MTT assay. (F) DAO (10 µM), Stsp (3 µM) or vehicle (0.1% DMSO) were incubated with EA, choline (Chol) or L-serine (L-Ser) (50 mM, each) for 2 hrs at 37 °C and subsequently extracted as described above. Extracts containing adducts or unreacted agents (in ethanol as vehicle) were added to monocytes for 3 hrs (left panel) or 48 hrs (right panel), and cell viability was assessed by MTT assay. Data are means ± S.E, n = 3. *p < 0.05, **p < 0.01, ***p < 0.001, ****p < 0.0001 vs vehicle control; ANOVA plus Bonferroni post hoc test.

Figure S2: Markers subcellular fractionation.

HeLa cells were incubated with DAO (5 µM) or vehicle (0.1% DMSO) 15 min. Subcellular fractions were generated by hypotonic cell lysis and differential centrifugation. Respective fractions were analyzed by Western blot for specific fraction proteins. Western blots are representative for three independent experiments.

Figure 4: Subcellular locales of DAO-PE interactions and consequences for PE contents and membrane stability.

HeLa cells were incubated with DAO (5 µM) or vehicle (0.1% DMSO) for the indicated time points. Subcellular fractions were generated by hypotonic cell lysis and differential centrifugation. (A) Subcellular distribution of PE in HeLa cells after 15 min (left panel) and 3 hrs (right panel). (B) Subcellular distribution of DAO-PE adducts. The DAO-PE adducts formed within 15 min (left panel) or after 3 hrs (right panel) were extracted with $CHCl_3$/MeOH (3:1), cleaved by phospholipase D from PE, and then analyzed with UPLC-MS/MS. (C, D, E) HeLa cells were pre-incubated with 5 µM DAO for 3 hrs (C) or 15 min only (D). PE species were extracted by the Bligh and Dyer method and were analyzed by UPLC-MS/MS. (E) Correlation of PE species obtained after 15 min and after 3 hrs to total PE. (F) Correlation of PE species obtained after 15 min and after 3 hrs to vehicle control, shown as heat map. Data are given as mean + S.E, n = 3. *p < 0.05, **p < 0.01, ***p < 0.001 vs vehicle control; ANOVA plus Bonferroni post hoc test. (G) Liposomal leakage test. Liposomes (LUVs) composed of DOPC or DOPC/DOPE (1:1) containing HPTS/DPX were incubated with DAO (10 µM) and the fluorescence was measured. Liposomal leakage is expressed as % of the positive control

incubated with Triton X-100 (=100%). (H) Monocytes were incubated with DAO at the indicated concentrations or vehicle (0.1% DMSO) for 15 min or 60 min, acidic vesicles (red) were stained with the Lysotracker probe for 5 min. Fluorescence microscopy pictures (left panel) are representative of four independent experiments. Acidification of vesicles (right panel) was assessed by fluorescence measured by NOVOstar®. Acidification is expressed in correlation to Hoechst staining of each cell per sample with vehicle = 100%. Data are given as mean + S.E, n = 3. *p < 0.05, **p < 0.01, ***p < 0.001 vs vehicle control; ANOVA plus Bonferroni post hoc test.

Figure S3: Liposomal leakage test.

Liposomes (LUVs) composed of DOPC or DOPC/DOPE (1:1) containing HPTS/DPX were incubated with vehicle (DMSO, negative control) or DAO (10 µM) and the fluorescence was measured. Results are representative for n=3 independent experiments.

References

1. Bohnert, M., et al., *In vitro cytotoxicity of melleolide antibiotics: structural and mechanistic aspects.* Bioorg Med Chem Lett, 2011. **21**(7): p. 2003-6.
2. Bohnert, M., et al., *Cytotoxic and antifungal activities of melleolide antibiotics follow dissimilar structure-activity relationships.* Phytochemistry, 2014. **105**: p. 101-8.
3. Bohnert, M., et al., *Melleolides induce rapid cell death in human primary monocytes and cancer cells.* Bioorg Med Chem, 2014. **22**(15): p. 3856-61.
4. Misiek, M., et al., *Structure and cytotoxicity of arnamial and related fungal sesquiterpene aryl esters.* J Nat Prod, 2009. **72**(10): p. 1888-91.
5. Momose, I., et al., *Melleolides K, L and M, new melleolides from Armillariella mellea.* J Antibiot (Tokyo), 2000. **53**(2): p. 137-43.
6. Dorfer, M., et al., *Melleolides impact fungal translation via elongation factor 2.* Org Biomol Chem, 2019.17(19):4906-16
7. Konig, S., et al., *Melleolides from Honey Mushroom Inhibit 5-Lipoxygenase via Cys159.* Cell Chem Biol, 2019. **26**(1): p. 60-70 e4.
8. Chang, W.H., et al., *Armillaridin induces autophagy-associated cell death in human chronic myelogenous leukemia K562 cells.* Tumour Biol, 2016. **37**(10): p. 14291-14300.
9. Chen, Y.J., C.C. Chen, and H.L. Huang, *Induction of apoptosis by Armillaria mellea constituent armillarikin in human hepatocellular carcinoma.* Onco Targets Ther, 2016. **9**: p. 4773-83.
10. Yin, X., T. Feng, and J.-K. Liu, *Structures and cytotoxicities of three new sesquiterpenes from cultures of Armillaria sp.* Nat Prod and Bioprospect, 2012. **2**(6): p. 245-248.
11. Chen, C.C., et al., *Three New Sesquiterpene Aryl Esters from the Mycelium of Armillaria mellea.* Molecules, 2015. **20**(6): p. 9994-10003.
12. Chi, C.W., C.C. Chen, and Y.J. Chen, *Therapeutic and radiosensitizing effects of armillaridin on human esophageal cancer cells.* Evid Based Complement Alternat Med, 2013. **2013**: p. 459271.
13. Liu, T.P., et al., *Armillaridin, a Honey Medicinal Mushroom, Armillaria mellea (Higher Basidiomycetes) Component, Inhibits Differentiation and Activation of Human Macrophages.* Int J Med Mushrooms, 2015. **17**(2): p. 161-8.
14. Clarke, P.G., *Developmental cell death: morphological diversity and multiple mechanisms.* Anat Embryol (Berl), 1990. **181**(3): p. 195-213.
15. Galluzzi, L., et al., *Cell death modalities: classification and pathophysiological implications.* Cell Death Differ, 2007. **14**(7): p. 1237-43.

16. Kroemer, G. and M. Jaattela, *Lysosomes and autophagy in cell death control.* Nat Rev Cancer, 2005. **5**(11): p. 886-97.
17. Taylor, R.C., S.P. Cullen, and S.J. Martin, *Apoptosis: controlled demolition at the cellular level.* Nat Rev Mol Cell Biol, 2008. **9**(3): p. 231-41.
18. Mizushima, N., *Autophagy: process and function.* Genes Dev, 2007. **21**(22): p. 2861-73.
19. Levine, B. and G. Kroemer, *Autophagy in the pathogenesis of disease.* Cell, 2008. **132**(1): p. 27-42.
20. Festjens, N., T. Vanden Berghe, and P. Vandenabeele, *Necrosis, a well-orchestrated form of cell demise: signalling cascades, important mediators and concomitant immune response.* Biochim Biophys Acta, 2006. **1757**(9-10): p. 1371-87.
21. Golstein, P. and G. Kroemer, *Cell death by necrosis: towards a molecular definition.* Trends Biochem Sci, 2007. **32**(1): p. 37-43.
22. Vance, J.E., *Phospholipid synthesis and transport in mammalian cells.* Traffic, 2015. **16**(1): p. 1-18.
23. Emoto, K., et al., *Exposure of phosphatidylethanolamine on the surface of apoptotic cells.* Exp Cell Res, 1997. **232**(2): p. 430-4.
24. Dowhan, W. and M. Bogdanov, *Lipid-dependent membrane protein topogenesis.* Annu Rev Biochem, 2009. **78**: p. 515-40.
25. van den Brink-van der Laan, E., J.A. Killian, and B. de Kruijff, *Nonbilayer lipids affect peripheral and integral membrane proteins via changes in the lateral pressure profile.* Biochim Biophys Acta, 2004. **1666**(1-2): p. 275-88.
26. Verkleij, A.J., et al., *Non-bilayer structures in membrane fusion.* Ciba Found Symp, 1984. **103**: p. 45-59.
27. Bottinger, L., et al., *Phosphatidylethanolamine and cardiolipin differentially affect the stability of mitochondrial respiratory chain supercomplexes.* J Mol Biol, 2012. **423**(5): p. 677-86.
28. Birner, R., et al., *Roles of phosphatidylethanolamine and of its several biosynthetic pathways in Saccharomyces cerevisiae.* Mol Biol Cell, 2001. **12**(4): p. 997-1007.
29. Ichimura, Y., et al., *A ubiquitin-like system mediates protein lipidation.* Nature, 2000. **408**(6811): p. 488-92.
30. Rockenfeller, P., et al., *Phosphatidylethanolamine positively regulates autophagy and longevity.* Cell Death Differ, 2015. **22**(3): p. 499-508.
31. Menon, A.K. and V.L. Stevens, *Phosphatidylethanolamine is the donor of the ethanolamine residue linking a glycosylphosphatidylinositol anchor to protein.* J Biol Chem, 1992. **267**(22): p. 15277-80.
32. Falcieri, E., et al., *The protein kinase inhibitor staurosporine induces morphological changes typical of apoptosis in MOLT-4 cells without concomitant DNA fragmentation.* Biochem Biophys Res Commun, 1993. **193**(1): p. 19-25.
33. Green, D.R. and G. Kroemer, *The pathophysiology of mitochondrial cell death.* Science, 2004. **305**(5684): p. 626-9.
34. Hemmings, B.A., *Akt signaling: linking membrane events to life and death decisions.* Science, 1997. **275**(5300): p. 628-30.
35. Watanabe, T., et al., *Apoptosis Signal-regulating Kinase 1 (ASK1)-p38 Pathway-dependent Cytoplasmic Translocation of the Orphan Nuclear Receptor NR4A2 Is Required for Oxidative Stress-induced Necrosis.* J Biol Chem, 2015. **290**(17): p. 10791-803.
36. Dunai, Z.A., et al., *Staurosporine induces necroptotic cell death under caspase-compromised conditions in U937 cells.* PLoS One, 2012. **7**(7): p. e41945.
37. Mebarek, N., et al., *Polymeric micelles based on poly(methacrylic acid) block-containing copolymers with different membrane destabilizing properties for cellular drug delivery.* Int J Pharm, 2013. **454**(2): p. 611-20.
38. Campbell, W.G., *The chemistry of the white rots of wood: The effect on wood substance of Armillaria mellea (Vahl.) Fr., Polyporus hispidus (Bull.) Fr., and Stereum hirsutum Fr.* Biochem J, 1931. **25**(6): p. 2023-7.
39. Richard, C., *[Antibiotic activity of Armillaria mellea].* Can J Microbiol, 1971. **17**(11): p. 1395-9.

40. Donnelly, D.M., et al., *Antibacterial sesquiterpene aryl esters from Armillaria mellea.* J Nat Prod, 1985. **48**(1): p. 10-6.
41. Obuchi, T., et al., *Armillaric acid, a new antibiotic produced by Armillaria mellea.* Planta Med, 1990. **56**(2): p. 198-201.
42. Evidente, A., et al., *Herbicidal potential of ophiobolins produced by Drechslera gigantea.* J Agric Food Chem, 2006. **54**(5): p. 1779-83.
43. Chidley, C., et al., *The anticancer natural product ophiobolin A induces cytotoxicity by covalent modification of phosphatidylethanolamine.* Elife, 2016. **5**.
44. Morrison, R., et al., *Ophiobolin A, a sesterpenoid fungal phytotoxin, displays different mechanisms of cell death in mammalian cells depending upon the cancer cell origin.* International Journal of Oncology, 2017. **50**(3): p. 773-786.
45. Bury, M., et al., *Ophiobolin A induces paraptosis-like cell death in human glioblastoma cells by decreasing BKCa channel activity.* Cell Death Dis, 2013. **4**: p. e561.
46. Rodolfo, C., et al., *Ophiobolin A Induces Autophagy and Activates the Mitochondrial Pathway of Apoptosis in Human Melanoma Cells.* PLoS One, 2016. **11**(12): p. e0167672.
47. Bell, B.D., et al., *FADD and caspase-8 control the outcome of autophagic signaling in proliferating T cells.* Proc Natl Acad Sci U S A, 2008. **105**(43): p. 16677-82.
48. Yu, L., et al., *Regulation of an ATG7-beclin 1 program of autophagic cell death by caspase-8.* Science, 2004. **304**(5676): p. 1500-2.
49. Garscha, U., et al., *BRP-187: A potent inhibitor of leukotriene biosynthesis that acts through impeding the dynamic 5-lipoxygenase/5-lipoxygenase-activating protein (FLAP) complex assembly.* Biochem Pharmacol, 2016. **119**: p. 17-26.
50. MacDonald, R.C., et al., *Small-volume extrusion apparatus for preparation of large, unilamellar vesicles.* Biochim Biophys Acta, 1991. **1061**(2): p. 297-303.
51. Koeberle, A., et al., *Role of lysophosphatidic acid acyltransferase 3 for the supply of highly polyunsaturated fatty acids in TM4 Sertoli cells.* FASEB J, 2010. **24**(12): p. 4929-38.

Figure 1

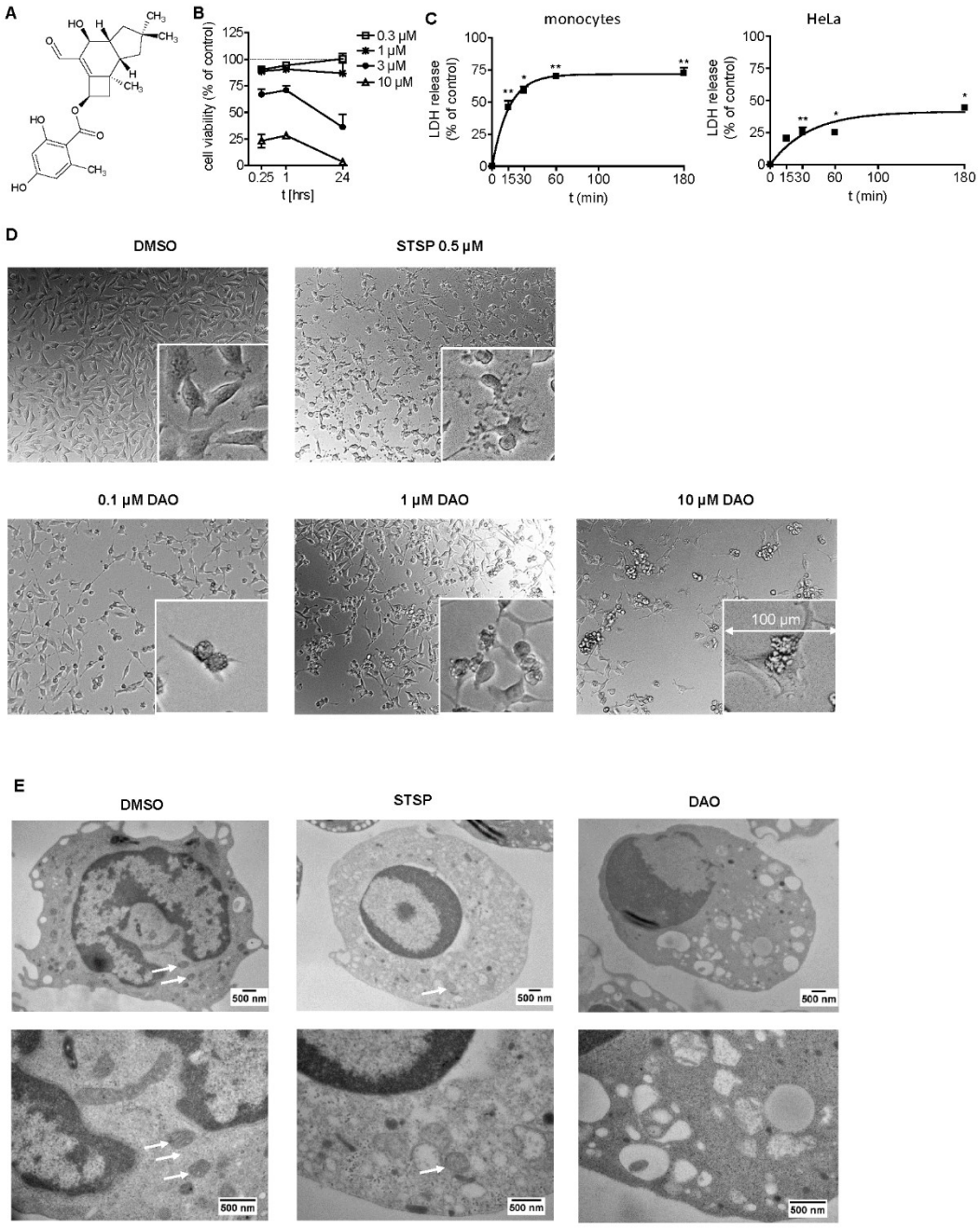
A
B
cell viability (% of control)
t [hrs]
0.3 µM
1 µM
3 µM
10 µM
C
monocytes
HeLa
LDH release (% of control)
t (min)
D
DMSO
STSP 0.5 µM
0.1 µM DAO
1 µM DAO
10 µM DAO
100 µm
E
DMSO
STSP
DAO
500 nm

Figure 2

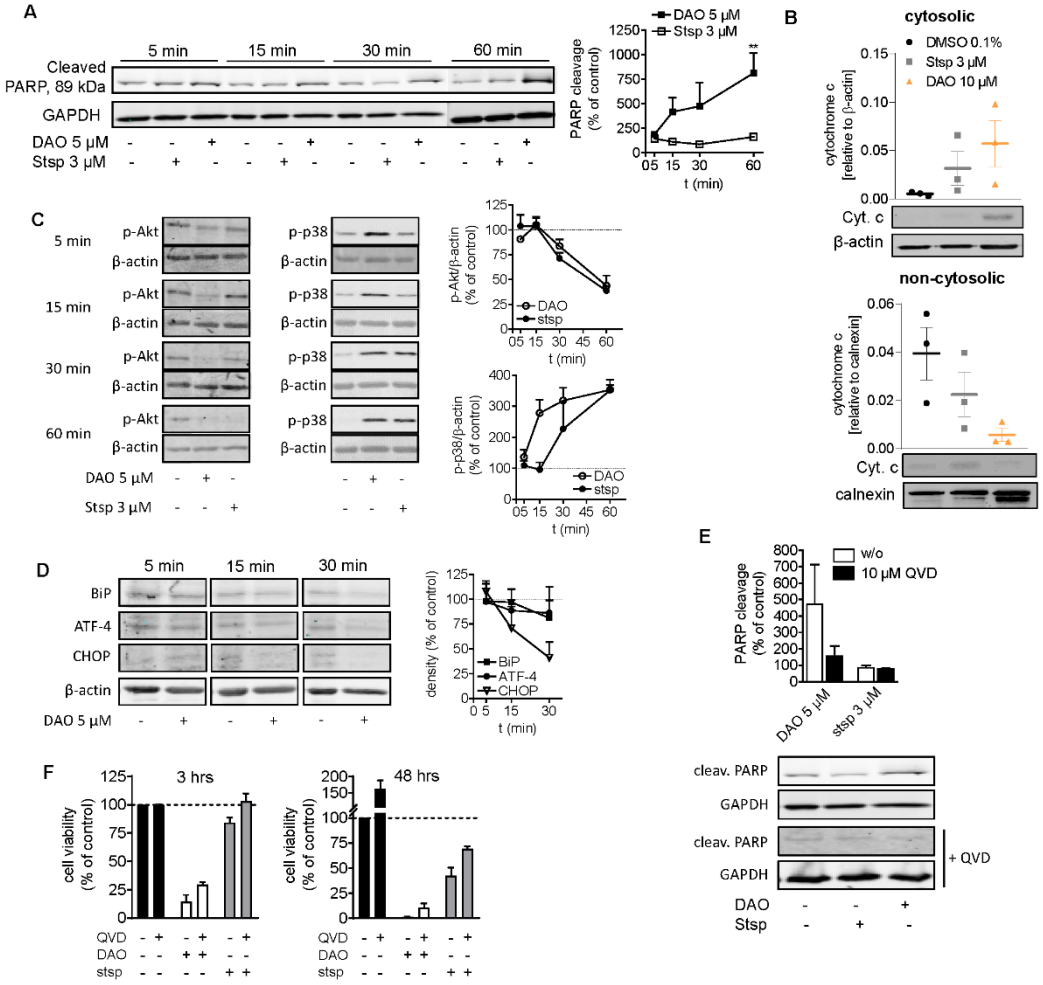
A
5 min
15 min
30 min
60 min
Cleaved PARP, 89 kDa
GAPDH
DAO 5 µM
Stsp 3 µM
PARP cleavage (% of control)
t (min)
B
cytosolic
DMSO 0.1%
Stsp 3 µM
DAO 10 µM
cytochrome c [relative to β-actin]
Cyt. c
β-actin
non-cytosolic
cytochrome c [relative to calnexin]
calnexin
C
p-Akt
p-p38
β-actin
p-Akt/β-actin (% of control)
p-p38/β-actin (% of control)
DAO
stsp
D
BiP
ATF-4
CHOP
density (% of control)
E
w/o
10 µM QVD
cleav. PARP
+ QVD
F
3 hrs
48 hrs
cell viability (% of control)
QVD
DAO
stsp

Figure 3

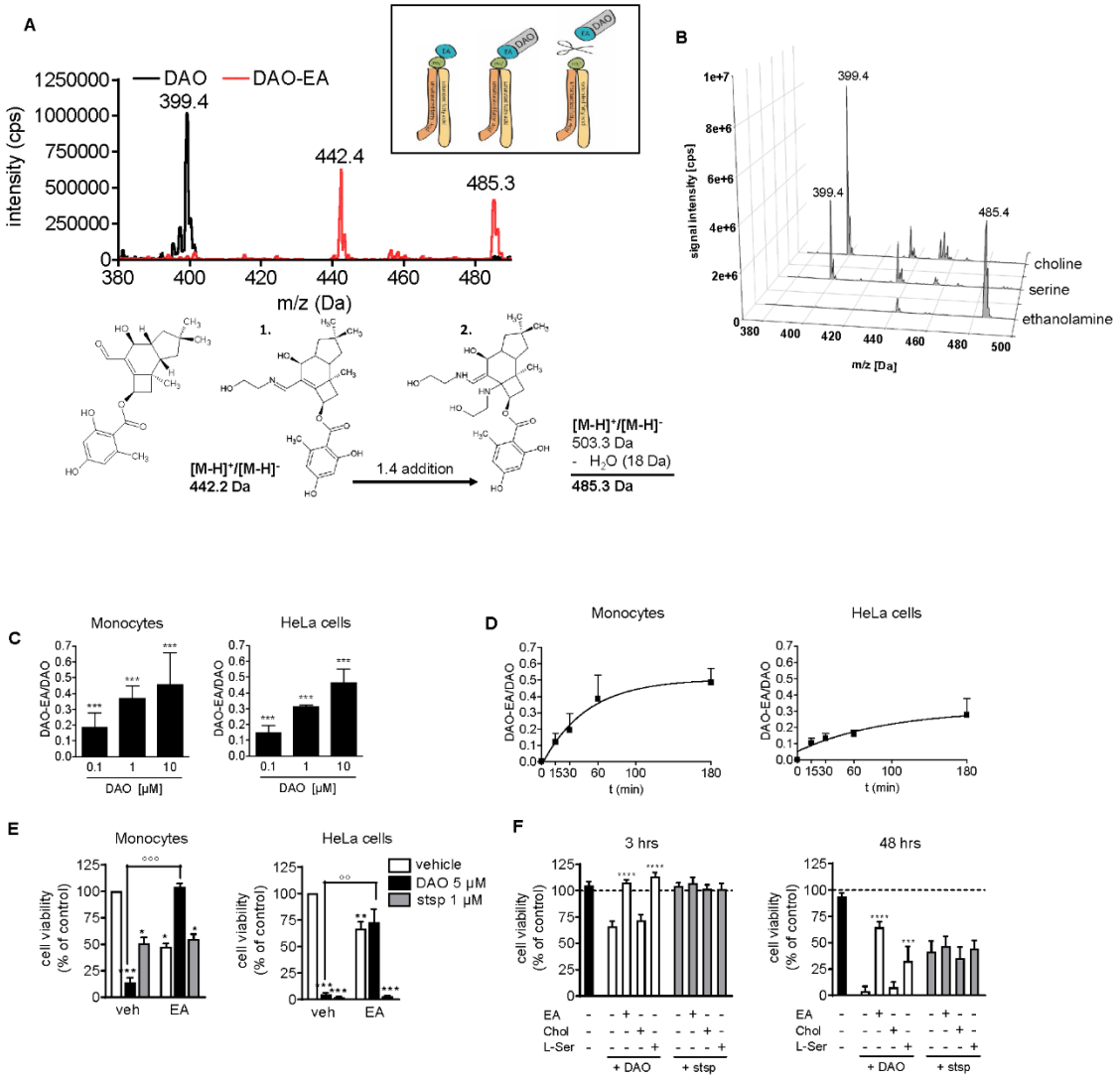
A
DAO
DAO-EA
399.4
442.4
485.3
intensity (cps)
m/z (Da)
[M-H]+/[M-H]- 442.2 Da
1.4 addition
[M-H]+/[M-H]- 503.3 Da
- H2O (18 Da)
485.3 Da
B
399.4
485.4
choline
serine
ethanolamine
signal intensity [cps]
m/z [Da]
C
Monocytes
HeLa cells
DAO-EA/DAO
DAO [µM]
D
Monocytes
HeLa cells
DAO-EA/DAO
t (min)
E
Monocytes
HeLa cells
vehicle
DAO 5 µM
stsp 1 µM
cell viability (% of control)
veh
EA
F
3 hrs
48 hrs
cell viability (% of control)
EA
Chol
L-Ser
+ DAO
+ stsp

Figure 4

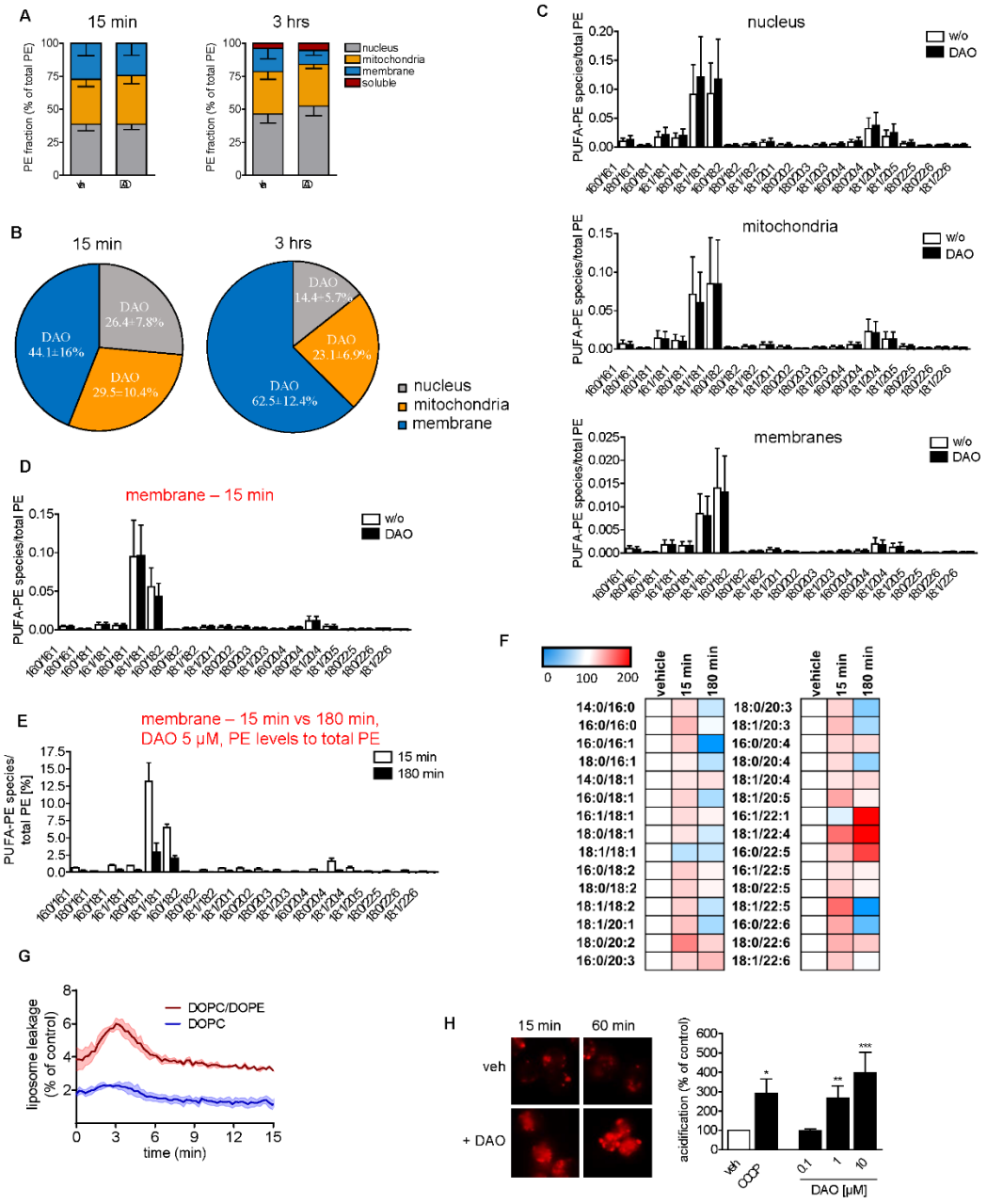
A
15 min
3 hrs
PE fraction (% of total PE)
nucleus
mitochondria
membrane
soluble
B
15 min
3 hrs
DAO 26.4±7.8%
DAO 44.1±16%
DAO 29.5±10.4%
DAO 14.4±5.7%
DAO 23.1±6.9%
DAO 62.5±12.4%
nucleus
mitochondria
membrane
C
nucleus
mitochondria
membranes
w/o
DAO
PUFA-PE species/total PE
D
membrane – 15 min
PUFA-PE species/total PE
E
membrane – 15 min vs 180 min,
DAO 5 µM, PE levels to total PE
15 min
180 min
PUFA-PE species/ total PE [%]
F
vehicle
15 min
180 min
14:0/16:0
16:0/16:0
16:0/16:1
18:0/16:1
14:0/18:1
16:0/18:1
16:1/18:1
18:0/18:1
18:1/18:1
16:0/18:2
18:0/18:2
18:1/18:2
18:1/20:1
18:0/20:2
16:0/20:3
18:0/20:3
18:1/20:3
16:0/20:4
18:0/20:4
18:1/20:4
18:1/20:5
16:1/22:1
18:1/22:4
16:0/22:5
16:1/22:5
18:0/22:5
18:1/22:5
16:0/22:6
18:0/22:6
18:1/22:6
G
liposome leakage (% of control)
DOPC/DOPE
DOPC
time (min)
H
15 min
60 min
veh
+ DAO
acidification (% of control)
veh
CCCP
0.1
1
10
DAO [µM]

Supplemental Figure 1

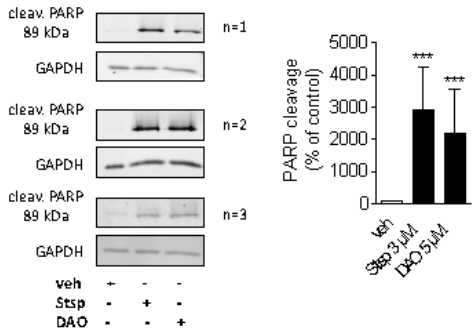

Supplemental Figure 2

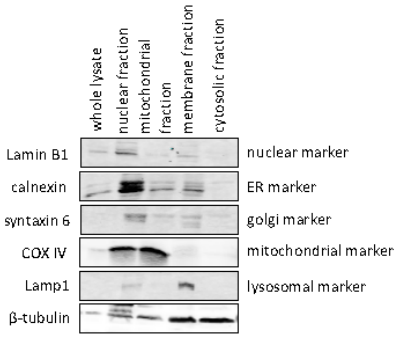

Supplemental Figure 3

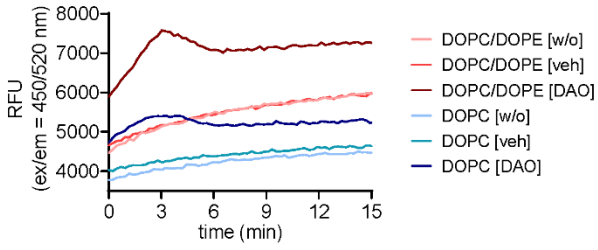

APPENDIX 3: AUTHORS´ CONTRIBUTIONS TO THE MANUSCRIPTS

Manuscript I

Author	Contribution
Stefanie König	Experimental design and performance of 5-LOX assays, immunofluorescence analysis, proximity ligation assays; assistance to HEK cell transfection; measurement of 5-LOX expression, FLAP expression, and phosphorylation of $cPLA_2$, ERK-1/2, p38 MAPK by Western Blot; maintenance of cell culture and performance of blood cell isolation; data analysis; writing the manuscript. Total contribution: 80%.
Erik Romp	HEK cell transfection with cysteine mutants; performance of [^{3}H]-labeled arachidonic acid release; support with immunofluorescence and PLA interpretation; maintenance of cell culture.
Verena Krauth	Performance of COX-1/COX-2 assays and $mPGES_1$ activity assay; assistance to 5-LOX assays; performance of blood cell isolation.
Michael Rühl	Performance of GSH incubation, standard peptide incubation, MALDI-MS measurement and data analysis.
Maximilian Dörfer	Isolation of DAO from *Armillaria mellea*.
Stefanie Liening	Performance of LTC_4S activity assay.
Bettina Hofmann	Supply of 5-LOX cysteine mutants; helped with interpretation of MALDI-MS data; experimental design.
Ann-Kathrin Häfner	Supply of 5-LOX cysteine mutants.
Dieter Steinhilber	Supply of 5-LOX cysteine mutants; experimental design.
Michael Karas	Performance of GSH incubation, standard peptide incubation, MALDI-MS measurement and data analysis; experimental design.
Dirk Hoffmeister	Isolation of DAO from *Armillaria mellea*; experimental design.
Ulrike Garscha	HEK cell transfection with cysteine mutants; support with immunofluorescence and PLA interpretation; experimental design.
Oliver Werz	Conceiving the project; experimental design, writing the manuscript.

Manuscript II

Author	Contribution
Stefanie König	Experimental design and performance of 5-LOX assays with several cell types, purified enzyme, agents, and stimuli, LM extraction for UPLC-MS/MS analysis; extraction of LM from animal samples and their analysis by UPLC-MS/MS and ELISA; experimental design, optimization and performance of epoxide hydrolase and aminopeptidase activity assays of LTA_4H; maintenance of cell culture and performance of blood cell isolation; data analysis; writing the manuscript. Total contribution: 75%..
Simona Pace	Experimental design and performance of animal models: peritonitis, pleurisy.
Helmut Pein	Experimental design, optimization and performance of aminopeptidase activity assay by UPLC-MS/MS.
Thorsten Heinekamp	Experimental design and performance of murine infection model with *A. fumigatus* conidia; cultivation of *A. fumigatus* and preparation of supernatants; histopathological investigations of murine lung tissue.
Jan Kramer	Performance of epoxide hydrolase activity by fluorescence-based assay; expression and purification of human recombinant LTA_4H; analysis of gliotoxin by UPLC-MS/MS after GSH incubation.
Erik Romp	Performance of sEH activity assay; maintenance of cell culture and performance of blood cell isolation.
Maria Straßburger	Assistance to performance of *A. fumigatus* experiments; histopathological investigations of murine lung tissue.
Fabiane Troisi	Assistance to performance of animal models: peritonitis, pleurisy.
Anna Proschak	Analysis of gliotoxin by UPLC-MS/MS.
Jan Dscherwak	Isolation of gliotoxin and derivatives from *A. fumigatus*.
Kirstin Scherlach	Isolation of gliotoxin and derivatives from *A. fumigatus*.
Antonietta Rossi	Experimental design and performance of animal models: peritonitis, pleurisy.
Lidia Sautebin	Experimental design and performance of animal models: peritonitis, pleurisy.

Jesper Z. Haeggström	Support with interpretation of LTA_4H data; experimental design.
Christian Hertweck	Isolation of gliotoxin and derivatives from *A. fumigatus.*
Axel Brakhage	Conceiving the project; experimental design.
Jana Gerstmeier	experimental design; helped with the interpretation of gliotoxin data.
Ewgenij Proschak	Performance of epoxide hydrolase activity by fluorescence-based assay; supply of human recombinant LTA_4H; analysis of gliotoxin by UPLC-MS/MS; experimental design.
Oliver Werz	Conceiving the project; experimental design, writing the manuscript.

Manuscript III

Author	**Contribution**
Sebastian Schieferdecker	Experimental design and performance of production and isolation of myxochelins; performance and design of isotope incorporation; performance of chrome azurol assay; cultivation of *Pyxidicoccus fallax*; data analysis; partially writing the manuscript.
Stefanie König	Experimental design and performance of 5-LOX assays with purified enzyme, purification of human recombinant 5-LOX from *E. coli*; coordination of mPGES-1 activity assay; data analysis; partially writing the manuscript. Total contribution: 30%.
Andreas Koeberle	Experimental design; coordination of mPGES-1 activity assay; support with the analysis of data from 5-LOX and mPGES-1 activity assays.
Hans-Martin Dahse	Performance of MTT assay with HeLa and K-562 cells.
Oliver Werz	Conceiving the project; experimental design, partially writing the manuscript.
Markus Nett	Conceiving the project; experimental design, partially writing the manuscript.

Manuscript IV

Author	Contribution
Markus Bohnert	Experimental design and performance of isolation of melleolides; partially writing the manuscript.
Olga Scherer	Experimental design and performance of MTT assays, inverse MTT and LDH assay; evaluation and performance of life cell imaging and flow cytometry experiments; data analysis; partially writing the manuscript.
Katja Wiechmann	Experimental design and performance of mitochondrial analysis; partially writing the manuscript.
Stefanie König	Experimental design and performance of MTT assays with DAO and staurosporine in human primary monocytes and HeLa cells; isolation of monocytes and cell culture; data analysis; partially writing the manuscript. Total contribution: 20%.
Hans-Martin Dahse	Performance of MTT assay with K-562 cells
Dirk Hoffmeister	Conceiving the project; experimental design, partially writing the manuscript.
Oliver Werz	Conceiving the project; experimental design, partially writing the manuscript.

Manuscript V

Author	Contribution
Stefanie König	Experimental design and performance of MTT and LDH assay, Western Blot analysis of phospho-p38 MAPK, phospho-Akt, BiP, CHOP, and ATF-4 in monocytes; experimental design and performance of measurement of non-cellular and cellular DAO-PE adducts for UPLC-MS/MS analysis after treatment with phospholipase D; extraction of cellular DAO-PE adducts and their analysis by UPLC-MS/MS; experimental design, optimization and performance of subcellular fractionation, Western Blot analysis of each fraction, extraction of cellular DAO-PE adducts and phospholipids in separated fractions and their analysis by UPLC-MS/MS; maintenance of cell culture

	and performance of blood cell isolation; data analysis; writing the manuscript. Total contribution: 70%.
Konstantin Löser	Experimental design, optimization and performance of subcellular fractionation, optimization and performance of measurements of DAO fragments with UPLC-MS/MS; partially writing the manuscript.
Helmut Pein	Experimental design, optimization and performance of DAO-PE binding assay with UPLC-MS/MS and measurements of DAO fragments with UPLC-MS/MS; partially writing the manuscript.
Konstantin Neukirch	Performance and analysis of MTT assay in monocytes with QVD pre-incubation and with ethanolamine, serine, and choline; performance and analysis of liposomal leakage test.
Anna Czapka	Western blot analysis of Cytochrome c levels in monocytes after fractionation in cytosolic and non-cytosolic fraction, performance of transmission electron microscopy (TEM).
Stephanie Hoeppener	Experimental design, optimization and performance of TEM
Maximilian Dörfer	Isolation of DAO from *Armillaria mellea*.
Dirk Hoffmeister	Conceiving the project; experimental design, partially writing the manuscript.
Oliver Werz	Conceiving the project; experimental design, partially writing the manuscript.

APPENDIX 3: ACKNOWLEGDMENTS

Ich möchte mich ganz besonders bei meinem Doktorvater Prof. Dr. Oliver Werz für das Vertrauen und die Möglichkeit bedanken dieses äußerst spannende Projekt im Rahmen der Förderung der Exzellenz Graduiertenschule Jena School for Microbial Communication in seinem Arbeitskreis bearbeiten zu dürfen. Ganz besonders bedanke ich mich für seine exzellente Betreuung, den regen wissenschaftlichen Austausch, seine Unterstützung, sein jederzeit offenes Ohr und die stetige Motivation für die Bearbeitung kniffliger Fragestellungen.

Des Weiteren danke ich Prof. Dr. Dirk Hoffmeister für die Möglichkeit am DAO Projekt teilzuhaben. Außerdem möchte ich mich bei Ihm und Maximilian Dörfer bedanken für die Bereitstellung der Melleolide, die erfolgreiche wissenschaftliche Zusammenarbeit und die interessanten Anregungen für das DAO Projekt.

Allen Gutachtern danke ich für die Bereitschaft, die Gutachten zu übernehmen und anzufertigen.

Ich bedanke mich bei Prof. Dr. Axel Brakhage und Dr. Thorsten Heinekamp für die hervorragende Zusammenarbeit bei der Erforschung des Wirkmechanismus von Gliotoxin, die Durchführung des *Aspergillus fumigatus*-Infektions-Tiermodells, die Bereitstellung der Δ*gliP A. fumigatus* Mutante, die Hilfe bei der Interpretation der Gliotoxin Daten und der Erstellung des Gliotoxin Manuskriptes.

Außerdem möchte ich mich herzlich bedanken bei Prof. Dr. Ewgenij Proschak und Jan Kramer für die Hilfe und Unterstützung bei der Erstellung des Gliotoxin Manuskriptes, für die Durchführung der Experimente mit reduziertem Gliotoxin, der MS-Analytik für das Manuskript und die Bereitstellung von Gliotoxin und rekombinanter LTA_4H.

Weiterhin danke ich den Frankfurter Arbeitskreisen von Prof. Dr. Dieter Steinhilber und Prof. Dr. Michael Karas mit Dr. Bettina Hofmann und Michael Rühl für die tatkräftige Unterstützung und die regen wissenschaftlichen Diskussionen bei der Analyse der Interaktion von DAO und Cysteinen innerhalb der 5-Lipoxygenase, der Bereitstellung der Plasmide der 5-LOX Cystein-Mutanten, der Peptid-Analytik und die MALDI-MS Messungen.

Herrn Prof. Dr. Markus Nett, Dr. Sebastian Schieferdecker und Juliane Korp danke ich für die Synthese und Bereitstellung vielfältiger Myxocheline und für die erfolgreiche und hervorragende Zusammenarbeit hinsichtlich gemeinsamer Publikationen.

Bedanken möchte ich mich außerdem bei Prof. Dr. Christian Hertweck und Dr. Kirstin Scherlach für die Bereitstellung von Gliotoxin und die Hilfe bei chemischen Fragen zu Gliotoxin.

Ich danke Prof. Dr. Lidia Sautebin, Dr. Antonietta Rossi und dem Arbeitskreis in Neapel für die Durchführung der Tiermodelle.

Allen Koautoren danke ich für die ausgezeichnete wissenschaftliche Zusammenarbeit!

Vielen Dank an die Transfusionsmedizin des Universitätsklinikums Jena für die Bereitstellung von Blutspenden.

Weiterhin danke ich der Jena School for Microbial Communication für die Finanzierung meines Projektes.

Von Herzen danke ich meinen ehemaligen Kollegen des Philosophenweg 14! Ohne sie wäre diese erfolgreiche Arbeit nicht möglich gewesen und die gemeinsame Zeit nicht so intensiv und unvergesslich geworden! Vielen Dank für jedes offene Ohr, für jede Motivation, für jede Unterstützung und die vielen wunderbaren, gemeinsamen und geselligen Abende! Vielen Dank an:

Herrn PD Dr. Andreas Koeberle für die geduldige Beantwortung und hilfreichen Ratschläge aller aufkommenden wissenschaftlichen Fragen!

Frau Dr. Ulrike Garscha für ihre große Hilfe in Fragen der Molekularbiologie, ihr offenes Ohr für Probleme jeglicher Art und die kritische Diskussion wissenschaftlicher Ergebnisse.

Frau Dr. Simona Pace für die erfolgreiche Zusammenarbeit bei Kadsurenin F- und Gliotoxin-Projekt und für die durchgeführten *in vivo* Experimente.

Katrin Fischer und Petra Wiecha möchte ich von Herzen danken für die großartige Unterstützung im alltäglichen Laborgeschehen, die Hilfe bei der Testung vielzähliger Substanzen, die Einführung im Umgang mit der HPLC und der Liebe zum ELISA, dem Messen von MS-Proben und der geordneten Koordination vieler Laborvorgänge! Weiterhin danke ich Nadja Gerlitz für das ausgezeichnete Laborbestellmanagement, die witzigen Unterhaltungen und jede Aufmunterung! Uwe Beck danke ich für seine Hilfsbereitschaft, sein handwerkliches Geschick und den ein oder anderen Tipp für manch kreative Idee! Ich bedanke mich bei Shanice Liebeskind und Theresa Hildebrandt für die Hilfestellung bei allen administrativen Fragestellungen. Bei Monika Listing, Bärbel Schmalwasser und Heidi Traber möchte ich mich für die Unterstützung bei der Testung von Natursubstanzen bedanken.

Von ganzem Herzen möchte ich mich bei Euch, meinen beiden Jungs, Konstantin Löser und Helmut Pein, für diese unvergessliche und intensive Zeit bedanken. Danke Euch für Eure Hilfe, Eure Unterstützung, Eure offenen Ohren, Eure Kritik, Eure verrückten Ideen und die gemeinsam verbrachte Zeit. Verena Krauth, danke Dir für die vielen schönen und geselligen Abende, Deine aufbauenden Worte, Deine Zeit und Deine Hilfsbereitschaft im Labor als auch im wahren Leben. Zusammen mit Stefanie Liening, Markus Werner, Erik Romp, Jana Fischer,

Petra Wiecha, Katrin Fischer, Ulrike Garscha, Nadja Gerlitz, Olga Sailer und Katrin Schubert habt ihr meine Promotionszeit zu etwas Besonderem gemacht und ohne euch wäre die Zeit nur halb so schön gewesen! Den beiden Computer-Spezialisten Helmut Pein und Markus Werner danke ich für die exzellente Behebung jegliches IT- und Computerproblems. Herzlichen Dank auch an Olga Sailer für die Einführung in das DAO Thema und die Übergabe vielfältiger Tipps und Tricks der jeweiligen Methoden. Außerdem bedanke ich mich bei allen anderen Mitarbeitern, Doktoranden, Diplomanden und Masteranden, die mich auf meinem Weg begleitet haben, für diese schöne Zeit!

Ein ganz besonderer Dank gebührt meiner Oma Erna, meinen Eltern und meinem Bruder, die mir diesen Weg ermöglicht haben und an mich bedingungslos glauben. Ohne meine langjährigen Freunde Judith und Martin mit Ferdi, Doreen und Martin mit Jakob, Claudia und Peter, Christina, Martin, Conny und Helmut mit Emil und Junus, Franzi und Konstantin mit Magda, Maria und Markus mit Willi, Anne und Markus mit Emil und Theo wäre ich heute nicht da, wo ich jetzt bin! Danke Euch für Eure Kraft, Eure Unterstützung, Euer Vertrauen und Eure Freundschaft! Ihr seid unendlich wertvoll für mich!

„Wer gar zu viel bedenkt, wird wenig leisten.“ – Friedrich Schiller

APPENDIX 4: PUBLICATIONS AND CONFERENCE CONTRIBUTIONS

A3.1 Publications

König S, Löser K, Pein H, Neukirch K, Czapka A, Hoeppener S, Dörfer M, Hoffmeister D, Koeberle A, Werz O. *"Rapid cell death induction by the honey mushroom mycotoxin dehydroarmillylorsellinate through covalent reaction with membrane phosphatidylethanolamines."* **manuscript in preparation**, planned submission 3rd quarter 2019 to **Cell Chem Biol**

Dörfer M, Heine D, **König S**, Gore S, Werz O, Hertweck C, Gressler M, Hoffmeister D (2019). *"Melleolides impact fungal translation via elongation factor 2."* **Org Biomol Chem** 17(19):4906-4916

König S, Pace S, Pein H, Heinekamp T, Kramer J, Romp E, Straßburger M, Troisi F, Proschak A, Dworschak J, Scherlach K, Rossi A, Sautebin L, Haeggström JZ, Hertweck C, Brakhage AA, Gerstmeier J, Proschak E, Werz O (2019). *"Gliotoxin from Aspergillus fumigatus Abrogates Leukotriene B_4 Formation through Inhibition of Leukotriene A_4 Hydrolase."* **Cell Chem Biol** 26(4):524-534

König S, Romp E, Krauth V, Rühl M, Dörfer M, Liening S, Hofmann B, Häfner AK, Steinhilber D, Karas M, Garscha U, Hoffmeister D, Werz O (2019). *"Melleolides from Honey Mushroom Inhibit 5-Lipoxygenase via Cys159."* **Cell Chem Biol** 26(1):60-70

Pein H, Ville A, Pace S, Temml V, Garscha U, Raasch M, Alsabil K, Viault G, Dinh CP, Guilet D, Troisi F, Neukirch K, **König S**, Bilancia R, Waltenberger B, Stuppner H, Wallert M, Lorkowski S, Weinigel C, Rummler S, Birringer M, Roviezzo F, Sautebin L, Helesbeux JJ, Séraphin D, Mosig AS, Schuster D, Rossi A, Richomme P, Werz O, Koeberle A (2018). *"Endogenous metabolites of vitamin E limit inflammation by targeting 5-lipoxygenase."* **Nat Commun** 9(1):3834

Guo H, Benndorf R, **König S**, Leichnitz D, Weigel C, Peschel G, Berthel P, Kaiser M, Steinbeck C, Werz O, Poulsen M, Beemelmanns C (2018). *"Expanding the Rubterolone Family: Intrinsic Reactivity and Directed Diversification of PKS-derived Pyrans."* **Chemistry** 24(44):11319-11324

Cheung SY, Werner M, Esposito L, Troisi F, Cantone V, Liening S, **König S**, Gerstmeier J, Koeberle A, Bilancia R, Rizza R, Rossi A, Roviezzo F, Temml V, Schuster D, Stuppner H, Schubert-Zsilavecz M, Werz O, Hanke T, Pace S (2018). *"Discovery of a benzenesulfonamide-based dual inhibitor of microsomal prostaglandin E_2 synthase-1 and 5-lipoxygenase that favorably modulates lipid mediator biosynthesis in inflammation."* **Eur J Med Chem** 156:815-830

Loeser K, Seemann S, **König S**, Lenhardt I, Abdel-Tawab M, Koeberle A, Werz O, Lupp A (2018). *"Protective Effect of Casperome®, an Orally Bioavailable Frankincense Extract, on Lipopolysaccharide- Induced Systemic Inflammation in Mice."* **Front Pharmacol** 9:387

Koeberle A, Henkel A, Verhoff M, Tausch L, **König S**, Fischer D, Kather N, Seitz S, Paul M, Jauch J, Werz O (2018). *"Triterpene Acids from Frankincense and Semi-Synthetic Derivatives That Inhibit 5-Lipoxygenase and Cathepsin G."* **Molecules** 23(2)

Garscha U, Romp E, Pace S, Rossi A, Temml V, Schuster D, **König S**, Gerstmeier J, Liening S, Werner M, Atze H, Wittmann S, Weinigel C, Rummler S, Scriba GK, Sautebin L, Werz O (2017). *"Pharmacological profile and efficiency in vivo of diflapolin, the first dual inhibitor of 5-lipoxygenase-activating protein and soluble epoxide hydrolase."* **Sci Rep** 7(1):9398

Wiechmann K, Müller H, **König S**, Wielsch N, Svatoš A, Jauch J, Werz O (2017). *"Mitochondrial Chaperonin HSP60 Is the Apoptosis-Related Target for Myrtucommulone."* **Cell Chem Biol** 24(5):614-623

Schieferdecker S, **König S**, Pace S, Werz O, Nett M (2017). *"Myxochelin-Inspired 5-Lipoxygenase Inhibitors: Synthesis and Biological Evaluation."* **ChemMedChem** 12(1):23-27

Korp J, **König S**, Schieferdecker S, Dahse HM, König GM, Werz O, Nett M (2015). *"Harnessing Enzymatic Promiscuity in Myxochelin Biosynthesis for the Production of 5-Lipoxygenase Inhibitors."* **Chembiochem** 16(17):2445-50

Schieferdecker S, **König S**, Koeberle A, Dahse HM, Werz O, Nett M (2015). *"Myxochelins target human 5-lipoxygenase."* **J Nat Prod** 78(2):335-8

Winekenstädde D, Angelis A, Waltenberger B, Schwaiger S, Tchoumtchoua J, **König S**, Werz O, Aligiannis N, Skaltsounis AL, Stuppner H (2015). *"Phytochemical profile of the aerial parts of Sedum sediforme and anti-inflammatory activity of myricitrin."* **Nat Prod Commun** 10(1):83-8

Schieferdecker S, **König S**, Weigel C, Dahse HM, Werz O, Nett M (2014). *"Structure and biosynthetic assembly of gulmirecins, macrolide antibiotics from the predatory bacterium Pyxidicoccus fallax."* **Chemistry** 20(48):15933-40

Bohnert M, Scherer O, Wiechmann K, **König S**, Dahse HM, Hoffmeister D, Werz O (2014). *"Melleolides induce rapid cell death in human primary monocytes and cancer cells."* **Bioorg Med Chem** 22(15):3856-61

Pergola C, Gaboriaud-Kolar N, Jestädt N, **König S**, Kritsanida M, Schaible AM, Li H, Garscha U, Weinigel C, Barz D, Albring KF, Huber O, Skaltsounis AL, Werz O (2014). *"Indirubin core*

structure of glycogen synthase kinase-3 inhibitors as novel chemotype for intervention with 5-lipoxygenase." **J Med Chem** 57(9):3715-23

A3.2 Conference contributions

A3.2.1 Oral presentations

Stefanie König, Maximilian Dörfer, Dirk Hoffmeister, Oliver Werz (October 2017). "Exploiting a melleolide from honey mushroom as tool for deciphering Cys159 in 5-lipoxygenase as determinant for regulation of leukotriene biosynthesis." JSMC Symposium, Jena, Germany

Stefanie König, Jana Gerstmeier, Kirstin Scherlach, Thorsten Heinekamp, Axel Brakhage, Christian Hertweck, Oliver Werz (November 2015). "Gliotoxin inhibits leukotriene A_4 hydrolase, the enzyme that synthesizes chemotactic leukotriene B_4." JSMC Retreat, Bad Sulza, Germany

A3.2.2 Poster presentations

Stefanie König, Maximilian Dörfer, Dirk Hoffmeister, Oliver Werz (September 2016). "The melleolide dehydroarmillylorsellinate (DAO) from honey mushroom inhibits 5-lipoxygenase and decreases eicosanoid biosynthesis in leukocytes." 6th European Workshop on Lipid Mediators (6EWLM 2016), Frankfurt, Germany

Stefanie König, Maximilian Dörfer, Dirk Hoffmeister, Oliver Werz (September 2016). "The melleolide dehydroarmillylorsellinate (DAO) inhibits 5-lipoxygenase and decreases eicosanoid biosynthesis in human leukocytes." 3rd EFMC Young Medicinal Chemist Symposium, Manchester, United Kingdom

Stefanie König, Jana Gerstmeier, Kirstin Scherlach, Thorsten Heinekamp, Axel Brakhage, Christian Hertweck, Oliver Werz (November 2015). "Gliotoxin inhibits leukotriene A_4 hydrolase, the enzyme that synthesizes chemotactic leukotriene B_4." JSMC Retreat, Bad Sulza, Germany

Stefanie König, Maximilian Dörfer, Dirk Hoffmeister, Oliver Werz (July 2015). "Dehydroarmillylorsellinate (DAO) from honey mushroom inhibits 5-lipoxygenase and suppresses eicosanoid biosynthesis in leukocytes." 14th International Conference of Bioactive Lipids in Cancer, Inflammation and Diseases, Budapest, Hungary

Stefanie König, Olga Scherer, Markus Bohnert, Dirk Hoffmeister, Oliver Werz (September 2014). "The melleolide DAO induces rapid cell death in human primary monocytes and cancer cells." JSMC Symposium, Jena, Germany

APPENDIX 5: CURRICULUM VITAE

PERSÖNLICHE DATEN

Name Stefanie König

APPENDIX 6: EIGENSTÄNDIGKEITSERKLÄRUNG

Hiermit erkläre ich, dass mir die Promotionsordnung der Fakultät für Biowissenschaften der Friedrich-Schiller-Universität Jena bekannt ist. Die vorliegende Dissertation habe ich selbst angefertigt, keine Textabschnitte eines Dritten oder eigener Prüfungsarbeiten ohne Kennzeichnung übernommen und alle von mir benutzten Hilfsmittel, persönliche Mitteilungen und Quellen wurden als solche kenntlich gemacht.

Ich versichere, dass ich die Hilfe eines Promotionsberaters nicht in Anspruch genommen habe und dass Dritte weder unmittelbar noch mittelbar geldwerte Leistungen von mir für Arbeiten erhalten haben, die im Zusammenhang mit dem Inhalt der vorgelegten Dissertation stehen.

Diese Dissertation wurde für keine staatliche oder andere wissenschaftliche Prüfung als Prüfungsarbeit von mir eingereicht. Weiterhin versichere ich, dass ich die gleiche, eine in wesentlichen Teilen ähnliche oder eine andere Abhandlung nicht bei einer anderen Universität als Dissertation eingereicht habe.

Ort, Datum	Stefanie König